



## **Production and characterisation of glycoside hydrolases from GH3, GH5, GH10, GH11 and GH61 for chemo-enzymatic synthesis of xylo- and mannoooligosaccharides**

**Dilokpimol, Adiphol; Abou Hachem, Maher ; Svensson, Birte**

*Publication date:*  
2010

*Document Version*  
Publisher's PDF, also known as Version of record

[Link back to DTU Orbit](#)

*Citation (APA):*

Dilokpimol, A., Abou Hachem, M., & Svensson, B. (2010). Production and characterisation of glycoside hydrolases from GH3, GH5, GH10, GH11 and GH61 for chemo-enzymatic synthesis of xylo- and mannoooligosaccharides. Kgs. Lyngby, Denmark: Technical University of Denmark (DTU).

## **DTU Library** Technical Information Center of Denmark

---

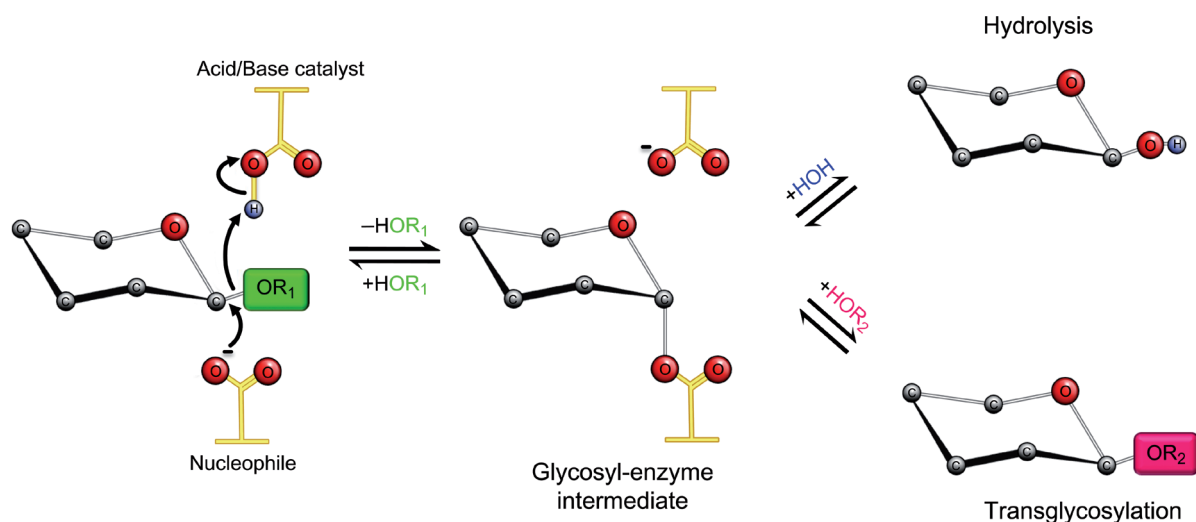
### **General rights**

Copyright and moral rights for the publications made accessible in the public portal are retained by the authors and/or other copyright owners and it is a condition of accessing publications that users recognise and abide by the legal requirements associated with these rights.

- Users may download and print one copy of any publication from the public portal for the purpose of private study or research.
- You may not further distribute the material or use it for any profit-making activity or commercial gain
- You may freely distribute the URL identifying the publication in the public portal

If you believe that this document breaches copyright please contact us providing details, and we will remove access to the work immediately and investigate your claim.

# Production and Characterisation of Glycoside Hydrolases from GH3, GH5, GH10, GH11 and GH61 for Chemo-Enzymatic Synthesis of Xylo- and Mannooligosaccharides

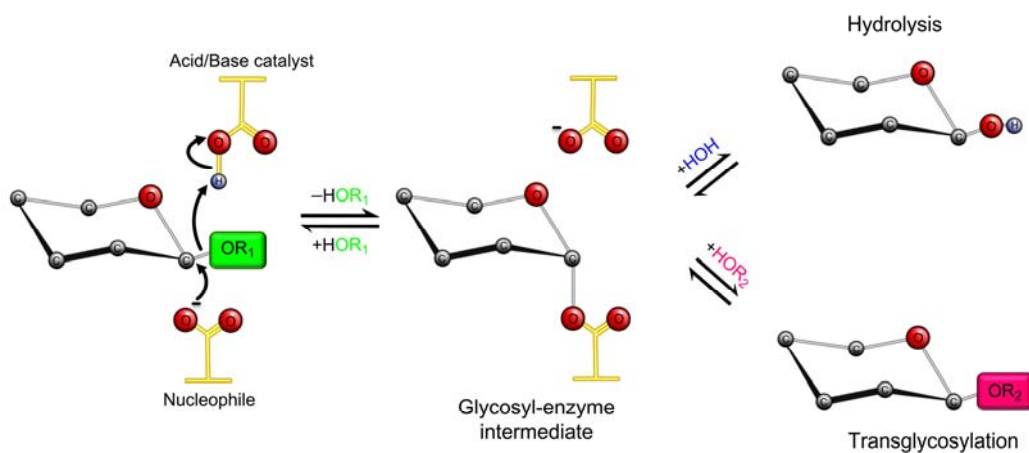


Adiphol Dilokpimol

Ph.D. Thesis

June 2010

# Production and characterisation of glycoside hydrolases from GH3, GH5, GH10, GH11 and GH61 for chemo-enzymatic synthesis of xylo- and manno oligosaccharides



**Adiphol Dilokpimol**

**Ph.D. Thesis**

**June 2010**

**Enzyme and Protein Chemistry**

**Department of Systems Biology**

**Technical University of Denmark**





## Preface

The present Ph.D. thesis entitled “Production and characterisation of glycoside hydrolases from GH3, GH5, GH10, GH11 and GH61 for chemo-enzymatic synthesis of xylo- and manno-oligosaccharides” summarises my work carried out under the supervision of Prof. Birte Svensson and Assoc. Prof. Maher Abou Hachem at Enzyme and Protein Chemistry (EPC), Department of Systems Biology, Technical University of Denmark (DTU) for the period of June 2007 to June 2010. This study was supported by the Danish Strategic Research Council’s Committee on Food and Health (FøSu, to the project ‘Biological Production of Dietary Fibres and Prebiotics’ no. 2101-06-0067).

This work has resulted in the following manuscripts:

**Dilokpimol, A.**, Nakai, H., Gotfredsen, C. H., Appeldoorn, M., Baumann, M. J., Nakai, N., Schols, H. A., Abou Hachem, M., Svensson, B. Enzymatic synthesis of  $\beta$ -xylosyl-oligosaccharides by transxylosylation using two  $\beta$ -xylosidases of glycoside hydrolase family 3 from *Aspergillus nidulans* FGSC A4, submitted to *Carbohydrate Research* (see 10.2.3.1)

**Dilokpimol, A.**, Nakai, H., Gotfredsen, C. H., Baumann, M. J., Nakai, N., Abou Hachem, M., Svensson, B. GH5 endo- $\beta$ -1,4-mannanases from *Aspergillus nidulans* FGSC A4 producing hetero manno-oligosaccharides by transglycosylation, to be submitted to *Biochimica et Biophysica Acta, Proteins and Proteomics* (see 10.2.3.2)

In addition, I am the coauthor of several publications and manuscripts (listed in 10.2) on results obtained in the same project.

Kgs. Lyngby, 3<sup>rd</sup> June 2010

---

Adiphol Dilokpimol

## Acknowledgements

This work could not have been accomplished without the help and support of many teachers, colleagues and friends.

First, I would like to express my deep appreciation and gratefully thankful to **Professor Birte Svensson** and **Associate Professor Maher Abou Hachem** for giving me the opportunity to carry out my Ph.D. study. I deeply appreciate all of your invaluable guidance and mental supports throughout the whole period. I would like to extend my heartiest thanks to **Dr. Hiroyuki Nakai** for his excellent and inspirational scientific supports in this study.

**Professor Anne S. Meyer** and **Professor Jørn D. Mikkelsen**, Center for Biological Production of Dietary Fibers and Prebiotics, DTU Chemical Engineering, and the **Steering Committee** for this project are sincerely thanked for their suggestions and discussions.

**Professor Stephen G. Withers**, University of British Columbia, Canada, **Professor Monica Palcic**, **Professor Ole Hindsgaul**, and **Dr. Karin Mannerstedt**, Carbohydrate Chemistry group, Carlsberg Laboratory, are thanked for providing and deacetylation of  $\alpha$ -xylosyl- and  $\alpha$ -xylobiosyl fluorides.

**Professor Henk A. Schols**, **Dr. Maaïke Appeldoorn**, and **Dr. Yvonne Westpahl**, Laboratory of Food Chemistry, Wageningen University, The Netherlands, are thanked for their excellent electrospray ionization mass spectrometry analysis and scientific discussions.

I would genuinely like to thank **Associate Professor Charlotte H. Gotfredsen** and **Anne Hector**, DTU Chemistry, not only for her superb nuclear magnetic resonance analysis of all transglycosylation products but also for generous and fruitful discussions. **Professor Jens Ø. Duus** and **Bent O. Petersen**, Carlsberg Laboratory, are thanked for assisting with the NMR assignment.

**Professor William G. T. Willats** and **Dr. Henriette Lodberg Pedersen**, Faculty of Life Sciences, University of Copenhagen, are thanked for performing analysis of the GH61 putative endo- $\beta$ -glucanase on carbohydrate microarray analysis.

**Professor Atsuo Kimura** and **Associate Professor Haruhide Mori**, Faculty of Agriculture, Hokkaido University, Japan, as well as **Dr. Nathalie Juge** and **Dr. Jean-Guy Berrin**, Institute of Food Research, Norwich Research Park, United Kingdom, are thanked for their kind support. **Professor Peter Roepstorff** and **Dr. Martin Zehl**, Department of Biochemistry and Molecular Biology, University of Southern Denmark, are thanked for electrospray ionization mass spectrometry analysis of Xyl-Cys. **Associate Professor Leila Lo Leggio**, Department of Chemistry, University of Copenhagen is thanked for stimulating discussions on  $\beta$ -xylosidase structure. **Associate Professor Mads H. Clausen**, DTU Chemistry, is thanked for the preparation of  $\beta$ -xylosyl fluoride. I apologise for my careless handling of the compound. I wish to thank **Anne Blicher** for

her excellent amino acid analysis. **PhD student Louise E. Rasmussen**, DTU Chemical Engineering, is thanked for kind assistance in the beginning of this project.

My thankfulness also goes to all former and present members of the **Enzyme and Protein Chemistry**, DTU Systems Biology, for their help in one way or another to make this study possible especially **Associate Professor Susanne Jacobsen, Dr. Martin J. Baumann, Dr. Per Hägglund, Dr. Eun Seong Seo, Dr. Malene B. Vester-Christensen, Susanne Blume, Karina Jansen, Birgit Andersen**, and **Bjarne G. Schmidt**. Special thanks to **Karen Marie Jakobsen** for her excellent administrative skills as well as **PhD student Marie S. Møller, PhD student Anders D. Jørgensen**, and **Brian S. Lassen** for kindly helping to translate ‘Danske resumé’.

The **Danish Strategic Research Council’s Committee on Food and Health (FøSu)** and **Danisco**, Denmark, are thanked for co-funding the PhD project in the Center for Biological Production of Dietary Fibers and Prebiotics with DTU.

Last but not least, I am thankful to my beloved parents, my family and my friends both in Denmark and Thailand, for their endless support and understanding throughout the difficult times. Without your love and support, I am sure that I would not be able to continue up till now.

## Summary

Plant cell wall hydrolysate by-products are resources for oligosaccharides which potentially can act as prebiotics stimulating the growth of probiotic bacteria and thus provide a number of health benefits to the host. The objective of the present research project is to produce novel prebiotics or biologically active oligosaccharides by enzyme catalysed transglycosylation of starting materials that are related to or derived from industrial plant by-products. Five recombinant glycoside hydrolases, *i.e.* one GH3  $\beta$ -xylosidase, two GH5 mannanases, one GH10 xylanase, and one GH11 xylanase from *Aspergillus nidulans* FGSC A4 were investigated for their transglycosylation activity aiming at production of  $\beta$ -xylo- and mannoooligosaccharides. The project includes characterisation of the produced enzymes.

The GH3  $\beta$ -xylosidase (BxlA) was produced as a His-tag fusion protein secreted by *Pichia pastoris* X-33 in a yield of 16 mg/L culture. BxlA displayed a  $K_m$  and  $k_{cat}$  towards *para*-nitrophenyl  $\beta$ -D-xylopyranoside of 1.3 mM and 112 s<sup>-1</sup>, respectively, and also hydrolysed *para*-nitrophenyl  $\alpha$ -L-arabinofuranoside albiet with two orders of magnitude lower catalytic efficiency ( $k_{cat}/K_m$ ). Among xylooligosaccharides (degree of polymerisation 2–6), BxlA preferably hydrolysed xylobiose, while the catalytic efficiency decreased slightly with increasing chain length. Transglycosylation reactions using 10 mono- and six disaccharides, two sugar alcohols, and two amino acids revealed that BxlA possesses broad acceptor specificity, while mannose, lyxose, and talose are preferred acceptors for BxlA with transglycosylation yields of 25%, 23%, and 22%, respectively. Moreover, four di- and two trisaccharides/glycosides produced with lyxose, L-fucose, talose, cysteine, sucrose, and turanose as acceptors are novel compounds and the structures of  $\beta$ -D-Xylp-(1→4)-D-Lyxp,  $\beta$ -D-Xylp-(1→4)- $\alpha$ -D-Glcp-(1→3)- $\beta$ -D-Fruf,  $\beta$ -D-Xylp-(1→4)- $\alpha$ -D-Glcp-(1→2)- $\beta$ -D-Fruf, and  $\beta$ -D-Xylp-(1→6)- $\beta$ -D-Fruf-(2→1)- $\alpha$ -D-Glcp, have been assigned by NMR and their molecular masses have been determined by ESI-MS. Glycosynthase mutants of BxlA (D307G, D307A, D307S, D307C) showed low glycosynthase activity using  $\alpha$ -xylosyl fluoride as donor with different acceptors and were not suitable for synthesis of xylosyl-oligosaccharides. The roles of Cys308 and Asn313 at subsite +1 of BxlA in transglycosylation were evaluated using subsite +1 mutants (C308W and N313R) created by site-directed mutagenesis. C308W essentially lost activity indicating that Cys308 is crucial for the activity of BxlA, whereas the transglycosylation yields catalysed by N313R were increased by 50–150% using hexoses and maltose as acceptors.

The GH5 mannanases (ManA and ManC, sharing 39% sequence identity) were produced recombinantly as His-tag fusion proteins by *P. pastoris* X-33 in a yield of 120 and 145 mg/L culture, respectively. ManA and ManC hydrolysed mannoooligosaccharides (degree of polymerisation 4–6) with highest  $k_{cat}$  of 193 and 134 s<sup>-1</sup> towards mannohexaose with  $K_m$  of 1.8 and 0.6 mM, respectively, but showed weak affinity towards mannotetraose. ManC had higher  $k_{cat}/K_m$  than ManA, while mannobiose was the main hydrolysis products from both ManA and ManC. In addition, ManC showed 30–80% higher activity towards konjac glucomannan, guar galactomannan, and locust bean gum galactomannan and possessed 8-fold higher transglycosylation activity than ManA. The maximum transglycosylation yield of mannopentaose and mannohexaose using ManC with 24 mM mannotetraose as donor and 100 mM mannotriose as acceptor was 7.13 mg/mL. Furthermore, in order to investigate the potential role of Trp283 at subsite +1 of ManC, which is equivalent to Ser289 in ManA, the subsite +1 mutants ManCW283S and ManAS289W were made. The subsite +1 mutants have lower



hydrolytic activity than the wild-type enzymes. ManAS289W showed lower  $K_m$  and the transglycosylation activity increased 50% compared to ManA wild-type, whereas ManCW283S showed higher  $K_m$  and the transglycosylation activity decreased 30–45% compared to ManC wild-type, indicating that Trp283 in ManC has some impact on the activity of mannanases, but is not a crucial residue in controlling transglycosylation and hydrolysis. Transglycosylation reactions using 12 mono-, 15 di-, and 9 trisaccharides revealed that ManA and ManC have relatively strict acceptor specificity. Apart from mannotriose, ManC can use isomaltotriose and melezitose as acceptors, but ManA accepts only mannotriose. Two penta- and two hexasaccharides were novel compounds produced by ManC using isomaltotriose and melezitose ( $\alpha$ -D-Glcp-(1→3)- $\beta$ -D-Furf-(2→1)- $\alpha$ -D-Glcp) as acceptors.

The GH10 (XlnC) and GH11 (XlnA) xylanases from *A. nidulans* FGSC A4 were recloned from *P. pastoris* expression host acquired from Fungal Genetics Stock Center (Kansas City, MO) and produced in *Escherichia coli* BL21(DE3) as His-tagged fusion proteins in a yield of 95 and 90 mg/L culture, respectively. XlnA showed higher activity than XlnC towards birchwood xylan, oat spelt arabinoxylan and wheat arabinoxylan with specific activity towards birchwood xylan of 330 and 280 U/mg, respectively. Transglycosylation using six disaccharides and two sugar alcohols revealed that XlnA has very strict acceptor specificity and can use only xylobiose as acceptor. XlnC has also rather narrow acceptor specificity, but can in addition to xylobiose use cellobiose, xylitol, and sorbitol as acceptors with transglycosylation yields of 3%, 22%, and 16%, respectively. The glycosynthase mutant of XlnC (E244A) was not properly functioning, since it showed low glycosynthase activity using  $\alpha$ -xylobiosyl fluoride as donor and the oligosaccharide products, moreover, were degraded by the trace hydrolytic activity of the E244A mutant.

The last part of the study was to perform enzyme discovery by applying a proteomics strategy. Previously, extracellular proteins from culture supernatant of *A. nidulans* FGSC A4 grown on 10 polysaccharides were separated by two-dimensional gel electrophoresis and identified after trypsin digestion by matrix-assisted laser desorption/ionization mass spectrometry (unpublished work by Kenji Maeda and Hiroyuki Nakai, Enzyme and Protein Chemistry, DTU Systems Biology). Among several potential novel carbohydrate active enzymes detected by this strategy, a GH61 putative endo- $\beta$ -glucanase (EglF) was chosen for further investigation. The *eglF* gene was obtained by mRNA isolation and cDNA cloning from a cell culture of *A. nidulans* FGSC A4 using barley  $\beta$ -glucan as substrate and cloned into *P. pastoris* X-33. EglF was produced recombinantly as His-tagged protein in a yield of 66 mg/L culture. EglF showed very low hydrolytic activity towards barley  $\beta$ -glucan and oat spelt arabinoxylan with specific activity of 180 and 145  $\mu$ U/mg, respectively, and no activity and binding were found by screening using carbohydrate microarrays (collaboration with Henriette Lodberg Pedersen and William G. T. Willats, University of Copenhagen). Recently, other GH61 proteins were proposed to be cellulase-enhancing factors, and the prepared EglF could be useful for further investigations on how GH61 proteins enhance cellulase activity.

## Dansk resumé

Biprodukter fra hydrolyse af plantecellevægge er kilder til oligosakkarider, som potentielt kan fungere som prebiotika ved at stimulere væksten af probiotiske bakterier, og dermed medføre en række sundhedsmæssige fordele for værten. Formålet med dette forskningsprojekt er, at producere nye prebiotika eller biologisk aktive oligosakkarider ved enzymkatalyseret transglykosylering af materialer, der er relateret til, eller stammer fra industrielle biprodukter. Fem forskellige rekombinante glykosidhydrolaser, dvs. en GH3  $\beta$ -xylosidase, to GH5 mannanaser, en GH10 xylanase, og en GH11 xylanase fra *Aspergillus nidulans* FGSC A4, blev undersøgt for deres transglykosyleringsaktivitet med det formål at producere  $\beta$ -xylo- og mannooligosakkarider. Projektet omfatter karakterisering af de producerede enzymer.

GH3  $\beta$ -xylosidase (BxlA) blev fremstillet som et His-tag-fusionsprotein, der udskilles af *Pichia pastoris* X-33, med et udbytte på 16 mg/L kultur.  $K_m$  og  $k_{cat}$  for *para*-nitrofenyl  $\beta$ -D-xylopyranosid var henholdsvis 1,3 mM og 112 s<sup>-1</sup>, og BxlA hydrolyserede også *para*-nitrofenyl  $\alpha$ -L-arabinofuranosid med to gange lavere katalytisk effektivitet ( $k_{cat}/K_m$ ). Blandt xylooligosakkarider (polymereringsgrad 2–6), hydrolyserede BxlA hovedsageligt xylobiose, mens den katalytiske effektivitet faldt en smule ved længere xylooligosakkarider. Transglykosyleringsreaktioner med 10 mono- og sex disakkarider, to sukkeralkoholer, og to aminosyrer viste, at BxlA har bred acceptor-specificitet, mens mannose, lyxose, og talose er foretrukne acceptorer for BxlA med transglykosyleringsudbytter på henholdsvis 25%, 23%, og 22%. Desuden, er fire di- og to trisakkarider produceret med lyxose, L-fukose, talose, cystein, sakkarose, og turanose som acceptorer, nye forbindelser, og strukturerne af  $\beta$ -D-Xylp-(1→4)-D-Lyxp,  $\beta$ -D-Xylp-(1→4)- $\alpha$ -D-Glcp-(1→3)- $\beta$ -D-Fruf,  $\beta$ -D-Xylp-(1→4)- $\alpha$ -D-Glcp-(1→2)- $\beta$ -D-Fruf, og  $\beta$ -D-Xylp-(1→6)- $\beta$ -D-Fruf-(2→1)- $\alpha$ -D-Glcp, er blevet bestemt med NMR og deres molekylvægt er blevet bestemt med ESI-MS. Glycosynthase mutanter af BxlA (D307G, D307A, D307S, D307C) viste lav glycosynthase aktivitet ved  $\alpha$ -xylosylfluorid som donor med forskellige acceptorer, og var ikke egnede til syntese af xylosylooligosakkarider. Rollerne for Cys308 og Asn313 på subsite +1 af BxlA for transglykosylering blev evalueret ved brug af subsite +1 mutanter (C308W og N313R) lavet ved site-directed mutagenese. C308W mistede næsten al aktivitet, hvilket indikerer, at Cys308 er afgørende for BxlA, hvorimod udbyttet af transglykosyleringen katalyseret af N313R blev øget med 50–150% ved brug af hexose og maltose som acceptorer.

GH5 mannanaserne (ManA og ManC, med 39% identisk sekvensdata) er blevet fremstillet rekombinant som His-tag-fusionsproteiner af *Pichia pastoris* X-33 med et udbytte på henholdsvis 120 og 145 mg/L kultur. ManA og ManC hydrolyserede mannooligosakkarider (polymerisationsgrad 4–6) med højeste  $k_{cat}$  på henholdsvis 193 og 134 s<sup>-1</sup> for mannohexaose med en  $K_m$  værdi på henholdsvis 1,8 og 0,6 mM, men viste svag affinitet overfor mannotetraose. ManC havde højere katalytiskeffektivitet ( $k_{cat}/K_m$ ) end ManA, mens mannobiose var det primære hydrolyseprodukt fra både ManA og ManC. Desuden viste ManC 30–80% højere aktivitet overfor konjac glucomannan, guar galactomannan, og johannesbrødkernemel galaktomannan og havde samtidig 8 gange højere transglykosyleringsaktivitet end ManA, og den maksimale transglykosyleringsproduktion var 7,13 mg/ml mannopentaose og mannohexaose ved 24 mM mannotetraose som donor, og 100 mM mannotriose som acceptor. Med henblik på at undersøge hvilken indfyldelse Trp283 ved subsite +1 af ManC, som svarer til Ser289 i

ManA, blev subsite +1 mutanterne, ManCW283S og ManAS289W, fremstillet. Subsite +1 mutanterne har lavere hydrolytisk aktivitet end vildtype enzymet. ManAS289W viste lavere  $K_m$  og transglykosyleringsaktiviteten steg 50% i forhold til vildtype ManA, mens ManCW283S viste højere  $K_m$  og transglykosyleringsaktiviteten faldt 30–45% i forhold til vildtype ManC. Det indikerer, at Trp283 i ManC har en indvirkning på aktiviteten af mannanaser, men er ikke en afgørende aminosyre for kontrollen af transglykosylering og hydrolyse. Transglykosyleringsreaktioner ved anvendelse af 12 mono-, 15 di- og 9 trisakkarider viste, at ManA og ManC har streng acceptorspecificitet. ManA accepterer kun mannotriose, mens ManC kan bruge både mannotriose, isomaltotriose og melezitose som acceptorer. To nye penta- og to hexasakkarid-forbindelser blev produceret af ManC ved hjælp af isomaltotriose og melezitose ( $\alpha$ -D-Glcp-(1→3)- $\beta$ -D-Fruf-(2→1)- $\alpha$ -D-Glcp) som acceptorer.

GH10 (XlnC) og GH11 (XlnA) xylanaserne blev genklonet fra *P. pastoris* kloner leveret af Fungal Genetics Stock Center (Kansas City, MO) og produceret i *Escherichia coli* BL21(DE3) som His-tag-fusionsproteiner med et udbytte på henholdsvis 95 og 90 mg/L kultur. XlnA viste højere aktivitet end XlnC mod birketræs-xylan, havre-spelt arabinoxylan og hvede arabinoxylan med specifik aktivitet på henholdsvis 330 og 280 U/mg for birketræs-xylan. Transglykosylering ved brug af sex disakkarider og to sukkeralkoholer viste, at XlnA har meget streng acceptorspecificitet, og kun kan bruge xylobiose som acceptor. XlnC har også ret streng acceptorspecificitet, men kan ud over xylobiose også bruge cellobiose, xylitol og sorbitol som acceptorer, med transglycosylationsudbytter på henholdsvis 3%, 22% og 16%. XlnC glycosynthase mutanten (E244A) var ikke velfungerende, da den viste lav glycosynthase-aktivitet ved brug af  $\alpha$ -xylobiosyl-fluorid som donor, og det producerede oligosakkarid var blevet nedbrudt af E244A mutantens sporadiske hydrolytiske aktivitet.

Den sidste del af undersøgelsen var at udføre enzym-detektion ved hjælp af en proteomics-strategi. Tidligere er ekstracellulære proteiner fra kultur-supernatant af *A. nidulans* FGSC A4, dyrket på 10 polysaccharider, blevet adskilt af 2-dimensional gel elektroforese, og identificeret efter trypsinfordøjelse af matrix-assisteret laser desorption/ioniseringsmassespektrometri (ikke-udgivet værk af Kenji Maeda og Hiroyuki Nakai, Enzyme and Protein Chemistry, DTU Systembiologi). Blandt flere potentielle nye kulhydrataktive enzymer opdaget ved brug af denne strategi, var en formodet GH61 endo- $\beta$ -glucanase (EglF), som blev udvalgt til nærmere undersøgelse. EglF-genet blev fremskaffet ved mRNA isolering og cDNA kloning fra en cellekultur af *A. nidulans* FGSC A4 ved hjælp af byg  $\beta$ -glucan som substrat, og klonet ind i *P. pastoris* X-33. EglF blev produceret rekombinant som His-tag-protein med et udbytte på 66 mg/L kultur. EglF viste meget lav hydrolytisk aktivitet mod byg  $\beta$ -glucan og havre-spelt arabinoxylaner med en specifik aktivitet på henholdsvis 180 og 145  $\mu$ U/mg, og ingen aktivitet eller bindinger blev fundet ved screening med kulhydratmicroarrays (samarbejde med Henriette Lodberg Pedersen og William G. T. Willats, Københavns Universitet). For nyligt blev der foreslået andre GH61 proteiner som cellulase-styrkende faktorer, og den preparerede EglF kunne være brugbar for yderligere undersøgelser af, hvordan GH61 proteiner øger cellulase-aktivitet.

## Abbreviations

2DE:	Two-dimensional gel electrophoresis
2D NMR:	Two-dimensional nuclear magnetic resonance spectroscopy
3D:	Three-dimensional
ACN:	Acetonitrile
Araf:	$\alpha$ -L-Arabinofuranoside
Arap:	$\alpha$ -L-Arabinopyranoside
BMGY:	Buffered glycerol-complex medium
BMM:	Buffered minimal methanol medium
BMMY:	Buffered methanol-complex medium
CAZy:	Carbohydrate-Active EnZymes Database
CBM:	Carbohydrate binding module family (families)
CCNFSDU:	Codex Commission on Nutrition and Foods for Special Dietary Uses
CE:	Combinatorial extension
Cys:	L-cysteine
DP:	Degree of polymerisation
ESI-MS:	Electrospray ionization mass spectrometry
ESI-Q-TOF MS:	Electrospray quadrupole time-of-flight mass spectrometry
FAO:	Food and Agriculture Organization of the United Nations
Gal:	$\alpha$ -D-Galactose / galactopyranoside
GalMan:	Galactomannan
GH:	Glycoside hydrolase family (families)
Glc:	$\beta$ -D-Glucose / glucopyranoside
GlcA:	$\alpha$ -D-Glucuronic acid / glucuronopyranoside
GlcMan:	Glucomannan
GT:	Glycosyltransferase family (families)
HEPES:	4-(2-hydroxyethyl)-1-piperazineethanesulfonic acid
HPAEC-PAD:	High performance anion exchange chromatography with pulsed amperometric detection
HPLC:	High performance liquid chromatography
IEF:	Isoelectric focusing
IMAC:	Immobilized metal ion affinity chromatography
IOM:	Institute of Medicine of the National Academies
Iso3:	Isomaltotriose
IUBMB:	International Union of Biochemistry and Molecular Biology
LB:	Luria Bertani (medium)
LBG:	Locust bean gum
M2–M6:	Mannobiose–mannohexaose
mAb:	Monoclonal antibody
MALDI-TOF MS:	Matrix assisted laser desorption/ionisation time-of-flight mass spectrometry
Man:	$\beta$ -D-Mannose / mannopyranoside
MeGlcA:	4-O-Methyl- $\alpha$ -D-glucuronopyranoside
Mel3:	Melezitose
MES:	2-( <i>N</i> -morpholino) ethanesulfonic acid
MP:	Low fat milk powder
NBT/BCIP:	Nitro blue tetrazolium and 5-bromo-4-chloro-3-indolyl phosphate

NMR:	Nuclear magnetic resonance spectroscopy
NMWL:	Nominal molecular weight limit
OD:	Optical density
PBS:	Phosphate buffered saline
PDB:	Protein Data Bank
<i>p</i> NP:	<i>para</i> -Nitrophenol
<i>p</i> NPA:	<i>para</i> -Nitrophenyl $\alpha$ -L-arabinofuranoside
<i>p</i> NPAP:	<i>para</i> -Nitrophenyl $\alpha$ -L-arabinopyranoside
<i>p</i> NPC2:	<i>p</i> NP $\beta$ -D-cellobioside
<i>p</i> NPX:	<i>para</i> -Nitrophenyl $\beta$ -D-xylopyranoside
ppi:	pixels per inch
SDS-PAGE:	Sodium dodecyl sulfate polyacrylamide gel electrophoresis
Ser:	L-serine
TIM:	Triosephosphate isomerase
USDA:	United States Department of Agriculture
X2–X6:	Xylobiose–xylohexaose
Xyl:	$\beta$ -D-Xylose / xylopyranoside
$\alpha$ X2F:	$\alpha$ -Xylobiosyl fluoride
$\alpha$ XF:	$\alpha$ -Xylosyl fluoride

# Content

Preface	i
Acknowledgements	ii
Summary	iv
Danske resumé	vi
Abbreviations	viii
Content	x
List of figures	xiv
List of tables	xvi
<b>1. The overall objective of the thesis project</b>	<b>1</b>
<b>2. Introduction</b>	<b>1</b>
2.1 Cell wall polysaccharides as source of dietary fibres and prebiotics	1
2.1.1 Plant cell wall composition	1
2.1.2 Dietary fibres and prebiotics	5
2.1.3 Oligosaccharides as prebiotics	6
2.1.4 Xylans and xylooligosaccharides	8
2.1.4.1 Structure and composition	8
2.1.4.2 Application of xylans and xylooligosaccharides	9
2.1.5 Mannans and mannoooligosaccharides	10
2.1.5.1 Structure and composition	10
2.1.5.2 Application of mannans and mannoooligosaccharides	11
2.1.6 Cellulose and cellooligosaccharides	11
2.1.6.1 Structure, composition, and applications	11
<b>3. Enzyme discovery</b>	<b>12</b>
<b>4. Hydrolysis, phosphorolysis, and transglycosylation mechanisms</b>	<b>13</b>
4.1 Enzyme catalysed transglycosylation	16
4.1.1 Reverse hydrolysis	17
4.1.2 Reverse phosphorolysis	17
4.1.3 Glycosynthase reaction	18
4.2 Xylanases and xylosidases	19
4.2.1 Enzymatic hydrolysis of xylans	19
4.2.2 GH10 and GH11 xylanases	22
4.2.3 GH3 xylosidases	23
4.2.4 Transglycosylation by xylanases and xylosidases	24
4.2.5 Objectives for investigation on GH3, GH10, and GH11	25
4.3 Mannanases	26
4.3.1 Enzymatic hydrolysis of mannans	26
4.3.2 GH5 mannanases	27
4.3.3 Transglycosylation by mannanases	27
4.3.4 Objective for investigation on GH5	28
4.4 Endo- $\beta$ -glucanase	28

4.4.1	Enzymatic hydrolysis of cellulose	28
4.4.2	GH61 putative endo- $\beta$ -glucanase	29
4.4.3	Objective for investigation on GH61	29
5.	<b>Materials and methods</b>	<b>31</b>
5.1	Materials	31
5.1.1	<i>Pichia pastoris</i> transformants and <i>Aspergillus</i> strain	31
5.1.2	Primers	31
5.1.3	Natural carbohydrate substrates	33
5.1.4	Synthetic carbohydrate substrates	33
5.2	Sequence comparison and homology modeling	33
5.3	Cloning and mutations	34
5.3.1	GH3 xylosidases	34
5.3.2	GH5 mannanases	35
5.3.3	GH10 and GH11 xylanases	35
5.4	Recombinant protein production and purification	35
5.4.1	GH3 xylosidases and mutants	36
5.4.2	GH5 mannanases and mutants	36
5.4.3	GH10, GH11 xylanases, and GH10 glycosynthase mutant	37
5.5	Protein characterisation	37
5.5.1	Protein concentration determination	37
5.5.2	Molecular mass determination	38
5.5.3	Glycosylation analysis	38
5.6	Enzyme activity and kinetics	38
5.6.1	GH3 xylosidases	38
5.6.1.1	<i>para</i> -Nitrophenyl $\beta$ -D-xylopyranoside and <i>para</i> -nitrophenyl $\alpha$ -L-arabinofuranoside	38
5.6.1.2	Xylooligosaccharides	39
5.6.2	GH5 mannanases	39
5.6.2.1	Galactomannan and glucomannan	39
5.6.2.2	Mannooligosaccharides	39
5.6.2.3	Hydrolysis action patterns	40
5.6.3	GH10 xylanase	40
5.6.3.1	Xylans	40
5.7	Transglycosylation screening and optimisation	40
5.7.1	GH3 xylosidases	40
5.7.2	GH5 mannanases	41
5.7.3	GH10 and GH11 xylanases	41
5.7.4	Glycosynthase reactions	42
5.8	Oligosaccharide production by transglycosylation for structural analysis	42
5.8.1	GH3 xylosidases	42
5.8.2	GH5 mannanases	43
5.9	Oligosaccharide characterisation	43
5.9.1	Nuclear magnetic resonance spectroscopy	43

5.9.2	Electrospray ionization mass spectrometry	44
5.9.3	Matrix-assisted laser desorption/ionisation-time of flight mass spectrometry	44
5.10	GH61 putative endo- $\beta$ -glucanase	44
5.10.1	Cultures of <i>Aspergillus nidulans</i> FGSC A4 on polymeric substrates	44
5.10.2	cDNA cloning	45
5.10.3	Production and purification of GH61 putative endo- $\beta$ -glucanase	45
5.10.4	Carbohydrate microarray analysis	45
5.10.4.1	Screening for EglF activity on carbohydrate microarrays <i>via</i> post-print epitope deletion	46
5.10.4.2	Screening for EglF binding to carbohydrate microarrays	46
<b>6.</b>	<b>Results</b>	<b>50</b>
6.1	GH3 xylosidase	50
6.1.1	Production and purification	50
6.1.2	Protein characterisation	50
6.1.3	Enzymatic specificity and kinetics	51
6.1.4	Transglycosylation	53
6.1.5	Characterisation of xylosyl-oligosaccharide products	56
6.1.6	Engineering of transglycosylation activity by glycosynthase and subsite +1 mutants	59
6.2	GH5 mannanases	62
6.2.1	Production and purification	62
6.2.2	Protein characterisation	64
6.2.3	Enzymatic specificity, kinetics, and hydrolysis action patterns	64
6.2.4	Transglycosylation catalysed by ManA and ManC	67
6.2.5	Transglycosylation catalysed by subsite +1 mutants	68
6.2.6	Characterisation of mannoooligosaccharide products	70
6.3	GH10 and GH11 xylanases	74
6.3.1	Production and purification	74
6.3.2	Enzymatic activity towards xylans	75
6.3.3	Transglycosylation	76
6.3.4	GH10 glycosynthase	76
6.4	GH61 putative endo- $\beta$ -glucanase	78
6.4.1	cDNA cloning	78
6.4.2	Production and purification	80
6.4.3	Protein characterisation and screening for activity	80
6.4.4	Carbohydrate microarrays	81
<b>7.</b>	<b>Discussion</b>	<b>82</b>
7.1	GH3 xylosidase	82
7.1.1	Production of BxlA	82
7.1.2	Comparison of hydrolytic activity of BxlA and BxlB	82
7.1.3	Transglycosylation and acceptor specificity of BxlA	83
7.1.4	Transglycosylation using amino acids as acceptors	85



7.1.5	Glycosynthase and subsite mutants of BxlA	85
7.2	GH5 mannanases	86
7.2.1	Production of ManAS289W and ManCW283S	86
7.2.2	Enzymatic properties of GH5 mannanases	86
7.2.3	Effect of subsites of GH5 mannanases	88
7.3	GH10 and GH11 xylanases	88
7.3.1	Production and activity of XlnC and XlnA	88
7.3.2	Transglycosylation by XlnC and XlnA	89
7.3.3	Glycosynthase of XlnC	90
7.4	GH61 putative endo- $\beta$ -glucanase	91
7.5	Novel oligosaccharides	93
<b>8.</b>	<b>Conclusions and future perspectives</b>	<b>95</b>
<b>9.</b>	<b>References</b>	<b>97</b>
<b>10.</b>	<b>Appendix</b>	<b>112</b>
10.1	Supplementary Figures	112
10.2	List of publications and presentations	121
10.2.1	Oral presentations	121
10.2.2	Poster presentations	121
10.2.3	Manuscripts and publications	123
10.2.3.1	Manuscript I	125
10.2.3.2	Manuscript II	145

## List of figures

Figure 1 Plant plasma membrane and cell-wall structure	3
Figure 2 Structure of xylans	9
Figure 3 Structure of mannans	11
Figure 4 Hydrolytic mechanisms of glycoside hydrolases	15
Figure 5 Hydrolysis, transglycosylation, and glycosynthase mechanisms of glycoside hydrolase	15
Figure 6 Schematic reaction mechanism of reverse hydrolysis and transglycosylation	17
Figure 7 Schematic reaction mechanism of reversible phosphorolysis	18
Figure 8 Xylanolytic (upper) and mannan degrading enzymes (lower) with their sites of attack on xylan and mannan substrates	22
Figure 9 Cartoon representation of 3D structures of GH10, GH11 xylanases, and GH3 xylosidase	24
Figure 10 Layout of carbohydrate microarrays	48
Figure 11 Overview of the experimental approach for carbohydrate microarray analysis.	49
Figure 12 Purification of BxlA	50
Figure 13 Molecular mass determination using SDS-PAGE and gel filtration, deglycosylation, and pI of BxlA	51
Figure 14 Effect of pH and temperature on activity and stability of purified BxlA and BxlB	52
Figure 15 Progress of transglycosylation with different acceptors catalysed by BxlA	54
Figure 16 HPAEC-PAD chromatograms monitoring transglycosylation with selected acceptors to illustrate different product formations	54
Figure 17 HPAEC-PAD chromatogram and ESI-Q-TOF mass spectra of Xyl-Cys	56
Figure 18 Cartoons representing the active site in 3D structures and homology models of GH3 enzymes	60
Figure 19 Glycosynthase reactions using D288A or D288C	61
Figure 20 Progress of transglycosylation with different acceptors by N313R	62
Figure 21 Purification of ManAS289W	63
Figure 22 Purification of ManCW283S	63
Figure 23 SDS-PAGE of purified and deglycosylated ManA, ManC, ManAS289W, and ManCW283S	64
Figure 24 Hydrolytic action patterns of ManA, ManAS289W, ManC, and ManCW283S towards mannoooligosaccharides	67
Figure 25 Time course of transglycosylation products formation of ManA and ManC	68
Figure 26 Cartoons representing the active site in 3D structures and homology models of GH 5 mannanases	69
Figure 27 Time course of transglycosylation products formation of ManAS289W and ManCW283S	70
Figure 28 Time course of total transglycosylation products formation from ManC acting on isomaltotriose and melezitose	71
Figure 29 Molecular masses of transglycosylation products from ManC	72
Figure 30 Preliminary productions of XlnA and XlnC	74
Figure 31 Purification of XlnC	75

Figure 32 Progress of transglycosylation with different acceptors catalysed by XlnC	76
Figure 33 Purification of E244A	77
Figure 34 Progress of glycosynthase reactions using E244A	78
Figure 35 Sequence alignment of GH61 putative endo- $\beta$ -glucanase gene	79
Figure 36 Purification of GH61 EglF	80
Figure 37 Molecular mass of EglF determined by SDS-PAGE and gel filtration, and pI of EglF	81
Figure 38 Conformation models of $\beta$ -D-xylopyranose and $\alpha$ -L-arabinofuranose	83
Figure 39 Illustration of transglycosylation products formation using manooligosaccharides	87
Figure 40 Cartoons representing active sites in the 3D structure of GH10 (XlnC) and a homology model of GH11 (XlnA) xylanases	90
Figure 41 Alignment of putative EglF with reported structures from GH61	92
Figure 42 Cartoons representing 3D structures and homology model of GH61 proteins	93
Supplementary Fig. 1 ESI-Q-TOF mass spectra of Xyl-Cys transglycosylation Reaction mixture	112
Supplementary Fig. 2 Amino acid sequence alignment of BxlA and BxlB	114
Supplementary Fig. 3 Amino acid sequence alignment of ManC and ManA	119

## List of tables

Table 1 Polymeric components of typical dicot and grass primary and secondary cell walls	4
Table 2 Typical oligosaccharides and polysaccharides with prebiotic effect	7
Table 3 Hemicellulolytic (and certain cellulolytic) enzymes, their classification, and current crystallographic data	20
Table 4 Enzymes identity and accession number	31
Table 5 Primers for construction of the expression plasmids	32
Table 6 Effect of metal ions on the hydrolytic activity towards <i>p</i> NPX of BxlA	51
Table 7 Kinetic parameters of BxlA and BxlB for hydrolysis of xylooligosaccharides, <i>p</i> NPX, and <i>p</i> NPA	53
Table 8 Maximum transglycosylation yields with different acceptors	55
Table 9 <sup>1</sup> H and <sup>13</sup> C NMR data assignments and molecular masses for xylosyl-oligosaccharides produced by enzymatic transglycosylation of BxlA	58
Table 10 Specific activity of subsite +1 mutants of BxlA towards 2 mM <i>p</i> NPX	60
Table 11 Maximum transglycosylation yields with different acceptors by N313R in comparison with BxlA	62
Table 12 Specific activity of ManA, ManAS289W, ManC, and ManCW283S towards mannan polymers	65
Table 13 Hydrolysis kinetic parameters of ManA, ManAS289W, ManC, and ManCW283S towards mannoooligosaccharides (M4–M6)	66
Table 14 Product formation from 0.5 mM mannoooligosaccharides hydrolysed by ManA, ManAS289W, ManC, or ManCW283S	66
Table 15 <sup>1</sup> H and <sup>13</sup> C NMR data assignments for mannoooligosaccharides produced by enzymatic transglycosylation of ManC	72
Table 16 Specific activity of purified XlnA and XlnC towards xylans	75
Table 17 Maximum transglycosylation yields with different acceptors by XlnC	76
Table 18 Kinetic parameters of GH3 β-xylosidases towards <i>p</i> NPX	83
Table 19 Kinetic parameters of GH5 β-mannanases towards mannoooligosaccharides (M4–M6)	87
Table 20 Novel oligosaccharide production by transglycosylation	94

## 1. The overall objective of the thesis project

To produce novel prebiotic candidates or biologically active oligosaccharides by enzymes catalysed transglycosylation of starting materials that are related to or derived from industrial plant by-products.

## 2. Introduction

### 2.1 Cell wall polysaccharides as source of dietary fibres and prebiotics

#### 2.1.1 Plant cell wall composition

The most abundant and renewable source of biopolymers in nature is the plant cell wall composed mainly of polysaccharides, *i.e.* cellulose, hemicelluloses, and pectins, which together with a phenolic polymer lignin and proteins form a complex and rigid structure (Fig. 1) (Sticklen 2008; Taiz and Zeiger, 1991; Waldron and Faulds, 2007). Cellulose, the most abundant polysaccharide in nature, consists of  $\beta$ -1,4 linked D-glucose units forming a linear polymeric chain that forms a flat ribbon, held together by hydrogen bonds between glucose units to form a crystalline structure, which is very stable and insoluble providing the rigidity to the plant cell wall (Taiz and Zeiger, 1991).

Hemicelluloses are heteropolysaccharides containing a variety of sugar units. Hemicelluloses are classified according to the main sugar residues: xylose, mannose, glucose, galactose, and arabinose, forming the backbone of the polymer. The major hemicelluloses are usually divided into four general groups of structurally different polysaccharide backbones: xylans, mannans, xyloglucans, and mixed-linkage  $\beta$ -glucans (Ebringerová, 2006). Xylans ( $\beta$ -1,4 linked D-xylose) are abundant in secondary cell wall of cereals, grasses, and hardwood<sup>1</sup>. Mannans, in the forms of galactomannan ( $\beta$ -1,4 linked D-mannose) and glucomannan ( $\beta$ -1,4 linked D-glucose and D-mannose), are found mainly in seed endosperm of legumes and secondary cell walls of softwood, respectively. The structure and composition of xylans and mannans will be discussed in detail later in this chapter. Xyloglucans ( $\beta$ -1,4 linked D-glucose substituted with xylose) are the major building material of primary cell walls in higher plants. They play an important role in interlacing the cellulose microfibrils and have been strongly implicated in the regulation of cell wall extension (involving xyloglucan endotransglycosylase) (Vincken et al., 1997; Waldron and Faulds, 2007). The last main hemicelluloses are mixed-linkage  $\beta$ -(1,3-1,4)-glucans or cereal  $\beta$ -glucans, found in cereals and grasses and located in the subaleurone and endospermic cell wall, where they associate with cellulose microfibrils during cell growth. The less abundant hemicelluloses including callose ( $\beta$ -1,3-glucans), galactan ( $\beta$ -1,3 linked D-galactose), and arabinan ( $\alpha$ -1,5 linked L-arabinose), are also present in

---

<sup>1</sup> Simple plant classification (adapted from Graham, et al., 2006)

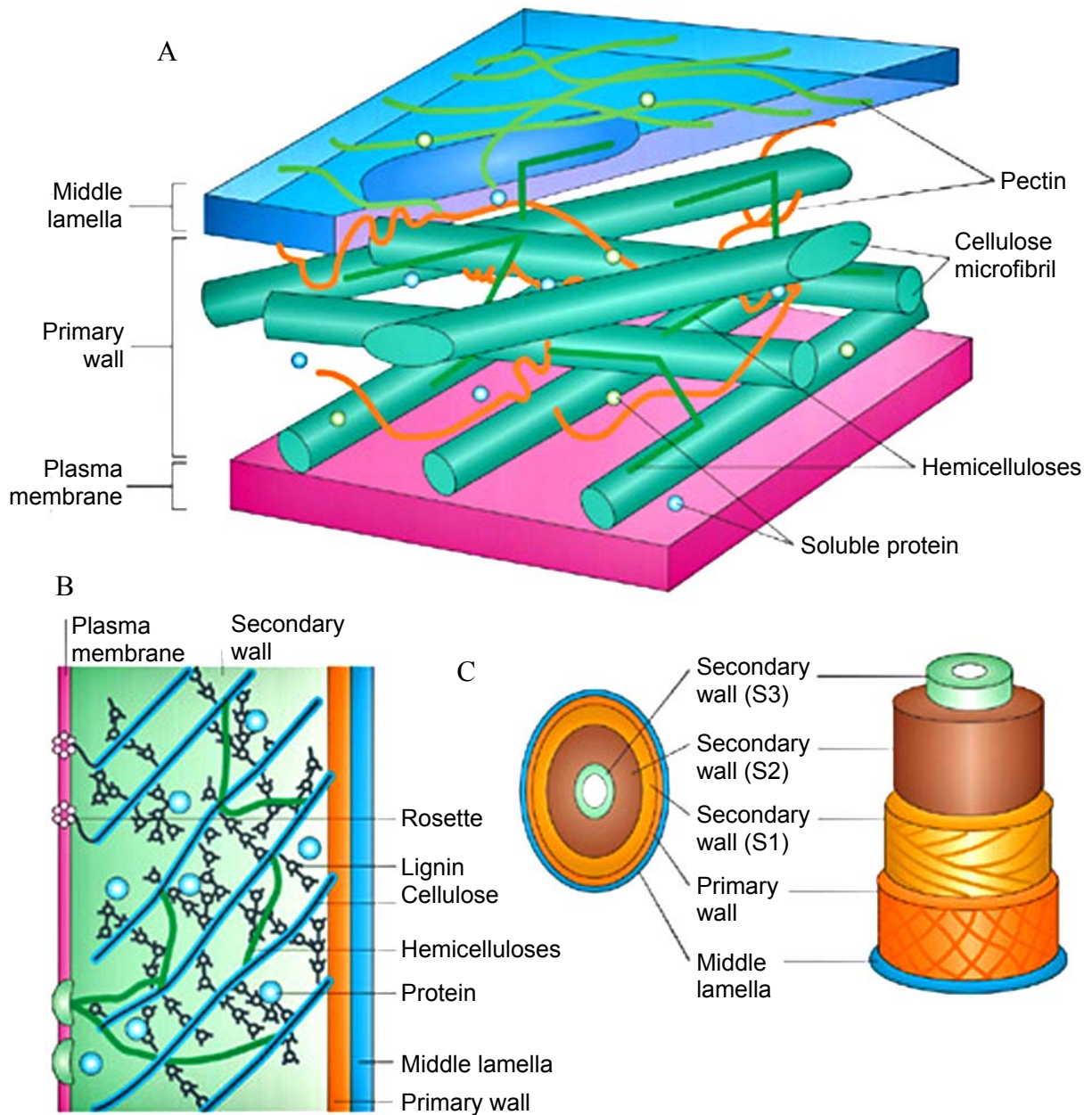
#### **Plant Kingdom:**

1. Non-vascular plants (Bryophytes: mosses, hornworts)
2. Vascular plants
  - a. Seedless plants (Pteridophytes: ferns)
  - b. Seed plants (Spermatophytes):
    - i. Softwood (Gymnosperms: pines and cycases)
    - ii. Hardwood (Angiospermes or flowering plants):
      - Grasses and cereal (Monocotyledons: wheat, barley, rice, and corn)
      - Fruits and vegetables (Dicotyledons: pea and apple)

particular tissues or plant species. The main chain sugars of hemicelluloses are modified by various side groups such as methylglucuronic acid, arabinose, galactose, and acetyl residues, making hemicelluloses branched and variable in structures (Aro, et al., 2005; Ebringerová, 2006; Waldron and Faulds, 2007).

Pectins are a family of complex polysaccharides comprised of polymers containing galacturonic acid and rhamnose as backbone with substitution of additional polymer chains rich in arabinose and galactose as well as several other sugars in less abundant quantities. Pectins are divided into two different types of regions: the smooth region, homogalacturonan that comprises a linear chain of  $\alpha$ -1,4 D-galacturonic acid residues, which can be methylated or acetylated, and the hairy region that consists of two different structures, D-xylose substituted galacturonan and rhamnogalacturonan to which long arabinan and galactan chains are linked *via* the rhamnose residues (for reviews of pectin structures see de Vries and Visser, 2003; Waldron and Faulds, 2007; Wong, 2008). Pectins and hemicelluloses are present in dicot primary walls in approximately equal amount, whereas hemicelluloses are more abundant in grasses and cereals (Table 1) (O'Neill and York, 2003).

Apart from the three major polysaccharides, the plant cell walls also contain lignin, a highly insoluble complex branched noncarbohydrate polymer of substituted phenylpropane units joined together by carbon-carbon and ether linkages forming an extensive cross-linked network within the cell wall and found in all vascular plants. It binds to cellulose fibers and hardens as well as strengthens the plant cell walls (Carpita and Gibeaut. 1993). The secondary walls of woody tissues and grasses are composed predominantly of cellulose, hemicellulose, and lignin (lignocelluloses). The cellulose fibrils are embedded in a network of hemicellulose and lignin (Fig. 1B). Cross-linking of these networks is believed to result in the elimination of water from the wall and the formation of a hydrophobic composite that limits accessibility of hydrolytic enzymes and is a major contributor to the structural characteristics of secondary walls (Carpita and Gibeaut. 1993). The function of plant cell wall is not only to protect the plant cells and maintain the cell shape, but also to play major roles in plant physiology involving with cell division, tissue extension, and support through ripening and senescence. The difference in molecular composition and structures of the plant cell wall depends on the cell, tissue, plant species, and the botanical origin. (Taiz and Zeiger, 1991; Waldron and Faulds, 2007).



Nature Reviews | Genetics

**Figure 1** Plant plasma membrane and cell-wall structure. A) Cell wall containing cellulose microfibrils, hemicellulose, pectin, lignin and soluble proteins. B) Cellulose synthase enzymes are in the form of rosette complexes, which float in the plasma membrane. C) Lignification occurs in the S1, S2, and S3 layers of the cell wall (O'Neill and York, 2003)

**Table 1** Polymeric components of typical dicot and grass primary and secondary cell walls

Polymer	Composition (% dry weight) <sup>1</sup>				Backbone	Side chain	
	Primary cell wall		Secondary cell wall			Carbohydrate	Non-carbohydrate
	Grass	Dicot	Grass	Dicot			
<b>Cellulose</b>	20–30	15–30	35–45	45–50	1,4 β-D-Glc	none	none
<b>Hemicellulose</b>							
Xyloglucan	1–5	20–25	Minor	Minor	1,4 β-D-Glc	α-D-Xyl, β-D-Gal, α-L-Fuc, β-L-Araf	acetyl esters
Mannan and Glucomannan	Minor	5–10	Minor	3–5	1,4 β-D-Man, 1,4 β-D-Man-1,4 β-D-Glc	α-D-Gal	acetyl
Xylan	20–40	5	40–50	20–30	1,4 β-D-Xyl	α-L-Araf, β-L-GlcA, 4-O-Me β-D-GlcA	acetyl, feruloyl and coumaryl esters
Mixed-linkage Glucan	10–30	Absent	Minor	Absent	1,3, 1,4 β-D-Glc		none detected
<b>Pectins</b> <sup>2</sup>	5	20–35	0.1	0.1	1,4 α-D-GalA, 1,4 α-D-GalA-1,2 α-L-Rha <sup>3</sup>	Not detected <sup>4,5,6</sup> β-D-Xyl, β-D-Apif <sup>7</sup>	methyl and acetyl esters and borate diester
<b>Phenolic esters</b>	1–5	Minor	0.5–1.5	Minor	feruloyl and coumaroyl esters (linked to xylans and pectins)		
<b>Lignin</b>	Minor	Minor	20	7–10	cross-linked racemic macromolecule (of the phenylpropanoids <i>p</i> -hydroxyphenyl, guaiacil, and syringal)		

Adapted from O'Neill and York, 2003; Vogel, 2008

<sup>1</sup> Approximate composition, may vary depending on the plant and tissue types

<sup>2</sup> Details of pectins see de Vries and Visser, 2003; Waldron and Faulds, 2007

<sup>3</sup> As rhamnogalacturonan I

<sup>4</sup> As rhomogalacturonan

<sup>5</sup> Side chain for rhamnogalacturonan I side chain: α-L-Araf, β-D-GalA, α-L-Fuc, β-D-GlcA, 4-O-Me β-D-GlcA

<sup>6</sup> Side chain for hamnogalacturonan II side chain: α-L-Rha, β-L-Rha, β-L-Araf, α-L-Ara, β-D-Gal, α-L-Acefa, β-D-Apif, α-L-Fuc, α-D-GalA, β-D-GalA, β-D-GlcA, 2-O-Me α-L-Fuc, β-D-Kdo, 2-O-Me α-D-Xyl, and β-D-Dha

<sup>7</sup> As xylogalacturonan and apiogalacturonan, respectively



## 2.1.2 Dietary fibres and prebiotics

As the most abundant biomass in nature, large amount of plant cell wall polysaccharide by-products or waste are generated through forestry and agricultural practices, pulp and paper industries, timber industries, and agro-industries as well as many food industries, *e.g.* sugar production, beer production, milling processing, and fruit and vegetable processing. The various biomasses are often disposed by burning or by landfill. However, the processed plant polysaccharide by-products can also be converted into different value-added bio-products including biofuel/bioethanol, organic chemicals, cheap energy sources for fermentation and improved animal feed and human nutrients (Howard et al., 2003). Among various opportunities, conversion of plant hydrolysate by-products into additives for functional foods gets increasing attention in recent years. Not only because this highly increases the by-product value, but also because these carbohydrates have functions involved with food physico-chemical properties (*e.g.* texture in canned vegetables, consistency in purees, and turbidity in fruit juice) (Fennema, 1996) and can improve human health, especially as dietary fibres (Kendall et al., 2010) and prebiotics (Mussatto and Mancilha, 2007; Swennen et al., 2006).

Codex Commission on Nutrition and Foods for Special Dietary Uses (CCNFSDU; 2008) defined dietary fibre as carbohydrate polymers with ten or more monomeric units, which are not hydrolysed by endogenous enzymes in the small intestine of human beings and belong to the following three categories: 1) edible carbohydrate polymers naturally occurring in food as consumed, 2) carbohydrate polymers, which have been obtained from food raw material by physical, enzymatic, or chemical means and which have been shown to have physiological benefit to health, and 3) synthetic carbohydrate polymers, which have been shown to exert physiological benefit to health (Cummings et al., 2009). However, United States Department of Agriculture defined dietary fiber<sup>2</sup> consisting of nondigestible carbohydrates and lignin intrinsic in plants (Institute of Medicine, 2005). Hence, plant cell wall polysaccharides and lignin are generally considered as dietary fibres, similarly to chitin and chitosan, inulin, fructans, and resistant starch, whereas nondigestible sugars and sugar alcohols are not considered as dietary fibres. According to the new definition by CCNFSDU, nondigestible oligosaccharides (degree of polymerization; DP 3–9) are no longer considered as dietary fibres. Dietary fibres have health beneficial effects including laxation (fecal bulking and softening), blood cholesterol attenuation, blood glucose attenuation, and metabolic responses to glycaemic carbohydrates (for more details in health benefit of dietary fibres see Kendall et al., 2010).

Regarding human health, certain components of plant cell wall polysaccharides also able to act as prebiotics. Prebiotics were first defined as a nondigestible food ingredient that beneficially affects the host by selectively stimulating the growth, activity, or both of one or a limited number of bacterial species (*i.e.* probiotics<sup>3</sup>) already resident in the colon (Gibson and Roberfroid, 1995). In 2007, Food and Agriculture Organization of the United Nations (FAO) defined prebiotic as a non-viable food component that confers a health benefit on the host associated with modulation of the microbiota. A food ingredient to be classified, as a prebiotic must fulfill the three following criteria: 1) neither be hydrolyzed nor absorbed in the upper part of the gastrointestinal tract; 2) be a selective substrate for one or a limited number of potentially beneficially bacteria in the

---

<sup>2</sup> Dietary fibres: naturally occurred in food, Functional fibres: added into food, including polydextrose and resistant dextrins, Total fibres: sum of both fibres (IOM, 2005)

<sup>3</sup> Probiotics are live microorganisms which when administered in adequate amount confer a health benefit on the host (FAO, 2001)

colon; and 3) alter the colonic microflora to a healthier composition (Collins and Gibson, 1999; Gibson and Roberfroid, 1995; for details on requirement see FAO, 2007). The combination of pro- and prebiotics (synbiotics) improves the survival of the probiotics and several health benefits are reported in the gastrointestinal tract and the immune system, such as prevention of diarrhea, inhibition of pathogen colonization, stimulation of the immune system, and prevention of colon cancer (for more details about pro-, pre- and synbiotics see Collins and Gibson, 1999; Davis and Milner, 2009; Steed et al., 2008; Swennen et al., 2006; Ziemer and Gibson 1998).

### 2.1.3 Oligosaccharides as prebiotics

The first generation of functional foods<sup>4</sup> was based on deliberate supplementation with vitamins and minerals. However, the last few years, the concept has moved towards and centered more on a positive effect on the gut microbiota in the form of pro- and prebiotics (Isolauri, et al., 2002; Swennen et al., 2006). Even though, the nondigestible oligosaccharides<sup>5</sup> (DP 3–9) are no longer considered as dietary fibres, according to the new definition by CCNFSDU, they still possess important food physico-chemical properties and some also act as prebiotics (Table 2) (for more details on the oligosaccharide functions as food additives see Nakakuki, 2002). The majority of reported prebiotic oligo- and polysaccharides focused on fructooligosaccharides, galactooligosaccharides, and inulin, which now have the status generally regarded as safe. The rest of the oligosaccharides have been studied to varying degrees *in vitro*, in animal feeding studies, but rarely in human feeding studies (Barreteau et al., 2006; FAO, 2007).

Plant hydrolysate by-products can be considered as a resource for development of novel prebiotic oligosaccharides, which may have better functionality than those currently found on the market. Enhanced persistence of the prebiotic effect along the colon, antipathogen effects, and more targeted prebiotics, might all be possible starting from plant cell wall polysaccharides. Traditionally, the nondigestible oligosaccharides can be obtained by direct extraction from natural sources, produced by chemical processes hydrolyzing polysaccharides, by enzymatic- or by a chemoenzymatic synthesis. At present advanced knowledge on plant cell wall polysaccharides and their degrading enzymes allows development of novel prebiotics, using two strategies i) controlled enzymatic hydrolysis of polysaccharides and ii) enzymatic synthesis of oligosaccharides (Barreteau et al., 2006; Rastall and Hotchkiss, 2003). The enzymatic depolymerization and modification of plant cell walls is a complex system requiring several enzymes for different type of polymers. Several of these enzymes, mainly from fungal sources, are industrially interesting and widely used in many biotechnological applications, particularly for production of second generation biofuel (for reviews on these enzymes see Aro et al., 2005; de Vries and Visser, 2001; Howard et al., 2003; Merino and Cherry, 2007; Shallom and Shoham, 2003). The following part will introduce the detailed structure and composition of xylans and mannans, the target substrates of the present study, as well as cellulose, a related substrate. The enzymes involved will be discussed further in chapter 4.

---

<sup>4</sup> Functional food is satisfactorily demonstrated to affect beneficially one or more target functions in the body, beyond adequate nutritional effects in a way relevant to either the state of well being and health and/or to reduction of the risk of a disease (Isolauri et al., 2002).

<sup>5</sup> Nondigestible oligosaccharides can be longer up to a degree of polymerization 60 (Swennen et al., 2006)

**Table 2** Typical oligosaccharides and polysaccharides with prebiotic effect

<b>Component</b>	<b>Origin/Manufacturing procedure</b>	<b>Backbone structure</b>	<b>Main linkage</b>	<b>Reference</b>
<i>Oligosaccharides</i>				
Fructooligosaccharide	Jerusalem artichokes, chicories, onions, garlic, leeks, asparaguses/Transglycosylation of sucrose	(Fru) <sub>n</sub> -Glc	β-(1,2)	Sabater-Molina et al., 2009
Galactooligosaccharide	Human milk/Enzymatic modification of lactose	(Gal) <sub>n</sub> -Glc	β-(1,4), β-(1,6)	Sako et al., 1999
Isomaltooligosaccharide	Honey/Enzymatic modification of starch	(Glc) <sub>n</sub>	α-(1,6)	Kuriki et al., 1993
Lactulose, lactitol, lactosucrose	Lactose derivatives	Gal-Fru, Gal-Glc-Fru	β-(1,4)	Sako et al., 1999
Mannooligosaccharide	Guar gum, locust bean gum, konjac/Mannan-containing hydrolysate	(Man) <sub>n</sub> , (Man-Glc) <sub>n</sub>	β-(1,4)	Asano et al., 2004
Soybean oligosaccharide	Soybean/Extract from soybean whey	(Gal) <sub>n</sub> -Glc-Fru	α-(1,6)	Espinosa-Martos and Ruperez, 2006
Xylooligosaccharide	Wheat bran, bamboo shoots/ Xylan-containing hydrolysate	(Xyl) <sub>n</sub>	β-(1,4)	Vázquez et al., 2000, Moure et al., 2006
<i>Polysaccharides</i>				
β-glucan	Bran of cereal grains, yeasts, mushrooms	(Glc) <sub>n</sub>	β-(1,4)	Snart et al., 2006
Inulin	As in fructooligosaccharides	(Fru) <sub>n</sub> -Glc	β-(1,2)	Van Loo et al., 1999
Pectin	Fruits and vegetables, legumes, potatoes	(GalA) <sub>n</sub> , (GalA-Rha) <sub>n</sub>	α-(1,4), α-(1,2)	Manderson et al., 2005
Resistant starch	Raw potatoes, green bananas, legumes/ Cooked and cooled starch (retrograded)	(Glc) <sub>n</sub>	α-(1,4)	Topping et al., 2003

Adapted from Mussatto and Mancilha, 2007; Sako et al., 1999; Van Loo et al., 1999.

## 2.1.4 Xylans and xylooligosaccharides

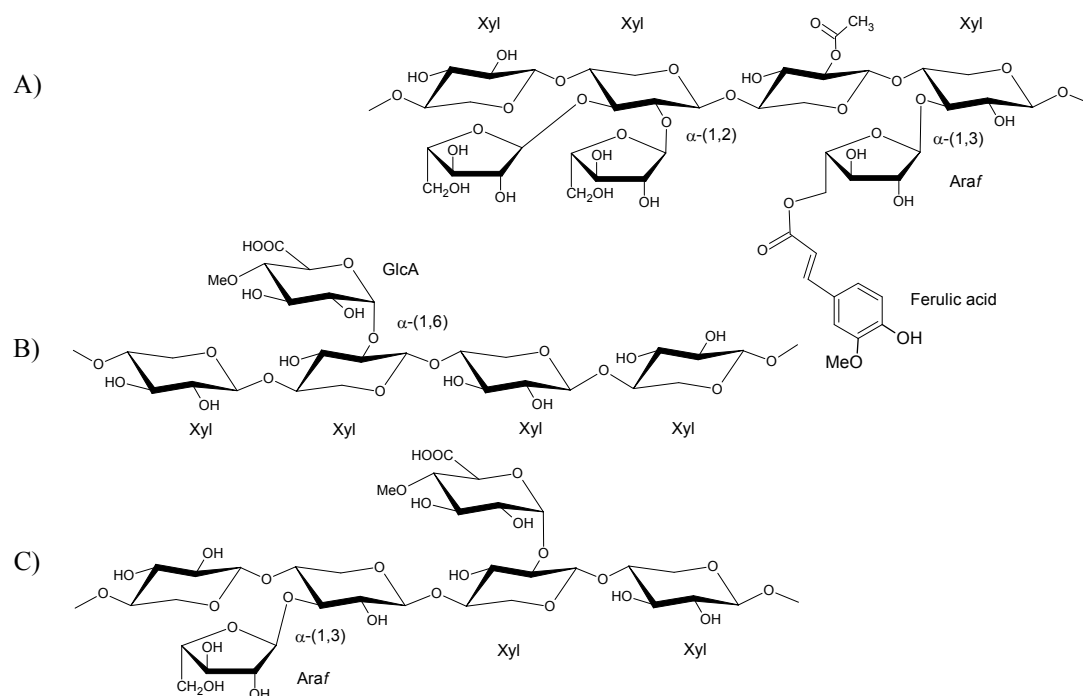
### 2.1.4.1 Structure and composition

Xylans are the predominant component of hemicelluloses and the second most abundant polysaccharide after cellulose, amounting to one third of all renewable organic compounds in nature (Collins et al., 2005). Xylans are found in high amounts in hardwoods, cereals, and grasses (up to 50% of the dry tissue in some cereals) and show large heterogeneity depending on the botanical source. Xylans have a backbone of 1,4-linked  $\beta$ -D-xylopyranosyl (Xyl) residues with different side chain substitutions such as  $\alpha$ -D-glucuronopyranosyl (GlcA), 4-*O*-methyl- $\alpha$ -D-glucuronopyranosyl (MeGlcA),  $\alpha$ -L-arabinofuranosyl (Araf), *O*-acetyl, feruloyl, or coumaroyl residues, and they can be grouped according to their side chains (de Vries and Visser, 2001; Ebringerová, 2006).

Cereal arabinoxylans (L-arabino-D-xylans) are found mostly in starchy endosperm (flour) and outer layer (bran) of cereals, grasses, and bamboo shoot. The side chain of cereal arabinoxylans comprises Araf substituted at position O2 and/or O3 (mono- or disubstitution) of xylose residues. A particular feature of arabinoxylan is the presence of phenolic acids (mainly ferulic and *p*-coumaric acids) esterified at position O5 of arabinose residues (Fig. 2A) (Ebringerová, 2006). Depending on the tissue, arabinoxylan can be extracted by water (water-extractable) or by alkaline solvent (water-unextractable). This behavior depends on the differences in chemical and/or physical interactions between arabinoxylans and other cell wall components and not on the content and distribution of arabinose side chains. Water-unextractable arabinoxylans are tightly embedded in the cell wall network by interactions with neighbour arabinoxylans through ferulic acid side chain cross-links, or other components such as protein, cellulose and lignin, while water extractable arabinoxylans are only loosely bound at the cell wall surface (Frederix et al., 2004 and Iiyama et al., 1994). These arabinoxylans have different physico-chemical and functional properties. Water-unextractable arabinoxylans are highly viscous and can be oxidatively cross-linked through ester-linked ferulic acids. Water-extractable arabinoxylans have a high water holding capacity. These properties strongly dictate the functional effects of arabinoxylans in biotechnological processes. In lignified tissues of grasses and cereals (straw, stems, stalks, outer pericarp of grains), the arabinoxylans are found in the form of (D-glucurono)-L-arabino-D-xylans (MeGlcA:Xyl:Araf 3–9:10:1–10) with partial *O*-acetylation (Ebringerová, 2006).

Glucuronoxylans (D-glucurono-D-xylans) are found in the secondary cell wall of dicots and hardwoods, containing single side chains of GlcA and/or its 4-methyl derivative (MeGlcA) attached at O2 position of xylose residues in the backbone (Fig. 2B) of a DP of 150–200. The xylan backbone can also be acetylated at O3 position and less at O2, the presence of these acetyl groups is responsible for partial solubility of xylan in water. In softwood, xylans, next to mannans constitute a minor hemicellulose in the form of arabinoglucuronoxylan ((L-arabino)-D-glucurono-D-xylans) (Fig. 2C), which resembles hardwood glucuronoxylans with addition of Araf residues attached at position O3 of the xylan backbone instead of acetylation. The degree of MeGlcA substitution in softwood is higher than in hardwood with less DP (70–130) of the backbone (Beg et al., 2001; Ebringerová, 2006). Apart from the three major xylans, homoxylans ( $\beta$ -1,3 and mixed  $\beta$ -1,3,  $\beta$ -1,4 linked xyloses) are present in some marine algae and seaweed, whereas the heteroxylans ( $\beta$ -1,4 linked xyloses heavily substituted by a variety of single and oligosaccharide side chains) are present in cereal bran, seeds, gum exudates, and various mucilages. These heteroxylans can form highly viscous solutions behaving similarly to plant exudate gums (Beg et al., 2001; Ebringerová, 2006).

The oligosaccharides of xylan, *i.e.* xylooligosaccharides, are produced from xylan containing lignocellulosic materials by chemical methods (such as, autohydrolysis with water, steam, or diluted mineral acids), enzymatic hydrolysis, or a combination of chemical and enzymatic treatments (Vazquez et al., 2000). The sources of xylans from plant cell wall by-products include barley hulls, brewery spent grains, corncobs, corn stover, rice hulls, wheat straw, and bamboo (Moure et al., 2006) (for reviews on manufacture of xylooligosaccharides see Moure et al., 2006; Vazquez et al., 2000).



**Figure 2** Structure of xylans. A) Arabinoxylan from cereals, arabinose residue can be esterified with ferulic and *p*-coumaric acid at position O5. B) Glucuronoxylan from hardwood. C) Arabinoglucuronoxylan from softwood (Ebringerová, 2006).

#### 2.1.4.2 Application of xylans and xylooligosaccharides

In the past decades, the main use of xylan-containing plant hydrolysate by-products for animal feed, fuel, compost, and soil conditioner (Howard et al., 2003). However, with the significant functions related to human and animal health benefits, more technical developments are focusing on production and application of xylooligosaccharides. The health-effects of xylooligosaccharides are mainly related to the gastrointestinal microflora proven a prebiotic effect. Moreover, xylans have ability to prevent gastrointestinal infections, to reduce duration of diarrhea, to maintain the fecal water content, and to enhance cecal epithelial cell proliferation. As food additive, xylooligosaccharides have acceptable odour, are low-caloric, and non-carcinogenic. They also show advantages over inulin and fructooligosaccharides in term of resistance to acids and heat allowing use in low-pH juices and carbonated drinks (Vazquez et al., 2000). In the last few years, xylooligosaccharides have shown a remarkable potential for practical utilization in several areas, including pharmaceuticals, feed formulations, and agricultural application, although the primary use is still in food-related applications.

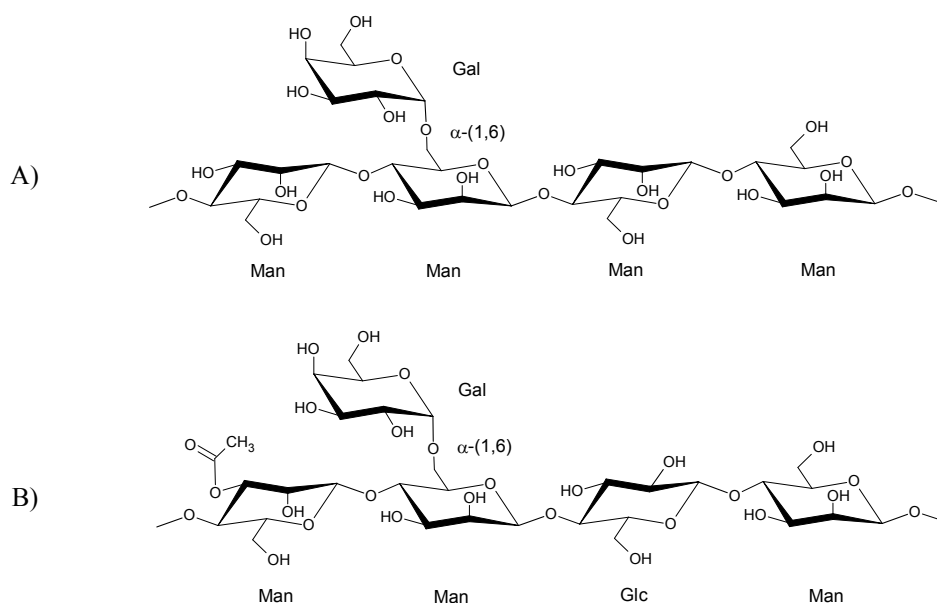
## 2.1.5 Mannans and manno oligosaccharides

### 2.1.5.1 Structure and composition

Whereas xylans are major constituents of hemicelluloses in grasses, cereals and hardwoods, the mannans (glucomannans or galactoglucomannans) are more abundant in softwoods. The mannans are classified into four groups: unsubstituted mannans, galactomannans, glucomannans, and galactoglucomannans, based on their backbone and galactose side chains (Moreira and Filho, 2008; Schröder et al., 2009).

Galactomannans (D-galacto-D-mannans) and unsubstituted mannans (D-mannans) consist of water-soluble 1,4 linked  $\beta$ -D-mannopyranosyl (Man) residues with side chains of single 1,6 linked  $\alpha$ -D-galactopyranosyl (Gal) groups attached along the chain of galactomannans (Fig. 3A). They are found predominantly in seed endosperms of legumes, such as guar, tara, and carobs (locust beans). In coffee seed arabinosyl residues are also present as side chains of mannans, attached at O6 position, whereas glucosyl residues are observed at reducing termini (Moreira and Filho, 2008). The galactose side chains are hydrophilic and increased degree of substitution result in higher solubility in water. The water retention makes galactomannans widely used as gelling agent or gum (Man:Gal of guar gum, tara gum, locust bean gum is approximately 2:1, 3:1, and 4:1, respectively). Pure mannans are defined to consist of at least 90% of linear mannan backbone with up to 10% substitution with single galactose residues.

Glucomannans (D-gluco-D-mannans) and galactoglucomannans ((D-galacto)-D-gluco-D-mannans) (Fig. 3B) are the major hemicelluloses in secondary cell walls of softwood. The backbone of glucomannans contain randomly arranged 1,4  $\beta$ -Man and 1,4 linked  $\beta$ -D-glucopyranosyl (Glc) residues with a DP greater than 200 in softwood. Like galactomannans, galactose side chains are present in glucomannans substituting at O6 of the mannan backbone with Man:Gal:Glc ratio of 3:1:0.1. Galactoglucomannans are glucomannans with higher substitution and Man:Gal:Glc ratio (3:1:1) and *O*-acetyl groups can substitute at O2 or O3 of the mannan backbone. Galactoglucomannan solubility in water is due to the content of galactose side chains that prevent the intermolecular interaction between backbone molecules and also act as flexible groups that can provide noncovalent connecting bridges with water and other cell wall polysaccharides (Dhawan and Kaur, 2007; Moreira and Filho, 2008; Waldron and Faulds, 2007).



**Figure 3** Structure of mannans. A) Galactomannan from seed endosperm of legumes. B) Galactoglucomannan from secondary cell wall of softwood (Ebringerová, 2006).

### 2.1.5.2 Application of mannans and manno oligosaccharides

Both galactomannans and glucomannans are widely used in the food industry. As mentioned above, galactomannans are used as gelling agent or gum. Guar and locust bean gums and their derivatives cause very high viscosity in aqueous solution. As food additives, these gums are widely used in gummy desserts, cream cheese, and salad dressing, as well as ice creams to improve texture and reduce melting. Galactomannans are, moreover, used also as thickening agent in the textile industry in dyebaths in printing and dyeing of fibers, fabrics, and carpets, particularly for sharp and bright patterns. Glucomannans are water-soluble dietary fibres, which are used widely in food industry as emulsifier and thickener. Konjac, as a rich source of glucomannans, that has been used in Asia for centuries in traditional foods, such as noodles, tofu and heat stable gelled food products. Glucomannans have been developed for biodegradable or soluble edible films as well as carrier material for drug delivery (Beneke et al., 2009; Mikkonen et al., 2010). Manno oligosaccharides are mainly produced by steam treatment at high pressure of natural sources such as coffee beans (Asano et al., 2003). They are used in food and feed industries to promote gastrointestinal health and performance (as both prebiotics and nondigestible oligosaccharides) with the extra effect to increase the amount of excreted fat and reduce the blood pressure (Asano et al., 2003; Hoshino-Takao et al., 2008; Kumao et al., 2006).

### 2.1.6 Cellulose and cello oligosaccharides

#### 2.1.6.1 Structure, composition, and applications

Cellulose, the major component of plant cell wall (40-45% of wood dry weight), consists of  $\beta$ -1,4 linked Glc units forming linear polymers. Each glucose unit rotates  $180^\circ$  from its neighbour and the chain contains 2000–8000 glucose units. In contrast to  $\alpha$ -1,4 glucosidically linked starch and glycogen, cellulose is a straight chain polymer with no coiling or branching. Approximately 150 (up to 250) glucan chains are condensed by

hydrogen bonds into a crystalline structure (Taiz and Zeiger, 1991; Waldron and Faulds, 2007). These crystalline structures are impermeable to water and their high strength provides strong resistance to chemical and enzymatic attack. In addition to this crystalline structure, cellulose contains noncrystalline (amorphous) regions within the microfibrils. The relative amount of crystalline and amorphous cellulose varies depending on the origin (de Vries and Visser, 2001; Waldron and Faulds, 2007). Cellooligosaccharides are short-chain cellulose with  $\beta$ -1,4 linked Glc units. These oligosaccharides are usually produced by controlled hydrolysis (partial hydrolysis) of cellulosic materials, which produces a mixture of cellooligosaccharides of different DP, that can be purified from the reaction mixture. Enzymatic hydrolysis of cellulose is an alternative option for cellooligosaccharide production (Akpinar and Penner, 2007). Cellooligosaccharides are commonly used as models for cellulose and in cellulase studies. Cellooligosaccharides are not hydrolyzed or absorbed by the human gastrointestinal tract (nondigestible oligosaccharides) and may have potential as prebiotics and/or non-caloric bulking agents in food products (Akpinar and Penner, 2007).

The main usage of cellulose is for pulp and paper as well as in textiles such as cotton, linen, and other plant fibres. Many products were generated from cellulose including cellophane, rayon, nitrocellulose, methylcellulose, and carboxymethyl cellulose. As a major source of plant cell wall polysaccharide, there are enormous developments focusing on bioconversion of industrial waste containing cellulose involving a combination of physico-chemical and enzymatic reactions (for reviews on bioethanol production see Duff and Murray; 1996, Howard et al., 2003; Merino and Cherry, 2007).

In recent years, production of oligosaccharides by chemical treatment has declined; instead, the manufacture is concentrated on enzymatic reactions, which are more suitable for preparation of food additives. Degradation and modification of plant cell wall polysaccharides require a number of different enzymes, which will be discussed further in the fourth chapter.

### **3. Enzyme discovery**

Enzymes are very specific catalysts of which only small quantities are required to perform the desired processes. The search for enzymes, which work optimally at specific conditions or discovery for novel enzymes, which provide valuable function, is challenging for many industries. Usually the enzyme screening and selection strategies are based on knowledge of the application and the physico-chemical conditions under which the enzyme must operate (Jones, 2007). The classical enzyme screening method is by screening natural isolates, based on culturing a broad diversity of plants, animals, or microorganisms, which in the latter case is the major source for industrial enzymes. The diversity should be reflected in taxonomy and phylogeny as well as physiological, biochemical and ecological variation. This classical screening has been successful including the discovery of extremophiles. However, random selection of microorganisms and screening of very large number of samples, which may also be redundant are the major problems of this approach.

By the aid of bioinformatics, molecular biology, and protein chemistry, several integrated approaches are developed involving molecular screening, genomic screening, environmental gene screening, and proteomics screening (Jones, 2007). Molecular screening, searching for homologous enzymes, takes the advantage of similarity of the genetic sequence, which can be used for prediction of protein function of the encoded enzyme. By using this information, a nucleotide primer probe can be designed and the



recombinant enzyme can be cloned and produced by using an appropriate expression system. The target homologous enzyme may have significantly different properties, enabling screening and cloning as an approach for improvement of pH or temperature stability. Several techniques, such as random shotgun (Staden, 1979) and nanopore technology (Kasianowicz et al., 1996), have been applied for the full genome sequencing. When the genome sequence is available, protein coding genes can be identified computationally either by *ab initio* gene prediction or by similarity search (Korf, 2004). The latter method is more reliable but depends on the availability of homologous genes. Even though molecular screening and genomic screening are very powerful techniques, they appear to be limited by the ability to grow target organisms and extract suitable DNA. Environmental gene screening applied several techniques to extract the DNA or RNA directly from microbial communities from the environment (Lorenz and Schleper, 2002). Although, extraction of the whole chromosomal DNA from the natural samples rarely gives a full-length genome, particularly in eukaryotes, isolation of total mRNA from a eukaryotic cell and cDNA library (Sambrook and Russell, 2001) can be done. The clones can then be screened for new enzyme-coding genes by techniques similar to those applied for classical screening without prior knowledge of homologous sequences. Proteomic screening approaches on the direct identification of protein function. Several separation and analysis techniques have been developed for the large-scale characterization of protein expression. Protein separation by two-dimensional gel electrophoresis (2DE) followed by identification by mass spectrometry is routinely utilized for this approach. An alternative to 2DE uses liquid chromatography after differential labeling of two protein mixtures with related isotope-coded affinity tags (Lai et al., 2004; Pohl, 2004; Uttamchandani et al., 2009). This approach can also make feasible to screen expression libraries of natural diversity (Jones, 2007).

#### **4. Hydrolysis, phosphorolysis, and transglycosylation mechanisms**

The enzymes catalyzing hydrolysis of glycosidic linkages are called glycoside hydrolases (glycosidases) and act as exo- (cleaving from an end, usually the non-reducing end) or endo- (cleaving interior bond in the substrate chain) glycosidases. These enzymes are involved in a series of important biological events from energy metabolism by degradation of carbohydrates to expression regulation as well as microbial defense mechanisms. Plant cell wall polysaccharides are chemically and physico-chemically highly complex and enzymatic biodegradation of plant cell walls requires a mixture of several endo- and exo-glycoside hydrolases as well as esterases, which are found in many microorganisms particularly in filamentous fungi (Collins et al., 2005; de Vries and Visser, 2001; Polizeli et al., 2005). Glycoside hydrolases are classified into EC 3.2.1.x<sup>6</sup> as enzymes acting on *O*- or *S*-glycosides, according to the International Union of Biochemistry and Molecular Biology (IUBMB) (Webb, 1992). The IUBMB enzyme nomenclature is based on the specificity of the enzyme and does not reflect its structural and mechanistic features. Different enzymes catalyzing the same reaction have the same EC number and certain enzymes catalyzing several reactions belong to more than one class. For structural and mechanistic enzymology, classification is made in the Carbohydrate-Active EnZymes Database<sup>7</sup> (CAZy; <http://www.cazy.org>; Cantarel et al.,

---

<sup>6</sup> The Enzyme Commission number (EC number) is a numerical classification scheme for enzymes (Webb 1992).

<sup>7</sup> CAZy database describes the families of structurally-related catalytic and carbohydrate-binding modules (or functional domains) of enzymes that degrade, modify, or create glycosidic bonds, which covers four of

2009). CAZy classification is based on amino acid sequence similarities. The sequence-based classification allows predicting the mechanism (retaining/inverting, see below), the active site residues and possible substrates as well as the function for newly sequenced enzymes for which function has not been biochemically demonstrated. CAZy classifies enzymes into glycoside hydrolase families (GH) clustered into clans reflecting conserved folding (Cantarel et al., 2009; Henrissat, 1991; Henrissat et al., 1995).

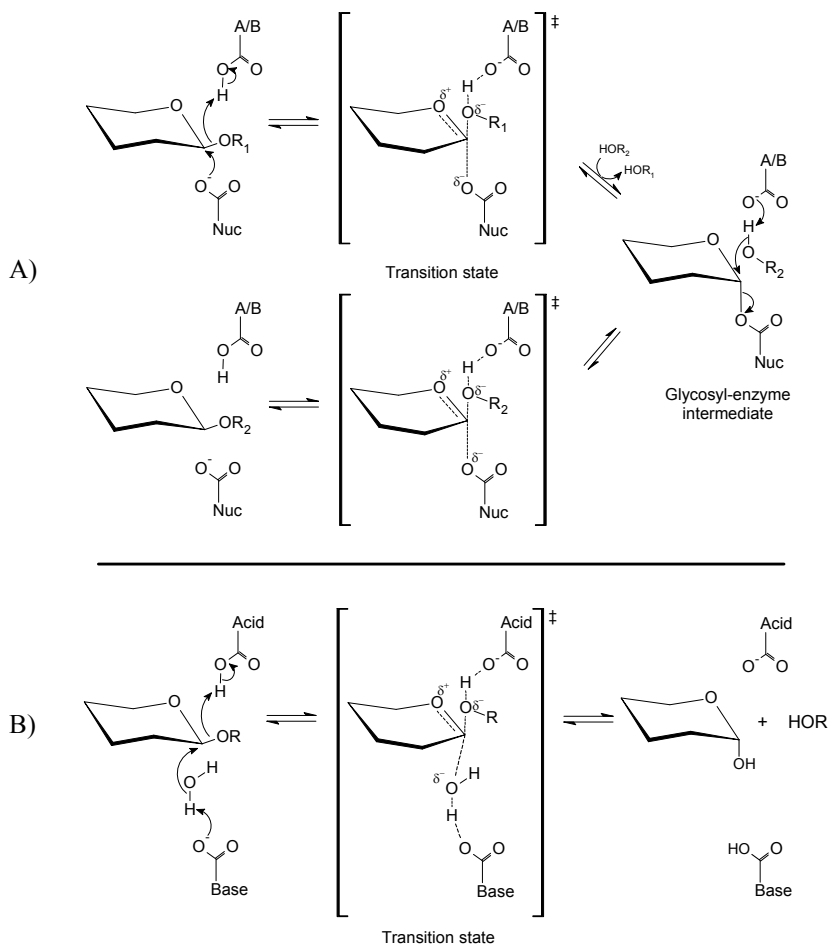
The hydrolytic mechanisms of glycoside hydrolases mostly follow general acid-base catalysis performed by two catalytic residues, typically glutamic acid or aspartic acid: an acid/base proton donor and a nucleophile (Jakeman and Withers, 2002). Depending on the spatial position of the catalytic residues, there are two reaction mechanisms resulting in either retention or inversion of the substrate anomeric configuration in the product. Retaining glycoside hydrolases, hydrolyze with net retention of configuration by a double-displacement or two-step mechanism involving a covalent glycosyl-enzyme intermediate with an oxocarbenium ion-like transition state (Fig. 4A). The two catalytic carboxylates positioned on opposite sides of the sugar ring plane catalyse this reaction by first (glycosylation step) protonating the glycosidic oxygen and, at the same time, the second carboxylic residue acts as nucleophile attacking the anomeric centre to cleave the glycosidic bond and form a glycosyl-enzyme intermediate (Fig. 4A). In the second step (deglycosylation), the glycosyl-enzyme intermediate is hydrolyzed by water. The first catalytic residue acts as a base to deprotonate the incoming nucleophile (a water molecule) as it attacks the intermediate resulting in release of product from the enzyme. Different from the retaining mechanism is found a one-step or single-displacement reaction with attack of water at the same time occurs in the inverting mechanism, which involves two catalytic carboxylates acting as acid and base catalysts resulting in product with opposite anomeric configuration of the substrate (Fig. 4B). The distance between the two carboxylates is approximately 5.5 Å for retaining and 6–11 Å for inverting glycoside hydrolases, since the inverting mechanism requires accommodating a water molecule next to the sugar rings to perform the hydrolysis (Davies and Henrissat, 1995; Henrissat and Davies, 1997).

Phosphorolysis is a reaction that cleaves a glycosidic bond by attack of a phosphate group, analogous to hydrolysis, however, phosphorolysis is reversible in contrast to hydrolysis (Berg et al., 2002). The enzymes catalyzing phosphorolysis are called phosphorylases. Several phosphorylases are reported to act on glycogen, sucrose, maltose, cellobiose, cellodextrin, trehalose, kojibiose, and starch (Cantarel et al., 2009). Phosphorylases are classified into EC 2.4.1.x as glycosyltransferases, which transfer hexose sugar to a phosphate acceptor, whereas they belong to four GH (GH13, GH65, GH94, and GH112) and three glycosyltransferase families (GT; GT3, GT4, and GT35).

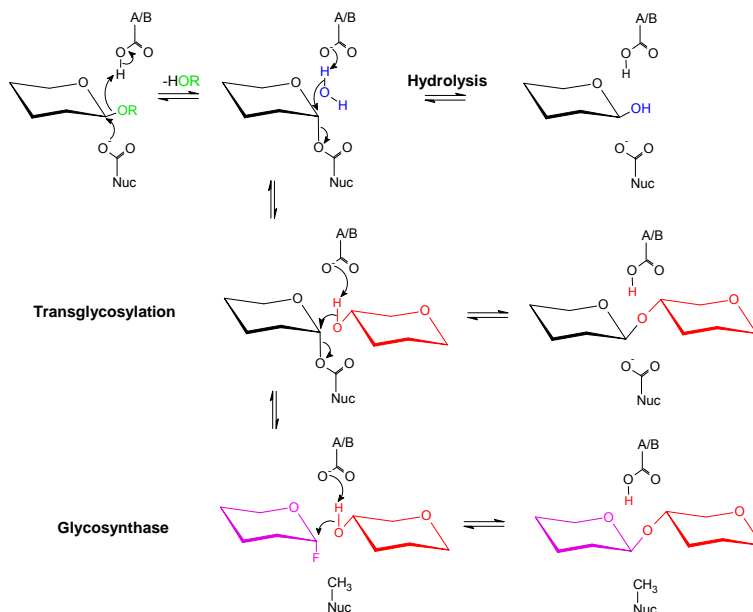
The transglycosylation (transfer reaction) applies the same mechanism as in hydrolysis. In the glycosylation step, the glycosyl residue, which attach to the enzyme forming a glycosyl-enzyme intermediate is referred to as donor (or glycosyl donor). However, in the deglycosylation step, instead of a water molecule, other molecules, such as carbohydrates, alcohols, or peptides can attack the intermediate resulting in release of a product with a new glycosidic linkage. The molecule, which accepts the glycoside donor, is referred to as acceptor. In other words, hydrolysis by glycoside hydrolases can be considered as transglycosylation reaction, in which the acceptor is the water molecule (Fig. 5) (Shaikh and Withers, 2008).

---

enzymes categories (glycoside hydrolases, glycosyltransferases, polysaccharide lyases, and carbohydrate esterases) and the carbohydrate-binding modules (Cantarel et al., 2009).



**Figure 4** Hydrolytic mechanisms of glycoside hydrolases. A) Retaining mechanism of  $\beta$ -glycosidase. B) Inverting mechanism of  $\beta$ -glycosidase (Davies and Henrissat, 1995). AB, catalytic acid/base residue; Nuc, catalytic nucleophile; R and R<sub>1</sub>, aglycone side of the substrate; R<sub>2</sub>, hydrogen in water (hydrolysis) or other molecule with hydroxyl group (transglycosylation).



**Figure 5** Hydrolysis, transglycosylation, and glycosynthase mechanisms of glycoside hydrolase (Shaikh and Withers, 2008). Nuc, catalytic nucleophile; A/B, catalytic acid base; F, fluoride; R, aglycone side of the substrate; acceptor molecule is in red; glycosyl fluoride is in magenta.

## 4.1 Enzyme catalysed transglycosylation

In general, the glycosylation is considered to be an important method for structural modification of carbohydrate-containing compounds with useful biological activities. The glycosidic linkage, joining carbohydrate to another carbohydrate or other molecule, is one of the most important chemical characteristics of a saccharide. The synthesis of a glycosidic linkage can be performed by either chemical or enzymatic reactions. Chemical synthesis of the glycosidic linkage usually utilises a sugar unit as precursor of an intermediate oxacarbenium ion that has significant positive charge at the anomeric carbon atom. Sugar units have more than one possible site of reaction and each of these sites often shows very similar reactivity, resulting in several positions where a linkage can be introduced. Thus, masking by protecting groups is essential to direct coupling to the right position. For this reason, protection and deprotection of functional groups are used extensively for the chemical synthesis of carbohydrates. In addition, a difficulty in synthesis of oligosaccharides is to ensure the correct stereochemistry of the glycosidic linkage formed (Stick, 2001). The enzymatic glycosylation has several advantages over the chemical synthesis since it is usually more stereo- and regioselective and can be performed under mild reaction conditions without additional steps for protection and deprotection. Moreover, enzymatic glycosylation is more suitable for the modification of biologically active substances particularly in the food or cosmetic fields, where in general harsh conditions or use of toxic catalysts are undesirable (Murata and Usui, 2006).

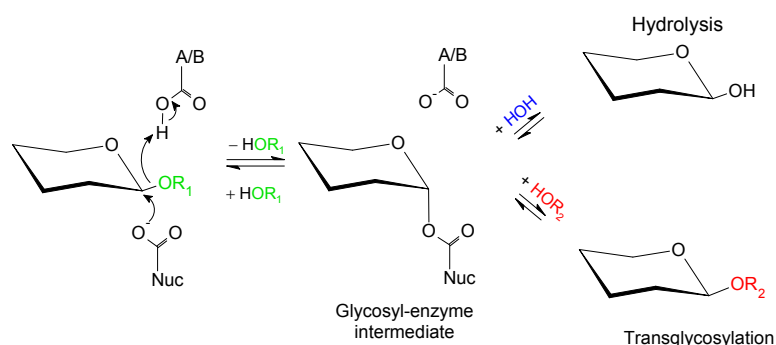
The enzymes responsible for the synthesis of glycosidic linkage have been recognised as glycosyltransferases, which transfer sugar moieties from activated donor molecules to specific acceptors, forming a specific glycosidic bond *in vivo* (Qian et al., 2002; Sinnott, 1990). Together with glycosidases, they form the major catalytic machinery for synthesis and degradation of glycosidic bonds. The main advantage of using glycosyltransferases is the high efficiency and high regio- and stereoselectivity exhibited by the enzymes; however, the disadvantage is the inaccessibility of the transferases and the high-cost and instability of the activated nucleoside phosphate donors. Even though recombinant glycosyltransferases recently became available and the concept of using nucleotide sugar regeneration has been pursued, the use of these enzymes is limited (Murata and Usui, 2006).

Glycoside hydrolases, in contrast, hydrolyse glycosidic linkages and transglycosylation is commonly observed as a side reaction, which sometimes provides a possibility to achieve efficient synthesis of carbohydrates. Although, the regioselectivity of glycosidases is rarely absolute and their yields are lower than those of glycosyltransferases, their glycosyl donor substrates are relatively inexpensive, chemically simple, and readily available. Both endo- and exo-glycosidases can perform transglycosylation. Most glycoside hydrolases used for oligosaccharide synthesis are exo-glycosidases, which usually transfer a non-reducing terminal monosaccharide unit from a donor to a variety of acceptors, while endo-glycosidases are possibly capable of transferring longer oligosaccharides or a whole carbohydrate block to a new acceptor. By this approach, new bioactive saccharides can be created, including neoglycoproteins and neoglycolipids (Crout and Vic, 1998; Murata and Usui, 2006). Glycoside hydrolase equilibrium is shifted towards hydrolysis of the substrates; this, however, obviously represents a source of degradation of the transglycosylation products. Hence, to achieve oligosaccharide synthesis, the transglycosylation reaction must be faster than hydrolysis and the rate of hydrolysis of the transglycosylation products should be slow. Furthermore, to improve the transglycosylation ability of glycoside hydrolases, several techniques have been developed. The three major strategies in enzymatic synthesis of oligosaccharides are

briefly described below.

#### 4.1.1 Reverse hydrolysis

Even though reactions catalysed by GHs are by far in the direction of hydrolysis for majority of the enzymes, the reverse reaction is possible depending on individual enzyme characteristics in an equilibrium-controlled condition to concur the thermodynamic barrier of the enzymes. Instead of breaking the glycosidic linkage by reaction with water, the reverse hydrolysis links two saccharide molecules by transfer of donor, after departure of the leaving group, to the acceptor molecule and release of a water molecule (Fig. 6). A shift of the thermodynamic equilibrium towards synthesis can be achieved by increasing the concentration of sugar donor substrate and acceptor (typically alcohols, or monosaccharides) together with reaction at medium high temperature (usually above 50°C) and high concentration of co-solvents (80–90%), if the acceptor is not alcohol, to reduce water activity (Plou et al., 2007). The reverse hydrolysis reaction is simple from a mechanistic point of view and moderate yield can be obtained particularly in synthesis of alkyl-saccharides. However, this same level of efficiency is not typical for oligosaccharide synthesis, because of a number of shortcomings, including enzyme instability at high temperature and solubility of saccharides in organic solvents, as well as separation of products from excessive amount of substrate (Crout and Vic, 1998; Murata and Usui, 2006; Stick, 2001; for examples of reverse hydrolysis see Ajisaka et al., 1987; Drouet et al., 1994; Singh et al., 2000).

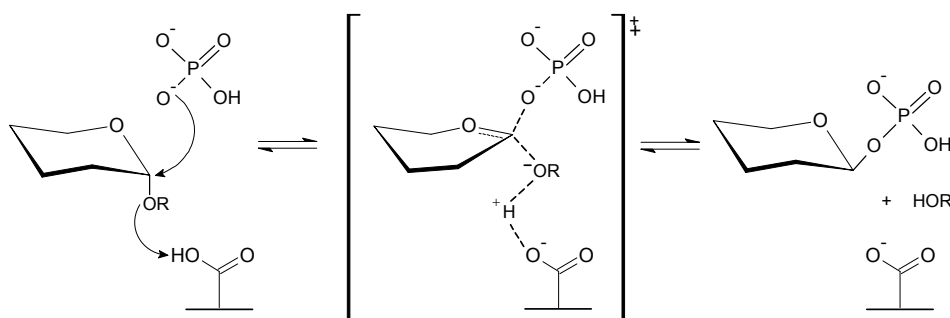


**Figure 6** Schematic reaction mechanism of reverse hydrolysis and transglycosylation (adapted from Shaikh and Withers, 2008). Nuc, catalytic nucleophile; A/B, catalytic acid base; R<sub>1</sub>, aglycone side of the substrate; R<sub>2</sub>, other saccharide with hydroxyl group marked in red.

#### 4.1.2 Reverse phosphorolysis

In a reversible reaction of phosphorolysis, the substrate of the phosphorylase can be synthesised, this is referred to as reverse phosphorolysis. This approach was demonstrated by using maltose phosphorylase from *Lactobacillus brevis* (Tsumuraya et al., 1990). Maltose phosphorylase promotes the cleavage of maltose and releases β-glucose 1-phosphate (maltose + phosphate = D-glucose + β-D-glucose 1-phosphate) (Wood and Rainbow, 1961). By reverse phosphorolysis, β-D-glucosyl fluoride was used instead of β-D-glucose 1-phosphate as donor and D-glucose was used as acceptor, when incubating with maltose phosphorylase, maltose and HF were detected at a rapid rate as products of reverse phosphorolysis (β-D-glucosyl fluoride + D-glucose = maltose + HF) (Tsumuraya

et al., 1990). Furthermore, this approach was developed for production of novel oligosaccharides using cellobiose phosphorylase from *Cellvibrio gilvus* (Percy et al., 1998a, 1998b), cellodextrin phosphorylase from *Clostridium thermocellum* YM4 (Shintate et al., 2003), and maltose phosphorylase from *L. acidophilus* NCFM (Nakai et al., 2009). The obvious advantage with this approach is a very efficient reaction and high regioselectivity similar to the glycosyl transferase reactions (Nakai et al., 2009; Shintate et al., 2003). Major limitations of the reverse phosphorolysis are the limited number of specificities found for phosphorylases and the amounts and price of 1-phosphate substrate required.



**Figure 7** Schematic reaction mechanism of reversible phosphorolysis (Nakai et al., 2009). R, a carbohydrate residue.

#### 4.1.3 Glycosynthase reaction

A very efficient approach for chemoenzymatic glycoside synthesis came with the aid of protein engineering, and is referred to as the glycosynthase reaction. Glycosynthases are glycoside hydrolase mutants in which the catalytic nucleophile was changed to an amino acid residue unable to act as a catalytic group by site-directed mutagenesis. These mutants essentially lost the hydrolytic activity and, instead catalyse the formation of glycosidic linkages when presented with a glycosyl fluoride with the opposite anomeric configuration of the normal substrate (Fig. 5). The first glycosynthase work was made with a retaining exo-glycosidase,  $\beta$ -glucosidase from *Agrobacterium* sp., in which the catalytic nucleophile glutamic acid was mutated to alanine that catalysed the formation of  $\beta$ -1,4 linked glycosides of glucose and galactose from  $\alpha$ -glucosyl and  $\alpha$ -galactosyl fluorides as donors (Mackenzie et al., 1998; Withers et al., 1992). The glycosynthase has been developed for several enzymes and both exo- and endo-retaining glycosidases have produced different oligosaccharides containing glucose (Faijes et al., 2003; Mackenzie et al., 1998), galactose (Jakeman and Withers, 2002; Mackenzie et al., 1998), mannose (Jahn et al., 2003a), xylose (Ben-David et al., 2007; Kim et al., 2006; Sugimura et al., 2006), fucose (Wang, 2009), and glucuronic acid (Wilkinson et al., 2008) by mutating the catalytic nucleophile (aspartic or glutamic acid) to a small non-nucleophilic amino acid (such as alanine, glycine, cysteine, or serine). A more recent approach uses directed evolution to screen for amino acid substitutions that enhance glycosynthase activity (Mayer et al., 2000, 2001; Shaikh and Withers, 2008). Furthermore, the first inverting glycosynthase was pursued using aspartic acid to cysteine mutant of reducing-end xylose-releasing exo-oligoxyranase from *Bacillus halodurans* C-125 (Honda and Kitaoka, 2006). Glycosynthases are not only useful for oligosaccharide synthesis, but also for thioglycoside (*S*-glycosidic linkage) synthesis. This has been demonstrated by the use of retaining glycosidases that lack the catalytic acid/base amino

acid residue (thioglycoligases), which requires strong nucleophiles as acceptors that do not need general base catalysis. The two first thioglycoligases were glutamic acid to alanine mutants of  $\beta$ -glucosidase from *Agrobacterium* sp. and  $\beta$ -mannosidase from *Cellulomonas fimi* (Jahn et al., 2003b). Glycosynthases have been useful for the preparation of oligosaccharides; however, their use has certain limitations, for instance, the success rate to convert a given glycosidase into a glycosynthase is rather low and the availability and stability of specific glycosyl fluoride donors is for some cases problematical (Williams and Withers, 2000).

## **4.2 Xylanases and xylosidases**

### **4.2.1 Enzymatic hydrolysis of xylans**

The structures of xylans are heterogeneous and complex (see 2.1.4.1), hence a variety of glycoside hydrolases and esterases are required for their breakdown. These enzymes or enzyme systems are called xylan degrading or xylanolytic enzymes (Beg et al., 2001; Pastor et al., 2007). Xylanolytic enzymes are produced by a variety of microorganisms, mainly filamentous fungi as well as certain rumen microbiota, and they are widely used in industries, particularly pulp and paper as well as in animal feed, manufacture of bread, food and beverage, textiles, ethanol, and xylitol production (Beg et al., 2001). Since several xylan containing plant hydrolysate by-products are applied for second generation biofuels, xylanolytic enzymes are developed for complete hydrolysis of such materials.

Xylanolytic enzymes can be classified into two main groups: the xylan backbone degrading enzymes, *i.e.* endo- $\beta$ -1,4-xylanases and exo- $\beta$ -1,4-xylosidases, and the side chain degrading enzymes, *i.e.*  $\alpha$ -L-arabinofuranosidases,  $\alpha$ -D-glucuronosidases, acetyl xylan esterases, ferulic acid esterases, and *p*-coumaric acid esterases (Fig. 8 and table 3). Xylanases are responsible for hydrolysis of the xylan backbone and release shorter polysaccharides or xylooligosaccharides, while  $\beta$ -xylosidases are responsible for hydrolysis of unbranched xylooligosaccharides and thus contribute to prevent product inhibition of xylanases. The synergy between xylanases and xylosidases as well as the side chain degrading enzymes and esterases are required for complete xylan degradation (Beg et al., 2001; de Vries and Visser, 2001; Pastor et al., 2007).

**Table 3** Hemicellulolytic (and certain cellulolytic) enzymes, their classification, and current crystallographic data (adapted and updated from Shallom and Shoham, 2003)

Enzymes	Substrates	EC	CAZy		Catalytic mechanism <sup>1</sup>		Fold	3D structure <sup>2</sup>
			family	Clan	Re:	In:		
Endo- $\beta$ -1,4-xylanase	$\beta$ -1,4-xylan	3.2.1.8	GH5	A	Re:	E/E	$(\beta/\alpha)_8$	3GTN, 1NOF
			GH8	M	In:	D/E	$(\alpha/\alpha)_6$	1H12
			GH10	A	Re:	E/E	$(\beta/\alpha)_8$	1TA3, 1FXM, 1EXP...
			GH11	C	Re:	E/E	$\beta$ -jelly roll	1XYN, 1ENX, 1TE1...
			GH43	F	In:	D/E,D	5-fold $\beta$ -propeller	1UX7, 1W0N
Exo- $\beta$ -1,4-xylosidase	$\beta$ -1,4-xylooligomers, xylobiose	3.2.1.37	GH3	–	Re:	D/E	–	(1EX1), (3F93), (2X40)
			GH30	A	Re:	E/E	$(\beta/\alpha)_8$	(1OGS)
			GH39	A	Re:	E/E	$(\beta/\alpha)_8$	1W91, 1PX8
			GH43	F	In:	D/E,D	5-fold $\beta$ -propeller	1YRZ, 2EXH, 3C2U <sup>3</sup> ...
			GH52	–	Re:	E/D	–	Cryst.
$\alpha$ -L-Arabinofuranosidase	$\alpha$ -Arabinofuranosyl (1,2) or (1,3) xylooligomers,	3.2.1.55	GH3	–	Re:	D/E	–	(1EX1), (3F93), (2X40)
			GH43	F	In:	D/E,D	5-fold $\beta$ -propeller	3C7E, 3C2U <sup>3</sup>
			GH51	A	Re:	E/E	$(\beta/\alpha)_8$	2C7F, 1PZ2, 2VRK
			GH54	–	Re:	–	–	1WD3
			GH62	F	–	–	–	Cryst.
Endo- $\alpha$ -1,5-arabinanase	$\alpha$ -1,5-arabinan	3.2.1.99	GH43	F	In:	D/E,D	5-fold $\beta$ -propeller	1UV4, 3CU9, 1GYD...
$\alpha$ -Glucuronidase	(4- <i>O</i> -methyl)- $\alpha$ -glucuronic acid (1,2) xylooligomers	3.2.1.131	GH67	–	In:	–/E	$(\beta/\alpha)_8$	1K9D, 1K9E, 1GQI
			GH115	–	–	–	–	–
Endo- $\beta$ -1,4-mannanase	$\beta$ -1,4-mannan	3.2.1.78	GH5	A	Re:	E/E	$(\beta/\alpha)_8$	2MAN, 1VJZ, 1QNO...
			GH26	A	Re:	E/E	$(\beta/\alpha)_8$	2WHK, 2QHA, 1GVY...
			GH113	A	Re:	E/E	$(\beta/\alpha)_8$	3CIV
Exo- $\beta$ -1,4-mannosidase	$\beta$ -1,4-mannooligomers, mannobiose	3.2.1.25	GH1	A	Re:	E/E	$(\beta/\alpha)_8$	(1QOX)
			GH2	A	Re:	E/E	$(\beta/\alpha)_8$	2JE8
			GH5	A	Re:	E/E	$(\beta/\alpha)_8$	1UUQ
$\alpha$ -galactosidase	$\alpha$ -galactopyranosyl (1,6) mannooligomers	3.2.1.22	GH4	–	Re:	–	–	1S6Y
			GH27	D	Re:	D/D	$(\beta/\alpha)_8$	1R46, 1SZN, 3A5V...
			GH36	D	Re:	D/D	$(\beta/\alpha)_8$	1ZY9
			GH57	–	Re:	E/–	$(\beta/\alpha)_7$	(2B5D)
			GH97	–	In:	E/E	$(\beta/\alpha)_8$	3A24



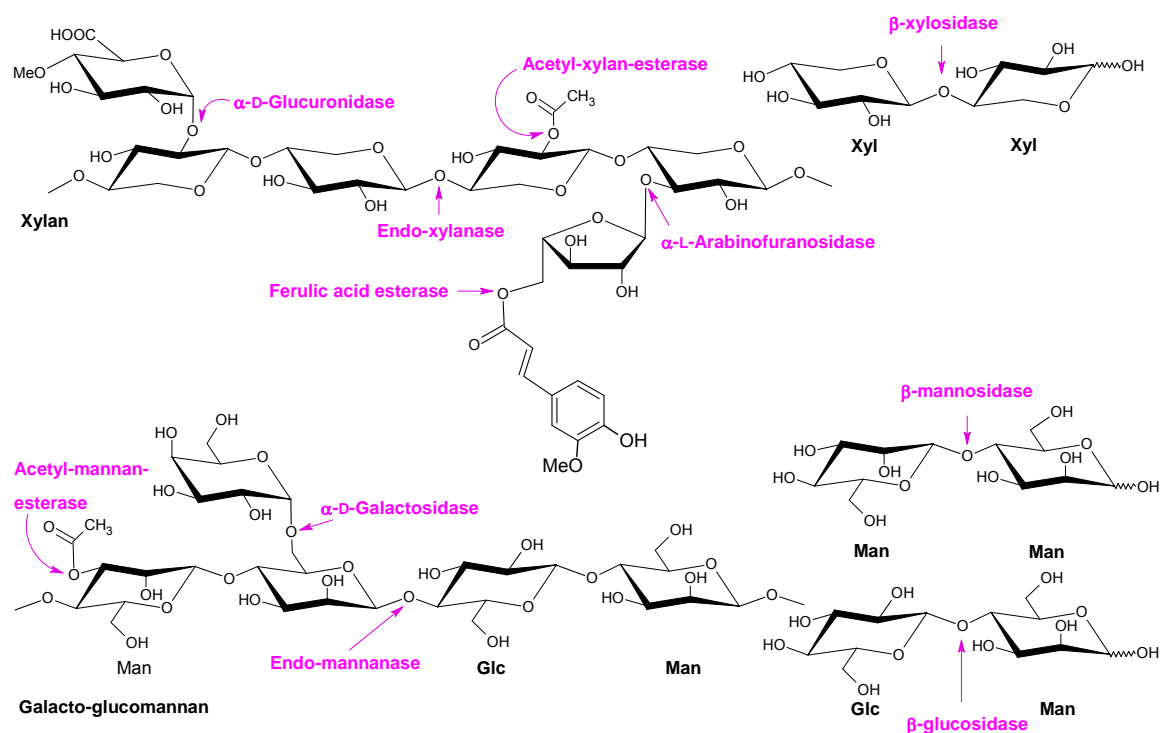
**Table 3** (continued)

Enzymes	Substrates	EC	CAZy		Catalytic		Fold	3D structure <sup>2</sup>
			family	Clan	mechanism <sup>1</sup>			
$\alpha$ -galactosidase (cont.)			GH97	–	Re:	D/E	( $\beta/\alpha$ ) <sub>8</sub>	
			GH110	–	In:	–	–	–
$\beta$ -glucosidase	$\beta$ -glucopyranosyl (1,4) mannopyranose	3.2.1.21	GH1	A	Re:	E/E	( $\beta/\alpha$ ) <sub>8</sub>	1BGA, 1GNX, 1QOX...
			GH3	–	Re:	D/E	–	2X40
			GH9	–	In:	D/E	( $\alpha/\alpha$ ) <sub>6</sub>	(1G87)
			GH30	A	Re:	E/E	( $\beta/\alpha$ ) <sub>8</sub>	(1OGS)
Endo-galactanase	$\beta$ -1,4-galactan	3.2.1.89	GH53	A	Re:	E/E	( $\beta/\alpha$ ) <sub>8</sub>	1R8L, 1FHL, 1HJQ...
Acetyl xylan esterase	2- or 3- <i>O</i> -acetyl xylan	3.1.1.72	CE1	–	–	–	( $\alpha/\beta/\alpha$ ) sandwich	(1JJF)
			CE2	–	–	–	( $\alpha/\beta/\alpha$ ) sandwich	2WAA, 2W9X, 2WAB
			CE3	–	–	–	( $\alpha/\beta/\alpha$ ) sandwich	2VPT
			CE4	–	–	–	( $\beta/\alpha$ ) <sub>7</sub> barrel	1HEH, 2C71, 2CC0
			CE5	–	–	–	( $\alpha/\beta/\alpha$ ) sandwich	1QOZ, 1G66
			CE6	–	–	–	( $\alpha/\beta/\alpha$ ) sandwich	1ZMB, 2AEA
			CE7	–	–	–	( $\alpha/\beta/\alpha$ ) sandwich	3FVR, 1L7A, 3FCY...
			CE12	–	–	–	( $\alpha/\beta/\alpha$ ) sandwich	(2W1W)
Acetyl mannan esterase	2- or 3- <i>O</i> -acetyl mannan	3.1.1.6	CE16	–	–	–	–	–
Feruloyl & <i>p</i> -coumaroyl esterases	5- <i>O</i> -feruloyl or <i>p</i> -coumaroyl arabinoxylan	3.1.1.73	CE1	–	–	–	( $\alpha/\beta/\alpha$ ) sandwich	1JJf, 1GKK
Endo- $\beta$ -1,4-glucanase	Cellulose	3.2.1.4	GH5, 6, 7, 8, 9, 12, 44, 45, 48, 51, 61, and 74					
Cellobiohydrolase	Cellulose (release cellobiose)	3.2.1.91	GH5, 6, 9, 48					
Exo- $\beta$ -1,4-glucanase	$\beta$ -1,4-cellooligomers	3.2.1.74	GH1, 3					

<sup>1</sup> Re: retaining, In: inverting, X/X: nucleophile/(acid/base) residues for retaining enzyme or general base/general acid for inverting enzyme, D: aspartic acid, E: glutamic acid.

<sup>2</sup> PDB code are reported, Cryst.: crystallization reported, ...: more structures have been reported, The PDB entries in parenthesis are from the relevant family but with different substrate specificity.

<sup>3</sup> Bifunctional enzyme



**Figure 8** Xylanolytic (upper) and mannan degrading enzymes (lower) with their sites of attack on xylan and mannan substrates (Shallom and Shoham, 2003).

#### 4.2.2 GH10 and GH11 xylanases

Xylanases (endo-β-1,4-xylanases, EC 3.2.1.8) catalyse the hydrolysis of the xylan backbone, yielding shorter polymer or xylooligosaccharides. In addition, they are active on xylooligosaccharides of DP greater than two, showing increase in affinity for xylooligomers of increasing length (Pastor et al., 2007). Xylanases of fungal origin are effective in the acidic pH range 4–6, while the xylanases from actinomycetes and bacteria are effective in a broader pH range 5–9. The optimum temperature for xylanases action ranges between 35–60°C. Several extremophilic xylanases are discovered which are still active up to 100°C or pH 2–11 (Beg et al., 2001). Xylanases can be classified roughly into two groups: low molecular weight (<30 kDa) with basic pI and high molecular weight (>30 kDa) with acidic pI (Wong et al., 1988). Xylanases are classified into five glycoside hydrolase families: 5, 7, 10, 11, and 43 according to the CAZy classification. GH5, GH7, GH10, and GH11 hydrolyse by a retaining mechanism with glutamic acids as both catalytic nucleophile and acid/base, whereas GH43 catalyses hydrolysis by an inverting mechanism with aspartic acid as general base and glutamic or aspartic acid as general acid (table 3) depend on the enzymes. In the present study, we have worked with GH10 and GH11 xylanases. These two families include xylanases of high molecular weight/low pI and low molecular weight/high pI, respectively (Pastor et al., 2007).

Kinetic and structural analysis by GH10 xylanases revealed that their active sites have four to five subsites (–3 or –2 to +2) (Biely et al., 1997; Charnock et al., 1998; Pell et al., 2004; Schmidt et al., 1999). The glycone (or donor) binding subsites are numbered negatively (–1, –2, etc) from the scissile bond towards the non-reducing end of the bound

substrate. The aglycone (or acceptor) binding subsites, heading away from the scissile bond towards the reducing end, are denoted by positive numbers (+1, +2, etc). The cleavage by definition takes place between subsites -1 and +1 (Biely et al., 1981; Davies et al., 1997). GH11 xylanases have up to three (-) subsites and three (+) subsites (Payan et al., 2004; Vardakou et al., 2008). On the hydrolytic activity, GH11 xylanases prefer linear xylans and unsubstituted regions of arabinoxylans to the decorated ones, whereas GH10 xylanases can cleave within decorated region, with the presence of MeGlcA, acetyl, or  $\alpha$ -Araf substitution. In general, GH10 xylanases exhibit wider catalytic versatility or lower substrate specificity than GH11 xylanases and can also exhibit low activity towards cellulosic substrates (Biely et al., 1997; Kolenová et al., 2006; Pastor et al., 2007). This reflects the shape of the active sites. GH10 xylanases are  $(\beta/\alpha)_8$  barrel or salad bowl-like shaped catalytic domains, with the larger radius on the top of the bowl where a shallow groove active site is situated. The structures of GH11 assume a  $\beta$ -jelly-roll fold in which two large  $\beta$ -pleated sheets and one  $\alpha$ -helix form a partially closed right hand-like shape, with the active sites (or the palm) formed by the cleft between the fingers and the thumb, which make obscure the binding of decorated substrate into the active sites (Fig. 9) (Berrin and Juge, 2008; Collins et al., 2005; Törrönen and Rouvinen, 1997). The variation of properties of arabinoxylans, such as water-extractable and water-unextractable arabinoxylans, affects the mode of action of xylanases. The relative activity of xylanases towards these substrates referred to as substrate selectivity illustrates the impact of enzyme functionality in cereal based biotechnology processes (Berrin and Juge, 2008; Frederix et al., 2004b; Moers et al., 2003; Moers et al., 2005).

#### 4.2.3 GH3 xylosidases

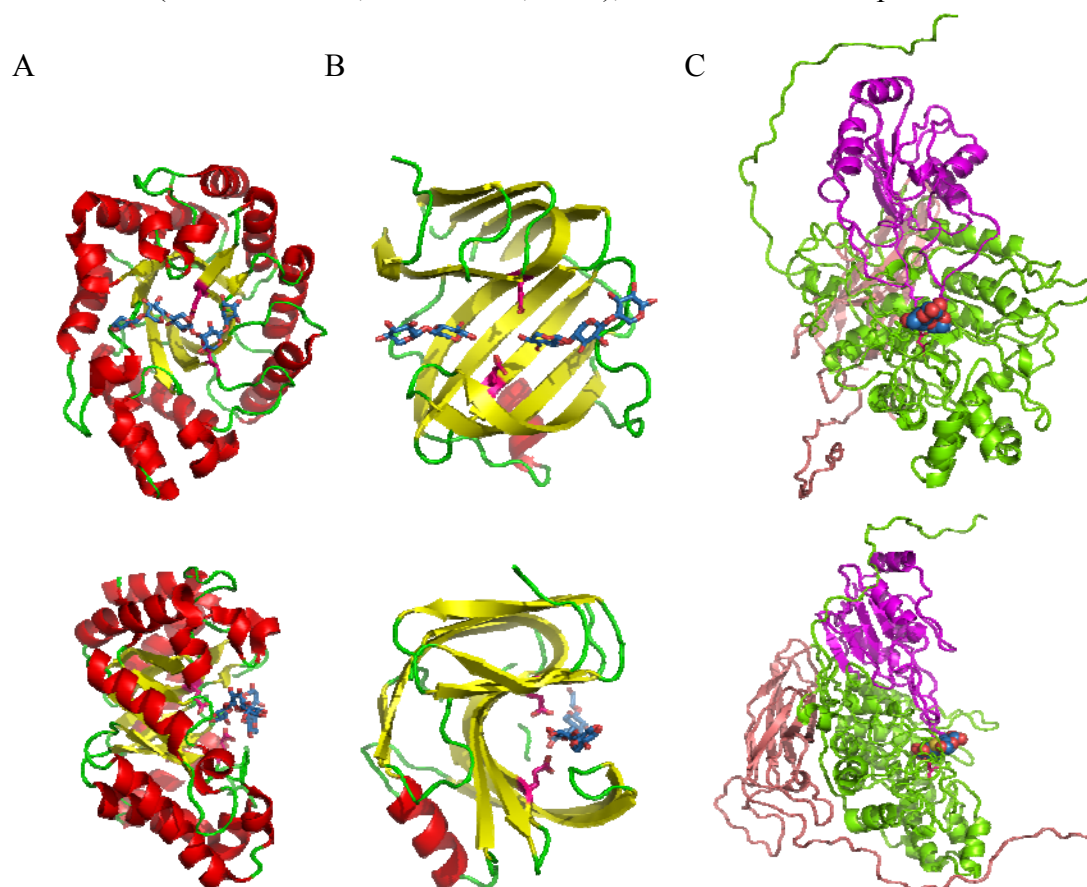
$\beta$ -Xylosidases (exo- $\beta$ -1,4-xylosidases, EC 3.2.1.37) catalyse hydrolysis of xylobiose and of xylooligosaccharides, generated by the action of xylanases by release of xylose from the non-reducing end. The affinity of  $\beta$ -xylosidases for xylooligosaccharides decreases with increasing of DP of the substrates (Beily, 2003; Pastor et al., 2007). Several  $\beta$ -xylosidases are reported to attack polymeric xylan in an exo-fashion (Beily, 2003).  $\beta$ -Xylosidases act synergistically with other xylan degrading enzymes and are required to accomplish complete hydrolysis of xylan, which is industrially important for the production of second generation biofuels from lignocellulosic biomass (Beg et al., 2001). The pH and temperature optimum of  $\beta$ -xylosidases are in the range of pH 3–5 and 50–70°C, respectively (Herrmann et al., 1996; Kurakake et al., 1997; Kumar and Ramon, 1996; Rasmussen et al., 2006).  $\beta$ -xylosidases are classified into five glycoside hydrolase families: 3, 30, 39, 43, and 52, (54)<sup>8</sup> according to the CAZy classification. GH3, GH30, GH39, and GH52 hydrolyse by a retaining mechanism, whereas GH43 hydrolyses according to an inverting mechanism (Table 3).

In the present study, we are interested in GH3  $\beta$ -xylosidases, which belong to a family that includes  $\beta$ -glucosidases (EC 3.2.1.21),  $\beta$ -N-acetylhexosaminidases (EC 3.2.1.52), glucon 1,3- $\beta$ -glucosidases (EC 3.2.1.58), glucon 1,4- $\beta$ -glucosidases (EC 3.2.1.74), exo-1,3-1,4-gluconases (EC 3.2.1.-) and  $\alpha$ -L-arabinofuranosidases (EC 3.2.1.55). The knowledge of structure-function relationships insight of GH3  $\beta$ -xylosidases is quite limited since there is no structure reported so far, while there are two exo-1,3/1,4- $\beta$ -gluconase structures from *Hordeum vulgare* and *Pseudoalteromonas* sp. BB1 (PDB ID: 1X38, Hrmova et al., 2005; 1EX1, Varghese et al., 1999; 3F93, Nakatani

---

<sup>8</sup> Bifunctional enzyme with main activity as  $\alpha$ -L-arabinofuranosidase

et al., to be published) and one  $\beta$ -glucosidase structure from *Thermotoga neapolitana* DSM 4359 (PDB ID: 2X40, Pozzo et al., 2010), which have been reported.



**Figure 9** Cartoon representation of 3D structures of GH10, GH11 xylanases, and GH3 xylosidase (upper: top view, lower: side view). A) *A. nidulans* GH10 xylanase (PDB ID: 1TA3) docking with X5 from xylanase from *Penicillium simplicissimum* (PDB ID: 1B3Z). B) 3D homology model of *A. nidulans* GH11 xylanase (using xylanase from *P. funiculosum*, PDB ID: 1TE1, as template; 67% sequence identity) docking with X2 and X3 from xylanase from *Escherichia coli* (PDB ID: 2VGD). C) 3D homology model of *A. nidulans* GH3 xylosidase ( $\beta$ -glucosidase from *Thermotoga neapolitana*, PDB ID: 2WT3, as template; 27% sequence identities) docking with thiocellobiose from exo-1,3/1,4- $\beta$ -glucanase from *Hordeum vulgare* (PDB ID: 1IEX), three colours representing three domains within the structure (for details on homologous modeling see 5.2, page 34), the enzyme structures were visualized by PyMOL v0.99.

#### 4.2.4 Transglycosylation by xylanases and xylosidases

It is generally accepted that transglycosylation naturally occurs as catalysed by glycoside hydrolases resulting in varying extent of transglycosylation. This also includes xylanases. During the characterization of GH10 and GH11 xylanases, transglycosylation is usually observed as a side activity when high concentration of oligosaccharide substrates is used. The enzymes can transfer xylooligosaccharide donors to create longer xylooligosaccharides (Berrin et al., 2006; Biely et al., 1981; Christakopoulos; 1996; Jiang et al., 2004; Kolenová et al., 2006; Yan et al., 2009). Moreover, the substrate donor is not only limited to short xylooligosaccharides, several transglycosylation reactions utilize xylans as substrate mixed directly with acceptor molecules, particularly different

alcohols. In the reactions using xylans as donor, xylanases can transfer mainly xylobiosyl to acceptor molecules. These have been identified by synthesis of alkyl xylooligosaccharides such as hexylxylobioside (Kadi and Crouzet, 2008), octylxylobioside (Matsumura et al., 1999), and benzylxylobioside (Kadi et al., 2002; Kadi and Crouzet, 2008) as well as alcoholic aroma xylooligosaccharide conjugates synthesized in the same fashion (Kadi et al., 2002). It is rare for xylanases to utilize other saccharides than xylooligosaccharides as acceptor due to the strict recognition, however, in one case; xylosylpsicoses<sup>9</sup> were synthesized by transglycosylation using xylanase from *A. sojae* (Oshima et al., 2006).

Moreover, GH3  $\beta$ -xylosidases are capable of catalysing transglycosylation at high substrate concentration, in which xylose from  $\beta$ -xylosyl donors, such as *para*-nitrophenyl  $\beta$ -D-xyloside or short xylo-oligosaccharides, are transferred to another xylosyl substrate forming *para*-nitrophenyl  $\beta$ -1,4 xylo-oligosaccharides or longer  $\beta$ -xylooligosaccharides with small amount of 1,3 glycosidic linkage (Eneyskaya et al., 2003; Rodionova et al., 1983; Win et al., 1988). Recently, transglycosylation using *A. niger* or *Aurebasidium pullulans*  $\beta$ -xylosidase was applied to produce *para*-nitrophenyl  $\beta$ -1,4-D-xylobioside, which is used as substrate in xylanase assay (Puchart and Biely 2007). Many  $\beta$ -xylosidases show broad acceptor specificity, including different mono-, disaccharides, sugar alcohols (Kurakake et al., 1997, 2005), alcohols (Shinoyama et al., 1988; Drouet et al., 1994), and hydroquinones (Sulistyo et al., 1994), which allows the formation of novel xylooligosaccharides, alkyl  $\beta$ -xylosides, and hydroquinone  $\beta$ -xylosides, respectively, under appropriate conditions. The heterogeneous transglycosylation using different non- $\beta$ -xylo-oligosaccharide acceptors has been tested by *A. awamori* K4 GH3  $\beta$ -xylosidase using xylobiose as donor with acceptors including three monosaccharides (arabinose, mannose, fructose), four disaccharides (trehalose, isomaltose, palatinose, maltose), and nine sugar alcohols (erythritol, xylitol, sorbitol, mannitol, dulcitol, maltitol, lactitol, palatinitol, myo-inositol) in yields of 44–69%, 0.8–50%, and 10–68%, respectively (Kurakake et al., 1997; 2005).

Being glycoside hydrolases, xylanases and xylosidases tend to hydrolyse the transglycosylation products. To circumvent this, glycosynthases can be used. So far, for xylanases, only glycosynthases from GH10 have been successfully obtained (Kim et al., 2006; Sugimura et al., 2006) and for the xylosidases, only GH52 xylosidase was reported as a glycosynthase (Ben-David et al., 2007).

#### 4.2.5 Objective for investigation on GH3, GH10, and GH11

*Objective for GH3 xylosidases:*

- To characterise hydrolytic and transglycosylation activity of recombinant GH3 xylosidases from *Aspergillus nidulans* FGSC A4 (BxlA).
- To synthesise and characterise novel xylooligosaccharides *via* transglycosylation by this GH3 xylosidase.
- To evaluate the effect of subsite +1 of BxlA in transglycosylation.
- To characterise the glycosynthases of BxlA

For GH3 xylosidase, we have reported hydrolytic activity of the enzyme towards different xylooligosaccharides (X2–X6), *para*-nitrophenyl  $\beta$ -D-xyloside (*p*NPX) and *para*-nitrophenyl  $\alpha$ -L-arabinofuranoside (*p*NPA), as well as pH and temperature optima

---

<sup>9</sup> Psicose (D-ribo-2-hexulose): C-3 epimer of D-fructose.

and stability, pI, and molecular mass of this enzyme in solution. The transglycosylation activity of this enzyme will also be described. The results will be compared with those for another  $\beta$ -xylosidase (BxlB) from the same origin, investigated by Dr. Hiroyuki Nakai (EPC, DTU). Furthermore, we are producing several novel xylooligosaccharides by transglycosylation, some of the structures were determined by nuclear magnetic resonance spectroscopy (NMR) and electrospray ionization mass spectrometry (ESI-MS).

Even though, the three-dimensional (3D) structure of GH3 xylosidase is not available, subsite +1 of BxlA can be tentatively identified by the aid of bioinformatics. In the present study, we evaluated the function of subsite +1 by the site-directed mutagenesis of Cys308 to Trp (C308W) and Asn313 to Arg (N313R) (the details of sequence comparison and homology modeling of this enzyme will be presented, 6.1.6, page 59). Since there is no glycosynthase reported from GH3, four glycosynthase mutants from BxlA were made by site-directed mutagenesis of Asp307, the catalytic nucleophile to Gly, Ala, Cys, and Ser.

*Objective for GH10 and GH11 xylanases:*

- To evaluate the potential transglycosylation activity of recombinant GH10 and GH11 xylanases from *Aspergillus nidulans* FGSC A4 (XlnC and XlnA, respectively) for production of novel xylooligosaccharides
- To evaluate the glycosynthase of XlnC

GH10 and GH11 are well-characterized families and many 3D structures have been reported (Table 3). In the xylanases study, we have investigated the possibility to use other disaccharides than xylobiose as well as sugar alcohols as acceptors in transglycosylation. In the preliminary acceptor screening, the XlnC showed possibility to transfer xylobiosyl to other acceptors than xylooligosaccharides; hence the glycosynthase of XlnC was made, by site-directed mutagenesis of Glu244 to Ala (E244A).

## 4.3 Mannanases

### 4.3.1 Enzymatic hydrolysis of mannans

Mannan degrading enzymes comprise four glycoside hydrolases and one esterase, *i.e.* endo- $\beta$ -1,4-mannanases, exo- $\beta$ -1,4-mannosidases,  $\alpha$ -galactosidases,  $\beta$ -glucosidases, and acetyl mannan esterases (Fig. 8 and Table 3) (Dhawan and Kaur, 2007 and Moreira and Filho, 2008). Mannanases are responsible for the cleavage of  $\beta$ -1,4-linked internal linkages of the mannan backbone in mannans including (galacto)glucomannans, while  $\beta$ -mannosidases cleave  $\beta$ -1,4-linked Man, releasing mannose from the non-reducing end of mannans and mannoooligosaccharides.  $\beta$ -Glucosidases are required to hydrolyse  $\beta$ -1,4-linked Glc at the terminal end of glucomannoooligosaccharides released by the hydrolysis of glucomannans and galactoglucomannans by mannanases.  $\alpha$ -Galactosidases, as debranching enzymes, catalyse the hydrolysis of  $\alpha$ -1,6-linked Gal side chain of galactomannans and galactoglucomannans, while acetyl mannan esterases catalyse the release of acetyl groups from galactoglucomannans (de Vries and Visser, 2001; Dhawan and Kaur, 2007; Moreira and Filho, 2008). Hydrolysis of mannans is affected by the extent and pattern of substitution by the Gal side chain in galactomannans and galactoglucomannans and the pattern of distribution of the Glc in glucomannans and galactoglucomannans backbone. Like the  $\beta$ -xylosidases in xylan degradation or  $\beta$ -glucosidases in cellulose degradation,  $\beta$ -mannosidases act synergistically with

mannanases and are essential to obtain complete hydrolysis of mannans (Dhawan and Kaur, 2007).

### 4.3.2 GH5 mannanases

Mannanases (endo- $\beta$ -1,4-mannanase, EC 3.2.1.78) classified into three glycoside hydrolase families: 5, 26, and 113 according to CAZy classification. All of these belong to clan GH-A and hydrolyses by a retaining mechanism with glutamic acids as both catalytic nucleophile and acid/base (Table 3; Moreira and Filho, 2008; Zhang et al., 2008). The degradation by mannanases is greatly affected by the extent and pattern of Gal substitution and the pattern of distribution of Glc residues on the main chain. The main products by complete hydrolysis of mannans by mannanases are mannobiose and mannotriose (Dhawan and Kaur, 2007; Moreira and Filho, 2008). In general, mannanases have pH and temperature optima at 3.0–7.5 and 45–70°C, respectively (Dhawan and Kaur, 2007). The mannanase from *Thermotoga neapolitana* 5068, an extremophilic bacterium, has highest activity at 92°C (Duffaud et al., 1997). Mannanases are mainly used in food, feed, and pulp and paper industries. Since mannans are the major hemicelluloses in softwood, mannanases are applied for aiding in enzymatic bleaching of softwood pulps. In food industries, mannanases are used for reducing the viscosity of coffee extracts as well as for modifying mannan containing materials (e.g. gums), which also have other technical application such as in oil drilling (Dhawan and Kaur, 2007).

In the present study we are interested in GH5, which is divided into 9 subfamilies<sup>10</sup> on the basis of sequence similarity (Béguin, 1990; Lo Leggio et al., 1997; Hilge et al., 1998; Larsson et al., 2006). Mannanases are classified into subfamilies 7 (eukaryotic mannanases), 8 (prokaryotic mannanases), and 10 (Hilge et al., 1998; Larsson, et al., 2006). Several crystal structures of GH5 mannanases have been reported. *Hypocrea jecorina* (anamorph: *Trichoderma reesei*; Sabini et al., 1999), *Thermomonospora fusca* (Hilge et al., 1998), and *Mytilus edulis* (Larsson et al., 2006) mannanases represent subfamilies 7, 8, and 10, respectively. GH26 and GH113 mannanases are exclusively of prokaryotic origin (Hogg et al., 2003). GH5 mannanases have five substrate binding subsites (–3 to +2) similar to GH26 and GH113 (Anderson, et al., 2008; Larsson et al., 2006; Sabini et al., 2000; Tailford et al., 2009). Binding to at least four subsites is required for efficient hydrolysis and the substitution of the substrate restricts hydrolysis, most likely by preventing substrate binding (Dhawan and Kaur, 2007).

### 4.3.3 Transglycosylation by mannanases

In the same manner as xylanases, mannanases can perform transglycosylation, which was observed during characterisation of the enzymes. Both microbial GH5 and GH113 are capable to perform transglycosylation (Gübitz et al., 1996; Harjunpää et al., 1995; Harjunpää et al., 1999; Hrmova et al., 2006; Zhang et al., 2008), whereas GH26 showed poor transglycosylation ability, which may stem from different subsite affinities (Anderson et al., 2008; Gilbert et al., 2008; Le Nours et al., 2005). Substrate donors for transglycosylation are usually mannoooligosaccharides (DP 4–6) and the transglycosylation products are longer mannoooligosaccharides. In plant, GH5 mannanase may play a significant role in modifying the structure of plant cell walls during cell expansion, seed germination, and fruit ripening, similarly to xyloglucan endotransglucosylase/hydrolase (Schröder et al., 2006, 2009). Currently, there are limited

---

<sup>10</sup> Subfamilies 5 and 6 are referred to as subfamily 5/6

details reported on reactions using different acceptors, such as alcohols or other saccharides (Hekmet, to be published) and no report on using mannans as donors.

#### 4.3.4 Objective for investigation on GH5

- To characterise hydrolytic and transglycosylation activity of recombinant mannanases of GH5 subfamily 7 from *Aspergillus nidulans* FGSC A4 (ManA and ManC) (in collaboration with Dr. Hiroyuki Nakai)
- To synthesise and characterise novel mannoooligosaccharides *via* transglycosylation catalysed by GH5 mannanases.
- To evaluate the effect of subsite +1 on transglycosylation of both GH5 mannanases.

For GH5 mannanases, we present hydrolytic activity towards different mannans, kinetics towards mannoooligosaccharides (M4–M6), hydrolysis patterns of these enzymes. The transglycosylation activity of these enzymes will be discussed. Furthermore, we produced novel mannoooligosaccharides by transglycosylation catalysed by ManC with isomaltotriose and melezitose<sup>11</sup> as acceptors. The structures of these products were determined by NMR and matrix assisted laser desorption ionisation time-of-flight mass spectrometry (MALDI-TOF MS).

The preliminary characterization of the two mannanases (by Dr. Hiroyuki Nakai) showed distinctly different transglycosylation activity. One of the reasons for this could be a structural difference at subsite +1. Since there are several structures of GH5 mannanases reported, subsite +1 of these mannanases can be identified by amino acid alignment and protein structure homologous modeling. Subsite +1 of ManA and ManC are well conserved except for Trp283 in ManC, corresponding to Ser289 in ManA. We are thus evaluating the effect of aromatic residue substitution at subsite +1 by the site-directed mutagenesis of both enzymes: Ser289 to Trp of ManA (ManAS289W) and Trp283 to Ser of ManC (ManCW283S; sequence comparison and homology modeling details are presented, 6.2.5, page 68).

### 4.4 Endo- $\beta$ -glucanase

#### 4.4.1 Enzymatic hydrolysis of cellulose

Cellulose is a polysaccharide consisting of a linear chain of  $\beta$ -1,4 linked Glc, which has an extremely rigid and compact structure. Cellulose degradation requires three types of cellulolytic enzymes, including cellobiohydrolases, endoglucanases, and  $\beta$ -glucosidases, as well as an accessory protein (swollenin) (Brotman et al., 2008; de Vries and Visser, 2001; Merino and Cherry, 2007). The endoglucanases, mainly referred to as cellulases, catalyse randomly the hydrolysis of  $\beta$ -1,4 linkages in cellulose and act mainly on the amorphous regions of cellulose, which also results in exposure of more chain termini for cellobiohydrolases. Cellobiohydrolases catalyse hydrolysis of cellulose both from the non-reducing and the reducing end, depending on the type of enzyme, and release mainly cellobiose. These enzymes are needed for hydrolysis of crystalline cellulose. With a tunnel-shaped active site, they may help open up the cellulose chain, under certain circumstances, and allow significant endoglucanase action (Kubicek, 1992; Xu et al., 2007).  $\beta$ -glucosidases degrade primarily cellobiose (and celloooligosaccharides), which reduces product inhibition by cellobiose on cellobiohydrolases and endoglucanases

---

<sup>11</sup> Melezitose ( $\alpha$ -D-Glcp-(1 $\rightarrow$ 3)- $\beta$ -D-Furf-(2 $\rightarrow$ 1)- $\alpha$ -D-Glcp)



and are essential for complete breakdown of cellulose (Kubicek, 1992; Xu et al., 2007). Swollenin, an expansin-like protein, helps making cellulose fibres more accessible by disrupting the crystalline structure of the cellulose, which supports the enzymatic degradation, particularly by endo-glucanases (Brotman et al., 2008; Saloheimo et al., 2002).

#### 4.4.2 GH61 putative endo- $\beta$ -glucanase

The functionally uncharacterised family GH61 has 116 members, which are solely from eukaryotes and mainly from filamentous fungi. The activity, function, and mechanism of this family are not clear. These putative enzymes remarkable have a carbohydrate binding module family (CBM)<sup>12</sup> 1, found in several members such as from *Agaricus bisporus* (CEL1; Armesilla et al., 1994), *A. kawachii* (Cel61A; Hara et al., 2003 or AkCel61A: Koseki et al., 2008) and *T. reesei* (EG IV; Saloheimo et al., 1997, renamed to Cel61A; Karlsson et al., 2001). GH61 was presumed to have some function in degradation of lignocellulose, possibly increasing the cellulase activity (Brown et al., 2005; Karlsson et al., 2001; Koseki et al., 2008; Liu et al., 2006). The proteins have very low levels of endo-glucanase activity, more than 10,000 times lower in activity than usual endo-glucanases, towards cellulose derivative substrates such as carboxymethyl cellulose and hydroxyethyl cellulose, as well as  $\beta$ -glucan and lichenan (Karlsson et al., 2001). Currently, there are two reported 3D structures from two different fungi: Cel61B from *Hypocrea jecorina* QM6A (PDB ID: 2VTC; Karkehabadi et al., 2008) and Cel61E from *Thielavia terrestris* NRRL 8126 (PDB ID: 3EII and 3EJA; Harris et al., 2010). Both protein structures contain mainly  $\beta$ -strands forming twisted  $\beta$ -sandwich with metal-binding sites, as nickel-binding for Cel61B and zinc-binding for Cel61E, without CBM. Even though two 3D structures from this family have been reported, there is still no clear identifiable carbohydrate binding cleft or catalytic pocket to guide to unravel the function of this putative endo-glucanase. The function for this protein is still under quest.

#### 4.4.3 Objective for investigation on GH61

- To demonstrate enzyme discovery by using a proteomics strategy.
- To produce and characterize the recombinant GH61 putative endo- $\beta$ -glucanase from *Aspergillus nidulans* FGSC A4 (EgIF).

In this part of the project, a proteomics strategy (Dr. Kenji Maeda, Dr. Hiroyuki Nakai, and PhD student Anders Dysted Jørgensen, EPC, DTU Systems Biology), was applied to analyse the culture supernatant of *A. nidulans* FGSC A4 growing on 10 different polysaccharides: potato starch, tamarind xyloglucan, birchwood xylan, oat spelt xylan, wheat arabinoxylan, sugar beet arabinan, larchwood arabinogalactan, guar galactomannan, carbo galactomannan, and konjac glucomannan (with glucose and without carbohydrate source as controls). The extracellular proteins were separated by 2DE and identified after trypsin digestion by MALDI-TOF MS. As a result, several novel and putative carbohydrate active enzymes were determined by the aid of genomic sequence of the fungus. Among several other novel carbohydrate active enzymes, a GH61 putative endo- $\beta$ -glucanase was discovered in the culture broth-containing oat spelt xylan.

---

<sup>12</sup> A carbohydrate-binding module (CBM) is defined as a contiguous amino acid sequence within a carbohydrate-active enzyme with a discreet fold having carbohydrate-binding activity (Tomme et al., 1995)

The actual function of this enzyme was unrevealed and the protein might be useful for synthesis of  $\beta$ -glucooligosaccharides by transglycosylation; hence this protein was selected for further investigation. The cDNA cloning of the GH61 (EglF), the production of the corresponding protein as well as its characterisation including carbohydrate microarrays screening have been performed.

## 5. Materials and methods

### 5.1 Materials

#### 5.1.1 *Pichia pastoris* transformants and *Aspergillus* strain

*Pichia pastoris* X-33 transformants harbouring full-length  $\beta$ -xylosidase, mannanase, and xylanase genes (Table 4) from *Aspergillus nidulans* FGSC A4 (Bauer *et al.*, 2006) and *Aspergillus nidulans* FGSC A4 (for cDNA cloning of GH61 putative endo- $\beta$ -glucanase) were purchased from Fungal Genetics Stock Center, School of Biological Sciences, University of Missouri, Kansas City, MO.

**Table 4** Enzymes identity and accession number

Name <sup>a</sup>	GH	Enzyme	Locus tag	FGSC database	
				accession no.	GenBank ID
BxlA	3	$\beta$ -xylosidase	AN2359.2	10077	EAA64470.1
BxlB	3	$\beta$ -xylosidase	AN8401.2	10125	EAA67023.1
ManA	5	Mannanase	AN3358.2	10088	EAA63326.1
ManC	5	Mannanase	AN6427.2	10106	EAA58449.1
XlnC	10	Xylanase	AN1818.2	10073	EAA64983.1
XlnA	11	Xylanase	AN3613.2	10092	EAA59821.1
EglF	61	Endo- $\beta$ -glucanase <sup>b</sup>	AN3860.2	–	EAA59125.1

<sup>a</sup> The enzyme names are according to Coutinho *et al.*, 2009

<sup>b</sup> putative endo  $\beta$ -glucanase or cellulase-enhancing factor (Harris *et al.*, 2010)

#### 5.1.2 Primers

The oligonucleotide primers (Table 5), constructed based on the *A. nidulans* genomic sequence (Galagan *et al.*, 2005) were purchased from Eurofins MWG Operon (Ebersberg, Germany).

**Table 5** Primers for construction of the expression plasmids of BxlA (GH3), BxlB (GH3), ManA (GH5), ManC (GH5), XlnC (GH10), XlnA (GH11), EglF (GH61), and their mutants

Primer	Primer sequence <sup>a</sup>	Restriction site
<i>bxlA</i>		
Sense	ATT <u>CTCGAG</u> AAAAGAGAGGGCTGAAGCTGCGAACACCAGCTACAC	XhoI
Antisense	ACT <u>CTAGAT</u> TAATGATGATGATGATGATGATGAGCAATAACATCCTGC	XbaI
D307G sense	CGTCTCCGGT <u>GGT</u> TGCGGTGCTGTC	–
D307G antisense	GACAGCACCGCA <u>ACC</u> ACCGGAGACG	–
D307A sense	CGTCTCCGGT <u>GCT</u> TGCGGTGCTGTC	–
D307A antisense	GACAGCACCGCA <u>AGC</u> ACCGGAGACG	–
D307C sense	CGTCTCCGGT <u>TGT</u> TGCGGTGCTGTC	–
D307C antisense	GACAGCACCGCA <u>ACA</u> ACCGGAGACG	–
D307S sense	CGTCTCCGGT <u>TCT</u> TGCGGTGCTGTC	–
D307S antisense	GACAGCACCGCA <u>AGA</u> ACCGGAGACG	–
C308W sense	CGTCTCCGGTGACT <u>TGG</u> GTGCTGTC	–
C308W antisense	GACAGCACCGCA <u>CA</u> GTCACCGGAGACG	–
N313R sense	GCGGTGCTGTCTAC <u>AGA</u> GTGTGGAACC	–
N313R antisense	GGTCCACACT <u>CT</u> GTAGACAGCACCGC	–
<i>bxlA</i> -sequencing 1	AACATCAACACTTTCCGACAC	–
<i>bxlA</i> -sequencing 2	AGACATCGACTGTGGAACCTC	–
<i>bxlA</i> -sequencing 3	AATTGACAACAATCGAAG	–
<i>bxlB</i>		
Sense	GGGGAATTCAACTACCCGGACTGCACAACGGGCCCTC	EcoRI
Antisense	CCCGGCGCCGCATCACTGTCGTTACCTGACAACGG	NotI
T1374C-sense	GGACAGAGGTGAA <u>CT</u> CGACAAGCACAGAC	–
T1374C-antisense	GTCTGTGCTTGTGCA <u>G</u> TTCACCTCTGTCC	–
<i>bxlB</i> -sequencing 1	CGCTATGTCAAAGAGTTTGTG	–
<i>bxlB</i> -sequencing 2	CGTTGACGAGACTATATACGAG	–
<i>bxlB</i> -sequencing 3	AGGAGGAACTCATTCTGGAAC	–
<i>manA</i>		
Sense	GGGGAATTCCCTCCCTCACGCGTCAACACCTGTGTACAC	EcoRI
Antisense	CCCGCGGCCGCCTACTTGGCACTCCTCTCAATCGTCTCG	NotI
S289W sense	CTTACCCGGAT <u>TGG</u> TGGGGCAC	–
S289W antisense	GTGCCCA <u>CCA</u> ATCCGGGTAGAG	–
<i>manC</i>		
Sense	GGGGAATTCCGCAAGGGCTTGTGACCACCAAAGGCG	EcoRI
Antisense	CCCGCGGCCGCCTACCGTCTCCGGTCAACTTGTTCACC	NotI
W283S sense	CTATCCGGA <u>AGT</u> TGGAGCAAGACC	–
W283S antisense	GGTCTTGCTCCA <u>ACT</u> ATCCGGATAG	–
<i>xlnC</i>		
Sense	TACATGCCATGGCCCAAAGCGCCAGCCTAAATGATCTT	NcoI
Antisense	AAGGAAAAAAGCGGCCGAGACAGAGCGTTGACGATTGACG	NotI
E244A sense	GCCATCACCG <u>CG</u> CTTGATATTGCGGG	–
E244A antisense	CCCGCAATATCAAG <u>CG</u> CGGTGATGGC	–
<i>xlnA</i>		
Sense	TACATGCCATGGCCACGCCGCTCGGGTCTGAAGACC	NcoI
Antisense	AAGGAAAAAAGCGGCCGCTAAACAGTAATAGAAGCCGACCCAC	NotI
<i>eglF</i>		
Sense	ATT <u>CTCGAG</u> AAAAGAGAGGGCTGAAGCTGGCCACGGATACGTGACG	XhoI
Antisense	ACT <u>CTAGAT</u> TAATGATGATGATGATGATGATGACCACTGTACAGCTCAGG	XbaI

<sup>a</sup> Restriction sites are underlined, mutation positions are doubly underlined

### 5.1.3 Natural carbohydrate substrates (with acceptors for transglycosylation)

For GH3  $\beta$ -xylosidases arabinose, lyxose, L-fucose, L-rhamnose, galactose, mannose, talose, fructose, maltose, sucrose, lactose, cellobiose, turanose, L-serine (Ser), and L-cysteine (Cys) were purchased from Sigma Aldrich (St. Louis, MO). Xylose (Xyl) was from Carl Roth (Karlsruhe, Germany). Glucose was from Merck (Darmstadt, Germany). Xylobiose (X2), xylotriose (X3), xylotetraose (X4), xylopentaose (X5), and xylohexaose (X6) were purchased from Megazyme (Wicklow, Ireland).

For GH5 mannanases mannose, melezitose<sup>13</sup> (Mel3), and locust bean gum galactomannan (LBG GalMan) were purchased from Sigma Aldrich. Guar galactomannan (guar GalMan) was from Carl Roth. Mannobiose (M2), mannotriose (M3), mannotetraose (M4), mannopentaose (M5), mannohexaose (M6) and konjac glucomannan (konjac GlcMan) were from Megazyme. Isomaltotriose (Iso3) was a gift from Assoc. Prof. Haruhide Mori and Prof. Atsuo Kimura, Faculty of Agriculture, Hokkaido University, Japan.

For GH10 and GH11 xylanases xylotriose, mannobiose, and wheat arabinoxylan (low viscosity) were purchased from Megazyme. Birchwood and oat spelt xylans were from Carl Roth. Cellobiose, isomaltose, and maltose were from Sigma Aldrich.

For GH61 putative endo-glucanases, oat spelt xylan was from Carl Roth and barley  $\beta$ -glucan was from laboratory preparation.

### 5.1.4 Synthetic carbohydrate substrates (with acceptors for transglycosylation)

Acetylated  $\alpha$ -xylosyl and  $\alpha$ -xylobiosyl fluorides were kind gifts from Prof. Stephen G. Withers (University of British Columbia, Canada). *para*-Nitrophenol (*p*NP), *p*NP  $\beta$ -D-xylopyranoside (*p*NPX), *p*NP  $\alpha$ -L-arabinofuranoside (*p*NPA),  $\alpha$ -L-arabinopyranoside (*p*NPAP), *p*NP  $\beta$ -D-cellobioside (*p*NPC2), xylitol, and sorbitol were purchased from Sigma Aldrich.

## 5.2 Sequence comparison and homology modeling

BLAST was used for homology search of protein sequences (<http://blast.ncbi.nlm.nih.gov/Blast.cgi>; Altschul et al., 1997). The sequence alignment was performed using T-Coffee (<http://tcoffee.vital-it.ch/cgi-bin/Tcoffee/tcoffee.cgi/index.cgi>; Notredame et al., 2000) and visualised using Easy Sequencing in Postscript (<http://escript.ibcp.fr/ESPript/ESPript>; Gouet et al., 1999). Homology models of BxlA, BxlB, ManA, and ManC were generated using HHpred-Homology server (<http://toolkit.tuebingen.mpg.de/hhpred>; Söding et al., 2005). For BxlA,  $\beta$ -glucosidase from *Thermotoga neapolitana* DSM 4359 (PDB ID: 2WT3; Pozzo et al., 2010) and  $\beta$ -glucanase from *Hordeum vulgare* (PDB ID: 1IEX; Hrmova et al., 2005) sharing 27% and 26% sequence identity, respectively served as templates. For GH5 mannanases,  $\beta$ -mannanase from *Hypocrea jecorina* RUTC-30 (PDB ID: 1QNR; Sabini et al., 2000) sharing 56% and 37% identity with ManA and ManC, respectively served as template. For putative GH61 endo- $\beta$ -glucanase, *H. jecorina* QM6A (PDB ID: 2VTC; Karkehabadi et al., 2008) sharing 44% sequence

---

<sup>13</sup> Melezitose ( $\alpha$ -D-Glcp-(1 $\rightarrow$ 3)- $\beta$ -D-Furf-(2 $\rightarrow$ 1)- $\alpha$ -D-Glcp)

identity served as template. The models were validated by the Combinatorial Extension (CE) Method (<http://cl.sdsc.edu/ce.html>; Shindyalov and Bourne, 1998) and ProQ-Protein Quality Predictor (<http://www.sbc.su.se/~bjornw/ProQ/ProQ.html>; Wallner and Elofsson, 2003).

For GH3  $\beta$ -xylosidase the root-mean-square deviations (rmsd) was 0.8 Å for 641 and 529 equivalent  $C_{\alpha}$  positions (out of 784 in BxlA) compared to 2WT3 and 1IEX with 7.7 and 7.5 Z-score. LGScore/MaxSub were 4.520/0.383 and 4.577/0.256, respectively, indicated that the models are of reasonable to good quality. Disulfide bonds of BxlA were predicted using DiANNA-Disulfide bond connectivity prediction (<http://clavius.bc.edu/~clotelab/DiANNA/>; Ferrèl and Clote, 2005). For GH5 mannanases rmsd were 0.3 Å for 343 equivalent  $C_{\alpha}$  positions (out of 372 in ManA and 381 in ManC) compared to 1QNR with 7.9 and 7.7 Z-score for ManA and ManC, respectively). LGScore/MaxSub values were 5.337/0.627 and 5.468/0.567 for ManA and ManC, respectively, indicated that the models are of good to very good quality. For GH61 putative endo- $\beta$ -glucanase rmsd was 0.7 Å for 224 equivalent  $C_{\alpha}$  positions (out of 230 in EglF) compared to 2VTC with 7.4 Z-score. LGScore/MaxSub was 3.200/0.319 indicated that the models are reasonable to good quality. All models were rendered and analysed using Pymol v0.99 (DeLano Scientific LLC, San Carlos, CA).

## 5.3 Cloning and mutations

### 5.3.1 GH3 xylosidases

*P. pastoris* X-33 transformants (*bxlA* – formerly *xlnD* and *bxlB*, Table 4), encode native full-length enzymes including signal peptides (Met1–Ser18 and Met1–Ser23 for *bxlA* and *bxlB*, respectively, predicted by SignalP 3.0 (<http://www.cbs.dtu.dk/services/SignalP/>; Bendtsen et al., 2004). The genes were therefore recloned to encode mature enzymes lacking signal peptides since the highly hydrophobic and the positively charged nature of signal peptides is likely to have significant effects on the properties of the gene product. Expand High Fidelity DNA polymerase (Roche Diagnostics GmbH, Mannheim, Germany) was used for DNA amplification using oligonucleotide primers (Table 5). The recloning of *bxlB* was performed by Dr. Hiroyuki Nakai. The silent mutation (1374T>C) of the EcoRI site in *bxlB* was introduced by overlap PCR (Sambrook et al., 1989) using the primer pair in Table 5. PCR products were digested by XhoI and XbaI for *bxlA* or EcoRI and NotI for *bxlB* (New England BioLabs, Ipswich, MA), and cloned into the pPICZ $\alpha$ A vector (Invitrogen, Carlsbad, CA). The plasmids (pPIC $\alpha$ A-BxlA and pPIC $\alpha$ A-BxlB) were transformed into *Escherichia coli* DH5 $\alpha$  (Invitrogen) and transformants were selected on low salt Luria-Bertani (LB; 1% tryptone, 0.5% yeast extract, 0.5% NaCl, pH 7.0) supplemented with 25  $\mu$ g/mL Zeocin. Purified plasmids (QIAprep Spin Miniprep; QIAGEN, Hilden, Germany) were fully sequenced (Eurofins MWG Operon, Ebersberg, Germany). The pPIC $\alpha$ A-BxlA was linearised by PmeI (New England BioLabs) and transformed into *P. pastoris* X-33 (Invitrogen) by electroporation (Micropulser; Bio-Rad Laboratories Inc, Hercules, CA). Transformants were selected on yeast peptone dextrose (1% yeast extract, 2% peptone, 2% dextrose) plates containing 1 M sorbitol and 100  $\mu$ g/mL Zeocin at 30°C for 3 days.

The glycosylase and subsite mutants of BxlA were obtained by site-directed mutagenesis (QuikChange Lightning Site-Directed Mutagenesis kit; Stratagene, La Jolla, CA) using D307G, D307A, D307C, and D307S primer pairs for glycosylase

mutants and C308W and N313R primer pairs for subsite +1 mutants (Table 5) with pPIC $\alpha$ A-BxlA as template. The mutated plasmids were transformed into *E. coli* DH5 $\alpha$ , verified by fully sequencing, and transformed into *P. pastoris* X-33 as described above.

### 5.3.2 GH5 mannanases

*P. pastoris* X-33 transformants harbouring full-length  $\beta$ -mannanase genes *manA* and *manC* (Table 4) encoded native full-length enzymes including signal peptides (Met1–Ala18 for *manA* and *manC* predicted by SignalP 3.0; Bendtsen et al., 2004), therefore the genes were recloned to encode the mature enzymes lacking signal peptides. The recloning of  $\beta$ -mannanase genes was conducted by Dr. Hiroyuki Nakai using Expand High Fidelity DNA polymerase (Roche Diagnostics GmbH) for DNA amplification using oligonucleotide primers (Table 5). PCR products were digested by EcoRI and NotI (New England BioLabs) for both *manA* and *manC*, and cloned into the pPICZ $\alpha$ A vector (Invitrogen). The plasmids (pPICZ $\alpha$ A-ManA and pPICZ $\alpha$ A-ManC) were transformed into *Escherichia coli* DH5 $\alpha$  (Invitrogen). Transformants were selected on low salt LB supplemented with 25  $\mu$ g/mL Zeocin and purified plasmids were fully sequenced (Eurofins MWG Operon). The plasmids were linearised by PmeI and transformed into *P. pastoris* X-33 as described in 5.3.1.

Substitution of Ser289 to Trp in ManA (ManAS289W) was obtained by site-directed mutagenesis (QuikChange Lightning Site-Directed Mutagenesis kit; Stratagene) using S289W primer pair (Table 5) with pPICZ $\alpha$ A-ManA as template. Substitution of Trp283 to Ser in ManC (ManCW283S) was prepared using W283S primer pair with pPICZ $\alpha$ A-ManC as template. Mutated plasmids were transformed into *E. coli* DH5 $\alpha$ , verified by full sequencing, and transformed into *P. pastoris* X-33 as described in 5.3.1.

### 5.3.3 GH10 and GH11 xylanases

*P. pastoris* X-33 transformants harbouring full-length xylanase genes *xlnA* and *xlnC* (Table 4) encoded native full-length enzymes including signal peptides (Met1–Ala19 for *xlnA* and *xlnC*, predicted by SignalP 3.0; Bendtsen et al., 2004), therefore the genes were reconstructed to encode the mature enzymes without signal peptides. Expand High Fidelity DNA polymerase (Roche Diagnostics GmbH) was used for DNA amplification using oligonucleotide primers (Table 5). PCR products were digested by NcoI and NotI (New England BioLabs) for both *xlnA* and *xlnC*, and cloned into the pET28-a(+) vector (Novagen, Merck KGaA, Darmstadt, Germany). The plasmids (pET28-a(+)-XlnA and pET28-a(+)-XlnC) were transformed into *E. coli* BL21(DE3) (New England BioLabs) by heatshock at 42°C. Transformants were selected on LB (1% tryptone, 0.5% yeast extract, 1% NaCl, pH 7.0) supplemented with 30  $\mu$ g/mL kanamycin and purified plasmids were confirmed by full-length sequencing (Eurofins MWG Operon).

The glycosylase mutant of XlnC was prepared by site-directed mutagenesis (QuikChange Lightning Site-Directed Mutagenesis kit; Stratagene) using E244A primers pair (Table 5) with pET28-a(+)-XlnC as template. The mutated plasmids were transformed into *E. coli* BL21(DE3) and verified by full-length sequencing as described above.

## 5.4 Recombinant protein production and purification

### 5.4.1 GH3 xylosidases and mutants

*P. pastoris* X-33 harbouring BxlA wild type or mutants was grown in 3 × 1 L buffered glycerol-complex medium (BMGY; 1% yeast extract, 2% peptone, 100 mM potassium phosphate pH 6.0, 1.34% yeast nitrogen base with ammonium sulfate, 4 × 10<sup>-5</sup>% biotin, 1% glycerol) in 3 × 2.5 L plastic shake flask at 30°C for 24 h to OD<sub>600</sub> of 25–32. Cells were harvested (3000g, 5 min, 4°C) and resuspended in 1 L buffered minimal methanol medium (BMM; 100 mM potassium phosphate pH 6.0, 1.34% yeast nitrogen base with ammonium sulfate, 4 × 10<sup>-5</sup>% biotin, 1% methanol, 1% casamino acid) in 2.5 L plastic shake flask. The induction was continued at 22°C for 72 h. Methanol was supplemented to a final concentration of 1% (v/v) every 24 h until harvest by centrifugation (13,500g, 4°C, 1 h). Then, the culture supernatant was concentrated and buffer-exchanged to 10 mM MES pH 6.0 (Pellicon tangential flow filtration systems, nominal molecular weight limit (NMWL) 10 kDa; Millipore, Billerica, MA), and applied to a Resource Q 6 mL column (GE Healthcare, Uppsala, Sweden) equilibrated with the same buffer. After washing with 37.5 mM NaCl in the same buffer, protein was eluted by a 37.5–325 mM NaCl linear gradient (flow rate: 2 mL/min, 144 mL). Fractions containing activity were pooled, concentrated (Amicon Ultra-15, NMWL 30 kDa, Millipore), and applied to a Hiload 26/60 Superdex G200 column (GE Healthcare) equilibrated with 20 mM MES, 0.25 M NaCl, pH 6.0 (flow rate: 1 mL/min). Fractions containing BxlA, verified by activity assay (5.6.1.1) and/or SDS-PAGE (5.5.1)<sup>14</sup>, were pooled, concentrated, and buffer-exchanged to 10 mM MES pH 6.0. All purification steps were performed using an ÄKTAexplorer chromatograph (GE Healthcare) at 4°C. The anion exchange chromatography was used instead of immobilized metal ion affinity chromatography (IMAC) due to the instability of BxlA at pH 7.5 and the very poor yield (<20% activity recovery) by IMAC at lower pH.

### 5.4.2 GH5 mannanases and mutants

ManA and ManC were produced and purified by Dr. Hiroyuki Nakai. *P. pastoris* X-33 harbouring ManAS289W and ManCW283S were grown in 3 × 1 L of BMGY at 30°C in 3 × 2.5 L plastic shake flask for 24 h to OD<sub>600</sub> of 34 (ManAS289W) and 28 (ManCW283S). The cells were harvested (3000g, 5 min, 4°C) and resuspended in 1 L BMM (containing 0.5% methanol) in 2.5 L plastic shake flask. The induction was continued at 22°C for 72 h and methanol was supplemented to the culture to a final concentration of 0.5% (v/v) every 24 h. The culture supernatants were harvested (13,500g, 4°C, 1 h), adjusted pH to 7.5 with 1 M K<sub>2</sub>HPO<sub>4</sub>, filtered (0.22 µm; TPP, Trasadingen, Switzerland), and applied to a 5 mL HisTrap HP column (GE Healthcare) equilibrated with 20 mM HEPES, 0.5 M NaCl, 10 mM imidazole, pH 7.5. After washing with 20 mM HEPES, 0.5 M NaCl, 22 mM imidazole, pH 7.5, followed by elution using a 22–400 mM imidazole linear gradient (flow rate: 1.0 mL/min, 25 mL) fractions containing enzymes, verified by SDS-PAGE, were pooled, concentrated (Centriprep YM30, Millipore), and applied to a Hiload 26/60 Superdex G75 column (GE Healthcare) equilibrated with 20 mM MES,

---

<sup>14</sup> For glycosynthase mutants, the fraction were verified only by SDS-PAGE



0.15 M NaCl, pH 7.0, flow rate 0.5 mL/min. Fractions containing enzymes were pooled, concentrated, and buffer-exchanged to 20 mM HEPES pH 7.0. All purification steps were performed at 4°C.

### 5.4.3 GH10, GH11 xylanases, and GH10 glycosynthase mutant

*E. coli* BL21(DE3) harbouring XlnA, XlnC, and XlnCE244A were grown in 1 L of LB containing 30 µg/mL kanamycin in 2.5 L plastic shake flask at 37°C to OD<sub>600</sub> of 0.6. Expression was induced by 0.1 mM isopropyl-1-thio-β-galactopyranoside and continued at 12°C for 24 h. Cells were harvested (10,000g, 10 min, 4°C) and resuspended in 30 mL BugBuster Protein Extraction Reagent (Novagen) containing 1 µL Benzonase Nuclease (Sigma Aldrich). Following 30 min incubation at 4°C with rotating mixing, the supernatants were collected (16,000g, 4°C, 20 min), filtered (45 µm; GE Infrastructure Water & Process Technologies Life Science Microseparations, Trevose, PA), and applied to a 5 mL HisTrap HP column (GE Healthcare) equilibrated with 20 mM HEPES, 0.5 M NaCl, 10 mM imidazole, pH 7.5. After washing with 20 mM HEPES, 0.5 M NaCl, 22 mM imidazole, pH 7.5, followed by elution using a 22–400 mM imidazole linear gradient (flow rate: 1.0 mL/min 25 mL) fractions containing enzymes were pooled, concentrated (Centriprep YM10, Millipore), and applied to a Hiload 26/60 Superdex G75 column (GE Healthcare) equilibrated with 20 mM HEPES, 0.15 M NaCl, pH 7.0 (flow rate: 0.5 mL/min). Fractions containing enzymes, verified by activity assay (5.6.3.1) and/or SDS-PAGE (5.5.1)<sup>15</sup> were pooled, concentrated, and buffer-exchanged to 20 mM HEPES pH 7.0. All purification steps were performed at 4°C.

## 5.5 Protein characterisation

### 5.5.1 Protein concentration determination

The Protein concentration was determined spectrophotometrically at 280 nm using extinction coefficients  $E^{0.1\%} = 1.79$  (BxlA, D307G, D307A, D307C, D307S, N313R), 1.82 (C308W), 2.26 (ManA), 2.57 (ManC), 2.33 (ManAS289W), 2.51 (ManCW283S), 1.86 (EglF) as determined by amino acid analysis, conducted by Anne Blicher (EPC, DTU Systems Biology), or theoretical extinction coefficients  $E^{0.1\%} = 2.78$  (XlnA) and 2.08 (XlnC, E244A) (<http://www.expasy.ch/tools/protparam.html>; Gasteiger et al., 2005).

Protein purity was assessed by sodium dodecyl sulfate polyacrylamide gel electrophoresis (SDS-PAGE) using NuPAGE Novex Bis-Tris 4–12% gels (Invitrogen) in 1% MES buffered polyacrylamide NuPAGE minigel Novex system with reducing agent added in the sample preparation and antioxidant in the buffer system according to the manufacturer's recommendation followed by Coomassie Brilliant Blue G-250 staining (Candiano et al., 2004).

Isoelectric focusing (IEF) was carried out using 400–800 ng enzyme and Pharmacia PhastSystem (GE Healthcare) with 4 cm polyacrylamide PhastGel IEF, pH

---

<sup>15</sup> For glycosynthase E244A, the fractions were verified only by SDS-PAGE

range 4.0–6.5 using the low range pI (pH 2.5–6.5) calibration kit (GE Healthcare) as marker and stained using PlusOne Silver Stain Kit, Protein (GE Healthcare).

### 5.5.2 Molecular mass determination

The molecular mass of the enzymes was estimated by SDS-PAGE (as described in 5.5.1) and by analytical gel filtration performed using precalibrated Hiload 16/60 Superdex G75 or G200 columns (flow rate: 1 mL/min; Gel Filtration Calibration Kits; GE Healthcare).

### 5.5.3 Glycosylation analysis

*N*-glycosylation was predicted using NetNGlyc 1.0 Server (<http://www.cbs.dtu.dk/services/NetNGlyc/>; Gupta et al., 2004). Deglycosylation of purified enzymes (5–7  $\mu$ g of enzymes) was carried out using Endoglycosidase H (New England BioLabs). The carbohydrate content was quantified by the phenol-sulfuric acid carbohydrate assay (Dubois et al., 1956) using glucose and mannose as standards.

## 5.6 Enzyme activity and kinetics

### 5.6.1 GH3 xylosidases

#### 5.6.1.1 *para*-Nitrophenyl $\beta$ -D-xylopyranoside and *para*-nitrophenyl $\alpha$ -L-arabinofuranoside

$\beta$ -Xylosidase activity was assayed toward 2 mM *p*NPX at 40°C for 10 min in 50 mM sodium acetate pH 5.0 for BxlA or pH 5.2 for BxlB (50  $\mu$ L reaction mixture). The reaction was terminated by addition of 1 M Na<sub>2</sub>CO<sub>3</sub> (100  $\mu$ L) and the absorbance of released *p*NP was measured at 410 nm, with a standard curve of 0.05–0.5 mM *p*NP, by a microtiter plate reader (Bio-Tek Instrument Inc., Winooski, VT). One unit was defined as the amount of enzyme liberating 1  $\mu$ mol of *p*NP per min under the assay condition. Activity and kinetics of BxlB were determined by Dr. Hiroyuki Nakai. The effect of metal ions on activity of BxlA was determined by addition to a final concentration of 5 mM of CaCl<sub>2</sub>, CuCl<sub>2</sub>, MgCl<sub>2</sub>, AgNO<sub>3</sub>, or ZnCl<sub>2</sub> in the assay buffer.

The pH optimum of 71 nM BxlA and 79 nM BxlB was determined using 2 mM *p*NPX in 40 mM Britton-Robinson buffer (Britton and Robinson, 1931) in the pH range 2.0–10.0. The temperature optimum was determined in the range 25–80°C in 50 mM sodium acetate pH 5.0 (BxlA) or pH 5.2 (BxlB) using the same enzyme concentrations. The dependence of stability on pH and temperature was deduced from residual activity measured using  $\beta$ -xylosidase activity assay for 355 nM BxlA and 395 nM BxlB. The pH stability was analysed at 40°C for 5 h in 40 mM Britton-Robinson buffer pH 2.0–10.0, and the temperature stability was determined in 50 mM sodium acetate pH 5.0 at 25–80°C, 5 h.

The initial rates of hydrolysis towards 8 different concentrations of *p*NPX (0.1–8.0 mM) and *p*NPA (0.2–2.0 mM) were measured using 40 nM (for *p*NPX) and 465 nM (for *p*NPA) of BxlA, and towards 11 different concentrations of *p*NPX (0.1–8.0 mM) and *p*NPA (0.1–8.0 mM) using 66 nM (for *p*NPX) and 328 nM (for

*p*NPA) of BxlB. *p*NP was quantified spectrophotometrically at 410 nm using a standard curve of 0.05–0.5 mM *p*NP. Kinetic parameters,  $K_m$  and  $k_{cat}$ , were determined by fitting the Michaelis-Menten equation to the initial rate data using SigmaPlot v. 9.0.1 (Systat Software Inc. San Jose, CA). For *p*NPA having higher  $K_m$  than the highest substrate concentration used, the  $k_{cat}/K_m$  was calculated as slope of the plot of velocity per enzyme concentration ( $v/[E]$ ) as a function of substrate concentration.

### 5.6.1.2 Xylooligosaccharides

The initial rates of hydrolysis toward 8 different concentrations of xylooligosaccharides (X2–X6, 0.4–6.0 mM) were measured using 32 nM (for X2–X5), and 35 nM (for X6) BxlA. Eleven different concentrations of X2 (1.0–8.0 mM), X3–X4 (0.8–8.0 mM), and X5–X6 (1.0–8.0 mM) were analysed using 66 nM (for *p*NPX and X2–X6) and 328 nM (for *p*NPA) BxlB. The hydrolytic activity towards xylooligosaccharides was assayed in 50 mM sodium acetate pH 5.0 for BxlA or pH 5.2 for BxlB (100  $\mu$ L reaction mixture). The reaction was terminated by addition of 2% *p*-bromoaniline (w/v) in glacial acetic acid with 4% thiourea (w/v) (500  $\mu$ L) and the mixture was incubated in the dark at 70°C for 10 min followed by incubating at 37°C for 60 min. The absorbance at 520 nm, using standard curve of 0.25–5.0 mM xylose, was measured on a microtiter plate reader (Bio-Tek Instrument Inc.), as the formation of furfural from pentoses in acetic acid containing thiourea with *p*-bromoaniline acetate (Deschatelets and Yu, 1986; Roe and Rice, 1948). Kinetic parameters,  $K_m$  and  $k_{cat}$ , were determined by fitting the Michaelis-Menten equation to the initial rate data using SigmaPlot v. 9.0.1 (Systat Software Inc. San Jose, CA).

## 5.6.2 GH5 mannanases

### 5.6.2.1 Galactomannan and glucomannan

$\beta$ -Mannanase activity was assayed toward 0.5% (w/v) of three mannans: konjac glucomannan, guar galactomannan, and locust bean gum galactomannan. All substrates (1 g) were dissolved in 6 mL 95% ethanol and stirred in 90 mL deionized water with heating until boiling, and the stirring was continued until the mixture was cooled. The volume of the solution was adjusted to 100 mL with deionized water. The enzyme (40  $\mu$ L) was incubated with mannan solution (180  $\mu$ L) and 200 mM sodium acetate pH 5.5 with 0.01% BSA (180  $\mu$ L) at 37°C for 5 min. The reducing sugars liberated in the reaction mixture were determined by adding 3,5-dinitrosalicylic acid solution (600  $\mu$ L), incubating at 95°C for 15 min, cooling on ice for 10 min, and measuring the absorbance at 540 nm (Miller, 1959; Mohun and Cook, 1962) in a 96 well microtiter plate (Bio-Tek Instrument Inc.). One unit was defined as the amount of enzyme liberating 1  $\mu$ mol of mannose per min under the assay condition, using mannose as a standard.

### 5.6.2.2 Mannooligosaccharides

Initial rates of hydrolysis toward M4–M6 (0.2–6.0 mM) were measured using 60 nM (for M4), 30 nM (for M5), and 10 nM (for M6) of ManA, 75 nM (for M4), 15 nM (for M5), and 12 nM (for M6) of ManC, 50 nM (for M4), 28 nM (for M5), and 12

nM (for M6) of ManAS289W, and 120 nM (for M4), 32 nM (for M5), and 20 nM (for M6) of ManCW283S in 100 mM sodium acetate, 0.005% BSA, pH 5.5. The released reducing sugar was quantified by using copper bicinchoninate and measuring the absorbance at 540 nm using mannose as standard (McFeeters, 1980; Mori et al., 2001). Kinetic parameters,  $K_m$  and  $k_{cat}$ , were determined by fitting to the Michaelis-Menten equation to the initial rate data using SigmaPlot v. 9.0.1 (Systat Software Inc).

### 5.6.2.3 Hydrolysis action patterns

The hydrolysis patterns towards 0.5 mM M4–M6 were investigated using the same enzyme concentration for ManA, ManAS289W, ManC, and ManCW283S as in the kinetic assay in 100 mM sodium acetate pH 5.5 at 37°C. Aliquots (6  $\mu$ L) were removed at appropriate intervals and added into 100 mM NaOH (294  $\mu$ L) to stop reaction. The reaction mixtures were quantified based on peak areas of high performance anion exchange chromatography with pulsed amperometric detection (HPAEC-PAD; ICS3000 system; Dionex Corporation, Sunnyvale, CA) equipped with CarboPac PA200 anion exchange column (3  $\times$  250 mm with 3  $\times$  50 mm guard column; Dionex) using isocratic elution of 37.5 mM NaOH for 35 min at 25°C, flow rate: 0.35 mL/min, calibrated with mannose and M2–M6.

## 5.6.3 GH10 xylanase

### 5.6.3.1 Xylans

$\beta$ -Xylanase activity was assayed toward 1% (w/v) birchwood glucuronoxylan and 0.5% (w/v) wheat (low viscosity) and oat spelt arabinoxylans. All substrates (1 or 0.5 g) were dissolved in 80 mL of 50 mM sodium acetate pH 5.0 and heating until clear by microwaving and stirred until the mixture was cooled overnight. The volume of the solution was adjusted to 100 mL with acetate buffer. Enzyme (40  $\mu$ L) was incubated with xylan solution (360  $\mu$ L) at 40°C for 5 min. The released reducing sugar was determined by adding 3,5-dinitrosalicylic acid solution (600  $\mu$ L), incubating at 95°C for 15 min, cooling, and measuring the absorbance at 540 nm in a 96 well microtiter plate (Miller, 1959 and Mohun and Cook, 1962). One unit was defined as the amount of enzyme liberating 1  $\mu$ mol of xylose per min under the assay condition.

## 5.7 Transglycosylation screening and optimization

### 5.7.1 GH3 xylosidases

The transglycosylation reactions (1 mL) containing 200 nM BxlA, 30 mM *p*NPX and 200 mM acceptor candidate (xylose, arabinose, lyxose, L-fucose, L-rhamnose, glucose, galactose, mannose, talose, fructose, xylitol, sorbitol, maltose, sucrose, lactose, cellobiose, turanose, lactulose, L-cysteine, or L-serine) in 50 mM sodium acetate (10 mM for L-cysteine and L-serine reactions) pH 5.0, were incubated at 40°C for 5 h. The products were quantified based on peak areas of HPAEC-PAD (ICS-3000 IC system; Dionex Corporation) equipped with CarboPac PA200 anion exchange column (3  $\times$  250 mm with 3  $\times$  50 mm guard column; Dionex) using a linear 0–75 mM sodium acetate gradient in 100 mM NaOH for 35 min at 25°C, flow rate

0.35 mL/min) using xylobiose and xylotriose as standards for di- and trisaccharide products, respectively. The transglycosylation yield was estimated based on the *p*NPX concentration. Aliquots of 5  $\mu$ L were removed at appropriate intervals during five h and transferred to 100 mM NaOH (195  $\mu$ L) stop solution.

To evaluate the transglycosylation ability of xylosidase subsite +1 mutants, the time course was followed of the transglycosylation reaction (1 mL) of 200 nM C308W or 200 nM N313R, 30 mM *p*NPX and 200 mM acceptor (xylose, galactose, mannose, fructose, or maltose) in 50 mM sodium acetate pH 5.0, at 40°C for 16 h. The products were quantified as described above. Aliquots of 5  $\mu$ L were removed at appropriate intervals during 16 h and transferred to 100 mM NaOH (195  $\mu$ L) stop solution.

### 5.7.2 GH5 mannanases

To evaluate the transglycosylation ability of mannanase subsite +1 mutants, the time course of transglycosylation (1 mL) of 330 nM (ManA and ManAS289W) or 145 nM (ManC and ManCW283S) with 30 mM M4 (without acceptor) or 24 mM M4 with 100 mM M3 in 100 mM sodium acetate pH 5.5, were performed at 37°C for 150–300 min. The reaction mixtures were quantified using HPAEC-PAD (Dionex) as described above using isocratic elution of 50 mM NaOH for 35 min at 25°C (flow rate: 0.35 mL/min) using mannopentaose and mannohexaose as standards for penta- and hexasaccharide products, respectively. The transglycosylation yield was estimated based on the M4 concentration. Aliquots (5  $\mu$ L) were removed at 0, 2.5, 5, 10, 15, 20, 25, 30, 35, 40, 45, 60, 80, 100, 120, and 150 min for ManA and ManC; and at 0, 2.5, 5, 10, 20, 30, 45, 60, 90, 120, 150, 180, 210, 240, 270, and 300 min for ManAS289W and ManCW283S, and added to 100 mM NaOH (245  $\mu$ L) to stop the reaction.

To optimize the novel manno oligosaccharide production by ManC, time course transglycosylation reactions (1 mL) of 145 nM ManC containing 24 mM M4 with 200 mM isomaltotriose or melezitose in 100 mM sodium acetate pH 5.5, were performed at 37°C for 180 min. Aliquots (5  $\mu$ L) were removed at 0, 2.5, 5, 10, 15, 20, 25, 30, 35, 40, 45, 60, 80, 100, 120, 140, 160, and 180 min and added to 100 mM NaOH (245  $\mu$ L) to stop the reaction.

### 5.7.3 GH10 and GH11 xylanases

The transglycosylation reaction mixtures (1 mL), contained 1  $\mu$ M XlnA or XlnC, 20 mM X3 and 200 mM acceptor (xylobiose, cellobiose, maltose, isomaltose, lactose, mannobiose, xylitol, or sorbitol) in 50 mM sodium acetate pH 5.0, at 37°C for 5 h. The products were quantified based on peak areas of HPAEC-PAD (ICS-3000 IC system; Dionex Corporation) equipped with CarboPac PA200 anion exchange column (3  $\times$  250 mm with 3  $\times$  50 mm guard column; Dionex) using 0–75 mM sodium acetate linear gradient in 100 mM NaOH for 35 min at 25°C, flow rate: 0.35 mL/min) using xylotriose, xylotetraose, xylopentaose and xylohexaose as standards for tri-, tetra-, penta-, and hexasaccharide products, respectively. The transglycosylation yield was estimated based on the X3 concentration. Aliquots of 5  $\mu$ L were removed at 0, 5, 15, 30, 45, 60, 120, 180, 240, and 300 min and transferred to 100 mM NaOH (195  $\mu$ L) stop solution.

## 5.7.4 Glycosynthase reactions

Acetylated  $\alpha$ -xylosyl and  $\alpha$ -xylobiosyl fluorides received from Prof. Stephen G. Withers (University of British Columbia, Canada) were deacetylated in collaboration with Dr. Karin Mannerstedt, Prof. Monica Palcic, and Prof. Ole Hindsgaul (Carlsberg Laboratory) for glycosynthase reaction using the catalytic nucleophile mutants of GH3 xylosidase and GH10 xylanase, respectively. Tri-*O*-acetyl  $\alpha$ -xylosyl fluoride (99.6 mg) and hepta-*O*-acetyl  $\alpha$ -xylobiosyl fluoride (51.8 mg) was dissolved in dry methanol (10 and 15 mL, respectively) at 0°C with bubbling of NH<sub>3</sub> gas for 5 min. The reaction was stirred at 0°C without NH<sub>3</sub> gas until all the starting material was deacetylated (1 and 3 h, respectively), as monitored by thin layer chromatography (TLC; aluminium-coated silica gel 60 F<sub>254</sub>, Merck) developed by CHCl<sub>3</sub>/methanol (6:1, v/v for xylosyl fluoride) and ethylacetate/methanol/water (17:2:1, v/v for xylobiosyl fluoride), respectively, soaked with 8% sulfuric acid followed by tarring at 120°C. The deacetylated substrates were rotary evaporated without heating and dissolved in 5 mM ammonium bicarbonate pH 7.0 (to 100 mM final concentration). The  $\alpha$ -xylosyl and  $\alpha$ -xylobiosyl fluoride solutions were immediately frozen and stored at -80°C. The  $\alpha$ -xylosyl and  $\alpha$ -xylobiosyl fluorides are stable at -80°C. The purity of the fluoride substrates was analysed using electrospray ionization mass spectra (ESI-MS; Bruker Esquire 3000-Plus Ion Trap instrument, Bruker Daltonik, Bremen, Germany).

GH3  $\beta$ -xylosidase glycosynthase mutants D288A and D288C (50  $\mu$ M) were incubated with 2 mM  $\alpha$ -xylosyl fluoride ( $\alpha$ XF) as donor and 2 mM acceptor (*p*NP  $\alpha$ -L-arabinopyranoside (*p*NP*A**p*), lyxose, galactose, or cellobiose) in 100 mM sodium acetate (pH 5.0, pH 5.5, pH 6.0) or 100 mM phosphate buffer (pH 6.5, pH 7.0) at 30°C for 40 h. The reaction products were monitored by thin layer chromatography (TLC) developed by 100% acetonitrile (for reaction with *p*NP*A**p*) or acetonitrile/water (85:15, v/v; for reaction with sugars), sprayed with 2% orcinol in sulphuric acid/water/ethanol (10:10:80, v/v/v) followed by tarring at 120°C.

GH10 xylanase glycosynthase mutant E244A 87  $\mu$ M was incubated with 10 mM  $\alpha$ -xylobiosyl fluoride ( $\alpha$ X2F) as donor and 5 mM X2 or X3 as acceptors in 100 mM sodium acetate pH 5.0 at 30°C for 24 h. Control reactions were performed by incubating the E244A mutant with either 10 mM  $\alpha$ X2F donor or 5 mM of each acceptor to monitor hydrolytic activity of E244A and incubating 10 mM  $\alpha$ X2F without E244A mutant to monitor stability of fluoride substrate during the reaction. The reaction products were monitored by TLC developed by acetonitrile/water (80:20, v/v; twice), sprayed with 2% orcinol solution followed by tarring at 120°C.

## 5.8 Oligosaccharides production by transglycosylation for structural analysis

### 5.8.1 GH3 xylosidases

Xylooligosaccharide products were obtained in 1 mL reaction mixtures containing 200 nM BxlA and 30 mM *p*NPX with 200 mM acceptor (xylose, arabinose, lyxose, L-fucose, glucose, mannose, talose, sucrose, or turanose) incubated at 40°C in 50 mM sodium acetate pH 5.0. The reaction time for each reaction was according to maximum transglycosylation yield obtained from 5.7.1. The reaction was terminated by heat inactivation (95°C, 10 min), centrifuged (18,000g, 4°C, 5 min), desalted (Amberlite MB-20; Fluka, Sigma Aldrich), and filtered (0.45  $\mu$ m nylon filter;

Frisenette Aps, Knebel, Denmark). The xylooligosaccharide products were purified using high performance liquid chromatography (HPLC; UltiMate 3000 Standard LC system; Dionex) equipped with a TSKgel Amide-80 column (5  $\mu\text{m}$ , 4.6  $\times$  250 mm with 4.6  $\times$  10 mm guard column; TOSOH, Tokyo, Japan) and refractive index detector (RI-101; Showa Denko, Kanagawa, Japan) at constant flow rate 1 mL/min of mobile phase (acetonitrile/water 80:20 or 85:15, v/v) at 70°C. The purity was confirmed by TLC (aluminium-coated silica gel 60 F<sub>254</sub>, Merck) developed by acetonitrile/water (80:20, v/v), sprayed with 2% orcinol solution followed by tarring at 120°C.

## 5.8.2 GH5 mannanases

Mannooligosaccharide products were obtained in 1 mL reaction mixtures containing 145 nM ManC and 24 mM M4 with acceptors; 100 mM mannotriose; 200 mM isomaltotriose or 200 mM melezitose incubated at 37°C (60 min for mannotriose, 120 min for isomaltotriose, 180 min for melezitose) in 100 mM sodium acetate, pH 5.5. The reaction was terminated by heat inactivation at 95°C for 10 min, centrifuged (18,000g, 4°C, 5 min), desalted (Amberlite MB-20; Fluka, Sigma Aldrich), and filtered (0.45  $\mu\text{m}$  nylon filter; Frisenette Aps). The mannoooligosaccharide products were purified using HPLC (UltiMate 3000 Standard LC system; Dionex) equipped with a TSKgel Amide-80 column (5  $\mu\text{m}$ , 4.6  $\times$  250 mm with 4.6  $\times$  10 mm guard column; TOSOH) and refractive index detector (RI-101; Showa Denko) under a constant flow rate (1 mL/min) of mobile phase (acetonitrile/water 70:30, v/v) at 70°C. The purity was confirmed by TLC (aluminium-coated silica gel 60 F<sub>254</sub>, Merck) developed by acetonitrile/water (70:30, v/v) twice, sprayed with 2% orcinol solution followed by tarring at 120°C.

## 5.9 Oligosaccharide characterisation

### 5.9.1 Nuclear magnetic resonance spectroscopy

500  $\mu\text{L}$  of 1–2 mM purified xylooligosaccharide products were vacuum dried (Savant SVC100 SpeedVac Concentrator; Savant Instruments, Inc. Farmingdale, NY) or freeze dried (CoolSafe -55°C; ScanLaf A/S, Lyngø, Denmark) and dissolved in deuterium oxide. Nuclear magnetic resonance spectroscopy (NMR) was performed in collaboration with Assoc. Prof. Charlotte H. Gotfredsen (DTU Kemi). The structure of transglycosylation products was determined by <sup>1</sup>H- and <sup>13</sup>C-NMR analysis. Spectra were recorded on a Varian Unity Inova 500 MHz NMR spectrometer and a few on a Bruker Avance 800 MHz spectrometer (at the Danish Instrument Center for NMR Spectroscopy of Biological Macromolecules). A series of two-dimensional homo- and heteronuclear correlated spectra: Double-Quantum Filtered COrrrelation Spectroscopy (DQF-COSY), Nuclear Overhauser Enhancement Spectroscopy (NOESY), gradient Heteronuclear Single Quantum Coherence (gHSQC), and gradient Heteronuclear Multiple Bond Correlation (gHMBC), were acquired using standard pulse sequences. The NMR data used for the structural assignment were acquired in D<sub>2</sub>O. The chemical shifts were referenced to the solvent  $\delta_{\text{H}}$  4.78 ppm and the carbon shifts were references according to C5 of xylose at 66.1 ppm.

### 5.9.2 Electrospray ionization mass spectrometry

Molecular mass of xylooligosaccharide products as determined in collaboration with Ph.D. student Yvonne Westphal, Dr. Maaïke Appeldoorn, and Prof. Henk A. Schols (Laboratory of Food Chemistry, Wageningen University, The Netherlands) by electrospray ionization mass spectrometry (ESI-MS) using an LTQ XL ion trap MS (Thermo Scientific, San Jose, CA). Samples were vacuum dried (Savant SVC100 SpeedVac Concentrator; Bx1A) or freeze dried (CoolSafe -55°C; Bx1B) and dissolved in milliQ water (100 µg/mL) prior to introduction through a Thermo Accela UHPLC system equipped with a Hypercarb (100 × 2.1 mm, 3 µm) column (Thermo Scientific) eluted with a gradient of deionized water/acetonitrile and 0.2% trifluoroacetic acid (0.4 mL·min<sup>-1</sup>; 70°C). MS detection was performed in the positive mode using a spray voltage of 4.5 kV and a capillary temperature of 260°C and auto-tuned on glucosyltransferase (Westphal et al., 2010).

Electrospray quadrupole time-of-flight mass spectrometry (ESI-Q-TOF MS) was used for detecting the products from the reaction of L-cysteine and L-serine. The ESI-Q-TOF MS was performed in collaboration with Dr. Martin Zehl and Prof. Peter Roepstorff (Department of Biochemistry and Molecular Biology, University of Southern Denmark, Odense, Denmark). The sample mixtures (200 nM Bx1A, 30 mM *p*NPX and 200 mM L-cysteine or L-serine in 10 mM sodium acetate pH 5.0, 40°C reacted for 60 min) were diluted 100 fold in isopropanol/water (1:1, v/v) and introduced into an orthogonal ESI ion source at a flow rate of 5 µL/min. Measurements were performed using a Waters SYNAPT-HDMS System (Waters Corporation, Milford, MA) in positive ion V mode. CID fragment ions of Glu-Fibrinopeptide were used for calibration.

### 5.9.3 Matrix-assisted laser desorption/ionisation-time of flight mass spectrometry

The molecular masses of mannooligosaccharides were determined by Matrix-assisted laser desorption/ionisation-time of flight mass spectrometry (MALDI-TOF MS) using an Ultraflex II TOF/TOF instrument (Bruker Daltonics GmbH, Bremen, Germany) equipped with all solid-state laser system. The mass spectrometer was selected for positive ions and analysed at 25040 V and detected using reflector mode. High (75%) laser power was required to obtain good spectra and at least 100 spectra were collected. The mass spectrometer was calibrated using mannopentaose, mannohexaose, and trypsin-digested β-lactoglobulin (mass range *m/z* 851–2313, as Na<sup>+</sup> adducts for M5 and M6). The matrix solution was prepared by dissolving 10 mg 2,5-dihydroxybenzoic acid in 1 mL of acetonitrile/water (30:70, v/v) containing 10 mM NaCl. The 0.2 mM (for M5 and manno-isomaltotrioses) or 0.1 mM (for M6 and manno-melezitoses) of samples (1 µL) and matrix (1 µL) were pipetted onto a MALDI-TOF-target plate (Bruker Daltonics) and the mixtures were air-dried prior to analysis.

## 5.10 GH61 putative endo-β-glucanase

### 5.10.1 Cultures of *Aspergillus nidulans* FGSC A4 on polymeric substrates



To demonstrate enzyme discovery by using the proteomic strategy and to investigate the function of GH61 putative endo- $\beta$ -glucanase from *A. nidulans* FGSC A4 (see 4.4.3), cDNA cloning and recombinant production of this putative enzyme was performed. *A. nidulans* FGSC A4 was grown on minimal agar medium (0.6% NaNO<sub>3</sub>, 0.052% KCl, 0.052% MgSO<sub>4</sub>·7H<sub>2</sub>O, 1 mL trace element, 12 mM phosphate buffer pH 6.8, 1.25% agar; Barratt et al., 1965) containing 1% barley  $\beta$ -glucan or oat spelt xylan at 30°C for 5 days. The spores were suspended in 0.02% TWEEN-80 and grown in minimal medium without agar at 30°C for 1 day with shaking at 130 rpm. The cells were harvested by decanting the culture supernatant.

### 5.10.2 cDNA cloning

Two g of fungal cells was placed in a liquid nitrogen-cooled mortar with addition of liquid nitrogen and ground with a pestle until the cells became a fine powder. The mRNA isolation from the crushed fungal cells was performed using FastTrack 2.0 Kit for isolation of mRNA (Invitrogen) and the cDNA library was prepared using SuperScript III First Strand Synthesis System for reverse transcriptase polymerase chain reaction (Invitrogen). The *eglF* gene was obtained by amplification of target cDNA using Expand High Fidelity DNA polymerase (Roche Diagnostics GmbH) and oligonucleotide primers (Table 5, page 32), constructed based on genomic sequence (Galangan et al., 2005). The original signal peptide was Met1–Ala20 predicted by SignalP 3.0 (<http://www.cbs.dtu.dk/services/SignalP/>; Bendtsen et al., 2004). The PCR products were digested by XhoI and XbaI (New England BioLabs) and cloned into the pPICZ $\alpha$ A vector (Invitrogen). The plasmids were transformed into *Escherichia coli* DH5 $\alpha$  (Invitrogen) and transformants were selected on low salt LB supplemented with 25  $\mu$ g/mL Zeocin. The purified plasmids (QIAGEN plasmid midi kit; QIAGEN, Hilden, Germany) were confirmed by full-length sequencing (Eurofins MWG Operon). The plasmids were linearised by PmeI and transformed into *P. pastoris* strain X-33 as described in 5.3.1.

### 5.10.3 Production and purification of GH61 putative endo- $\beta$ -glucanase

*P. pastoris* X-33 transformant harbouring EglF was grown in 3  $\times$  1 L of BMGY at 30°C in 3  $\times$  2.5 L plastic shake flask for 24 h to OD<sub>600</sub> of 32. Cells were harvested (3000g, 5 min, 4°C) and resuspended in 1 L BMM in 2.5 L plastic shake flask. The induction was continued at 22°C for 72 h. Methanol was supplemented to a final concentration of 1% (v/v) every 24 h until harvest by centrifugation (13,500g, 4°C, 1 h). The putative endo- $\beta$ -glucanase was purified by anion exchange chromatography followed by gel filtration chromatography (as described in 5.4.1). Since this protein showed very low activity and had a low pI (4.0), anion exchange chromatography was used to avoid the effect of high pH as observed in case of BxlA (see 5.4.1) or metal inhibition, if any.

Endo- $\beta$ -glucanase activity was assayed toward 1% (w/v) barley  $\beta$ -glucan and 0.5% (w/v) oat spelt arabinoxylans in 50 mM sodium acetate pH 4.0–6.0 using 3,5-dinitrosalicylic acid solution as described in 5.6.3.1.

### 5.10.4 Carbohydrate microarray analysis

Carbohydrate microarray analysis was performed in collaboration with Dr. Henriette Lodberg Pedersen and Prof. William G. T. Willats (Department of Plant Biology and Biotechnology, Faculty of Life Sciences, University of Copenhagen, Denmark). The carbohydrate microarrays contain different mono-, oligo-, and polysaccharides extracted from plant cell walls (Fig. 10). The monoclonal antibodies against specific plant cell wall carbohydrate epitopes were probed to detect any epitope deletion as a result of enzyme hydrolysis (5.10.4.1; Moller et al., 2007; Øbro et al., 2007; Øbro et al., 2009) or anti-His antibody were probed to detect possible binding of the His-tagged protein to carbohydrates in the arrays (5.10.4.2). The experimental scheme is shown in Fig. 11.

#### **5.10.4.1 Screening for EglF activity on carbohydrate microarrays *via* post-print epitope deletion**

Arrays were initially blocked for 1 h at ambient temperature in 5% low fat milk powder (MP) in phosphate buffered saline (PBS: 140 mM NaCl, 2.7 mM KCl, 10 mM Na<sub>2</sub>HPO<sub>4</sub>, 1.7 mM KH<sub>2</sub>PO<sub>4</sub>, pH. 7.5). After blocking, the MP-PBS solution was discarded and the arrays were divided into two batches; one batch was probed with a panel of plant cell wall directed monoclonal antibodies (from PlantProbes, University of Leeds) in MP-PBS for 2 h at ambient temperature. The arrays were washed and probed with alkaline phosphatase conjugated anti-rat monoclonal antibody in MP-PBS for 2 h at ambient temperature followed by a second round of washing (3 × 10 min in PBS, 1 × 2 min H<sub>2</sub>O). The arrays were finally submerged for 5–10 min in AP buffer (100 mM Tris-base, 100 mM NaCl, 5 mM MgCl<sub>2</sub>, pH. 9.5) containing nitro blue tetrazolium (NBT) and 5-bromo-4-chloro-3-indolyl phosphate (BCIP). Binding of the antibodies was visualized as black spots, where binding strength correlates to spot intensity (pixels per inch, ppi). The second batch of arrays was incubated with EglF for 24 h at 25–28°C before the arrays were probed with the same panel of plant cell wall directed monoclonal antibodies as used for the first batch of arrays. Epitope deletion would be observed as a change in spot intensity between two arrays probed with the same antibody, but where one of the arrays initially were incubated with enzyme prior to antibody labeling (Moller et al., 2007; Øbro et al., 2007; Øbro et al., 2009).

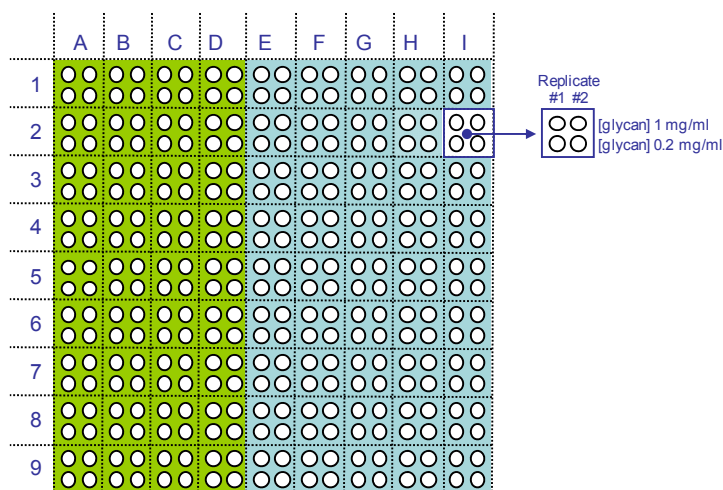
The experiment was executed 4 times:

1. The second batch of arrays was incubated with EglF (10 µg/mL) in MES buffer (20 mM MES, 0.5 mM MgCl<sub>2</sub>, pH 6.0)
2. The second batch of arrays was incubated with EglF (10 µg/mL) in HEPES buffer (20 mM HEPES, 0.5 mM MgCl<sub>2</sub>, pH 7.0)
3. The second batch of arrays was incubated with EglF (100 µg/mL) in HEPES buffer (20 mM HEPES, 0.5 mM MgCl<sub>2</sub>, pH 7.0)
4. The second batch of arrays was incubated with EglF (100 µg/mL) in acetate buffer (100 mM sodium acetate, 0.5 mM MgCl<sub>2</sub>, pH 4.5)

The plant cell wall directed mAbs used in the experiments were selected such that they collectively recognized the glycan structures presented on the carbohydrate microarrays.

#### **5.10.4.2 Screening for EglF binding to carbohydrate microarrays**

Two arrays were blocked in 5% MP in HEPES buffer (20 mM HEPES, 0.5 mM MgCl<sub>2</sub>, pH 7.0) or MES buffer (20 mM MES, 0.5 mM MgCl<sub>2</sub>, pH 6.0) for 1 h at ambient temperature. The blocking solution was discarded and the arrays were probed with EglF (20 µg/ml) in MP-buffer solution (the buffer corresponding to the buffer used for blocking) at ambient temperature. After 2 h, the arrays were washed (3 × 10 min in HEPES or MES buffer) and probed with alkaline phosphatase conjugated anti-His antibody in MP-buffer for 2 h at ambient temperature. Finally, the arrays were washed (3 × 10 min buffer, 1 × 2 min H<sub>2</sub>O) and developed in MP-buffer (pH 9.5) containing NBT and PBS for 20 min. Control arrays, where MP-buffer was applied instead of EglF solution, were included to reveal possible binding of the anti-His antibody to the epitopes displayed on the arrays.



### Oligosaccharides - BSA conjugated

A1	$\alpha$ -(1→4)-D-heptagalacturonate (DE 0%)
B1	$\alpha$ -(1→4)-D-pentagalacturonate (DE 0%)
C1	$\beta$ -D-galactose
D1	$\beta$ -(1→4)-D-galactotetraose
A2	$\alpha$ -L-arabinose
B2	$\alpha$ -(1→5)-L-arabinobiose
C2	$\alpha$ -(1→5)-L-arabinotriose
D2	$\alpha$ -(1→5)-L-arabinotetraose
A3	$\alpha$ -(1→5)-L-arabinopentaose
B3	$\alpha$ -(1→5)-L-arabinohexaose
C3	$\alpha$ -(1→5)-L-arabinoheptaose
D3	$\beta$ -(1→4)-D-glucopentaose
A4	$\beta$ -D-mannose
B4	$\beta$ -(1→4)-D-mannotriose
C4	$\beta$ -(1→4)-D-mannotetraose
D4	$\beta$ -(1→4)-D-mannopentaose
A5	$\beta$ -D-xylose
B5	$\beta$ -(1→4)-D-xylotriase
C5	$\beta$ -(1→4)-D-xylotetraose
D5	$\beta$ -(1→4)-D-xylopentaose
A6	Xyloglucan heptamer XXX(G)-
B6	Xyloglucan octamer XXL(G)-
C6	Xyloglucan nonamer XLL(G)-
D6	6 <sup>1</sup> - $\alpha$ -D-galactosyl- $\beta$ -(1→4)-D-mannobiose
A7	(1→3),(1→4)- $\beta$ -D-glucotriose [G4G3G(G)-]
B7	(1→3),(1→4)- $\beta$ -D-glucotetraose [G3G4G4G(G)-]
C7	(1→3),(1→4)- $\beta$ -D-glucopentaose [G3G4G3G4G(G)-]
D7	6 <sup>3</sup> ,6 <sup>4</sup> -di galactosyl- $\beta$ -(1→4)-D-mannotetraose
A8	$\alpha$ -(1→4)-D-glucobiose
B8	$\alpha$ -(1→4)-D-glucopentaose
C8	$\alpha$ -(1→6)-D-glycosyl- $\alpha$ -(1→4)-D-maltotriose G6G4G
D8	$\alpha$ -(1→6)-D-glycosyl- $\alpha$ -(1→4)-D-maltosyl-maltose G6G4G4G6G4G
A9	$\beta$ -D-glucose
B9	$\beta$ -(1→3)-D-glucotriose
C9	$\beta$ -(1→3)-D-glucotetraose
D9	$\beta$ -(1→3)-D-glucopentaose

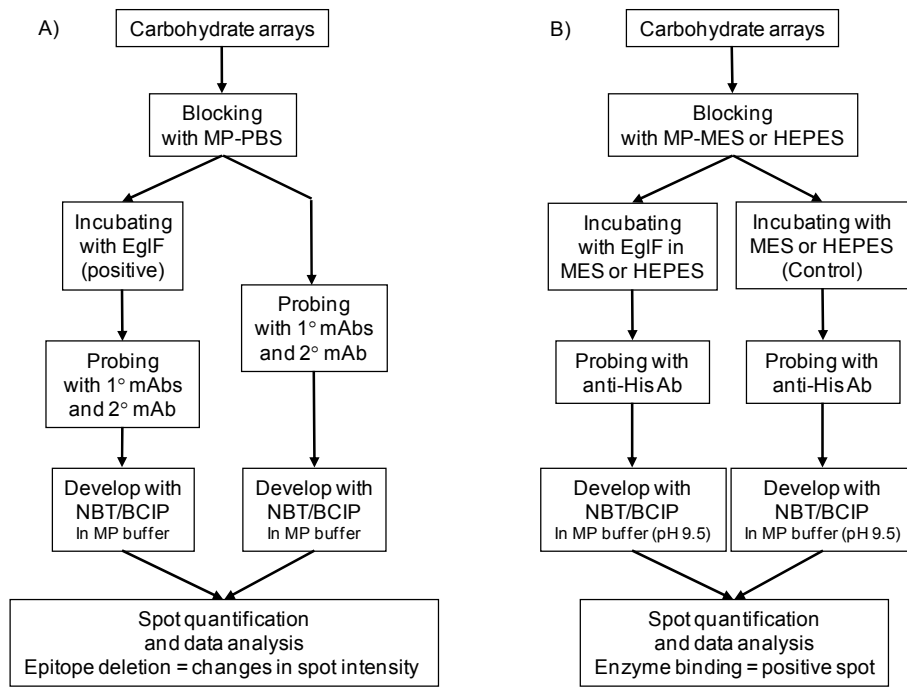
\* DE; degree of methyl esterification

### Polysaccharides

E1	Lime pectin, DE 11% (Danisco #F11)
F1	Lime pectin, DE 43% (Danisco #F43)
G1	Lime pectin DE 0% (Danisco #B00)
H1	Lime pectin, DE 16% (Danisco #P16)
I1	Sugar beet pectin (Danisco #SBP6232)
E2	Pectic galactan #1 (lupin, INRA/Nantes)
F2	Pectic galactan #2 (potato, INRA/Nantes)
G2	Pectic galactan #3 (lupin, Megazyme)
H2	Pectic galactan #4 (tomato, J. Paul Knox)
I2	RGI1 enriched pectin (red wine)
E3	RGI #1 (soy bean, Megazyme)
F3	RGI #2 (carrot, INRA/Nantes)
G3	RGI #3 (sugar beet, INRA/Nantes)
H3	RGI #4 (Arabidopsis, INRA/Nantes)
I3	Seed mucilage (Arabidopsis, INRA/Nantes)
E4	Arabinan (sugar beet, Megazyme)
F4	Arabinan, de-branched (sugar beet, Megazyme)
G4	(1→5)- $\alpha$ -L-arabinan (sugar beet, Megazyme)
H4	RGI #5 (potato, Megazyme)
I4	Xylogalacturonan, XGA (apple, INRA/Nantes)
E5	Xylan (birch wood, Sigma-Aldrich)
F5	Arabinoylan (wheat, Megazyme)
G5	4-Methoxy-glucoronoarabinoxylan (birch, Sigma-Aldrich)
H5	Xyloglucan, non fucosylated (tamarind seed, Megazyme)
I5	Xyloglucan, fucosylated (pea, INRA/Nantes)
E6	Carboxymethyl-cellulose, CM-cellulose (Avicel)
F6	Hydroxymethyl-cellulose, MeO-cellulose (Avicel)
G6	Hydroxyethyl-cellulose, EtO-cellulose (Avicel)
H6	(1→6),(1→3)- $\beta$ -D-glucan (laminarin, Sigma-Aldrich)
I6	(1→3)- $\beta$ -D-glucan (pachyman)
E7	$\beta$ -glucan #1 (lichenan, icelandic moss, Megazyme)
F7	$\beta$ -glucan #2 (barley, Megazyme)
G7	$\beta$ -glucan #3 (oat, Megazyme)
H7	$\beta$ -glucan #4 (yeast)
I7	(1→6),(1→4)- $\alpha$ -D-glucan (pullulan)
E8	Glucomannan
F8	Galactomannan
G8	Gum guar
H8	Gum Arabic (Sigma-Aldrich)
I8	Locust bean gum (Megazyme)
E9	Xanthan gum (Danisco #R80)
F9	Carrageenan #1 (Danisco #I00)
G9	Carrageenan #2 (Danisco #201)
H9	Alginate, sodium salt (Danisco #FD-155)
I9	Sugar beet arabinan (Megazyme)

**Figure 10** Layout of carbohydrate microarrays (adapted from Øbro et al., 2009)

figure courtesy of Dr. Henriette Lodberg Pedersen.



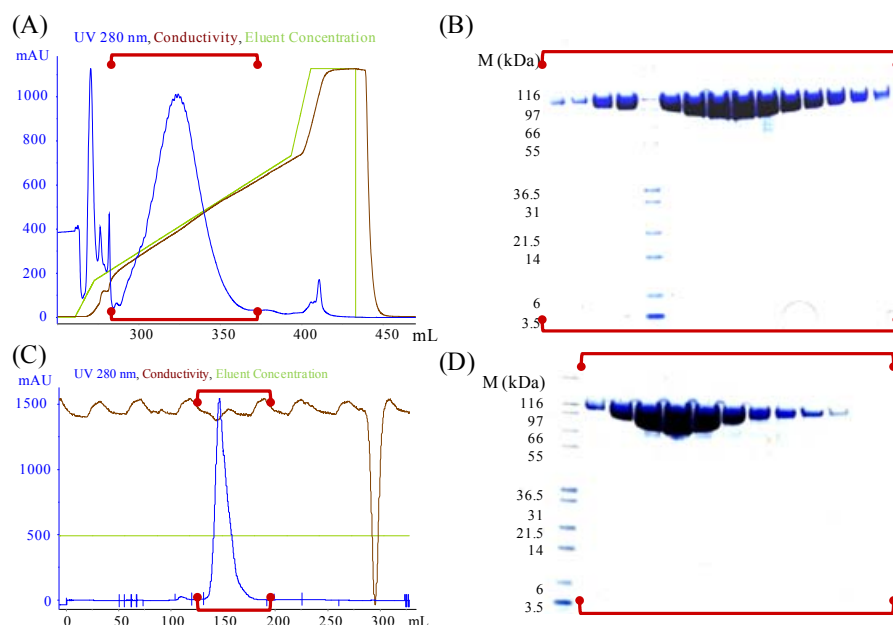
**Figure 11** Overview of the experimental approach for carbohydrate microarray analysis. A) Screening for EglF activity on carbohydrate microarrays *via* post-print epitope deletion, B) screening for EglF binding to carbohydrate microarrays. 1° mAbs, plant cell wall directed monoclonal antibodies (from Plant Probes, Leeds University); 2° mAb, alkaline phosphatase conjugated anti-rat monoclonal antibody; anti-His Ab, alkaline phosphatase conjugated anti-His antibody.

## 6. Results

### 6.1 GH3 xylosidases

#### 6.1.1 Production and purification

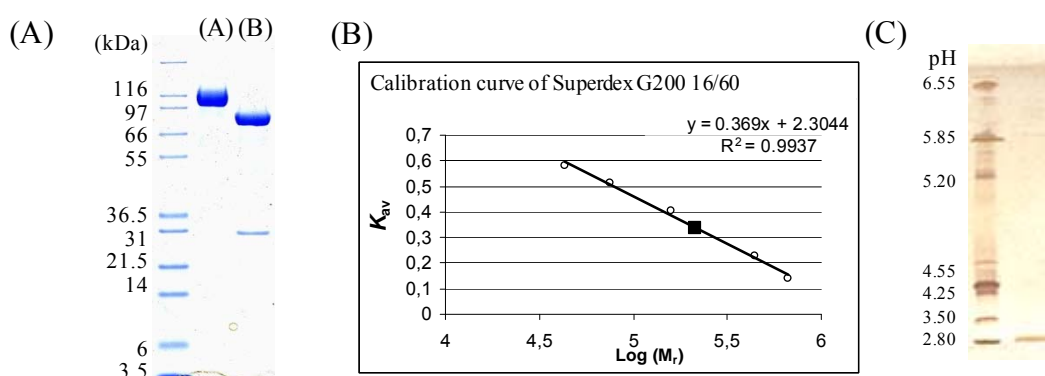
The  $\beta$ -xylosidase BxlA from *A. nidulans* FGSC A4 was produced recombinantly as His-tag fusion protein in *P. pastoris* X-33 secreted as directed by the  $\alpha$ -factor secretion signal peptide. BxlA was purified by anion exchange chromatography (Fig. 12A,B) followed by gel filtration chromatography (Fig. 12C,D) in a yield of 16 mg/L culture.



**Figure 12** Purification of BxlA. A) anion exchange chromatogram. B) SDS-PAGE of BxlA purified using a Resource Q 6 mL column; 15  $\mu$ L samples loaded. C) gel filtration chromatogram of pooled BxlA fractions from (A). D) SDS-PAGE of BxlA purified by Hiload 26/60 Superdex G200 column; 20  $\mu$ L samples loaded; marker, Mark12 unstained protein standard marker (Invitrogen). The red bars in (A) and (C) show the fractions which are analysed by SDS-PAGE in (B) and (D) (see 5.4.1).

#### 6.1.2 Protein characterisation

BxlA migrated as a single band in SDS-PAGE with an estimated size of 110 kDa (Fig. 13A). This value is larger than the theoretical mass of  $M_r = 86045.2$  and Endoglycosidase H treatment reduced the molecular mass to 86 kDa (Fig. 13A). BxlA contains 10 possible *N*-glycosylation sites and the carbohydrate content was estimated to 29% and 17% by phenol-sulphuric method using glucose and mannose as standards, respectively. These contents are in excellent agreement with the apparent molecular mass found by SDS-PAGE. Gel filtration gave a value of 220 kDa (Fig. 13B) indicating that BxlA is a dimer in solution. The isoelectric point (pI) of BxlA was 3.0 (Fig. 13C) resembling native BxlA (called XlnD)  $\beta$ -xylosidases from *A. nidulans* having values of 3.4 (Kumar and Ramon, 1996).



**Figure 13** Molecular mass determination using SDS-PAGE and gel filtration, deglycosylation, and pI of BxlA. A) SDS-PAGE of purified and deglycosylated BxlA; left lane, marker, Mark12 unstained protein standard marker (Invitrogen); lane (A) 7  $\mu$ g BxlA; lane (B) 7  $\mu$ g deglycosylated BxlA, endoglycosidase H presented as a band at 29 kDa. B) calibration of superdex G200 16/60 column (open circle), BxlA has molecular weight of 220 kDa (filled square). C) isoelectric focusing of 400  $\mu$ g purified BxlA using polyacrylamide PhastGel IEF (pH 4–6.5) with low range pI (pH 2.5–6.5) calibration standard (GE Healthcare).

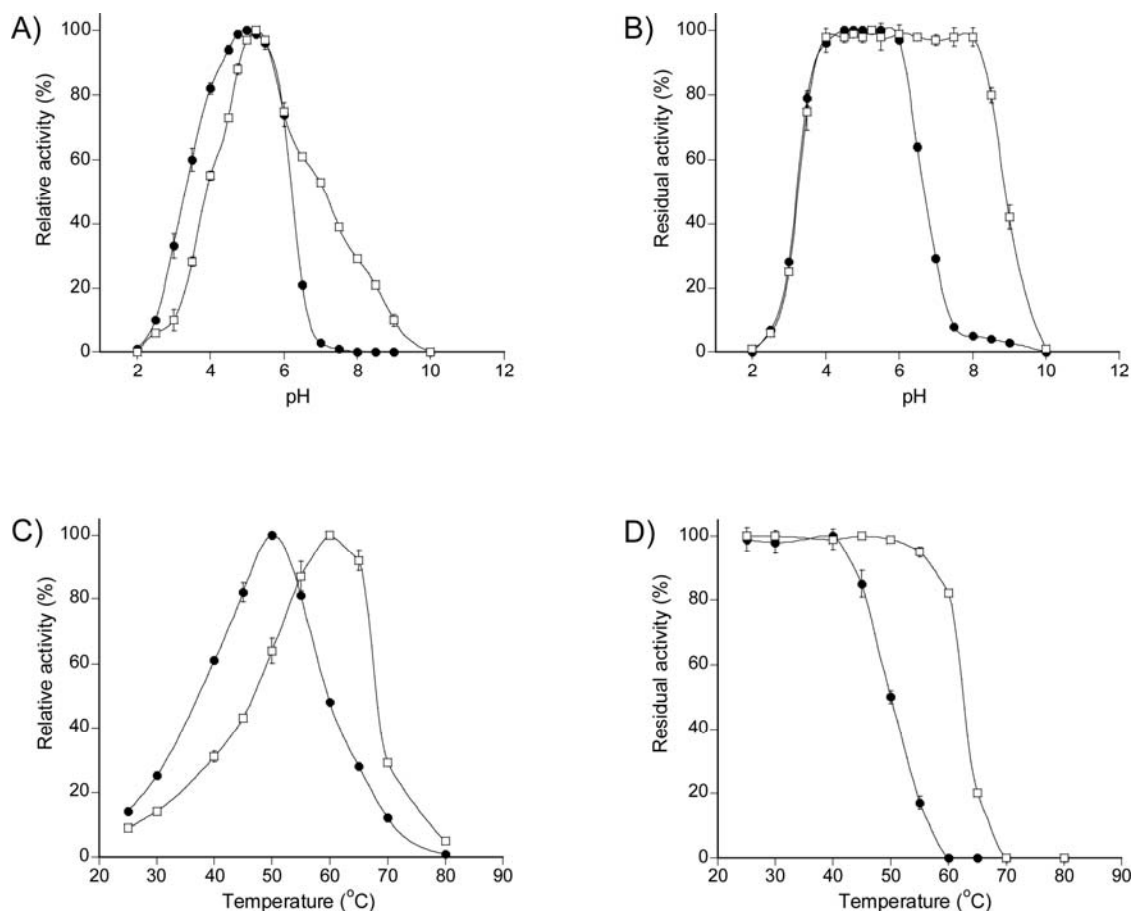
### 6.1.3 Enzymatic specificity and kinetics

BxlA had a specific activity of  $32 \pm 1.6$  U/mg and  $2 \pm 0.2$  U/mg towards 2 mM *p*NPX and *p*NPA, respectively. Among five tested metal ions, BxlA was inhibited importantly by  $\text{Ag}^{2+}$  and  $\text{Cu}^{2+}$  (Table 6). The pH optima for hydrolysis of *p*NPX by BxlA and BxlB (sharing 45% sequence identity, see 4.2.5 and Table 4) were 5.0 and 5.2, respectively (Fig. 14A). The enzymes were stable at pH 4.0–6.0 and 4.0–8.0 (>95% residual activity), respectively (Fig. 14B). BxlA and BxlB showed maximum activity at 50 and 60°C (Fig. 14C) and retained activity up to 40 and 55°C after 5 h incubation (>95% residual activity), respectively (Fig. 14D).

**Table 6** Effect of metal ions on the hydrolytic activity towards *p*NPX of BxlA.

5 mM Metal salt	Relative activity (%)	
	BxlA	XlnD <sup>a</sup>
CaCl <sub>2</sub>	100	111
CuCl <sub>2</sub>	35	9
MgCl <sub>2</sub>	100	114
AgNO <sub>3</sub>	1	7
ZnCl <sub>2</sub>	100	50

<sup>a</sup> From Kumar and Ramón, 1996



**Figure 14** Effect of pH and temperature on activity and stability of purified BxlA (black circle) and BxlB (white square). A) pH-dependence for hydrolysis of *p*NPX by 71 nM BxlA and 79 nM BxlB in 40 mM Britton-Robinson buffer; B) pH-stability of 355 nM BxlA and 395 nM BxlB in 40 mM Britton-Robinson buffer and 5 h incubation; C) temperature-activity dependence for 71 nM BxlA and 79 nM BxlB at 25–80°C with 10 min reaction; D) stability of 355 nM BxlA and 395 nM BxlB in the temperature range 25–80°C for 5 h. Each experiment was made in triplicate. Standard deviations are shown as error bars

Kinetics hydrolysis parameters of BxlA and BxlB towards xylooligosaccharides (X2–X6), *p*NPX, and *p*NPA are shown in Table 7. Among the xylooligosaccharides, both enzymes have highest catalytic efficiency ( $k_{cat}/K_m$ ) towards xylobiose, whereas the efficiency decreased slightly with longer oligosaccharides due to small decreases and increases in  $k_{cat}$  and  $K_m$ , respectively. The catalytic efficiency towards *p*NPX by BxlA was slightly higher than by BxlB for xylobiose, while BxlB showed the same catalytic efficiency towards these substrates. Both enzymes hydrolysed *p*NPA albeit with two and one orders of magnitude lower efficiency, respectively, compared to *p*NPX. BxlA and BxlB have poor affinity for *p*NPA and only  $k_{cat}/K_m$  values were determined.



**Table 7** Kinetic parameters of BxlA and BxlB for hydrolysis of xylooligosaccharides, *p*NPX, and *p*NPA.

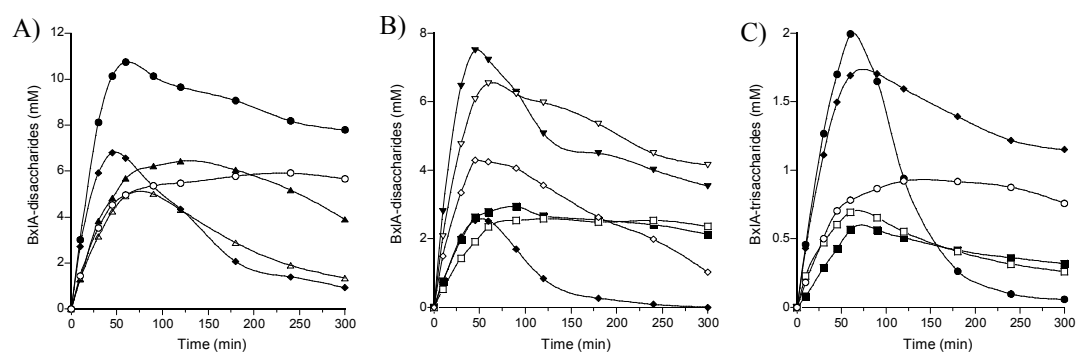
Substrate	BxlA			BxlB		
	$k_{\text{cat}}$ s <sup>-1</sup>	$K_{\text{m}}$ mM	$k_{\text{cat}}/K_{\text{m}}$ s <sup>-1</sup> ·mM <sup>-1</sup>	$k_{\text{cat}}$ s <sup>-1</sup>	$K_{\text{m}}$ mM	$k_{\text{cat}}/K_{\text{m}}$ s <sup>-1</sup> ·mM <sup>-1</sup>
X2	139 ± 7.8	2.0 ± 0.07	70	36 ± 0.7	2.5 ± 0.40	14
X3	122 ± 7.8	2.1 ± 0.14	58	28 ± 0.1	3.0 ± 0.06	9
X4	104 ± 1.1	2.5 ± 0.11	42	25 ± 0.2	3.2 ± 0.15	8
X5	93 ± 4.7	2.8 ± 0.15	33	23 ± 0.2	4.3 ± 0.15	5
X6	65 ± 1.5	3.0 ± 0.14	22	22 ± 0.5	5.2 ± 0.58	4
<i>p</i> NPX	112 ± 1.3	1.3 ± 0.16	90	18 ± 0.4	1.3 ± 0.11	14
<i>p</i> NPA	–	–	0.9	–	–	1.1

Standard deviations were calculated from triplicate experiments (see 5.6.1.1 for experimental details)

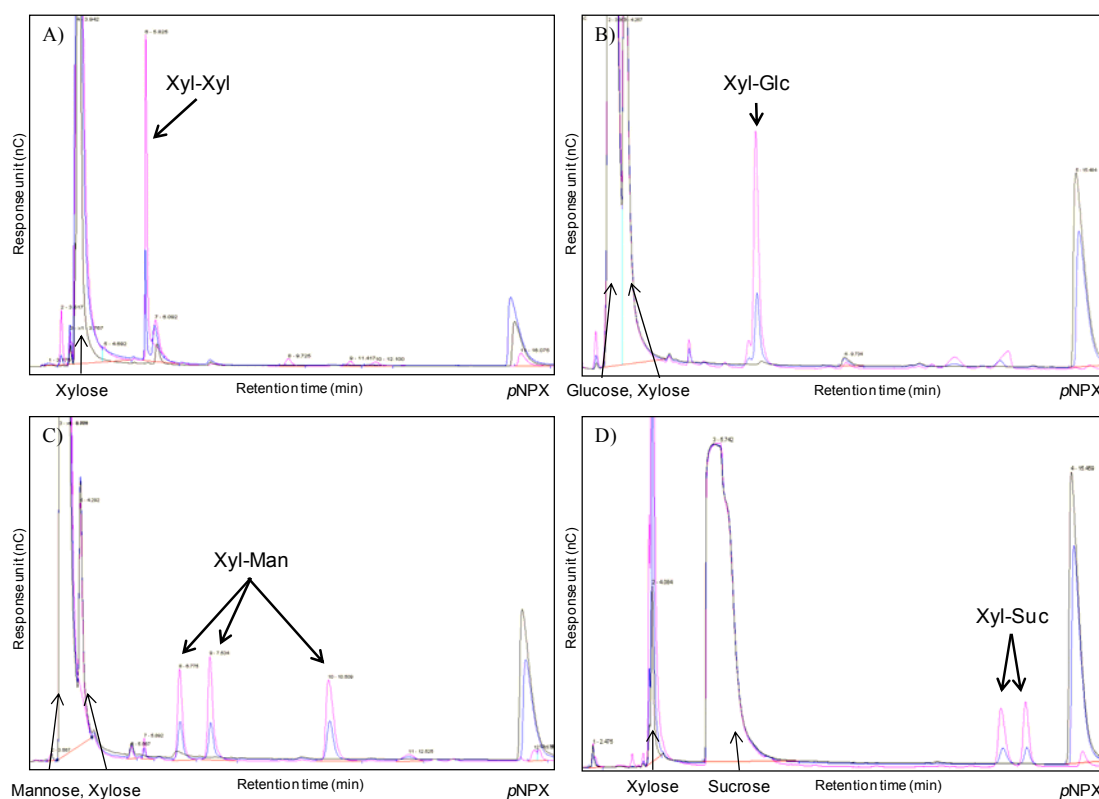
#### 6.1.4 Transglycosylation

The acceptor specificity in transglycosylation for BxlA was investigated using *p*NPX as donor with 10 monosaccharides, six disaccharides, two sugar alcohols, and two amino acids as candidate acceptors. Progress of transglycosylation using 30 mM *p*NPX donor with 200 mM acceptor was monitored by HPAEC-PAD during 5 h (Fig. 15). In many transglycosylation reactions, more than one transglycosylation products were formed as detected by HPAEC-PAD (Fig. 16). The mixed products may be due to the formation of products with different linkages, different forms ( $\alpha$ ,  $\beta$ , furanosyl, pyranosyl), or longer chains (in case the enzyme uses a transglycosylation product as acceptor in a second transglycosylation reaction), therefore the total product yields (products/donor, mM/mM) for each acceptor was estimated by the maximum formation of products during the observation period (Table 8).

All tested monosaccharides except L-rhamnose were accommodated as acceptors by BxlA, which showed preference, however, for mannose, talose, lyxose, and xylitol, as gave similar yield to xylose and was less efficient in accepting glucose, galactose and fructose. BxlA poorly used disaccharides as acceptors, even though it showed preference to use turanose and sucrose to lactulose, maltose, and cellobiose, and could not use lactose as acceptor



**Figure 15** Progress of transglycosylation with different acceptors catalysed by BxlA. Reactions containing 200 nM BxlA, 30 mM *p*NPX, and 200 mM acceptor; A) acceptor: xylose ( $\blacktriangle$ ), arabinose ( $\triangle$ ), lyxose ( $\blacklozenge$ ), xylitol ( $\bullet$ ), sorbitol ( $\circ$ ); B) acceptor: glucose ( $\blacksquare$ ), galactose ( $\square$ ), mannose ( $\blacktriangledown$ ), talose ( $\nabla$ ), fructose ( $\blacklozenge$ ), L-fucose ( $\diamond$ ); C) acceptor: maltose ( $\blacksquare$ ), sucrose ( $\blacklozenge$ ), cellobiose ( $\square$ ), turanose ( $\bullet$ ), lactulose ( $\circ$ ).



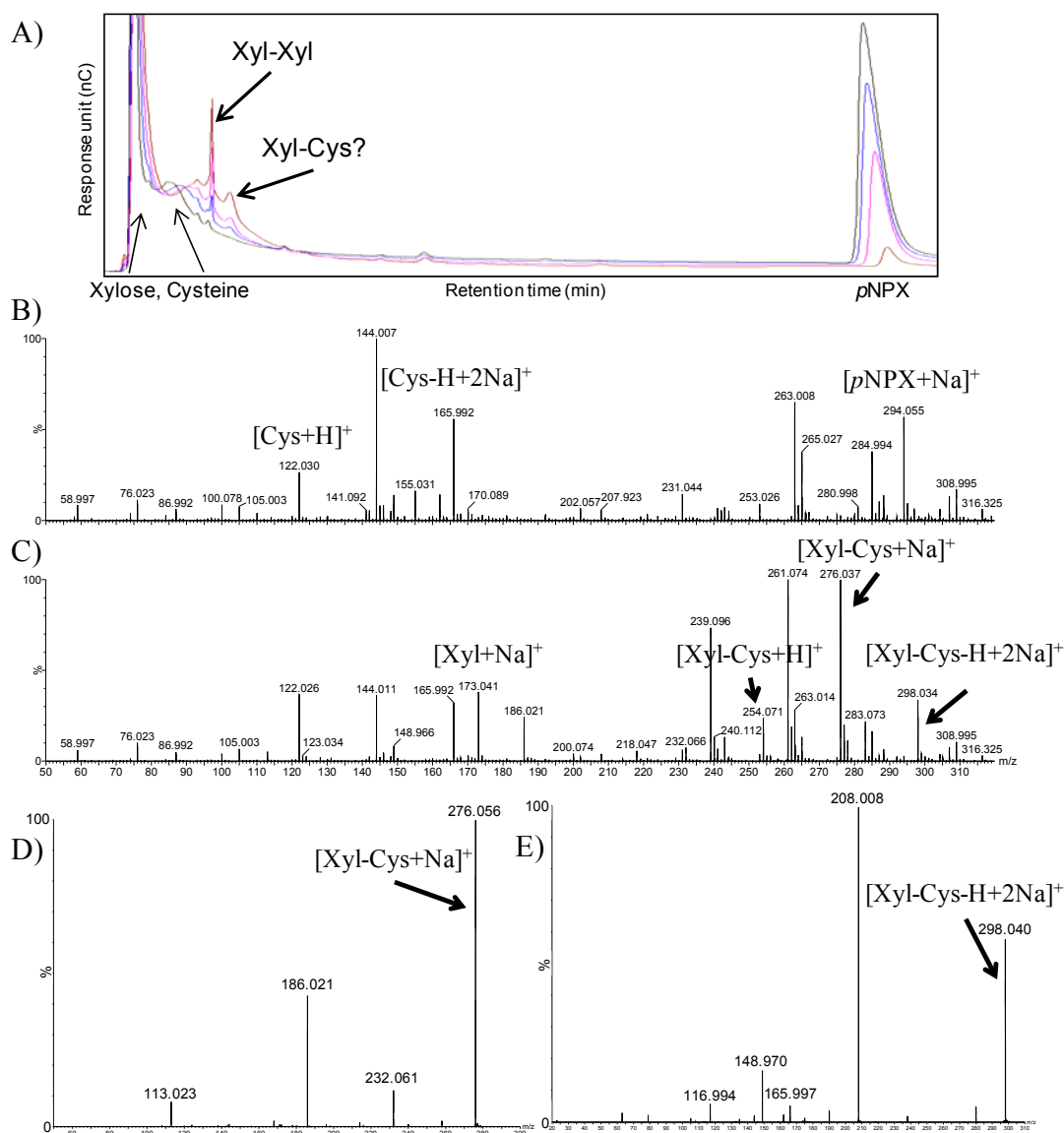
**Figure 16** HPAEC-PAD chromatograms monitoring transglycosylation with selected acceptors to illustrate different product formations; A) xylose; B) glucose; C) mannose; D) sucrose; black line, reaction time: 0 min; blue line, reaction time: 10 min; magenta line; reaction time: 60 min for glucose, mannose, sucrose, and 120 min for xylose.

**Table 8** Maximum transglycosylation yields with different acceptors.

Acceptor	Yield (%)	Production (mg/mL)	No. of major TG peaks
<u>Monosaccharides</u>			
<b>D-xylose</b>	<b>21</b>	<b>1.81</b>	<b>1</b>
<b>D-arabinose</b>	<b>17</b>	<b>1.41</b>	<b>2</b>
<b>D-lyxose</b>	<b>23</b>	<b>1.92</b>	<b>3</b>
<b>L-fucose</b>	<b>14</b>	<b>1.27</b>	<b>3</b>
L-rhamnose	n.d.	n.d.	n.d.
<b>D-glucose</b>	<b>10</b>	<b>0.92</b>	<b>1</b>
D-galactose	9	0.81	1
<b>D-mannose</b>	<b>25</b>	<b>2.34</b>	<b>3</b>
<b>D-talose</b>	<b>22</b>	<b>2.04</b>	<b>3</b>
D-fructose	8	0.79	2
<u>Sugar alcohols</u>			
Xylitol	36	3.05	2
Sorbitol	20	1.85	2
<u>Disaccharides</u>			
Maltose	2	0.27	2
<b>Sucrose</b>	<b>6</b>	<b>0.81</b>	<b>2</b>
Lactose	n.d.	n.d.	n.d.
Cellobiose	2	0.33	1
<b>Turanose</b>	<b>7</b>	<b>0.95</b>	<b>2</b>
Lactulose	3	0.44	2

Products were quantified by HPAEC-PAD using xylobiose and xylotriose as standards for di- and trisaccharides, respectively. The total yield was estimated as percentage of product/donor concentration (mM/mM); n.d., not detected. Products in bold were purified for structural analysis.

Two amino acids, L-cysteine and L-serine, were also tested as acceptors; the formation of Xyl-Cys and Xyl-Ser could not be clearly monitored either by TLC or by HPAEC-PAD, but have been evaluated by ESI-Q-TOF MS (Fig. 17). The peak of cysteine from HPAEC-PAD chromatogram was broadened over time and overlapped with the transglycosylation products (Fig. 17A). Xyl-Cys could be detected in the form of Xyl-Cys+H ( $m/z$  254), Xyl-Cys+Na<sup>+</sup> ( $m/z$  276), and Xyl-Cys-H+2Na<sup>+</sup> ( $m/z$  298), whereas the formation of Xyl-Ser as Xyl-Ser+Na<sup>+</sup> ( $m/z$  260) could not be confirmed by MS/MS. The thio-glycoside linkage of Xyl-Cys was additionally supported by the lack of reaction with iodoacetamide, which would form *S*-carbamidomethylcysteine with a free thiol. ESI-MS showed no *S*-carbamidomethylation of Xyl-Cys, while *S*-carbamidomethyl cysteine formed with the L-cysteine itself (data not shown).



**Figure 17** HPAEC-PAD chromatogram and ESI-Q-TOF mass spectra ( $m/z$  50-320) of Xyl-Cys transglycosylation reaction mixture containing 200 nM BxlA, 30 mM *p*NPX, and 200 mM L-cysteine in 10 mM sodium acetate pH 5.0 at 40°C. A) HPAEC-PAD chromatogram. Black, reaction time: 0 min; blue, reaction time: 30 min; magenta; reaction time: 60 min; brown, reaction time: 120 min; B) reaction with L-cysteine at 0 min; C) reaction with L-cysteine at 60 min reaction time; D) ESI-Q-TOF MS/MS spectrum of Xyl-Cys at  $m/z$  276; E) ESI-Q-TOF MS/MS spectrum of Xyl-Cys at  $m/z$  298 (see Appendix Figure 1 for details in Fig. 17B-E, page 113–114).

### 6.1.5 Characterisation of xylosyl-oligosaccharide products

Among the tested transglycosylations, nine products (from xylose, arabinose, lyxose, L-fucose, glucose, mannose, talose, sucrose, and turanose) formed by BxlA were purified by HPLC and subjected to structure-determination by two-dimensional nuclear magnetic resonance spectroscopy (2D NMR) and ESI-MS. The molecular masses for all products gave signals corresponding to the calculated molecular masses of  $\text{Li}^+$  adducts of the acceptor conjugate of xylose. Chemical shifts for NMR linkage analysis were assigned based on 2D NMR spectra and chemical shifts of selected

products are presented in Table 9. The xylobiose formation using xylose as well as the transglycosylation products from arabinose and lyxose acceptors were linked mainly with  $\beta$ -1,4 linkages as identified by long range proton-carbon bond correlations between the non-reducing anomeric proton and C-4 of the substituted position and as confirmed by inter NOE correlation. In contrast the transglycosylation products from mannose and glucose acceptors linked mainly with  $\beta$ -1,6 linkages as identified by the downfield shift of the C6 or by inter NOE correlation across the glycosidic bond. The presence of  $\beta$ -1-6 linkages might be because the 6-OH as primary alcohol is less steric hindered and the enzymes having a loose acceptor binding site. The preference for a primary alcohol is in agreement with the  $\beta$ -xylosidase from *A. awamori* (Kurakake et al., 2005). In case of disaccharide acceptors, the xylosyl residues could form  $\beta$ -1,4 or  $\beta$ -1,6 linked to either reducing or non-reducing ends of the disaccharides, which may depend on the accessibility or less steric hindrance configuration of the disaccharide acceptors.

The structures of four novel transglycosylation products including:  $\beta$ -D-xylopyranosyl-(1 $\rightarrow$ 4)-D-lyxopyranoside,  $\beta$ -D-xylopyranosyl-(1 $\rightarrow$ 4)- $\alpha$ -D-glucopyranosyl-(1 $\rightarrow$ 3)- $\beta$ -D-fructofuranoside,  $\beta$ -D-xylopyranosyl-(1 $\rightarrow$ 4)- $\alpha$ -D-glucopyranosyl-(1 $\rightarrow$ 2)- $\beta$ -D-fructofuranoside, and  $\beta$ -D-xylopyranosyl-(1 $\rightarrow$ 6)- $\beta$ -D-fructofuranosyl-(2 $\rightarrow$ 1)- $\alpha$ -D-glucopyranoside have been assigned by 2D NMR (Table 9). The structures of transglycosylation products from L-fucose and talose as acceptors, which are also novel xylosyl-oligosaccharides cannot be solved by NMR due to the presence of mixtures of compounds, but ESI-MS confirmed that they are disaccharides with molecular masses of  $m/z$  303 and 319, respectively.

**Table 9**  $^1\text{H}$  and  $^{13}\text{C}$  NMR data assignments and molecular masses for  $\beta$ -xylosyl-oligosaccharides produced by enzymatic transglycosylation of BxlA.

Compound (molecular mass) <sup>1</sup>	Chemical shifts ( $\delta$ , p.p.m.)					
	H-1 C-1	H-2 C-2	H-3 C-3	H-4 C-4	H-5a/H-5b C-5	H-6a/H-6b C-6
$\beta$ -Xylp-(1,4)-	4.43	3.23	3.4	3.6	3.95/3.28	–
	102.7	73.6	76.4	70.1	66.1 <sup>2</sup>	–
$\alpha$ -Xylp	5.16	3.52	n.d.	n.d.	3.80/3.73	–
	92.9	72.2	72	74.3	59.7	–
$\beta$ -Xylp ( <i>m/z</i> 289)	4.56	3.22	3.52	3.76	3.35/4.04	–
	97.3	~74.9	~74.9	77.3	63.8	–
$\beta$ -Xylp-(1,4)-	4.43	3.32	3.42	3.62	3.26/3.93	–
	102.3	73.8	76.6	70.2	66.1 <sup>2</sup>	–
$\alpha$ -Arap	5.22	3.79	3.91	4.1	3.78/3.96	–
	93.4	n.d.	n.d.	77.2	61	–
$\beta$ -Arap ( <i>m/z</i> 289)	4.53	3.48	3.68	4.05	3.60/4.00	–
	97.3	73	72.5	76.8	64.6	–
$\beta$ -Xylp-(1,4)-	4.47	3.26	3.42	3.6	3.30/3.94	–
	103.6	73.7	76.6	70.2	66.1 <sup>2</sup>	–
$\alpha$ -Lyxp	4.95	3.74	4.03	3.91	3.80/3.88	–
	94.9	70.8	~70.2	77	62.4	–
$\beta$ -Lyxp ( <i>m/z</i> 289)	4.88	3.92	n.d.	n.d.	n.d.	–
	95.2	n.d.	n.d.	n.d.	n.d.	–
$\beta$ -Xylp-(1,6)-	4.43	3.28	3.42	3.6	3.31/3.94	–
	104.4	73.9	76.4	70.2	66.1 <sup>2</sup>	–
$\alpha$ -Manp	5.14	3.91	3.81	3.69	3.93	3.85/4.09
	95	~72.1	~71	~67.6	~72.2	~69.9
$\beta$ -Manp ( <i>m/z</i> 319)	4.87	3.92	3.63	3.59	3.49	3.82/4.13
	94.6	71.8	~73.8	70.1	~76	~69.9
$\beta$ -Xylp-(1,6)-	4.42	3.27	3.43	3.6	3.29/3.93	–
	104.2	73.9	76.6	70	66.1 <sup>2</sup>	–
$\alpha$ -Glc p	5.19	3.5	3.68	3.4	3.93	3.84/4.10
	92.9	72.3	73.3	70.5	71.1	~69.8
$\beta$ -Glc p ( <i>m/z</i> 319)	4.61	3.22	3.45	3.94	3.58	3.80/4.12
	96.9	75	76.5	71.3	76	~69.9
$\beta$ -Xylp-(1,4)-	4.43	3.33	3.42	3.63	3.93/3.26	–
	102.1	73.6	70.2	70.1	66.1 <sup>2</sup>	–
$\alpha$ -Glc p-(1,3)-	5.31	3.56	3.72	3.4	3.71	3.83/3.77
	101.5	73	73.7	76.5	73.7	61.4
$\beta$ -Fruf ( <i>m/z</i> 481)	3.48/3.73	–	3.97	4.16	4.12	3.84/3.97
	64.7	n.d.	77	70.2	70.2	61.8
$\beta$ -Xylp-(1,4)-	4.41	3.27	3.41	3.61	3.96/3.28	–
	104.2	74	76.6	70.1	66.1 <sup>2</sup>	–
$\alpha$ -Glc p-(1,2)-	5.37	3.55	3.81	3.62	3.93	3.82/3.88
	92.9	71.9	71.9	78.8	72.1	60.3
$\beta$ -Fruf ( <i>m/z</i> 481)	3.66/3.59	–	4.18	3.99	3.85	3.75/3.80
	62.1	104.6	77.3	74.9	82.2	63.4
$\beta$ -Xylp-(1,6)-	4.47	3.27	3.42	3.59	3.94/3.29	–
	104.3	74	76.5	70.1	66.1 <sup>2</sup>	–
$\beta$ -Fruf-(2,1)-	n.d.	–	4.18	4.03	4.02	3.95
	n.d.	104.9	77	75.4	81	n.d.
$\alpha$ -Glc p ( <i>m/z</i> 481)	5.37	3.52	3.73	3.44	3.81	3.78/3.82
	93.2	72	n.d.	n.d.	n.d.	n.d.

<sup>a</sup> molecular mass as  $\text{Li}^+$  adduct (estimated mass + *m/z* 7) determined by ESI-MS

<sup>b</sup> reference carbon shifts according to C5

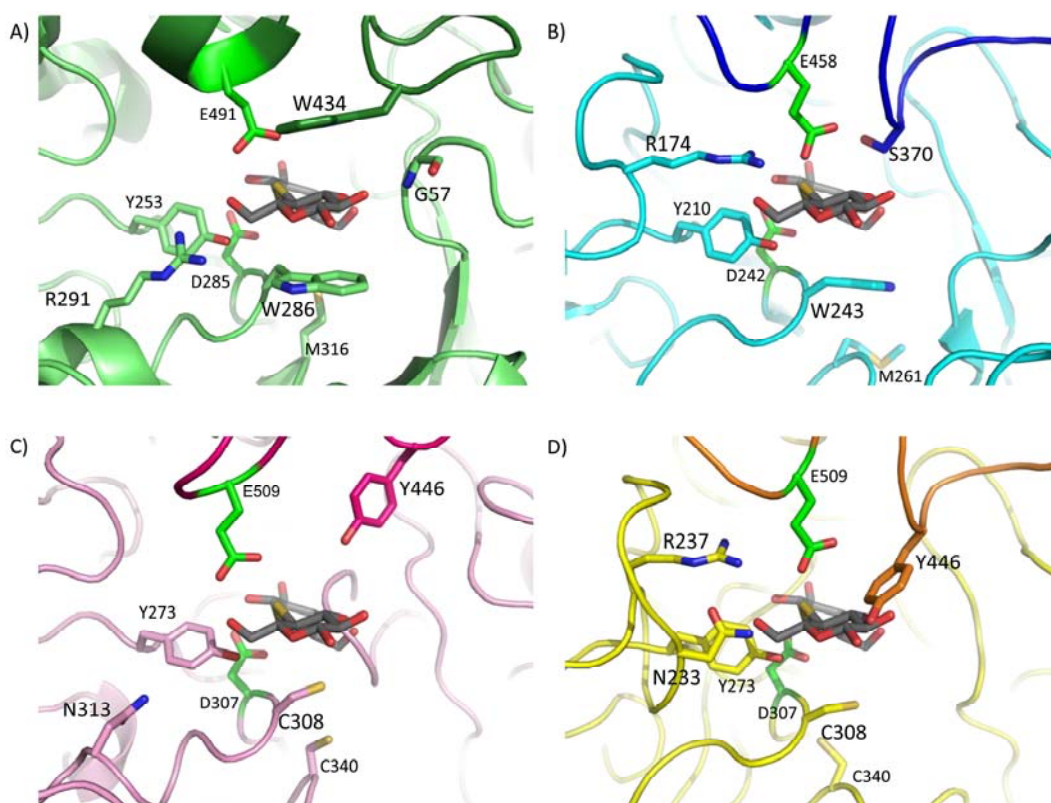
n.d., not detected.

### 6.1.6 Engineering of transglycosylation activity by glycosynthase and subsite +1 mutants

The first reported GH3 structure, exo-1,3/1,4- $\beta$ -glucanase from *Hordeum vulgare* (ExoI; Fig 18A; Varghese et al., 1997) has two domains: a TIM barrel (domain 1) and a six-stranded  $\beta$ -sandwich (domain 2), whereas the structure of  $\beta$ -glucosidase from *Thermotoga neapolitana* DSM 4359 (Bgl3B; Fig 18B; Pozzo et al., 2010) has three domains: a TIM barrel (domain 1), a five-stranded  $\alpha/\beta$  sandwich (domain 2), and a fibronectin type III domain (domain 3). No structure is reported of GH3  $\beta$ -xylosidases, however, small-angle X-ray scattering data of a GH3  $\beta$ -xylosidase of *Trichoderma reesei*, indicates three domains (Seidle et al., 2005). The 3D models of BxlA have two (Fig. 18C) and three domains (Fig. 18D) corresponding to the template structures of ExoI and Bgl3B. The quality of the protein models is reasonable to good, as verified by CE method and ProQ (see 5.2, page 33). In general, domain 1 is well conserved among GH3 enzymes and the catalytic nucleophile of all query sequences align together in this domain. Domains 2 and 3 have no highly conserved sequence motifs, which make it difficult to unambiguously identify the catalytic acid/base residue; therefore these were identified according to the templates of each homology modelling.

The subsite +1 mutants C308W and N313R on domain 1 in BxlA were designed based on the alignment of BxlA with related GH3 enzymes (Fig. 18 and Appendix Fig. 2, page 115). Cys308 of BxlA is situated next to its catalytic nucleophile Asp307, whereas in case of GH3  $\beta$ -glucanase and  $\beta$ -glucosidase, the corresponding residue was Trp (Trp 286 for ExoI and Trp243 for Bgl3B) that formed a stacking interaction to the sugar ring at acceptor binding site (subsite +1) as shown for  $\beta$ -glucanase from barley (*Hordeum vulgare*) ExoI (PDB ID: 1IEX; Hrmova et al., 2005). However, Cys308 was predicted to form a disulfide with Cys340 (see 5.2). The substitution of Cys308 to Trp in BxlA (C308W) could increase transglycosylation activity of BxlA by providing a stacking interaction at subsite +1 or it could cause the loss of a disulfide in BxlA and affect its structural integrity. Asn313 of BxlA is equivalent to Arg291 of ExoI, which can form a hydrogen bond to 6-OH of the sugar ring at subsite +1, however it is equivalent to Asn248 of Bgl3B, which located far ( $>15\text{\AA}$ ) from the active site and may not be involved in acceptor interaction. The substitution of Asn313 by Arg in BxlA (N313R) was made to investigate the role of this residue and in an attempt to increase the transglycosylation activity of BxlA towards hexose acceptors.

The production and purification of BxlA glycosynthase and subsite +1 mutants were done essentially as for BxlA (see 5.4.1) with yields of 9, 13, 11, 8, 11, and 12 mg/L culture for D307G, D307A, D307C, D307S, C308W, and N313R BxlA, respectively. The specific activities of the mutants are shown in Table 10. The activity of the glycosynthase mutants and C308W decreased by three orders of magnitude, whereas that of N313R was decreased three fold. The severe reduction in activity of C308W indicated that Cys308 is essential for BxlA. This could be because Cys308 forms disulfide bond with Cys340 (3.3  $\text{\AA}$  from Cys308) as found by using the DiANNA-Disulfide bond connectivity prediction.



**Figure 18** Cartoons representing the active site in 3D structures and homology models of: A) exo-1,3/1,4- $\beta$ -glucanase from *H. vulgare* (ExoI; PDB ID: 1IEEX), B)  $\beta$ -glucosidase from *T. neapolitana* DSM 4359 (Bgl3B; PDB ID: 2WT3), C) model structure of BxlA (using 1IEEX as template), D) model structure of BxlA (using 2WT3 as template; see 5.2). The thiocellobiose in grey from the complex with ExoI was superimposed on the modelled structures of BxlA as well as on the 3D structure of Bgl3B; green sticks show catalytic nucleophile (Asp) and acid/base (Glu) residues.

**Table 10** Specific activity of subsite +1 mutants of BxlA towards 2 mM *p*NPX.

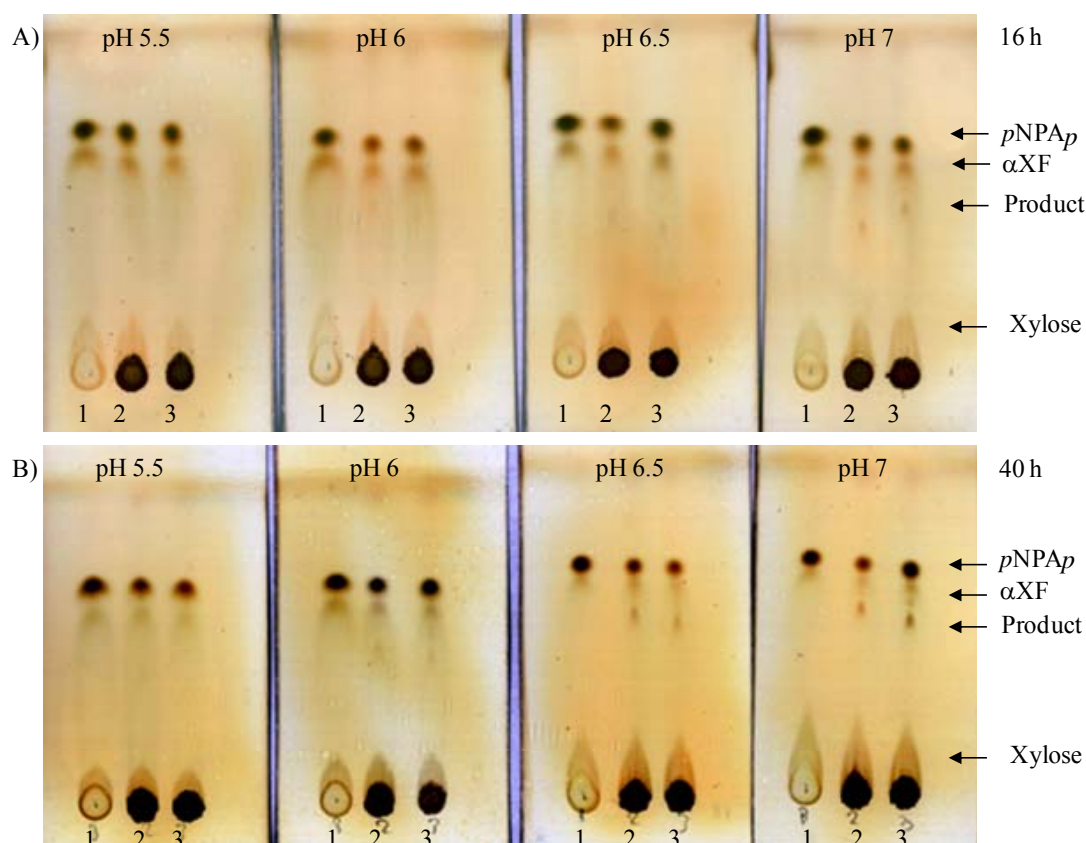
Enzyme	Specific activity (U/mg)	Ratio <sup>1</sup>
BxlA	32 $\pm$ 1.64	1
D307G	0.027 $\pm$ 0.0032	8 $\times$ 10 <sup>-4</sup>
D307A	0.028 $\pm$ 0.0023	9 $\times$ 10 <sup>-4</sup>
D307C	0.034 $\pm$ 0.0027	11 $\times$ 10 <sup>-4</sup>
D307S	0.029 $\pm$ 0.0061	9 $\times$ 10 <sup>-4</sup>
C308W	0.027 $\pm$ 0.0014	9 $\times$ 10 <sup>-4</sup>
N313R	11 $\pm$ 0.80	0.3

<sup>1</sup> normalized with activity of BxlA

Standard deviations were calculated from 4 experiments

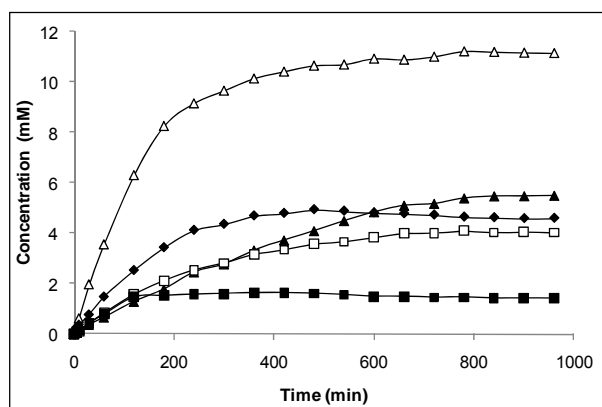


The glycosynthase reactions of GH3  $\beta$ -xylosidase D307A and D307C catalytic nucleophile mutants were done by first screen for pH suitable for the reaction in the pH range 5.0–7.0 (Fig. 19; data not shown for pH 5.0). *pNPAP* was used as acceptor for the screening since aryl sugars bind well to the subsite of glycoside hydrolases. After 16 h incubation, the product could be visualized at pH 7 by TLC and it became clearly visible after 40 h. The glycosynthase reactions were slow and the mutants showed quite low activity. When replacing *pNPAP* by lyxose, galactose, or cellobiose, the glycosynthase products could not be detected neither by TLC nor HPAEC-PAD (data not shown), confirming the weak glycosynthase activity by these mutants.



**Figure 19** Glycosynthase reactions using 50  $\mu$ M D307A or D307C with 2 mM  $\alpha$ XF as donor and 2 mM *pNPAP* as acceptor in 100 mM sodium acetate (pH 5.5, pH 6.0) or 100 mM phosphate buffer (pH 6.5, 7.0) at 30°C for: 16 h (A) and 40 h (B). Lane 1, control reaction without enzyme; lane 2, 50  $\mu$ M D307A; lane 3, 50  $\mu$ M D307C. The TLC was developed with 100% acetonitrile (see 5.7.4 for TLC method).

C308W showed three orders of magnitude diminished hydrolytic activity as seen also for the glycosynthase mutants compared to BxlA and no transglycosylation activity was detected after incubation for 24 h using 200 nM C308W with 30 mM *pNPX* and 200 mM acceptor (xylose, galactose, mannose, fructose, or maltose) confirming the loss of its activity. N313R showed three folds decrease in hydrolytic activity compared to BxlA wild-type. The transglycosylation activity of N313R toward hexoses increased 1.5–2 fold and up to three folds towards maltose, but slightly decreased towards xylose (Fig. 20 and Table 11), indicating that this residue may be involved in binding to 6-OH of hexose acceptors as predicted by 3D model of BxlA using 1IEX as template (Fig. 18C).



**Figure 20** Progress of transglycosylation with different acceptors by N313R. Reactions containing 200 nM N313R with 30 mM *p*NPX and 200 mM acceptor; xylose (▲), galactose (□), mannose (Δ), fructose (◆), or maltose (■).

**Table 11** Maximum transglycosylation yields with different acceptors by N313R in comparison with BxlA.

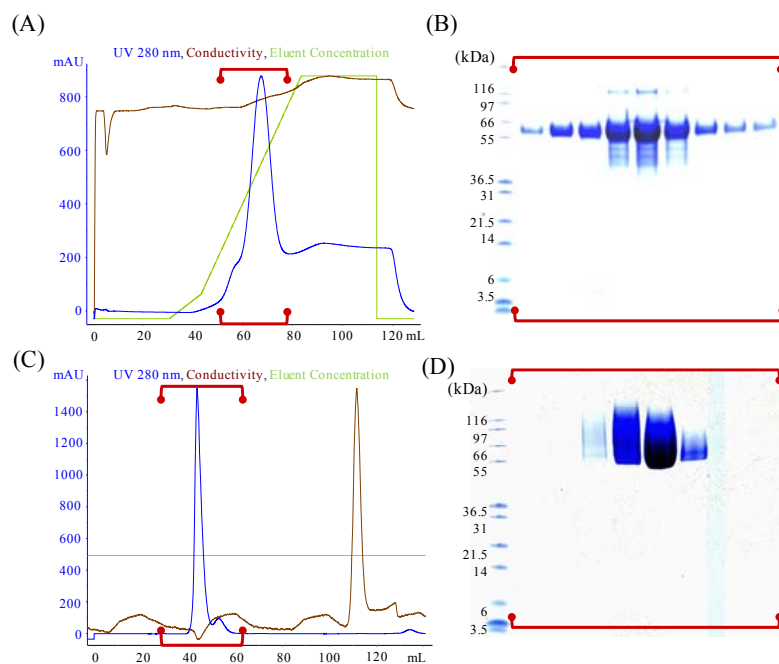
Acceptor	N313R		BxlA		Ratio <sup>1</sup>
	Yield (%)	Production (mg/mL)	Yield (%)	Production (mg/mL)	
<u>Monosaccharides</u>					
D-xylose	18	1.55	21	1.81	0.8
D-galactose	14	1.28	9	0.81	1.6
D-mannose	37	3.50	25	2.34	1.5
D-fructose	16	1.54	8	0.79	1.9
<u>Disaccharides</u>					
Maltose	5	0.78	2	0.27	2.7

<sup>1</sup> Normalized by transglycosylation yield of BxlA

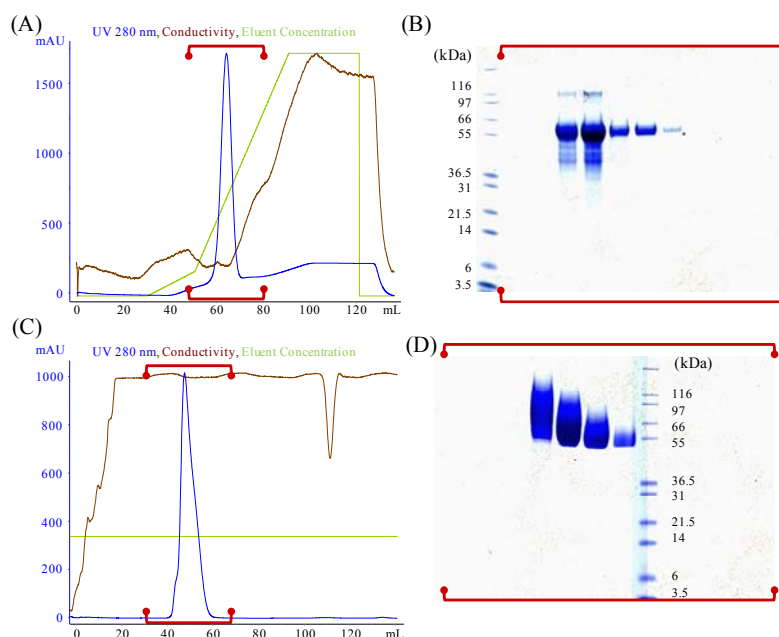
## 6.2 GH5 mannanases

### 6.2.1 Production and purification

Two subsite +1 mutants ManAS289W and ManCW283S of ManA and ManC, respectively, from *A. nidulans* FGSC A4 were produced recombinantly as His-tag fusion proteins in *P. pastoris* X-33 (Fig. 21 and 22). The enzymes were purified by nickel chelating chromatography followed by gel filtration in a yield of 12 and 24 mg/L culture for ManAS289W and ManCW283S, respectively. The ManA and ManC wild-type enzymes were produced by Dr. Hiroyuki Nakai by induction with buffered methanol-complex medium (BMGY with 0.5% methanol without glycerol) for 5 days and purified in the same protocol as their subsite +1 mutants in a yield of 120 and 145 mg/L culture, respectively (see manuscript 2).



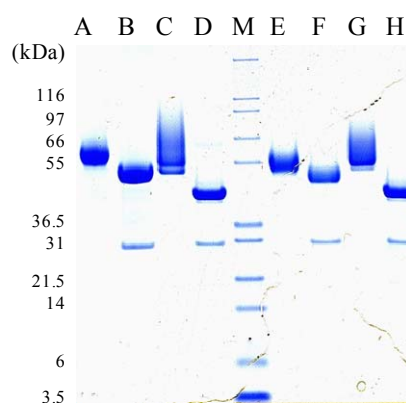
**Figure 21** Purification of ManAS289W. A) immobilized metal ion affinity chromatogram. B) SDS-PAGE of purified ManAS289W by HisTrap 5 mL column; 25  $\mu$ L samples loaded. C) gel filtration chromatogram of pooled ManAS289W fraction from (A). D) SDS-PAGE of ManAS289W purified by Hiload 26/60 Superdex G75 column; 25  $\mu$ L samples loaded; marker, Mark12 unstained protein standard marker (Invitrogen). The red bars in (A) and (C) show the fractions which are analysed by SDS-PAGE in (B) and (D) (see 5.4.2, page 36).



**Figure 22** Purification of ManCW283S. A) immobilized metal ion affinity chromatogram. B) SDS-PAGE of purified ManCW283S by HisTrap 5 mL column; 20  $\mu$ L samples loaded. C) gel filtration chromatogram of pooled ManCW283S fraction from (A). D) SDS-PAGE of ManCW283S purified by Hiload 26/60 Superdex G75 column; 20  $\mu$ L samples loaded; marker, Mark12 unstained protein standard marker (Invitrogen). The red bars in (A) and (C) show the fractions which are analysed by SDS-PAGE in (B) and (D) (see 5.4.2, page 36).

## 6.2.2 Protein characterisation

The recombinant ManCW283S migrated in SDS-PAGE as a single band similarly to ManC with an estimated size of 56 kDa (Fig. 23, Lane A), whereas ManAS289W migrated as a smear similarly to ManA with lowest band of 56 kDa and the smearing up to 90 kDa (Fig. 23, Lane C). The theoretical masses were 43946.2 and 46544.6 Da, for ManAS289W and ManCW283S, respectively. Deglycosylation by Endoglycosidase H reduced the molecular mass of ManCW283S by 5 kDa (Fig. 23, Lane B), and of ManAW283S by 10 kDa (Fig. 23, Lane D), while the smear bands became a sharp band at 45 kDa. *N*-glycosylation was predicted to occur and the enzymes have 4 and 2 possible sites for ManAW283S and ManCW283S, respectively, which correspond well with the reduced molecular masses after deglycosylation. This indicated slight glycosylation is in agreement with what was found for ManA and ManC (Fig. 23E–H).



**Figure 23** SDS-PAGE of purified and deglycosylated ManA, ManC, ManAS289W, and ManCW283S. Lane A, 7  $\mu$ g ManCW283S; lane B, 7  $\mu$ g deglycosylated ManCW283S; lane C, 5  $\mu$ g ManAS289W; lane D, 5  $\mu$ g deglycosylated ManAS289W; lane E, 5  $\mu$ g ManC; lane F, 5  $\mu$ g deglycosylated ManC; lane G, 5  $\mu$ g ManA; lane H, 5  $\mu$ g deglycosylated ManA; lane M, Mark12 unstained protein standard marker (Invitrogen); endoglycosidase H is seen as a 29 kDa band in lane B, D, E, and H.

## 6.2.3 Enzymatic specificity, kinetics, and hydrolysis action patterns

The activity towards konjac glucomannan (konjac GlcMan), guar galactomannan (guar GalMan), and locust bean gum galactomannan (LBG GalMan) is shown in table 12. ManC showed 30–80% higher activity towards polymeric mannans than ManA and also showed preference to LBG GalMan with 20% and 40% higher activity towards guar GalMan and konjac GlcMan, respectively. In contrast, ManA showed no different in specific activity on LBG and guar GalMans, but showed 15% lower specific activity on konjac GlcMan than on both types of GalMans. LBG and guar GalMans have different degree of Gal substitution (Gal:Man, 1:4 and 1:2, respectively; see 2.1.5.1, page 10). Thus, ManA seems to be less discriminate regarding different substitution in GalMans as well as the backbone composition in case of konjac GlcMan, whereas ManC appears to have a preference towards less substitution mannans.

The subsite +1 mutants showed decreased activity towards polymeric mannans. The specific activity of ManAS289W towards LBG GalMan was 15% and 20% higher than that of guar GalMan and konjac GlcMan, respectively, whereas the specific activity of ManCW283S on LBG GalMan showed only 5% and 15% higher specific activity towards guar GalMan and konjac GlcMan. Thus, substitution of Trp283 in ManC reduced the impact of Gal substitution and *vice versa* in case of ManA mutation. This could be because the bulky Trp obscure the side chain of mannan to bind to the substrate binding site.

**Table 12** Specific activity of ManA, ManAS289W, ManC, and ManCW283S towards mannan polymers

Enzyme	Substrate (0.5%)	Specific activity
		U/mg
ManA	Konjac GlcMan	340 ± 2
	LBG GalMan	400 ± 4
	Guar GalMan	390 ± 6
ManAS289W	Konjac GlcMan	220 ± 1
	LBG GalMan	300 ± 1
	Guar GalMan	250 ± 1
ManC	Konjac GlcMan	430 ± 4
	LBG GalMan	730 ± 2
	Guar GalMan	600 ± 2
ManCW283S	Konjac GlcMan	270 ± 1
	LBG GalMan	320 ± 4
	Guar GalMan	300 ± 1

Standard deviations were calculated from triplicate experiments (see 5.6.2.1 for experimental details).

The kinetic parameters towards mannoooligosaccharides (M4–M6) are shown in Table 13. Both mannanase wild-type and mutant enzymes have highest  $k_{cat}$  towards M6 and their catalytic efficiency ( $k_{cat}/K_m$ ) increased with increasing length of mannoooligosaccharides, which is typical behavior for endo-acting enzymes having 5–6 substrate binding subsites. All mannanases showed weak affinity towards M4, therefore only  $k_{cat}/K_m$  values were reported. ManC showed higher catalytic efficiency than ManA. Both mannanase subsite +1 mutants showed slightly lower  $k_{cat}$  than the corresponding wild-type enzymes but the effect was even smaller than for the specific activity towards mannans (Table 12). The catalytic efficiency of ManCW283S decreased approximately 50%, but  $K_m$  was slightly increased compared with ManC. The  $K_m$  value of ManAS289W was slightly decreased, whereas the catalytic efficiency was quite similar compared with ManA. These could be the effect of the Trp substitution, which affected the substrate binding affinity of both mutants.

To gain further understanding of the hydrolysis action patterns of ManA and ManC, 0.5 mM M4–M6 were hydrolysed by ManA, ManAS289W, ManC, and ManCW283S, and the time course of the hydrolysis was monitored by HPAEC-PAD (Table 14 and Fig. 24). Both ManA and ManC form mannobiose as major hydrolysis










product from M4–M6, indicating that ManA and ManC may have strong substrate binding affinity at subsite –2, +2 or both. M1 and M3 were also produced importantly from M4 in case of ManA, which may be due to the weak affinity as shown in the kinetics analysis towards M4 giving some flexibility in the productive binding positioning at the active site. From the hydrolysis action patterns of M5 and M6, subsite –3 and/or +3 of the ManA could play role also in substrate binding and hence the trisaccharide was produced. In case of the subsite +1 mutants, ManAS289W and ManCW283S also formed mannobiose as main hydrolysis product from M4–M6 and their hydrolysis action pattern showed no obvious different from their wild-type enzymes (Table 14 and Fig. 24 D–F, J–L).

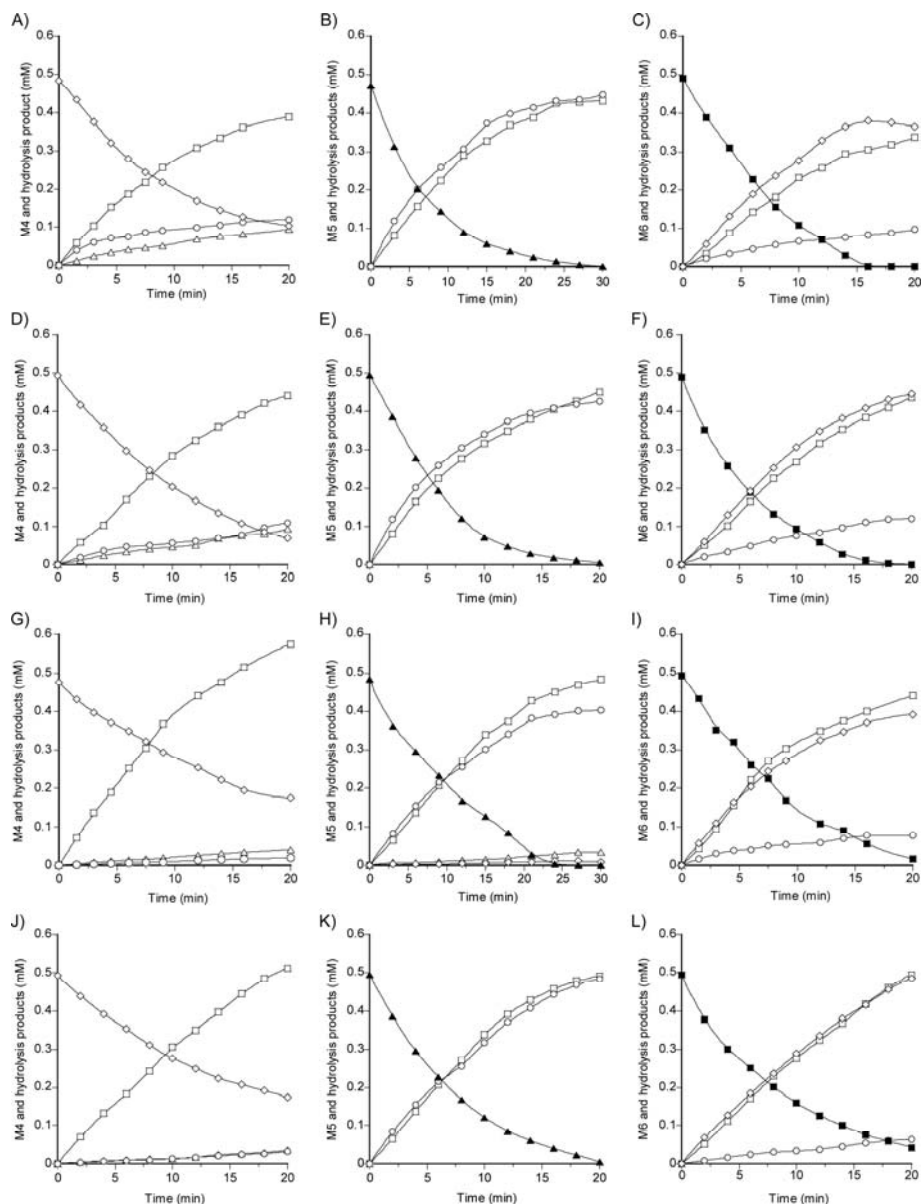
**Table 13** Hydrolysis kinetic parameters of ManA, ManAS289W, ManC, and ManCW283S towards mannoooligosaccharides (M4–M6).

Enzyme	Substrate	$k_{cat}$ s <sup>-1</sup>	$K_m$ mM	$k_{cat}/K_m$ s <sup>-1</sup> mM <sup>-1</sup>
ManA	M4	–	–	6
	M5	67 ± 2.8	2.9 ± 0.03	23
	M6	193 ± 5.8	1.8 ± 0.08	109
ManAS289W	M4	–	–	10
	M5	42 ± 2.5	1.6 ± 0.16	27
	M6	148 ± 1.7	1.3 ± 0.05	115
ManC	M4	–	–	7
	M5	112 ± 8.1	1.8 ± 0.13	61
	M6	134 ± 5.2	0.6 ± 0.04	215
ManCW283S	M4	–	–	3
	M5	98 ± 3.1	2.8 ± 0.13	36
	M6	117 ± 3.3	1.0 ± 0.03	118

Standard deviations were calculated from triplicate experiments (see 5.6.2.2 for experimental details)

**Table 14** Hydrolysis product formation from 0.5 mM mannoooligosaccharides hydrolysed by ManA, ManAS289W, ManC or ManCW283S for 20 min.

Substrate	ManA	ManA S289W	ManC	ManC W283S
M4 	64%	68%	91%	88%
 }  } 	36%	32%	9%	12%
M5 	100%	100%	96%	100%
 } 				
M6 	88%	88%	92%	94%
	12%	12%	8%	6%

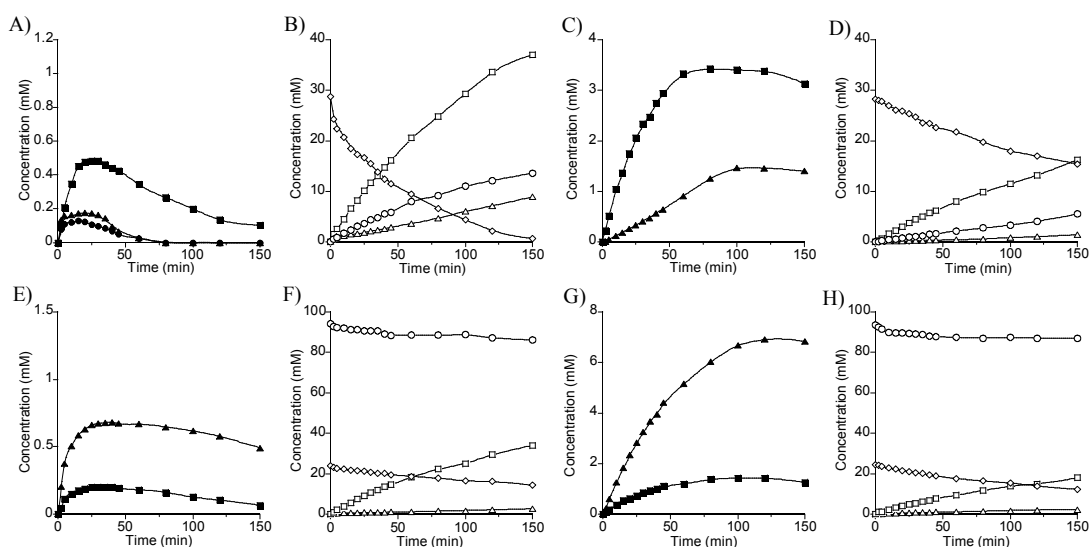


**Figure 24** Hydrolysis action patterns of ManA (A–C), ManAS289W (D–F), ManC (G–I), and ManCW283S (J–L) towards 0.5 mM M4–M6 in 100 mM sodium acetate pH 5.5 at 37°C. A), 60 nM ManA with M4; B), 30 nM ManA with M5; C), 10 nM ManA with M6; D), 50 nM ManAS289W with M4; E), 28 nM ManAS289W with M5; F), 12 nM ManAS289W with 0.5 mM M6; G), 75 nM ManC with M4; H), 15 nM ManC with M5; I), 12 nM ManC with M6; J), 120 nM ManCW283S with M4; K), 32 nM ManCW283S with M5; L), 20 nM ManCW283S with M6; M1, ( $\Delta$ ); M2, ( $\square$ ); M3, ( $\circ$ ); M4, ( $\diamond$ ); M5, ( $\blacktriangle$ ); M6, ( $\blacksquare$ ).

#### 6.2.4 Transglycosylation catalysed by ManA and ManC

The time course of transglycosylation catalysed by ManA and ManC was studied using either 30 mM M4 without addition of acceptor or 24 mM M4 with 100 mM M3 as acceptor as monitored during 150 min at 37°C by HPAEC-PAD. When using 30 mM M4, M5–M7 were produced by ManA (Fig. 25A), whereas ManC produced only M5 and M6 (Fig. 25C). The total product yields (M5+M6) were 2% and 16% for ManA and ManC, respectively. M7 was predicted from HPAEC-PAD

profile thus not included when estimating the total transglycosylation yield because there is no M7 standard available and the low yields hampered producing enough M7 for use as standard. The concentration of M7, however, was estimated by using standard curve of M6. Addition of M3 helped increasing the transglycosylation ability of both ManA and ManC by approximately 50%. The total product yields (M5+M6) were 4% and 25% for ManA and ManC, respectively (Fig. 25E-25H). In both cases, ManC possessed higher transglycosylation ability than ManA by almost 10-fold.



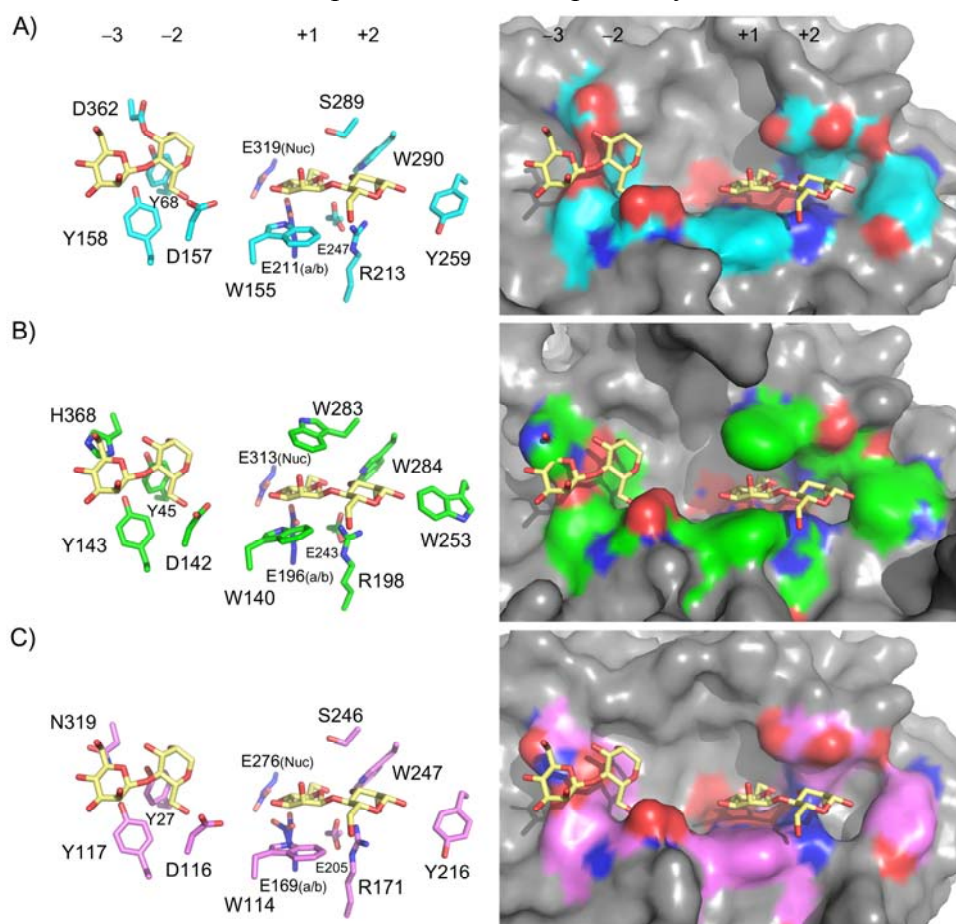
**Figure 25** Time course of transglycosylation products formation of ManA and ManC using 30 mM M4 or 24 mM M4 with 100 mM M3. A) transglycosylation products of 330 nM ManA with 30 mM M4; B) hydrolysis products and substrate of 330 nM ManA with 30 mM M4; C) transglycosylation products of 145 nM ManC with 30 mM M4; D) hydrolysis products and substrate of 145 nM ManC with 30 mM M4; E) transglycosylation products of 330 nM ManA with 24 mM M4 and 100 mM M3; F) hydrolysis products and substrate of 330 nM ManA with 24 mM M4 and 100 mM M3; G) transglycosylation products of 145 nM ManC with 24 mM M4 and 100 mM M3; H) hydrolysis products and substrate of 145 nM ManC with 24 mM M4 and 100 mM M3; M1, ( $\Delta$ ); M2, ( $\square$ ); M3, ( $\circ$ ); M4, ( $\diamond$ ); M5, ( $\blacktriangle$ ); M6, ( $\blacksquare$ ); M7, ( $\bullet$ ); see also Fig. 39, page 88.

### 6.2.5 Transglycosylation catalysed by subsite +1 mutants

3D homology modelling of ManA and ManC was performed using GH5 mannanase from *H. jecorina* RUTC-30 complexed with mannobiose at subsite +1 and +2 (PDB ID: 1QNR) as template and superimposed with mannobiose (subsite -2 to -3) from *Thermobifida fusca* KW3 (PDB ID: 2MAN; Hilge et al., 1998) to investigate possible substrate binding site interactions of ManA and ManC (Fig. 26 and Appendix Fig. 3, page 119). ManA and ManC models showed quite similar substrate binding sites to *H. jecorina* mannanase. The mannobiose from structure of *T. fusca* mannanase was used for illustrating possible substrate binding at the donor binding subsites, although it belongs to subfamily 8, which is less conserved to ManA and ManC (subfamily 7). Both ManA and ManC shared 39% sequence identity with a quite conserved possible subsite +1 and +2 except for a Trp residue (Trp283) at subsite +1 of ManC, which is equivalent to Ser289 of ManA. To investigate the effect



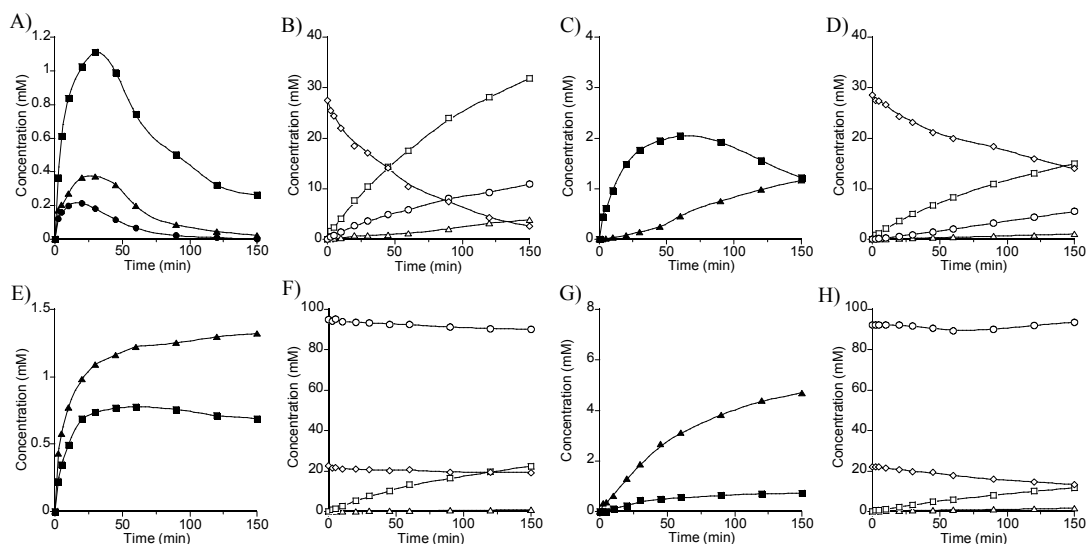
of this Trp283 of ManC, ManCW283S and ManAS289W mutants were made to mimic Ser289 of ManA and Trp283 of ManC, respectively.



**Figure 26** Cartoons representing the active site as sticks and surface in 3D structure of mannanase from *H. jecorina* RUTC-30 and homology models of ManA and ManC. A), Model structure of ManA; B), model structure of ManC; C), structure of *H. jecorina* RUTC-30 in complex with mannobiose along subsite +1 and +2 (PDB ID: 1QNR, Sabini et al., 2000); mannobiose along subsite -2 to -3 was from *T. fusca* KW3 mannanase (PDB ID: 2MAN; Hilge et al., 1998); Nuc, catalytic nucleophile; a/b, acid/base catalyst.

The transglycosylation catalysed by subsite +1 mutants were investigated by using 30 mM M4 without addition of acceptor or 24 mM M4 with 100 mM M3 in the same fashion as ManA and ManC. ManAS289W and ManCW283S showed similar transglycosylation pattern as the wild-type enzymes. Using 30 mM M4, ManAS289W produced M5–M7 (Fig. 27A), whereas ManCW283S produced only M5 and M6 (Fig. 27C). ManAS289W increased the total product yield (M5+M6) up to 55% and the total product yield (M5+M6) was 5%, using 30 mM M4, whereas ManCW283S gave 45% yield decreased and the total product yield (M5+M6) was found to be 9%. Addition of M3 helps increasing the transglycosylation ability of ManAS289W and ManCW283S by approximately 50% as observed for ManA and ManC. The total product yields (M5+M6) were 8% and 24% for ManAS289W and ManCW283S (Fig. 27E–27H), respectively. The transglycosylation yield (M5+M6) thus increased 50% in case of ManAS289W and decreased 31% in case of ManCW283S compared to

ManA and ManC, respectively. The changes in transglycosylation yield in both subsite +1 mutants showed that the Trp283 of ManC helped to increase transglycosylation yield possibly by increasing acceptor binding affinity at subsite +1 as indicated by decreasing of  $K_m$  in case of ManAS289W and increasing of  $K_m$  in case of ManCW283S from kinetics analysis.



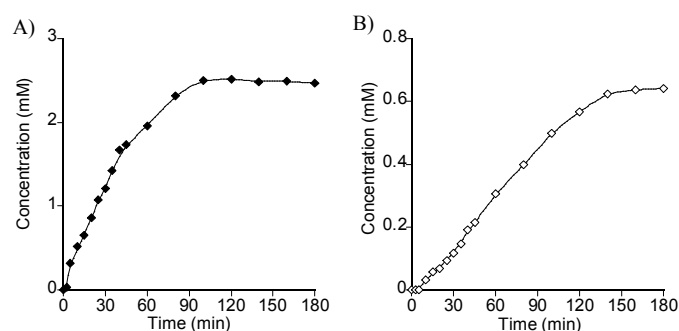
**Figure 27** Time course of transglycosylation products formation of ManAS289W and ManCW283S using 30 mM M4 or 24 mM M4 with 100 mM M3. A) transglycosylation products of 330 nM ManAS289W with 30 mM M4; B) hydrolysis products and substrate of 330 nM ManAS289W with 30 mM M4; C) transglycosylation products of 145 nM ManCW283S with 30 mM M4; D) hydrolysis products and substrate of 145 nM ManCW283S with 30 mM M4; E) transglycosylation products of 330 nM ManAS289W with 24 mM M4 and 100 mM M3; F) hydrolysis products and substrate of 330 nM ManAS289W with 24 mM M4 and 100 mM M3; G) transglycosylation products of 145 nM ManCW283S with 24 mM M4 and 100 mM M3; H) hydrolysis products and substrate of 145 nM ManCW283S with 24 mM M4 and 100 mM M3; M1, ( $\Delta$ ); M2, ( $\square$ ); M3, ( $\circ$ ); M4, ( $\diamond$ ); M5, ( $\blacktriangle$ ); M6, ( $\blacksquare$ ); M7, ( $\bullet$ ).

## 6.2.6 Characterisation of manno oligosaccharide products

ManA and ManC wild-type enzymes were screened for suitable acceptors using 14 mM M2 as donor and 400 mM of different mono- to trisaccharides as acceptors (performed by Dr. Hiroyuki Nakai, EPC, DTU Systems Biology; see manuscript 2). ManC possesses higher transglycosylation activity than ManA as shown by its 8-fold higher production of M5 within 30 min screening reaction, using M3 as acceptor. ManC can also use isomaltotriose and melezitose as acceptors, whereas ManA strictly accepts only M3.

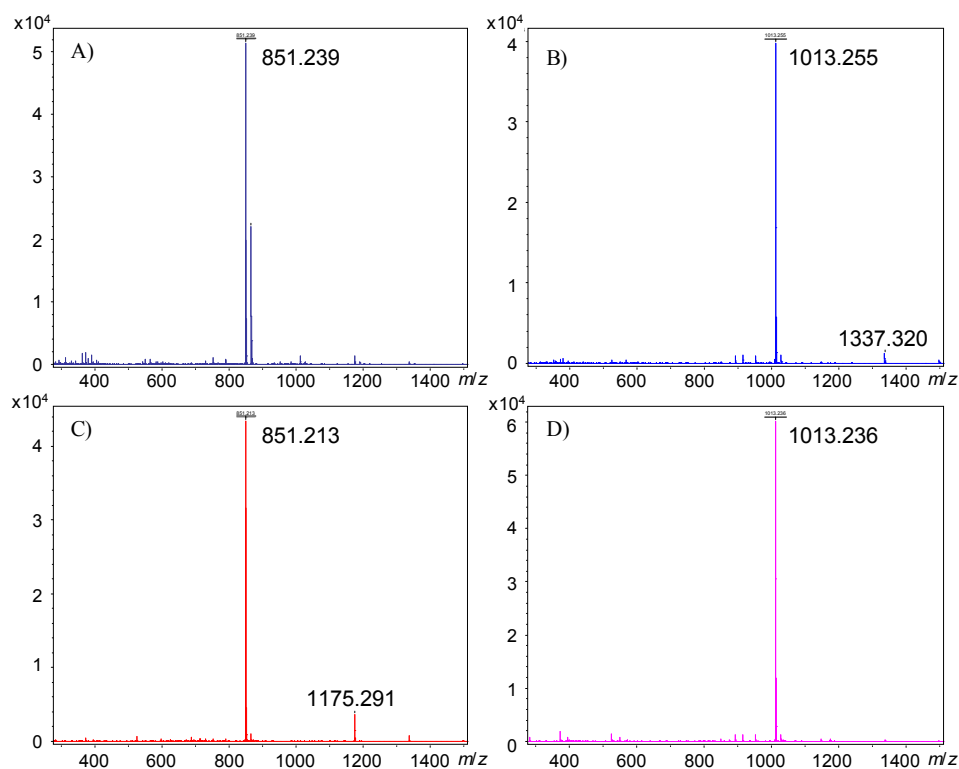
Even though ManAS289W increased the transglycosylation ability of ManA by 50%, ManC wild-type produced higher concentration of transglycosylation products. Therefore, ManC was used for the production of transglycosylation products for structural analysis. Time course of the reactions using 145 nM ManC with 24 mM M4 and 200 mM isomaltotriose or melezitose is shown as total product formation in Fig. 28. The concentration of acceptors was reduced from 400 mM to

200 mM here because of the low solubility of acceptors in acetonitrile used in the HPLC purification (see 5.8.2) and high acceptor concentrations present practical challenges in purification of the transglycosylation products due to broad acceptor peaks masking the products. The transglycosylation reactions using isomaltotriose and melezitose as acceptors resulted in two transglycosylation products from each acceptor with ratio of about 5:1 based on peak area. The mixed products occurred mainly because ManC transferred mannobiosyl and mannotriosyl to the acceptors. The maximum production of manno-isomaltotrioses and manno-melezitoses were 2.51 and 0.64 mM at 120 and 180 min corresponding to 10% and 3% total product yields, respectively, compared with the M4 donor concentration (mM/mM).



**Figure 28** Time course of total transglycosylation products formation from 145 nM ManC acting on 200 mM isomaltotriose (A) and 200 mM melezitose (B).

The molecular masses of M5 and M6 produced by transglycosylation of ManC using 24 mM M4 and 100 mM M3 as well as the two forms of manno-isomaltotriose and manno-melezitose were  $m/z$  851 and 1013 determined by MALDI-TOF MS (Fig. 29), indicating formation of a pentasaccharide as predominant and a hexasaccharide as a minor product, respectively (analysed as  $\text{Na}^+$  adducts). The structures of major transglycosylation products from manno-isomaltotriose and manno-melezitose as well as M5 produced by transglycosylation of ManC were assigned by 2D NMR (Table 15). The mannobiosyl isomaltotriose and mannobiosyl melezitose showed  $\beta$ -1,4 linked between mannobiosyl donor and trisaccharide acceptor, as identified by the downfield shift of the C6, similarly to structure of M5 confirming the regioselectivity as  $\beta$ -1,4 glycosidic linkage formation by ManC. Noticeably, mannobiosyl melezitose also contained minor compounds which were identified as mannobiosyl  $\beta$ -1,6 linked to fructose residue of melezitose and two mannobiosyl linked to one melezitose acceptor, which in later case also visualised as a small peak at  $m/z$  1175.3 in MALDI-TOF MS chromatogram (Fig. 29C).



**Figure 29** Molecular masses of transglycosylation products as  $\text{Na}^+$  adducts (mass range  $m/z$  300–1500). A) Manno-isomaltotriose (1):  $m/z$  851.239; B) manno-isomaltotriose (2):  $m/z$  1013.255; C) manno-melezitose (1):  $m/z$  851.213 with trace of heptasaccharide at  $m/z$  1175.291; D) manno-melezitose (2):  $m/z$  1013.236 (see 5.9.3 for MALDI-TOF MS method).

**Table 15**  $^1\text{H}$  and  $^{13}\text{C}$  NMR data assignments for manno oligosaccharides produced by enzymatic transglycosylation of ManC.

Compound (molecular mass) <sup>1</sup>	Chemical shifts ( $\delta$ , p.p.m.)					
	H-1 C-1	H-2 C-2	H-3 C-3	H-4 C-4	H-5 C-5	H-6a/H-6b C-6
$\beta$ -Manp-(1,4)-	4.70	4.01	3.6	3.51	3.39	3.89/3.68
$\beta$ -Manp-(1,4)-	n.d.	n.d.	n.d.	n.d.	n.d.	n.d.
$\beta$ -Manp-(1,4)-	4.7	4.08	3.77	3.77	3.51	3.87/3.71
$\beta$ -Manp-(1,4)-	n.d.	n.d.	n.d.	n.d.	n.d.	n.d.
$\beta$ -Manp-(1,4)-	4.7	4.08	3.77	3.77	3.51	3.87/3.71
$\beta$ -Manp-(1,4)-	n.d.	n.d.	n.d.	n.d.	n.d.	n.d.
$\beta$ -Manp	5.13	3.94	3.85	n.d.	n.d.	n.d.
$\beta$ -Manp	n.d.	n.d.	n.d.	n.d.	n.d.	n.d.
$\alpha$ -Manp	4.86	n.d.	n.d.	n.d.	n.d.	n.d.
$\alpha$ -Manp ( $m/z$ 851)	n.d.	n.d.	n.d.	n.d.	n.d.	n.d.

<sup>1</sup> molecular mass as  $\text{Na}^+$  adduct (estimated mass +  $m/z$  23) determined by MALDI-TOF MS

**Table 15 (continued)**

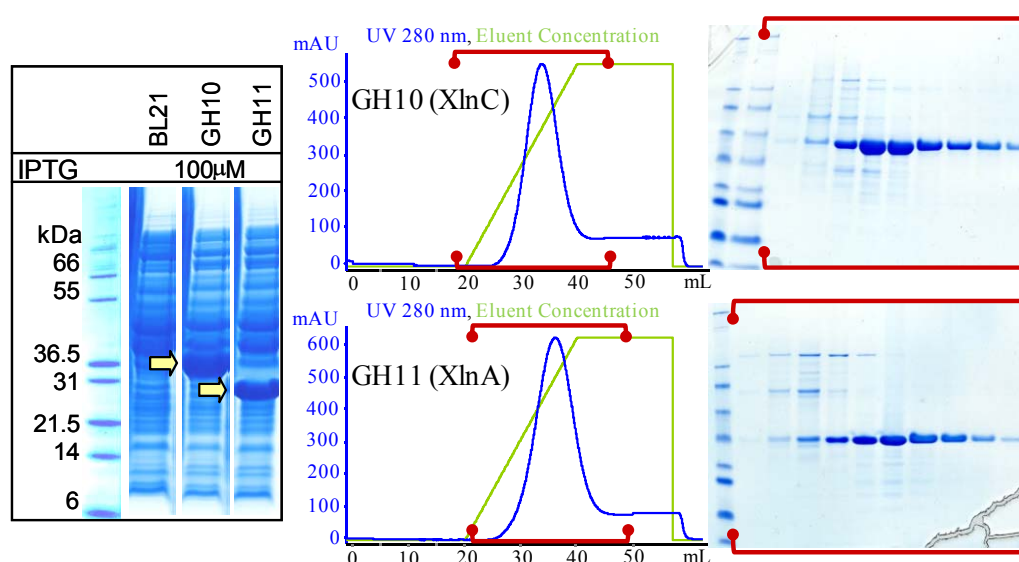
Compound (molecular mass) <sup>1</sup>	Chemical shifts ( $\delta$ , p.p.m.)					
	H-1 C-1	H-2 C-2	H-3 C-3	H-4 C-4	H-5 C-5	H-6a/H-6b C-6
$\beta$ -Manp-(1,4)-	4.79 101.2	4.14 71	3.82 72.4	n.d. n.d.	n.d. n.d.	n.d. n.d.
$\beta$ -Manp-(1,4)-	4.75 101.3	4.08 71.5	3.68 n.d.	3.58 76.1	n.d. n.d.	n.d. n.d.
$\alpha$ -Glc $\rho$ -(1,6)-	4.98 98.8	3.62 72.1	3.91 72.7	3.71 79.7	3.85 n.d.	3.78/3.86 61.2
$\alpha$ -Glc $\rho$ -(1,6)-	4.98 98.8	3.6 72.3	3.75 n.d.	3.52 n.d.	3.93 71.2	3.79/3.98 66.7
$\alpha$ -Glc $\rho$	5.26 93.2	3.56 n.d.	n.d. n.d.	n.d. n.d.	n.d. n.d.	n.d. n.d.
$\beta$ -Glc $\rho$	4.69 97.2	3.28 75	3.49 77.1	n.d. n.d.	n.d. n.d.	n.d. n.d.
( $m/z$ 851)	97.2	75	77.1	n.d.	n.d.	n.d.
$\beta$ -Manp-(1,4)-	4.75 100.1	4.12 69.7	3.81 71.4	3.55 66.7	3.55 n.d.	3.97/n.d. n.d.
$\beta$ -Manp-(1,4)-	4.72 100.1	4.05 n.d.	3.65 n.d.	3.56 74.9	3.81 n.d.	n.d. n.d.
$\alpha$ -Glc $\rho$ -(1,3)-	5.18 100.3	3.57 71.3	3.72 72.7	3.43 76.3	3.89 72.4	3.75/3.89 60.3
$\beta$ -Fru $\rho$ -(2,1)-	n.d. n.d.	– 103.3	4.31 82.9	4.32 73.5	4.06 79.7	3.99/4.12 70.3
$\alpha$ -Glc $\rho$	5.42 91.7	3.53 74.8	3.64 72.7	3.41 69.4	3.92 72	3.75/3.91 60.3
( $m/z$ 851)	91.7	74.8	72.7	69.4	72	60.3

<sup>1</sup> molecular mass as Na<sup>+</sup> adduct (estimated mass +  $m/z$  23) determined by MALDI-TOF MS

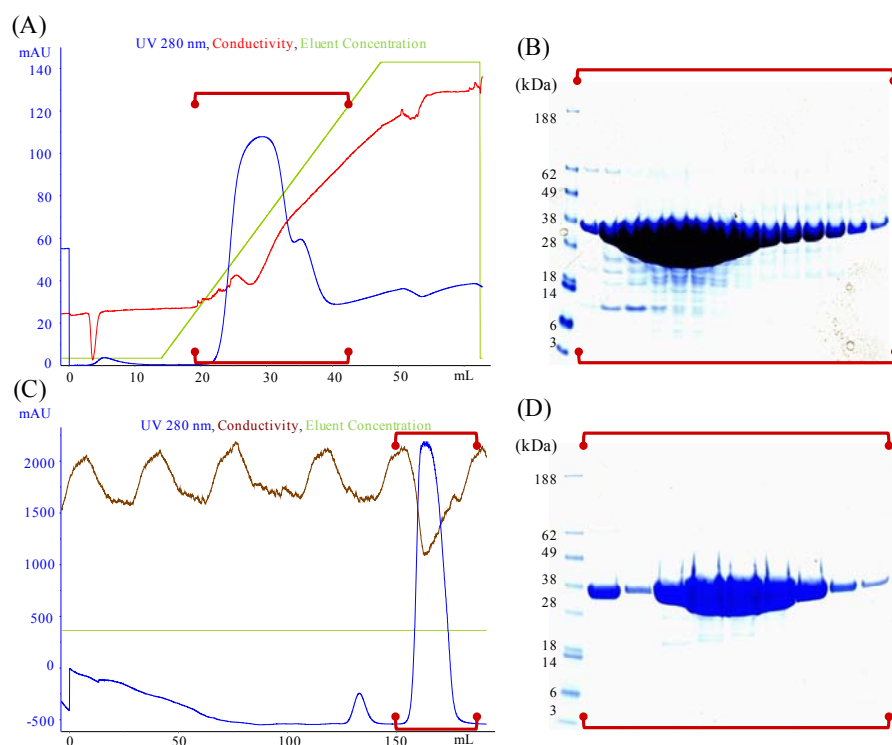
## 6.3 GH10 and GH11 xylanases

### 6.3.1 Production and purification

GH10 (XlnC) and GH11 (XlnA) xylanases from *A. nidulans* FGSC A4 were produced recombinantly as His-tag fusion proteins in *E. coli* BL21(DE3). The enzymes were first tested for expression in 100 mL scale with 10–100  $\mu$ M IPTG induction (data not shown) and purified by immobilized metal ion affinity chromatography using a HisTrap 1 mL column (Fig. 30). The highest enzyme production was obtained with 100  $\mu$ M IPTG in yields of 9 and 8 mg/100 mL culture for XlnA and XlnC, respectively. Afterward, XlnC was produced in 1 L scale and purified by nickel chelating chromatography followed by gel filtration in a yield of 95 mg/L culture (Fig. 31). Both enzymes migrated as a single band in SDS-PAGE and the molecular masses were in agreement with the theoretical masses of  $M_r = 23976.8$  and 33501.3 Da for XlnA and XlnC, respectively (Fig. 30).



**Figure 30** Preliminary productions of XlnA and XlnC; Left, SDS-PAGE of supernatant from BugBuster treated cell, the corresponding bands to XlnC (GH10) and XlnA (GH11) are marked with light yellow arrows. Center, immobilized metal ion affinity chromatograms. Right, SDS-PAGE of XlnA and XlnC, 20  $\mu$ L samples loaded. The red bars in show the fractions which are analysed by SDS-PAGE (see 5.4.3).



**Figure 31** Purification of XlnC. A) immobilized metal ion affinity chromatogram. B) SDS-PAGE of purified XlnC by HisTrap 5 mL column; 15  $\mu$ L samples loaded. C) gel filtration chromatogram of pooled XlnC fractions from (A). D) SDS-PAGE of purified XlnC by Hiload 26/60 Superdex G75 column; 25  $\mu$ L samples loaded; Marker, SeeBlue pre-stained protein standard marker (Invitrogen). The red bars in (A) and (C) show the fractions which are analysed by SDS-PAGE in (B) and (D) (see 5.4.3).

### 6.3.2 Enzyme activity towards xylans

The activities towards birchwood glucuronoxylan, oat spelt arabinoxylan, and wheat arabinoxylan by XlnA and XlnC are shown in Table 16. XlnA and XlnC showed quite similar activity towards the tested xylans, even though on a molar basis XlnC had slightly higher activity than XlnA due to the lower molecular mass of XlnA.

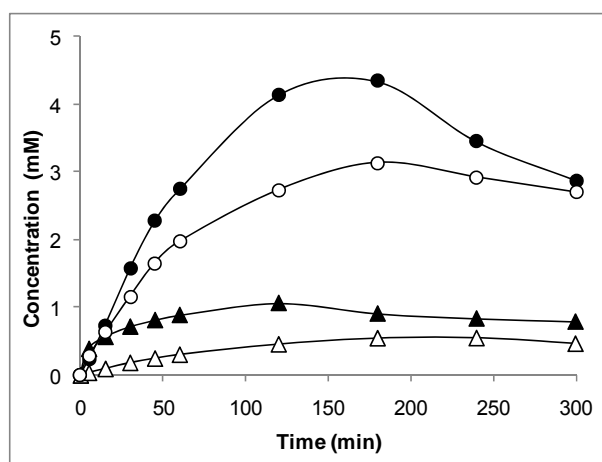
**Table 16** Specific activity of purified XlnA and XlnC towards xylans.

Enzyme	Substrate	Specific activity	
		U/mg	U/mol ( $\times 10^6$ )
XlnA	1.0% Birchwood xylan	330 $\pm$ 13	7,900
	0.5% Oat spelt arabinoxylan	290 $\pm$ 12	7,000
	0.5% Wheat arabinoxylan	350 $\pm$ 10	8,400
XlnC	1.0% Birchwood xylan	280 $\pm$ 9	9,500
	0.5% Oat spelt arabinoxylan	250 $\pm$ 9	8,500
	0.5% Wheat arabinoxylan	300 $\pm$ 10	10,200

Standard deviations were calculated from 4 experiments (see 5.6.3.1 for experimental details)

### 6.3.3 Transglycosylation

The preliminary screening of transglycosylation by XlnA and XlnC was done using six disaccharides (xylobiose, cellobiose, maltose, isomaltose, lactose, mannobiose) and two sugar alcohols (xylitol and sorbitol) as acceptor candidates and the reaction was monitored as product formation by TLC and MALDI-TOF MS (data not shown). XlnC can use xylobiose, cellobiose, xylitol, and sorbitol as acceptors, whereas XlnA can use only xylobiose. Therefore, XlnC was used for further investigation in an attempt to make novel oligosaccharides. The progress of transglycosylation by 1  $\mu$ M XlnC with 20 mM X3 and 200 mM acceptor (xylobiose, cellobiose, xylitol, or sorbitol) is shown in Fig. 32 and the total product yields with each acceptor is given in Table 17.



**Figure 32** Progress of transglycosylation with different acceptors catalysed by XlnC. Reaction mixtures contained 1  $\mu$ M XlnC, 20 mM X3 and 200 mM acceptor; X2 (▲), cellobiose (△), xylitol (●), and sorbitol (○).

**Table 17** Maximum transglycosylation yields with different acceptors by XlnC.

Acceptor	Yield (%)	Production (mg/mL)	No. of major TG product peaks
<u>Disaccharides</u>			
Xylobiose	5	0.58	2 <sup>1</sup>
Cellobiose	3	0.33	2
<u>Sugar alcohols</u>			
Xylitol	22	1.80	3
Sorbitol	16	1.40	3

<sup>1</sup> as xylotetraose and xylohexaose

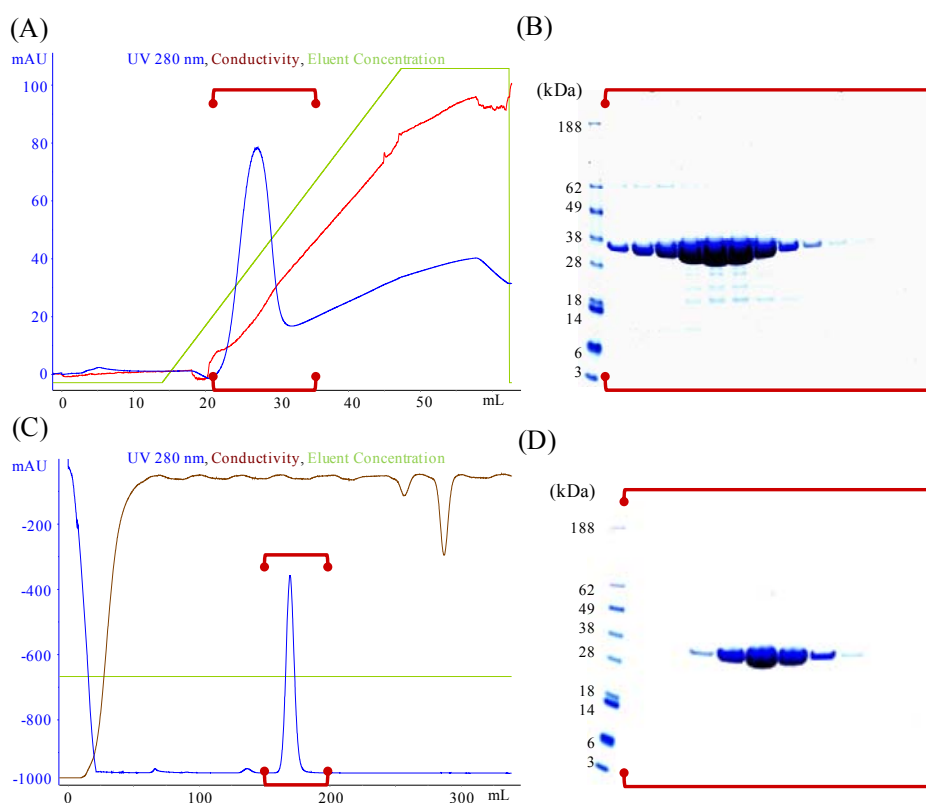
The yield was estimated as percentage of product/donor concentration (mM/mM)

### 6.3.4 GH10 glycosynthase

The GH10 glycosynthase mutant E244A from XlnC was produced recombinantly as His-tag fusion proteins in *E. coli* BL21(DE3). E244A was purified by nickel chelating chromatography followed by gel filtration in the same fashion as for XlnC and was obtained in a yield of 28 mg/L culture (Fig. 33). E244A had



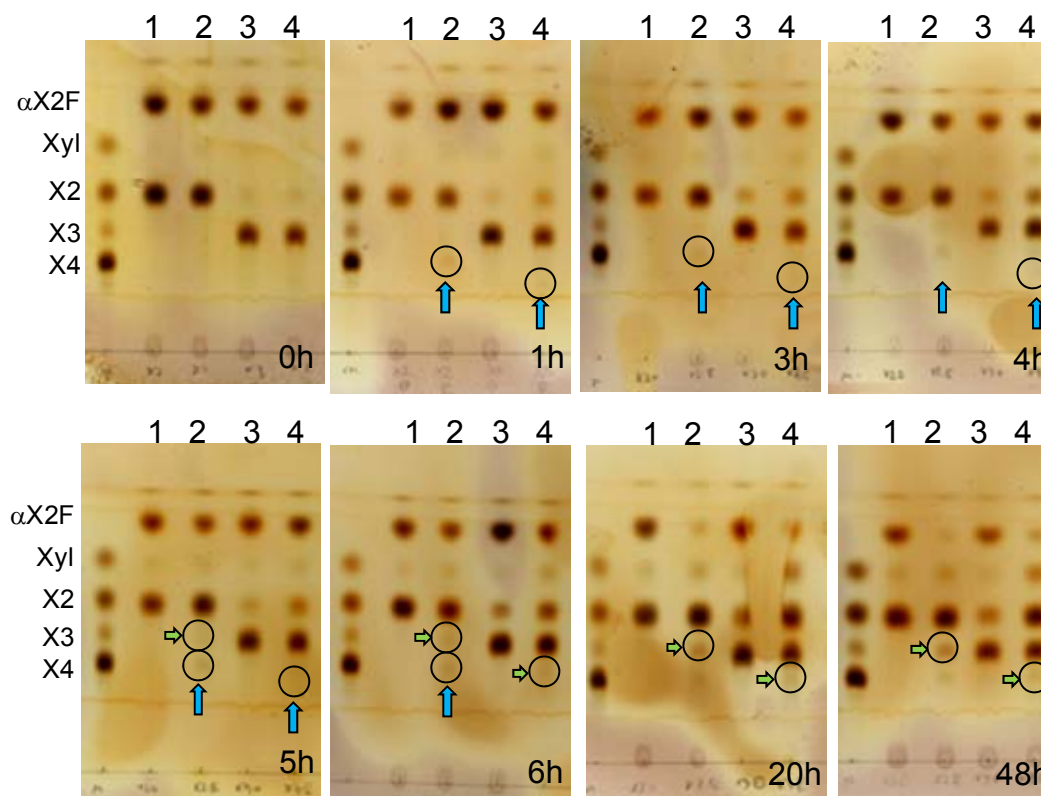
specific activity of 0.26 U/mg towards 1% birchwood xylan (see 5.6.3.1) which was two orders of magnitude lower than for XInC wild-type.



**Figure 33** Purification of E244A using immobilized metal ion affinity chromatography followed by gel filtration. A) immobilized metal ion affinity chromatogram, 15  $\mu$ L samples loaded; B) SDS-PAGE of purified E244A by HisTrap 5 mL column; C) gel filtration chromatogram of pooled E244A fractions from (A); D) SDS-PAGE of purified E244A by Hiload 26/60 Superdex G75 column; 20  $\mu$ L samples loaded; marker, SeeBlue marker (Invitrogen). The red bars in (A) and (C) show the fractions which are analysed by SDS-PAGE in (B) and (D) (see 5.4.3).

The glycosynthase reactions of 87  $\mu$ M E244A using  $\alpha$ -xylobiosyl fluoride ( $\alpha$ X2F) as donor and X2 or X3 as acceptor were monitored by TLC during 48 h at 30°C (Fig. 34). The reactions with donor and acceptor without addition of E244A were done in parallel with the glycosynthase reactions as controls.  $\alpha$ X2F was degraded during the incubation period seen as X2 in the control reaction with X3 as acceptor, but more than 50%  $\alpha$ X2F still remained after 48 h. No severe changes of pH of the reactions occurred during the incubation period as monitored by pH paper (MACHEREY-NAGEL GmbH & Co. KG, Düren, Germany). The glycosynthase products X4 and X5 from X2 and X3 as acceptors, respectively, were detected after 1 h incubation and increased until 5 h. However, the glycosynthase products were hydrolysed during the incubation because of the hydrolytic activity of E244A, therefore the glycosynthase products were not accumulated. In addition, E244A can carry out transglycosylation involving hydrolysis of acceptor *e.g.* X2, the enzyme hydrolyses X2 and transfer xylosyl residue to another X2 molecule resulting in X3, which can be visualised by the increased in X1 and X3 during the reaction. In case of X3 as acceptor, the transglycosylation product X4 was formed. The presence of

xylose in control reactions could be because of the degradation of  $\alpha$ XF, which is present as minor contaminant in  $\alpha$ X2F.



**Figure 34** Progress of glycosynthase reactions using 87  $\mu$ M E244A with 10 mM  $\alpha$ X2F as donor and 5 mM X2 or X3 as acceptor in 100 mM sodium acetate pH 5.0 at 30°C during 48 h, monitored by TLC. Lane 1, reaction with X2 as acceptor without E244A; lane 2, reaction with X2 as acceptor with E244A; lane 3, reaction with X3 as acceptor without E244A; lane 4, reaction with X3 as acceptor with E244A; developed by acetonitrile/water (80:20, v/v) twice and visualized by 0.2% orcinol solution (see 5.7.4); **blue arrows** indicate glycosynthase products (very faint); **green arrows** indicate transglycosylation products (very faint).

## 6.4 GH61 putative endo- $\beta$ -glucanase

### 6.4.1 cDNA cloning

The putative GH61 endo- $\beta$ -glucanase (*eglF*) gene from *A. nidulans* FGSC A4 was obtained by cDNA cloning, cloned into pPICZ $\alpha$ A vector (pPICZ $\alpha$ A-EglF), and transformed into *P. pastoris* (see 5.10, page 44). The pPICZ $\alpha$ A-EglF was fully sequenced using 5'AOX as sequencing primer (Fig. 35) confirmed the successful cloning of this gene. Sequence alignment of *eglF* with the AN3860 from *A. nidulans* FGSC A4 genome (Galagan et al., 2005) is shown in (Fig. 35) with the intron between 327 and 378 bases.

```

AN3860 -----
eglF_5AOX TTTTACGACACTTGAGAAGATCAAAAAACAACATAATTATTCGAAACGATGAGATTTCTCTT 60

AN3860 -----
eglF_5AOX CAATTTTTACTGCTGTTTTATTTCGCAGCATCTCCGCATTAGCTGCTCCAGTCAACACTA 120

AN3860 -----
eglF_5AOX CAACAGAAGATGAAACGGCACAAATTCGGCTGAAGCTGTCATCGGTTACTCAGATTTAG 180

AN3860 -----
eglF_5AOX AAGGGGATTTGATGTTGCTGTTTTGCCATTTTCCACAGCACAAATAACGGGTTATTGT 240

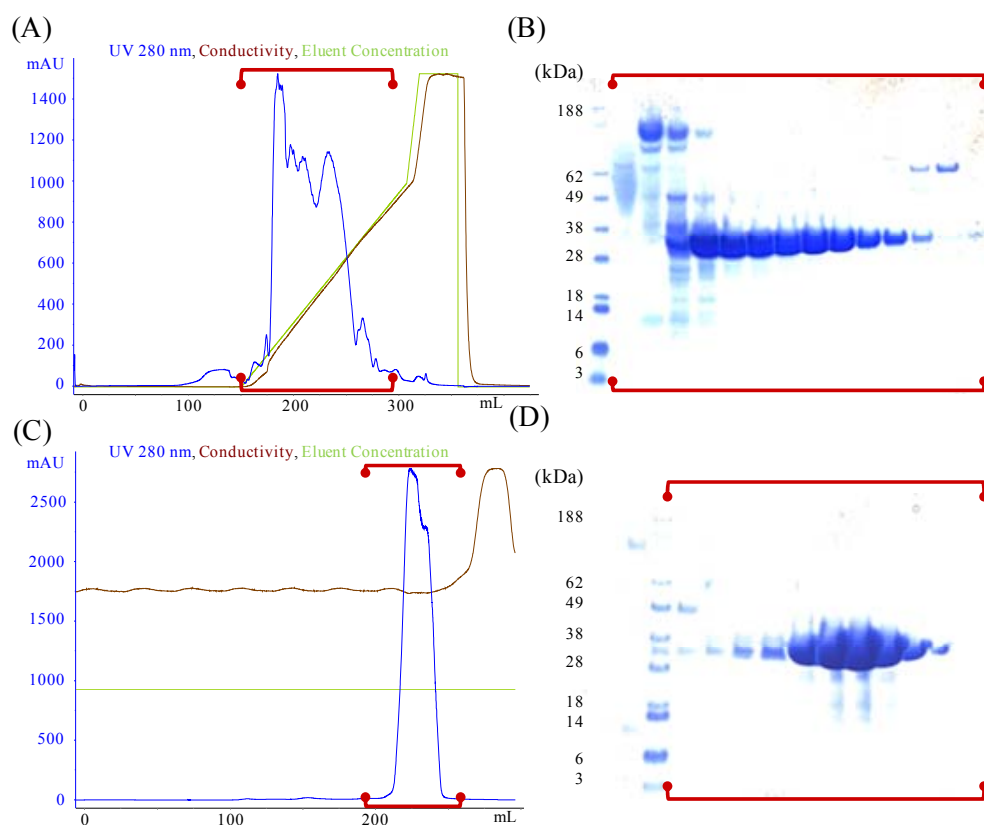
AN3860 -----ATGGCCATGTCGAAGATTGCTACCCTCGC-----GGGTCT-TCTCGCCTCTG 46
eglF_5AOX TTATAAATACTACTATTGTCAGCATTTGCTGCTAAAGAAGAGGGGTATCTCTCGAGAAAA 300
          * * * * *
AN3860 CTGGCCTCGTTGCAGGCCACGGATACGTGACGAAGATGACGATCGATGGAGAAGAATATG 106
eglF_5AOX GAGAGGCTGAAGCTGGCCACGGATACGTGACGAAGATGACGATCGATGGAGAAGAATATG 360
          * * * * *
AN3860 GTGGATGGCTCGCTGATAGCTATTACTACATGGACTCGCCGCCGGATAACTACGGATGGA 166
eglF_5AOX GTGGATGGCTCGCTGATAGCTATTACTACATGGACTCGCCGCCGGATAACTACGGATGGA 420
          * * * * *
AN3860 GTACGACAGTGACCGACAATGGCTTCGTCTCCCGCGATGCCTTTGGTACCGACGACATCA 226
eglF_5AOX GTACGACAGTGACCGACAATGGCTTCGTCTCCCGCGATGCCTTTGGTACCGACGACATCA 480
          * * * * *
AN3860 CCTGCCACAGGGGCGCCACTCCTGGTGTCTCTCTGCCCGGTGACAGCCGGCAGCAAGA 286
eglF_5AOX CCTGCCACAGGGGCGCCACTCCTGGTGTCTCTCTGCCCGGTGACAGCCGGCAGCAAGA 540
          * * * * *
AN3860 TCGATATCACTTGGAACACCTGGCCC GAATCTCAT AAGGGTGGGTATTAACCTTCAAATG 346
eglF_5AOX TCGATATCACTTGGAACACCTGGCCC GAATCTCAT AAGGG----- 580
          * * * * *
AN3860 CTTTTGCTTGTCTTACTAACAGATAATCAAGGCCCATCATCAACTACCTCGCAAATGC 406
eglF_5AOX -----CCCATCATCAACTACCTCGCAAATGC 608
          * * * * *
AN3860 AACGGCGACTGCTCTTCAGCCGACAAGACCAGCCTCGAATTCGTGAAGATCCAGGCCGAA 466
eglF_5AOX AACGGCGACTGCTCTTCAGCCGACAAGACCAGCCTCGAATTCGTGAAGATCCAGGCCGAA 668
          * * * * *
AN3860 GCGATTGTCGACGCTTCCACCAACACCTGGGTTACCGATGAACCTATTGAGAACTCCTTC 526
eglF_5AOX GCGATTGTCGACGCTTCCACCAACACCTGGGTTACCGATGAACCTATTGAGAACTCCTTC 728
          * * * * *
AN3860 ACTACTTCCGTTACGATCCCTGCCTCCATCGCCCCAGGTAACTACGTCTCCGACACGAG 586
eglF_5AOX ACTACTTCCGTTACGATCCCTGCCTCCATCGCCCCAGGTAACTACGTCTCCGACACGAG 788
          * * * * *
AN3860 ATCATCGCCCTCCACTCTGCAGGCCAGCAGAACGGTGC CCAAGCATACCTCAGTGTCTG 646
eglF_5AOX ATCATCGCCCTCCACTCTGCAGGCCAGCAGAACGGTGC CCAAGCATACCTCAGTGTCTG 848
          * * * * *
AN3860 AACCTGGTTGTCAGCGGCAGCGGTACTGACAACCATCTGGTACTCCTGGTACTCAGCTG 706
eglF_5AOX AACCTGGTTGTCAGCGGCAGCGGTACTGACAACCATCTGGTACTCCTGGTACTCAGCTG 908
          * * * * *
AN3860 TACTCTGCTAACGATGAGGGCATCGTCTTCGATATCTACTCGAACCCGACCTCGTACCCT 766
eglF_5AOX TACTCTGCTAACGATGAGGGCATCGTCTTCGATATCTACTCGAACCCGACCTCGTACCCT 968
          * * * * *
AN3860 ATGCCTGGTCTGAGCTGTACAGTGGTTAG----- 796
eglF_5AOX ATGCCTGGTCTGAGCTGTACAGTGGTACATCATCATCATTAATCTAGAACAAAA 1028
          * * * * *
AN3860 -----
eglF_5AOX ACTCATCTCAGAGA 1042

```

**Figure 35** Sequence alignment of GH61 putative endo- $\beta$ -glucanase (*eglF*) gene (using 5'AOX as sequencing primer) and the corresponding gene from genomic sequence (AN3860); the nucleic acids translated to mature protein is in red and the intron is in blue.

## 6.4.2 Production and purification

The *eglF* gene was first cloned into pET28-a(+) using *E. coli* BL21(DE3) as expression host, however *E. coli* was not able to produce this protein. Therefore, *eglF* was cloned into pPICZ $\alpha$ A vector to give the putative GH61 endo- $\beta$ -glucanase and expressed using *P. pastoris* X-33 as host. The putative GH61 endo- $\beta$ -glucanase (EglF) was produced recombinantly as a His-tag fusion protein and purified by anion exchange chromatography (Fig. 36A,B) followed by gel filtration chromatography (Fig. 36C,D) in a yield of 66 mg/L culture.

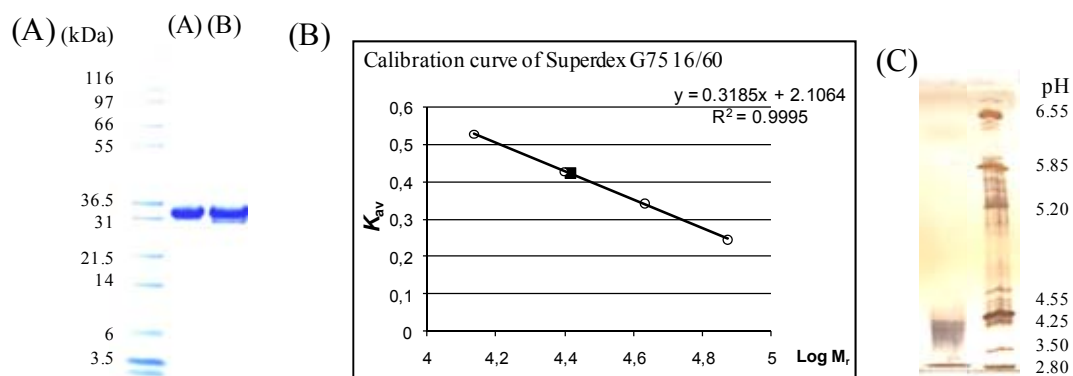


**Figure 36** Purification of GH61 EglF. A) anion exchange chromatogram; B) SDS-PAGE of purified EglF by Resource Q 6 mL column, 15  $\mu$ L samples loaded; C) gel filtration chromatogram of pooled EglF fraction from (A); D) SDS-PAGE of purified EglF by Hiload 26/60 Superdex G200 column, 15  $\mu$ L samples loaded; marker, SeeBlue marker (Invitrogen). The red bars in (A) and (C) show the fractions which are analysed by SDS-PAGE in (B) and (D) (see 5.4.1).

## 6.4.3 Protein characterisation and screening for activity

EglF migrated as a single band in SDS-PAGE with estimated size of 30 kDa (Fig. 37A). The theoretical mass ( $M_r$ ) of EglF was 25004.3 Da and gel filtration gave a value of 26 kDa (Fig. 37B), indicating that EglF is a monomer in solution. EglF contains two possible *N*-glycosylation sites, however, endoglycosidase H treatment showed no difference between untreated and treated protein forms. The isoelectric point of EglF was 4.0 (Fig. 37C). EglF showed very low specific activity towards barley  $\beta$ -glucan and oat spelt arabinoxylan with values of  $180 \pm 9.0$  and  $145 \pm 2.8$

$\mu\text{U}/\text{mg}$  (see 5.10.3), when incubated for 16 h, indicating that this protein was either not a typical  $\beta$ -glucanase or it was produced as an inactive enzyme.



**Figure 37** Molecular mass of EglF determined by SDS-PAGE (without and with endoglycosidase H treatment) and gel filtration, and pI of EglF. A) SDS-PAGE of purified and deglycosylated EglF; Left lane, marker, Mark12 unstained protein standard marker (Invitrogen); lane A, 7  $\mu\text{g}$  EglF; lane B, 7  $\mu\text{g}$  deglycosylated EglF, endoglycosidase H is seen as a band at 29 kDa; B) calibration curve of superdex G75 16/60 column (open circle) and EglF (black square), EglF has molecular weight of 26 kDa indicated by a black square; C) isoelectric focusing of 800  $\mu\text{g}$  purified EglF using polyacrylamide PhastGel IEF (pH 4–6.5) with low range pI (pH 2.5–6.5) calibration standard (GE Healthcare).

#### 6.4.4 Binding to carbohydrate microarrays

The putative GH61 endo- $\beta$ -glucanase EglF showed no binding towards the tested carbohydrate microarrays at pH 6 and 7 (see 5.10.4), indicating that the protein may not function as a binding protein, has very low affinity towards the tested carbohydrates, or has the specificity towards other carbohydrate than the tested ones.

## 7. Discussion

### 7.1 GH3 xylosidases

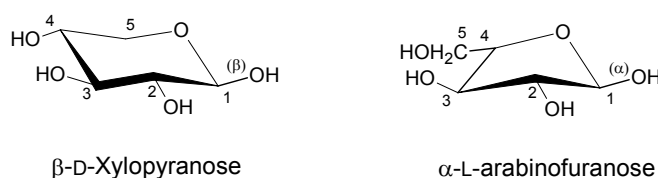
#### 7.1.1 Production of BxlA

The GH3  $\beta$ -xylosidase from *A. nidulans* FGSC A4 (BxlA) was secreted in recombinant form from *P. pastoris* as directed by the  $\alpha$ -factor secretion signal sequence from *S. cerevisiae*. The production of BxlA was much more efficient than the production by *A. nidulans* CECT2544 resulting in 0.5 mg/L (Kumar and Ramón, 1988) and was in the same range as found for the previously reported recombinant BxlA (as XlnD) in *A. nidulans* G191 host (Pérez-González et al., 1998). BxlA was glycosylated in *P. pastoris* (see Fig. 13, page 51) and the carbohydrate content corresponded well with its apparent molecular mass. However, the glycosylation was not present in native BxlA secreted from *A. nidulans* (Kumar and Ramón, 1988) hence this high glycosylation is a result of production by *P. pastoris*.

#### 7.1.2 Comparison of hydrolytic activity of BxlA and BxlB

In comparison with BxlB sharing 45% sequence identity with BxlA, Both BxlA and BxlB have quite similar pH optima of 5.0 and 5.2, respectively, but different temperature optima (50°C for BxlA and 60°C for BxlB). Additionally, BxlA is more sensitive to pH and temperature than BxlB (see Fig. 14, page 52). Most fungal GH3  $\beta$ -xylosidases, as well as BxlA and BxlB, have pH and temperature optima in the pH range 4–6 and 50–70°C (Herrmann et al., 1997; Knob et al., 2010; Kumar and Ramón, 1996; Kurakake et al., 1997). Additionally, BxlB has a wider pH stability range (pH 4–8) compared with most GH3  $\beta$ -xylosidases having pH 4–6 (Herrmann et al., 1997; Knob et al., 2010; Kumar and Ramón, 1996; Kurakake et al., 1997). Also the temperature stability up till 50–60°C of BxlB resembled that of other fungal GH3  $\beta$ -xylosidases (Herrmann et al., 1997; Knob et al., 2010; Kumar and Ramón, 1996; Kurakake et al., 1997; Rasmussen et al., 2006), whereas BxlA was sensitive to the temperatures >45°C. The incubation time of this experiment was 5 h, which was used to investigate the stability of the enzymes during transglycosylation reactions. In addition,  $\text{Ag}^{2+}$  and  $\text{Cu}^{2+}$  have strong effect on BxlA (see Table 6, page 51) as well as the native *A. nidulans* GH3  $\beta$ -xylosidases (XlnD; Kumar and Ramón, 1996). XlnD was found to be inhibited also by  $\text{Zn}^{2+}$ , whereas no inhibition was observed in BxlA. The metal inhibition may be due to the metal ion complex particularly with sulfhydryl groups (Whitaker, 1994). BxlA and BxlB have the capability to hydrolyse also  $\alpha$ -L-arabinofuranosidase (*p*NPA; see Table 7, page 53) with two and one orders of magnitude lower catalytic efficiency, respectively, compared to activity for *p*NPX. The low specificity towards *p*NPA has also been observed in some GH3  $\beta$ -xylosidases (Bauer et al., 2006; Herrmann et al., 1997; Lee et al., 2003). Structurally,  $\beta$ -D-xylopyranose, preferably forming a pyranose ring with chair conformation projecting the hydroxyl groups in equatorial positions away from the ring, is related to the  $\alpha$ -L-arabinofuranose, which forms a pucker conformation that resembles equatorial 2-OH and 3-OH of  $\beta$ -D-xylopyranose, and the hydroxyl configuration at the anomeric carbon of  $\alpha$ -L-arabinofuranose also resembles that of  $\beta$ -D-xylopyranose (Fig. 38). These conformations are energetically more favourable than other

configurations (Carpita and McCann, 2000) and may be the reason for  $\beta$ -xylosidase to have the side activity of  $\alpha$ -L-arabinofuranose. The  $K_m$  of 1.3 mM towards *p*NPX of BxlA and BxlB produced in this study is quite similar to that of the native BxlA from *A. nidulans* (Kumar and Ramón, 1996), but the  $k_{cat}$  of BxlA is three fold higher. The kinetic parameters of GH3  $\beta$ -xylosidases towards *p*NPX from different sources are shown in Table 18. BxlA has quite high hydrolytic activity towards *p*NPX, whereas BxlB gives values quite similar to other  $\beta$ -xylosidases. In addition, BxlA showed higher  $k_{cat}$  than BxlB towards all tested xylooligosaccharides (see Table 7, page 53). The kinetic parameters towards xylooligosaccharides (X2–X6) showed that both BxlA and BxlB prefer to hydrolyse xylobiose, while the catalytic efficiency decreased slightly towards longer xylooligosaccharides, as is the typical behaviour of exo-type enzymes and suggesting that BxlA and BxlB possibly possess with two substrate binding subsites (Biely, 2003; Herrmann et al., 1997; Matsuo and Yasui, 1984; Rasmussen et al., 2006).



**Figure 38** Conformation models of  $\beta$ -D-xylopyranose and  $\alpha$ -L-arabinofuranose

**Table 18** Kinetic parameters of GH3  $\beta$ -xylosidases towards *p*NPX.

Organism	$k_{cat}$ $s^{-1}$	$K_m$ mM	$k_{cat}/K_m$ $s^{-1} \cdot mM^{-1}$	Reference
<i>A. nidulans</i> (BxlA)	112	1.3	90	This study
<i>A. nidulans</i> (BxlB)	18	1.3	14	This study
<i>A. nidulans</i> (XlnD <sup>a</sup> )	37 <sup>b</sup>	1.1	34	Kumar and Ramón, 1996
<i>A. awamori</i>	11 <sup>c</sup>	4.1	2.7	Eneyskaya et al., 2003
<i>A. awamori</i>	17.5	0.25	70	Eneyskaya et al., 2007
<i>T. reesei</i>	176	0.42	419	Hermann et al., 1997
<i>Hordeum vulgare</i>	15.5	1.7	9.1	Lee et al., 2003

<sup>a</sup> BxlA was referred to as XlnD

<sup>b</sup> calculated from 25.6  $\mu$ mol/min/mg protein; MW: 85000 Da

<sup>c</sup> calculated from 5.3 nmol/min/ $\mu$ g protein; MW: 125000 Da

### 7.1.3 Transglycosylation and acceptor specificity of BxlA

BxlA displays broad acceptor specificity in transglycosylation and most of the transglycosylation reactions result in more than one product observed in HPAEC-PAD chromatograms (see Fig. 16 and Table 8, page 54–55). The minor products, possibly with different linkages or products synthesised from different forms of one acceptor ( $\alpha$ ,  $\beta$ , pyranosyl, furanosyl forms), complicates identification of their

structures. Thus, the heterogeneity of such samples hampers the assignment of NMR spectra and precludes assignment for some of the transglycosylation products.  $\beta$ -Xylosidases of GH3 from *A. niger* (Puchart and Biely, 2007), *A. awamori* (Eneyskaya et al., 2003), and *Penicillium wortmanni* (Win et al., 1988) were reported to possess transglycosylation activity, demonstrated by the synthesis of mainly  $\beta$ -1,4 linked xylooligosaccharides, whereas  $\beta$ -1,6 were formed predominantly when using hexose-containing acceptors (Kurakake et al., 1997; 2005). This is similar to the case of BxlA having mainly  $\beta$ -1,4 regioselectivity when using pentose acceptors (xylose, arabinose, lyxose) and mainly  $\beta$ -1,6 xylosidic-linkage when using hexose-containing acceptors (glucose, mannose; see Table 9, page 58). In case of disaccharide acceptors,  $\beta$ -1,4 and  $\beta$ -1,6 xylosyl linkage was found reflecting that BxlA has loose acceptor recognition.

BxlA displayed broad acceptor specificity in transglycosylation and had the highest transglycosylation yield using xylitol as acceptor and, among 10 tested monosaccharides, can transglycosylate mannose, lyxose, and talose in similar maximum total yields as xylose (>20% yield), while it was less efficiency in transglycosylate arabinose, glucose, galactose, and fructose and could not use L-rhamnose as acceptor (see Table 8, page 55). In general, BxlA as well as exo  $\beta$ -glucanase from *H. vulgare* (ExoI) and  $\beta$ -glucosidase from *T. neapolitana* (Bgl3B) seem to have loose acceptor recognition at subsite +1, which could be the reason for the broad acceptor specificity of BxlA. The loose acceptor recognition could allow the acceptor molecule to have some freedom to bind with different conformation resulting in different linkage formation as shown by the transglycosylation products from hexose and disaccharide acceptors (see Table 9, page 58). This may be affected by the accessibility or less steric hindrance configuration of the acceptors. The subsite +1 of BxlA is not quite clear on its 3D-models due to the not well conserved domain 2, however Tyr446 could be the key interaction with suitable acceptor molecules, which is equivalent to Trp434 in exo  $\beta$ -glucanase from *H. vulgare* and Ser370 in  $\beta$ -glucosidase from *T. neapolitana* (see Fig 18, page 60). According to the conformation of Tyr446 in 3D models, the hydroxyl group of this tyrosine could provide a hydrogen bond to 2-OH or 3-OH of a sugar acceptor at subsite +1 or it could form stacking interaction to the sugar ring by its aromatic residue. The thiocellobiose in the active site of the model structures was created by superimposition with ExoI to help illustrating structural details of subsite -1 and +1. In addition, disaccharides are generally poor acceptors for BxlA (2–7%) as compared to their monosaccharide counterparts (21–25%). The low transglycosylation yield using maltose in case of BxlA (2%) is in agreement with 0.8% yield of the GH3  $\beta$ -xylosidase from *A. awamori* (Kurakake et al., 2005) which tested four disaccharides: trehalose, palatinose, isomaltose, and maltose. This observation also supports the lack of recognition at subsites beyond +1 and is in agreement with the kinetics on hydrolysis of xylooligosaccharides. Noticeably, with the extended choices of mono- and disaccharide as acceptor candidates in transglycosylation screening, BxlA were able to produce 14 xylosyl oligosaccharides including five, which were not previously reported using lyxose, L-fucose, talose, sucrose, and turanose as acceptors.

In preliminary transglycosylation screening for BxlA, increasing acceptor/donor ratio (from 200/30 to 1000/40 mM; data not shown) resulted in a higher transglycosylation potency of BxlA. However, high acceptor concentrations present practical challenges in purification of the transglycosylation products due to broad acceptor peaks masking the products and decrease solubility of acceptors in acetonitrile used in the HPLC purification.



#### 7.1.4 Transglycosylation using amino acids as acceptors

Interestingly, this is the first report revealing the possibility to use amino acids as acceptors for transglycosylation catalysed by a wild-type glycoside hydrolase, which could be an alternative way to produce glycopeptides or thio-sugars. With Xyl-Cys (see Fig 17, page 56), we demonstrated that cysteine can be used as acceptor and forms a thio-glycosidic linkage. Such formation of thio-glycosidic linkage by protein engineered glycoside hydrolase was previously demonstrated by production of thio-sugar or thio-linked saccharides catalysed by thioglycosynthase of  $\beta$ -glucosidase from *Agrobacterium sp.* using  $\alpha$ -glucosyl fluoride as donor and *p*NP 4-deoxy-4-thio- $\beta$ -D-glucopyranoside as acceptor (Jahn and Withers, 2003; Müllegger et al., 2005). In case of L-serine as acceptor, very low amount of Xyl-Ser was observed, but this cannot be confirmed by MS/MS. This could be because L-serine is not a suitable acceptor for BxlA or the reaction conditions were not suitable. The use of low pH (pH 5.0) may not be suitable for Ser as well as Cys to be deprotonated (Whitaker, 1994). To investigate this reaction further, a suitable detection method is required to improve monitoring of the progress of the reaction. Tyrosine has hydroxyl group in the side chain, which makes it eligible as acceptor for transglycosylation by BxlA, but it was not tested because of its low solubility in aqueous solution.

#### 7.1.5 Glycosynthase and subsite mutants of BxlA

In case of glycosynthase and subsite +1 mutants of BxlA, the mutation has some effect on the recombinant protein production (see 6.1.6, page 59), and the yields were 50% lower as compared with BxlA wild-type enzyme. These mutant enzymes could be purified in soluble form which indicated that the overall structures are intact, although one cannot exclude major changes at the active site. The glycosynthase reactions are usually conducted at pH 6–7 (Fajies et al., 2003; Kim et al., 2006; Sugimura et al., 2006) to adapt to the stability of fluoride substrates. Even though BxlA glycosynthase mutants showed some activity (see Fig. 19, page 61), reactions by these glycosynthase mutants were considered as unsuccessful since the reaction consumed very high amount of enzymes and the enzymes cannot accept natural sugars (xylose, galactose, and cellobiose; see 6.1.6). Surprisingly, the highest activity was observed at pH 7.0, even though the BxlA wild-type enzyme was not stable at pH higher than 6. This may indicate that the enzyme still has intact structure at pH 7.0 and catalytic acid/base residue (Glu) can act as general base to perform glycosynthase reaction through the deglycosylation step (see Fig. 4 and 5, page 15). In case of subsite +1 mutants, the substitution of Cys308 to Trp caused severe reduction in hydrolytic activity similarly to nucleophile mutants and the enzyme could almost not hydrolyse *p*NPX as observed in transglycosylation reactions, indicating that Cys308 is essential for BxlA, and may form a disulfide bond as explained earlier in 6.1.6 (see also Fig. 18, page 60). In case of Asn313, N313R showed 50–150% increase in transglycosylation activity using hexoses and maltose, but a slight decrease using xylose as acceptors, which could show the effect of Arg residue on accepting the hexose ring by forming a hydrogen bond to 6-OH at subsite +1 as guided by the 3D model of BxlA using exo  $\beta$ -glucanase from *H. vulgare* as template (see Fig. 18C, page 60).

## 7.2 GH5 mannanases

### 7.2.1 Production of ManAS289W and ManCW283S

Two GH5 mannanases (ManA and ManC), sharing 38% sequence identity, from *A. nidulans* FGSC A4 and subsite +1 mutants (ManAS289W and ManCW283S) were secreted in recombinant forms as His-tag fusion proteins in *P. pastoris* X-33 as directed by the  $\alpha$ -factor secretion signal sequence. The production of subsite +1 mannanase mutants (ManAS289W and ManCW283S) was lower than that of ManA and ManC wild-type enzymes. This is because the difference in induction media (complex medium (BMMY) for wild-type and minimal medium (BMM) for mutant enzymes) and duration of induction (5 days for wild-type and 3 days for mutant enzymes). The use of BMM instead of BMMY is to overcome a technical problem during the production of the enzymes. Noticeably, in both cases, the production of the recombinant enzymes was more efficient than from the production of native enzymes from *A. niger* (Ademark et al., 1998) or *H. jecorina* (Arisan-Atac, et al., 1993; Stålblbrand, 1993) cultures or from the recombinant production in *S. cerevisiae* (Evodia Setati et al., 2001). Both ManAS289W and ManCW283S were slightly glycosylated similarly to their corresponding wild-type enzymes (see Fig. 23, page 64). The glycosylation has also been observed in native *H. jecorina* mannanase (Arisan-Atac, et al., 1993).

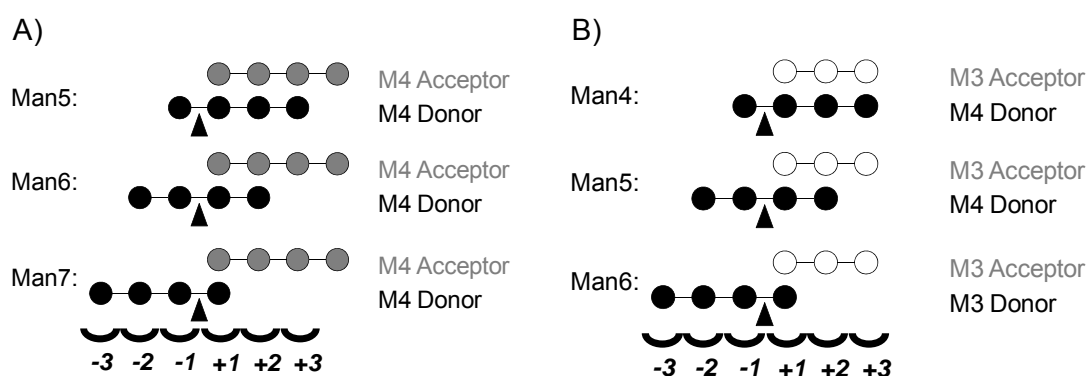
### 7.2.2 Enzymatic properties of GH5 mannanases

ManC showed higher activity towards mannans than ManA (see Table 12, page 65) and had slightly higher activity than *H. jecorina* and Aspergilli mannanases (Ademark et al., 1998; Evodia Setati et al., 2001; Hägglund et al., 2003; Kurakake and Komaki, 2001), which have specific activity in the range of 230–630 U/mg towards LBG GalMan. The kinetic parameters towards mannoooligosaccharides (M4–M6) of ManA and ManC are compared to *H. jecorina* and *M. edulis* GH5 mannanases (Table 19). The  $k_{cat}/K_m$  values of ManA and ManC were similar to those of *M. edulis* GH5 mannanase (Larsson et al., 2006), but lower than that from *H. jecorina* (Anderson, 2006) and showed increasing in  $k_{cat}/K_m$  with increasing chain length of mannoooligosaccharides, which is typical behavior of endo-acting enzymes and suggesting that ManA and ManC possibly possess with 5–6 substrate binding subsites. Both ManA and ManC wild-type enzymes have mannobiose as main hydrolysis products from M4–M6 (Table 14, page 66), which are also in agreement with the result from transglycosylation reactions. The possible formation of transglycosylation products is illustrated in Fig. 39, which was according to all transglycosylation products (Fig. 25, page 68). M5–M7 are the possible transglycosylation products using M4 as donor and acceptor, which were present in the reaction with 30 mM M4, while M6 was produced as the major product. M4–M6 are the possible products using M4 as donor and M3 as acceptor, which were present in the reaction using 24 mM M4 with 100 mM M3, while M5 was produced as the major product. Even though M4 as transglycosylation product cannot be monitored because of the use of M4 as donor (and M3 as acceptor), both cases confirmed that the mannobiosyl accumulated at the donor binding sites (“minus subsites”) during the first step of the hydrolysis and interact with an incoming M4 or M3 acceptor. This is in agreement with the hydrolysis action pattern analysis, which showed that M2 is the

main product from M4 and M6 hydrolysis. This clearly showed that the subsite –2 dominates binding at the glycone part of the active site cleft for both ManA and ManC. ManA produced more M1 and M3 from M4 than ManC in hydrolysis action pattern analysis, which may reflect either a higher affinity at subsite(s) –3 and/or +3 or weaker substrate affinity at subsite(s) –2 and/or +2 as compared to ManC. The hydrolysis action pattern on M6, however, does not support a difference in affinity of subsite(s) –3 and/or +3 for ManA and ManC, since they produce essentially the same amount of M3. The more likely explanation is that there is a difference in the –2 and/or +2 subsite(s) between these two enzymes.

**Table 19** Kinetic parameters of GH5  $\beta$ -mannanases towards mannoooligosaccharides (M4-M6).

Organism	Substrate	$k_{cat}$ $s^{-1}$	$K_m$ mM	$k_{cat}/K_m$ $s^{-1}\cdot mM^{-1}$	Reference
<i>A. nidulans</i> (ManA)	M4	–	–	6	This study
	M5	67	2.9	23	
	M6	193	1.8	109	
<i>A. nidulans</i> (ManC)	M4	–	–	7	This study
	M5	112	1.8	61	
	M6	134	0.6	215	
<i>H. jecorina</i> (Man5A)	M4	6.3	0.31	21	Anderson, 2006
	M5	13	0.08	163	
	M6	20	0.04	500	
<i>M. edulis</i> (Man5A)	M4	0.70	2.49	0.28	Larsson et al., 2006
	M5	45	1.61	28	
	M6	99	0.5	198	



**Figure 39** Illustration of transglycosylation products formation using A) M4 as donor and acceptor and B) M4 as donor and M3 as acceptor.

### 7.2.3 Effect of subsites of GH5 mannanases

According to 3D homology models of ManA and ManC (see Fig. 26, page 69), Asn319 of mannanase from *H. jecorina* (PDB ID: 1QNR) could form a hydrogen bond to 6-OH of the mannose residue at subsite -3, whereas the equivalent amino acid in ManA, Asp362 was oriented to bind with 3-OH of the mannose residue at subsite -2 (see Fig. 26A). In case of ManC, His368 equivalent to Asn319 of *H. jecorina* mannanase and Asp362 of ManA are exposed on the protein surface and may obscure substrate binding at subsite -3 (see Fig. 26B). As a consequence both ManA and ManC produced predominantly mannobiose as hydrolysis product as well as mannosyl bound to acceptor in transglycosylation reactions. The possible subsites +1 and +2 of ManA and ManC are well conserved, compared to *H. jecorina* mannanase, with one amino acid difference (Ser289 of ManA and Trp283 of ManC). Substitution of these residues (as ManAS289W and ManCW283S) showed that Trp283 of ManC had some impact on mannanases, but was not the critical residue controlling hydrolytic and transglycosylation ability of the enzymes. The changes in transglycosylation activity and substrate binding affinity (as  $K_m$ ) of ManAS289W and ManCW283S could be due to the effect of Trp238 of ManC. However, ManAS289W showed slightly lower  $K_m$  compared with ManA, whereas ManCW283S showed slightly higher  $K_m$  compared with ManC (see Table 13, page 66) indicating that this Trp has impact on the substrate binding ability and the changes in transglycosylation activity could be affected of the Trp substitution. More interestingly, the Trp283 of ManC seemed to involve in modulating the enzyme activity towards branched polymeric mannans possibly by defining a more restricted or open active site cleft at the proximal subsite -1 and +1. It is tempting to speculate that the more open active site cleft in ManA helps accommodating more branched substrates possibly aided by the space provided by the Trp to Ser substitution results in a looser affinity at the proximal subsites in ManA as compared to ManC (Fig. 26, page 69). Additionally, the homology models of ManA and ManC suggested that Tyr259 and Trp253, respectively, could act as subsite +3 and have a possible role in accepting the trisaccharides. These aromatic residues are strictly conserved among GH5 mannanases from fungi. Furthermore, GH5 mannanase from *H. jecorina* can accommodate a glucose residue at the acceptor recognition site ("plus subsites") which will advance the hydrolysis of glucomannan (Harjunpää et al., 1999), and which could be one reason for ManC to accept glucose residue from isomaltotriose and melezitose. In addition, these acceptors could have suitable conformation to bind at the plus subsites of ManC.

## 7.3 GH10 and GH11 xylanases

### 7.3.1 Production and activity of XlnC and XlnA

GH10 (XlnC) and GH11 (XlnA) xylanases were first reported together with another xylanase (XlnB) from *A. nidulans* distinguished by their molecular masses: 22 kDa for XlnA, 24 kDa for XlnB, and 34 kDa for XlnC (Fernández-Espinar et al., 1992). XlnC was further produced and purified from *A. nidulans* culture (Fernández-Espinar et al., 1994) and recloned into an *A. nidulans* expression host (MacCabe et al., 1996; MacCabe and Ramón, 2001) as well as into *S. cerevisiae* (Ganga et al., 1998).

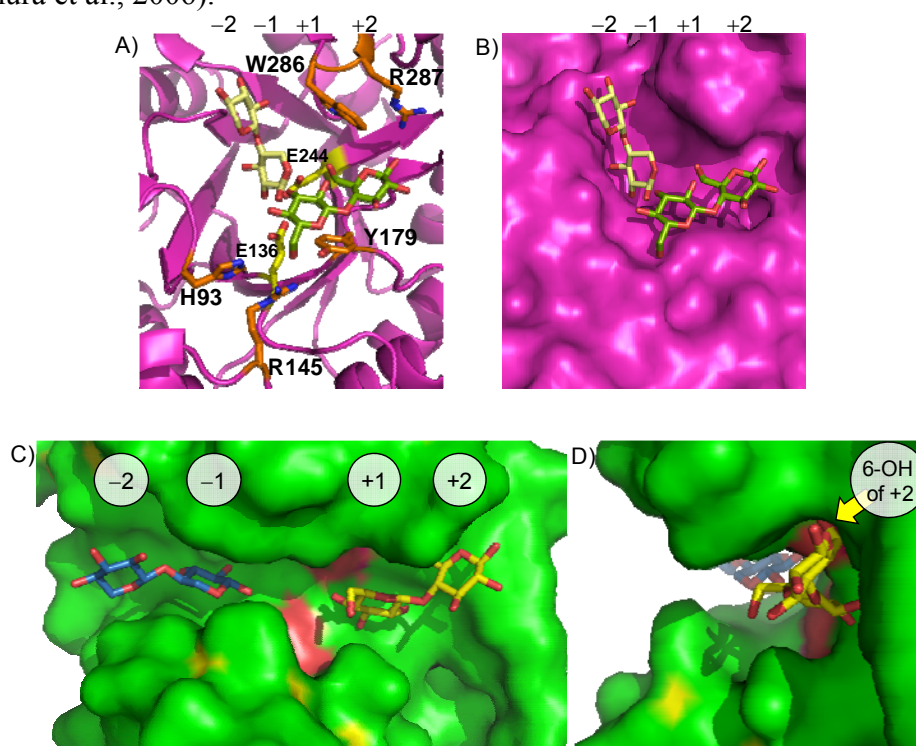
Together with XlnB, XlnA was cloned and produced in *S. cerevisiae* (Ganga et al., 1996; Pérez-González et al., 1996). In this study, we recloned *xlnA* and *xlnC* genes from the *P. pastoris* transformants harbouring these xylanase genes from *A. nidulans* FGSC A4 (Bauer et al., 2006) into *E. coli*, aiming to investigate the possibility of XlnA and XlnC to produce novel xylooligosaccharides *via* transglycosylation reactions. The recombinant production of XlnA and XlnC by *E. coli* (see 6.3.1, page 74) was more efficient than from the native host (5 mg/L for XlnC; Fernández-Espinar et al., 1994) or the recombinant production in *S. cerevisiae* (1.1 mg/L for XlnA and 1.0 mg/L for XlnC; Ganga et al., 1996). The activity towards birchwood xylan of XlnC (280 U/mg, Table 16, page 75) was 25% lower than that of native XlnC (379 U/mg; Fernández-Espinar et al., 1994), whereas the activity of XlnA (330 U/mg, Table 16, page 75) was in comparable with the reported GH11 xylanases (691 U/mg from *A. niger* BRFM281, Levasseur et al., 2005; 638 U/mg from *Streptomyces matensis* DW67, Yan et al., 2009; 420 and 101 U/mg from *T. reesei*; Tenkanen et al., 1992).

### 7.3.2 Transglycosylation by XlnC and XlnA

Xylanases usually possess transglycosylation as a side activity when high concentration of oligosaccharide substrates is used (see 4.2.4, page 24). Using six disaccharides (see 6.3.3, page 76) as acceptors, XlnA strictly accepted only xylobiose, whereas XlnC can use cellobiose, xylitol, and sorbitol as acceptors (see 6.3.3). Both XlnA and XlnC cannot use maltose, isomaltose, lactose, and mannobiose as acceptors. XlnC and GH10 xylanases have a shallow groove active site (see 4.2.2, page 22) with loose acceptor binding site at subsites +1 and +2 (Fig. 40A,B). The cellobiose can be situated in the acceptor binding site (“plus subsites”) and His93 and Arg145 can possibly form hydrogen bonds with 6-OH of the glucose residue at subsite +1. XlnA and GH11 xylanases have a deep and narrow cleft for active site, which restricts xylose molecule to be accommodated in the active site and the extra 6-OH of a hexose residue cannot fit in (Fig. 40C,D). The sugar alcohols gave higher yield than disaccharide acceptors in case of XlnC, which could be due to their more flexible conformations allowing multi-hydroxyl groups to attack the glycosyl-enzyme intermediate or they could behave as alcohol, which requires no interaction with the acceptor binding site. However, GH11 cannot use xylitol and sorbitol as acceptors indicating that the sugar alcohols need somehow to interact with acceptor binding site and the linear molecule makes it difficult for a sugar alcohol to enter the acceptor binding site. The transglycosylation products from XlnC were not purified further since these products are not novel. Xylobiosyl-cellobiose had been synthesised by reverse phosphololysis using recombinant cellodextrin phosphorylase from *Clostridium thermocellum* YM4 with  $\alpha$ -D-xylose 1-phosphate as donor and cellobiose as acceptor (Shintate et al., 2003). Xylotritol was synthesised together with xylitol and xylobitol in the production of reduced xylooligosaccharides as sweeteners (Shimizu et al., 1987). Xylobiosyl-sorbitol (xylobiosyl-D-glucitol) was synthesised as by-product from a chemical reaction for production of glycosyl-alditols (Sharkov et al., 1961) and as by-product from the synthesis of *N*-glycosyl derivatives of sodium sulfanilate (Kahl and Kuszlik-Jochym, 1964). The SciFinder search engine was used for evaluation of novelty of transglycosylation products (<https://scifinder.cas.org>; American Chemical Society, Columbus, Ohio).

### 7.3.3 Glycosynthase of XlnC

The GH10 glycosynthase mutant (E224A) was produced in three fold lower amounts than the XlnC wild-type enzyme and showed three orders of magnitude lower activity than wild-type (see 6.3.4, page 76). The glycosynthase activity of E244A was found to be rather low as judged by TLC (see Fig. 34, page 78) and, when using high concentration of the enzyme, remaining hydrolytic activity degrades the glycosynthase products (Fig. 34), therefore this glycosynthase is considered unsuccessful. The glycosynthase of GH10 xylanase has been reported by substituting the nucleophilic glutamic acid with Gly, Ala, and Ser (Kim et al., 2006; Sugimura et al., 2006). The glycine mutants exhibited highest glycosynthase activity and the alanine mutants showed good glycosynthase activity, whereas the serine mutants showed poor activity (Sugimura et al., 2006). The low activity of E244A could be due to the inappropriate substitution or the nature of this enzyme as in the study using glycosynthase mutants from different GH10 xylanases exhibited different activity (Sugimura et al., 2006).

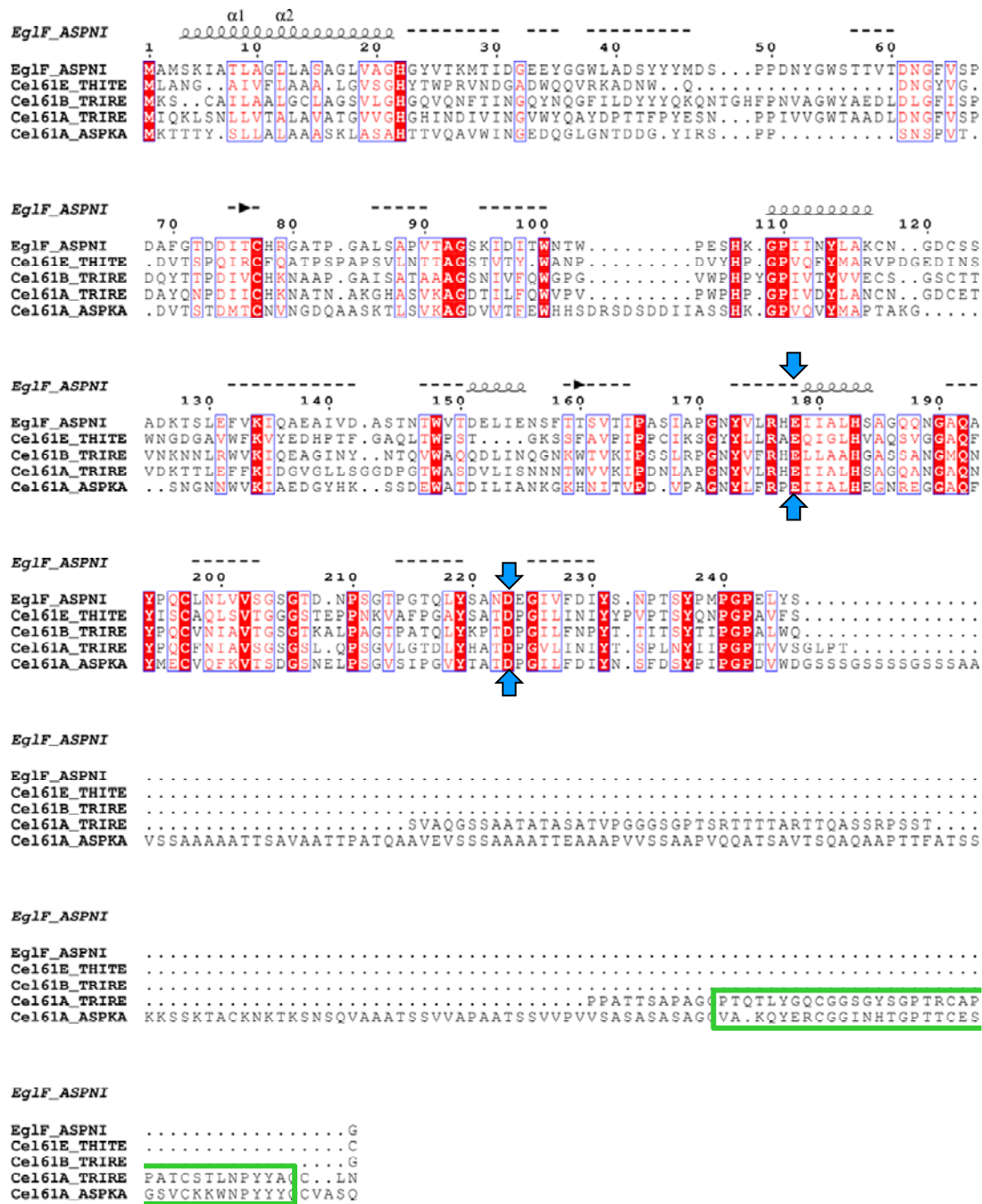


**Figure 40** Cartoons representing active sites in the 3D structure of GH10 (XlnC) and a homology model of GH11 (XlnA) xylanases. A) 3D structure of XlnC (PDB ID: 1TA3; Payan et al., 2004) superimposed with xylobiose (subsites -1 and -2, pale yellow●) and cellobiose (subsites +1 and +2, lime green●) from *P. simplicissimum* GH10 xylanase (PDB ID: 1B3Z; Schmidt et al., 1999), cellobiose was created by superimposition two  $\beta$ -glucoses on xylobiose at the acceptor binding sites; B) structure of XlnC similar to (A) with surface representation; C) model structure of XlnA using *P. funiculosum* xylanase as template (PDB: 1TE1; 67% sequence identity; Payan et al., 2004) and superimposed with xylobiose (subsites -1 and -2, blue●) and cellobiose (subsites +1 and +2, yellow●) from *Neocallimastix patriciarum* xylanase (PDB ID: 2VGD; Vardakou, et al., 2008), cellobiose was created by superimposition two  $\beta$ -glucoses on xylobiose on the acceptor binding sites; D) side view of the model structure of XlnA similar to (C).

## 7.4 GH61 putative endo- $\beta$ -glucanase

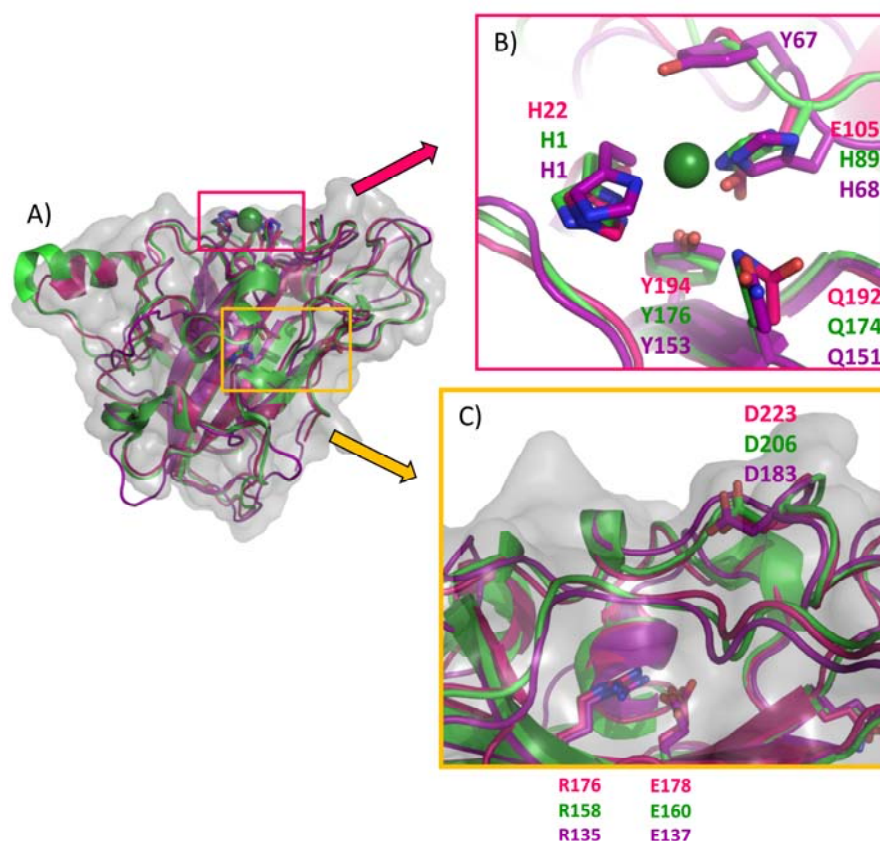
The objective for this part of the study was to perform enzyme discovery by applying a proteomics strategy. The proteomics strategy involved analysis of culture supernatants of *A. nidulans* FGSC A4 growing on 10 different polysaccharides (see 4.4.3, page 29) and was conducted by Dr. Kenji Maeda, Dr. Hiroyuki Nakai, and PhD student Anders Dysted Jørgensen, EPC, DTU Systems Biology. The GH61 putative endo- $\beta$ -glucanase from *A. nidulans* FGSC A4 (EglF) was successfully cloned into *P. pastoris* by the cDNA cloning technique (see 5.10.2, page 45) and secreted in recombinant form as directed by the  $\alpha$ -factor secretion signal sequence. The production of EglF (66 mg/L) was lower than the previously reported either from culture broth of *H. jecorina* (120 mg/L; Karlsson et al., 2001) or recombinant form of *H. jecorina* secreted by *P. pastoris* (280 mg/L; Liu et al., 2006) as Cel61A containing carbohydrate binding module family 1 (CBM1). Several GH61 proteins contain CBM1 at the C-terminal but EglF has no CBM (Fig 41). EglF showed extremely low activity towards barley  $\beta$ -glucan and oat spelt arabinoxylan and no binding ability was observed using carbohydrate microarrays. It is possible that the tested substrates or the reaction conditions have not been suitable for EglF showing very low activity towards barley  $\beta$ -glucan and oat arabinoxylan, or EglF has other functions. However, such extremely low activity was also observed in the other reports on GH61 proteins either from *A. kawachii* (Koseki et al., 2008) or *H. jecorina* (Harris et al., 2010; Karlsson et al., 2001; Saloheimo et al., 1997).

Two structures of GH61 proteins from *H. jecorina* (PDB ID: 2VTC) and *Thielavia terrestris* NRRL 8126 (PDB ID: 3EII) (see 4.4.2, page 29) showed no evidence of large surface clefts, crevices, or holes that would be possible binding pocket for soluble polysaccharides (Harris et al., 2010). There are two highly conserved carboxylic residues (Glu178 and Asp223 of EglF; Fig. 41 and 42) which may play a catalytic role. Glu178 is a buried residue and forms a salt bridge with a highly conserved Arg176, this has been proved to be important by mutagenesis of Glu137 of *T. terrestris* (3EII) resulting in lack of protein production (Harris et al., 2010). Even though Asp223 is surface accessible, it cannot act as catalytic residue, according to classical mode of action of glycoside hydrolases (Fig. 4, page 15), since it has no other carboxylic side chain close by (Karkehabadi et al., 2008). It is possible that GH61 may not follow a classical acid/base catalytic mechanism, but their activity is very low towards polysaccharides for being glycoside hydrolases. Several reports suggested that GH61 proteins may not act as glycoside hydrolases but have other functions (Brown et al., 2005; Harris et al., 2010; Karkehabadi et al., 2008; Liu et al., 2006). For example, a few reports suggested possible role of GH61 proteins as cellulase-enhancing factors which significantly improve the degradation of lignocellulosic biomass by cellulases (Brown et al., 2005; Harris et al., 2010; Liu et al., 2006). However several GH61 proteins from the same origin (different isoforms) are completely inactive as enhancers and some can act synergistically with cellulases from different sources making it ambiguous what is the true function of GH61 proteins (Harris et al., 2010). Therefore, the quest for understanding GH61 proteins still remains.



**Figure 41** Alignment of putative GH61 endo- $\beta$ -glucanase (EglF) with reported structures from *Thielavia terrestris* NRRL 8126 (Cel161E\_THITE; PDB ID: 3EII; Harris et al., 2010) and *H. jecorina* QM6A (Cel161B\_TRIRE; PDB ID: 2VTC; Karkehabadi et al., 2008) and two Cel61A containing CBM1 from *H. jecorina* RUTC-30 (Cel161A\_TRIRE; GenBank ID: CAA71999.1) and *A. kawachii* (Cel161A\_ASPKA; GenBank ID: BAB62318.1). Light blue arrows: two conserved Glu and Asp; green box: CBM1.





**Figure 42** Cartoons representing 3D structures and homology model of GH61 proteins. **Pink**, 3D model of EglF using structure from *H. jecorina* QM6A (PDB ID: 2VTC; Karkehabadi et al., 2008) as template; **green**, 3D structure of GH61 from *H. jecorina* QM6A (PDB ID: 2VTC; sharing 44% sequence identity); **purple**, 3D structure of *Thielavia terrestris* NRRL 8126 (PDB ID: 3EII; sharing 33% sequence identity; Harris et al., 2010). A) superimposition of three cartoons with grey surface from EglF model; B) metal ion-binding site; **dark green circle**, metal ion (nickel for 2VTC and zinc for 3EII); C) conserved acidic residues (Glu and Asp) with grey surface from EglF model.

## 7.5 Novel oligosaccharides

Several novel oligosaccharides were produced by the present study *i.e.* six novel xylosyl- and four novel manno oligosaccharides, using  $\beta$ -xylosidase (BxlA) and  $\beta$ -mannanase (ManC), respectively (Table 20). As mentioned in 7.1, several transglycosylation products were produced in more than one form (Table 8, page 55) possibly with different linkages or products synthesised from different forms of an acceptor ( $\alpha$ ,  $\beta$ , pyranosyl, furanosyl forms), all complicate identification of the structures of the obtained products.

Both xylo- and manno oligosaccharides act as prebiotics and are used as food additives in different food products due to these properties (see 2.1.4.2 and 2.1.5.2, page 9,11). Xylo oligosaccharides stimulate the growth of several intestinal Bifidobacteria (Grootaert et al., 2007; Moure et al., 2006; Vázquez et al., 2000; Zeng et al., 2007) and manno oligosaccharides can stimulate both Lactobacilli and Bifidobacteria (Asano et al., 2003), and both oligosaccharide types cannot be used by pathogenic bacteria *e.g.* *Staphylococcus*, *Clostridium* spp. and *Escherichia coli*

(Asano et al., 2003; Vázquez et al., 2000). Novel oligosaccharides produced *via* transglycosylation may exhibit the health benefits from both donor and acceptor and have better prebiotic effect than oligosaccharides present in nature by enhancing persistence of the prebiotic effect along the colon, antipathogen effects and more specific targeted prebiotics.

**Table 20** Novel oligosaccharide production by transglycosylation

Enzyme	Donor	Acceptor <sup>1</sup>	Yield (%)	Production (mg/mL)	Mass <sup>2</sup> (m/z)	NMR <sup>3</sup>
200 nM BxlA	30 mM <i>p</i> NPX	D-lyxose	23	1.92	289	✓
		L-fucose	14	1.27	303	✗
		D-talose	22	2.04	319	✗
		Sucrose <sup>4</sup>	6	0.81	481	✓
		Turanose	7	0.95	481	✓
		Cysteine	n.d.	n.d.	276, 298 <sup>5</sup>	✗
145 nM ManC	24 mM M4	Isomaltotriose	8.8	1.75	851	✓
			1.4	0.33	1013	✗
		Melezitose	3.0	0.62	851	✓
			0.5	0.13	1013	✗

<sup>1</sup> acceptor concentration = 200 mM.

<sup>2</sup> xylosyloligosaccharides were determined by ESI-MS as Li<sup>+</sup> adduct, mannoooligosaccharides were determined by MALDI-TOF MS as Na<sup>+</sup> adduct.

<sup>3</sup> see Table 9 and 15 for NMR assignment of xylosyl- and mannoooligosaccharides, respectively.

<sup>4</sup> Sucrose forms two transglycosylation products, *i.e.* β-xylopyranosyl-(1→4)-α-glucopyranosyl-(1→2)-β-fructofuranoside and β-xylopyranosyl-(1→6)-β-fructofuranosyl-(2→1)-α-glucopyranoside.

<sup>5</sup> determined by ESI-Q-TOF as Na<sup>+</sup> adduct and [Xyl-Cys-H+2Na]<sup>+</sup>.

n.d., not determined; ✓, the structures have been assigned by NMR; ✗, the structures cannot be assigned by NMR.

## 8. Conclusion and future perspectives

The present PhD project has demonstrated production of novel oligosaccharides by enzymes catalysed transglycosylation. Five glycoside hydrolases: one GH3  $\beta$ -xylosidase (BxlA), two GH5 mannanases (ManA and ManC), one GH10 xylanase (XlnC), and one GH11 xylanase (XlnA); from *Aspergillus nidulans* FGSC A4 were chosen for investigation of their transglycosylation ability. The use of different acceptors to investigate the acceptor specificity in transglycosylation of these enzymes also provides a route to produce novel oligosaccharides that might be useful as novel prebiotics or food ingredients. Six novel xylosyl- and four novel manno oligosaccharides were achieved by this study, using BxlA and ManC, respectively. Three other xylobiosyl-oligosaccharides achieved by transglycosylation catalysed by XlnC have been reported earlier by others.

The exo-acting enzyme BxlA showed broad acceptor specificity, which is useful as tool for synthesis of novel xylosyl oligosaccharides. *para*-Nitrophenyl xyloside was used as a donor containing a good leaving group which helps improving the transglycosylation yield. Optionally, using xylobiose, a natural substrate of  $\beta$ -xylosidase will decrease the transglycosylation yield, but will be more suitable for large-scale production of transglycosylation products for their usage as food ingredients. The endo-acting enzymes ManC and XlnC, in contrast, showed narrow acceptor specificity resulting in formation of a few different transglycosylation products in low yield (3-10% yield). Using high acceptor concentration can improve the transglycosylation yield, but is problematic for purification by HPLC to separate the products from their acceptors. In large-scale production, this problem could be solved by addition of purification step *e.g.* gel filtration to remove some of the acceptor prior further purification by HPLC. The cost of acceptors and donors for transglycosylation is also necessary to consider prior to large scale production. The substitution at subsite +1 in case of  $\beta$ -xylosidase and mannanase mutants showed impact on transglycosylation ability of these enzymes, but was not crucial. Even though it is possible to use the reported GH3  $\beta$ -glucosidase and  $\beta$ -glucanase as templates for homology models of GH3  $\beta$ -xylosidase, there is still some conflict between the models with different templates and missing information on the active sites, therefore the 3D structure of this enzyme is needed to gain more knowledge on the structural functional relationship of GH3  $\beta$ -xylosidase. Even though, glycosynthase is one of the powerful tools for synthesis of oligosaccharides, the glycosynthase reactions using GH3  $\beta$ -xylosidase and GH10 xylanase mutants in this study were not successful (see 6.1.6 and 6.3.4, respectively). No other attempts of using GH3 as glycosynthase have been reported.

In the last part of this PhD study, the GH61 putative endo- $\beta$ -glucanase from *A. nidulans* FGSC A4 (EglF) was chosen to apply enzyme discovery using a proteomics strategy (see 4.4.3). EglF was successfully cloned and produced recombinantly, but showed very low hydrolytic activity towards barley  $\beta$ -glucan and oat arabinoxylan as well as no detectable activity and binding ability by carbohydrate microarray analysis. The actual function of this putative enzyme has not been revealed, but recent publications proposed the possible role of GH61 protein as cellulase-enhancing factor (Brown et al., 2005; Harris et al., 2010; Liu et al., 2006). The mechanism behind this function remains unknown.

The present work has explored obvious enzymes to be used in chemo-enzymatic oligosaccharide synthesis and provides a basis for further developments either through protein engineering to increase yields or make new compounds, *e.g.* including glycosylated amino acids. It, moreover, adds to the understanding of the enigmatic GH61, and further work with the present prepared protein may contribute to shed light on the less known facts of cellulose degradation.

## 9. References

- Ademark, P, Varga, A, Medve, J, Harjunpaa, V, Drakenberg, T, Tjerneld, F, Stålbrand, H. Softwood hemicellulose-degrading enzymes from *Aspergillus niger*: Purification and properties of a  $\beta$ -mannanase. *J. Biotechnol.* 1998. 63: 199-210.
- Ajisaka, K, Nishida, H, Fujimoto, H. The synthesis of oligosaccharides by the reversed hydrolysis reaction of  $\beta$ -glucosidase at high substrate concentration and at high temperature. *Biotechnol. Lett.* 1987. 9: 243-248.
- Akpinar, O, Penner, MH. Preparation of cellooligosaccharides: Comparative study. *J Food Agric. Environ.* 2007. 6: 55-61.
- Altschul, SF, Madden, TL, Schäffer, AA, Zhang, J, Zhang, Z, Miller, W, Lipman, DJ. Gapped BLAST and PSI-BLAST: a new generation of protein database search programs. *Nucleic Acids Res.* 1997. 25: 3389-3402.
- Anderson, L. *Structure and Function of  $\beta$ -Mannanases from Glycoside Hydrolase Clan A: A study of hemicellulases from Microbes and a Mollusc*, PhD Thesis, Department of Biochemistry, Lund University, Sweden, 2006.
- Anderson, L, Hägglund, P, Stoll, D, Lo Leggio, L, Drakenberg, T, Stålbrand, H. Kinetics and stereochemistry of the *Cellulomonas fimi*  $\beta$ -mannanase studied using H-1-NMR. *Biocatal. Biotransfor.* 2008. 26: 86-95.
- Arisan-Atac, I, Hodits, R, Kristufek, D, Kubicek, CP. Purification, and characterization of a  $\beta$ -mannanase of *Trichoderma reesei* C-30. *Appl. Microbiol. Biot.* 1993. 39: 58-62.
- Armesilla, AL, Thurston, CF, Yagüe, E. CEL1: a novel cellulose binding protein secreted by *Agaricus bisporus* during growth on crystalline cellulose. *FEMS Microbiol. Lett.* 1994. 116: 293-299.
- Aro, N, Pakula, T, Penttila, M. Transcriptional regulation of plant cell wall degradation by filamentous fungi. *FEMS Microbiol. Rev.* 2005. 29: 719-739.
- Asano, I, Hamaguchi, K, Fujii, S, Iino, H. In vitro digestibility and fermentation of mannoooligosaccharides from coffee mannan. *Food Sci. Technol. Res.* 2003. 9: 62-66.
- Asano, I, Ikeda, Y, Fujii, S, Iino, H. Effects of mannoooligosaccharides from coffee on microbiota and short chain fatty acids in rat cecum. *Food Sci. Technol. Res.* 2004. 10: 273-277.
- Barkholt, V, Jensen, AL. Amino acid analysis: determination of cysteine plus half-cysteine in proteins after hydrochloric acid hydrolysis with a disulfide compound as additive. *Anal. Biochem.* 1989. 177: 318-322.
- Barreteau, H, Delattre, C, Michaud, P. Production of oligosaccharides as promising new food additive generation. *Food Technol. Biotech.* 2006. 44: 323-333.
- Bauer, S, Vasu, P, Persson, S, Mort, AJ, Somerville, CR. Development and application of a suite of polysaccharide-degrading enzymes for analyzing plant cell walls. *PNAS* 2006. 130: 11417-11422.
- Beg, QK, Kapoor, M, Mahajan, L, Hoondal, GS. Microbial xylanases and their industrial applications: a review. *Appl. Microbiol. Biot.* 2001. 56: 326-338.
- Béguin, P. Molecular biology of cellulose degradation. *Annu. Rev. Microbiol.* 1990. 44: 219-248.
- Ben-David, A, Bravman, T, Balazs, YS, Czjzek, M, Schomburg, D, Shoham, G, Shoham, Y. Glycosynthase activity of *Geobacillus stearothermophilus* GH52  $\beta$ -xylosidase: efficient synthesis of xylooligosaccharides from  $\alpha$ -D-xylopyranosyl fluoride through a conjugated reaction. *ChemBiochem.* 2007. 8: 2145-2151.

- Beneke, CE, Viljoen, AM, Hamman, JH. Polymeric plant-derived excipients in drug delivery. *Molecules*. 2009. 14: 2602-2620.
- Berg, JM, Tymoczko, JL, Stryer, L. *Biochemistry: International edition, fifth ed.*, W. H. Freeman and Company, Madison Avenue, NY, 2002.
- Biely P. Xylanolytic enzymes, in: J.R. Whitaker, A.G.J. Voragen, D.W.S. Wong (Eds), *Handbook of Food Enzymology*, Marcel Dekker Inc., New York, 2003, pp. 879-916.
- Berrin, J-G, Ajandouz EH, Georis, J, Arnaut, F, Juge, N. Substrate and product hydrolysis specificity in family 11 glycoside hydrolases: an analysis of *Penicillium funiculosum* and *Penicillium griseofulvum* xylanases. *Appl. Microbiol. Biot.* 2006. 74: 1001-1010.
- Berrin, J-G, Juge, N. Factors affecting xylanase functionality in the degradation of arabinoxylans. *Biotechnol. Lett.* 2008. 30:1139-1150.
- Biely, P. Xylanolytic enzymes, in: J.R. Whitaker, A.G.J. Voragen, D.W.S. Wong (Eds), *Handbook of Food Enzymology*, Marcel Dekker Inc., New York, 2003, pp. 879-916.
- Biely, P, Vrsanska, M, Kratky, Z. Mechanisms of substrate digestion by endo-1,4- $\beta$ -xylanase of *Cryptococcus albidus* lysozyme-type pattern of action. *Eur. J. Biochem.* 1981. 119: 565-571.
- Biely, P, Vrsanská, M, Tenkanen, M, Kluepfel, D. Endo- $\beta$ -1,4-xylanase families: differences in catalytic properties. *J. Biotechnol.* 1997. 57: 151-166.
- Blom, N, Sicheritz-Ponten, T, Gupta, R, Gammeltoft, S, Brunak, S. Prediction of post-translational glycosylation and phosphorylation of proteins from the amino acid sequence. *Proteomics*. 2004. 4: 1633-49.
- Britton, HTK, Robinson, RA. Universal buffer solutions and the dissociation constant of veronal. *J. Chem. Soc.* 1931: 1456-1462.
- Brotman, Y, Briff, E, Viterbo, A, Chet, I. Role of swollenin, an expansin-like protein from *Trichoderma*, in plant root colonization. *Plant Physiol.* 2008. 147: 779-789.
- Brown, K, Harris, P, Zaretsky, E, Re, E, Vlasenko, E, McFarland, K, Lopez de Leon, A. Polypeptides having cellulolytic enhancing activity and polynucleotides encoding same. WO 2005/074647. 28 January 2005.
- Candiano, G, Bruschi, M, Musante, L, Santucci, L, Ghiggeri, GM, Carnemolla, B, Orecchia, P, Zardi, L, Righetti, PG. Blue silver: a very sensitive colloidal Coomassie G-250 staining for proteome analysis. *Electrophoresis*. 2004. 25: 1327-1333
- Cantarel, BL, Coutinho, PM, Rancurel, C, Bernard, T, Lombard, V, Henrissat, B. The Carbohydrate-Active EnZymes database (CAZy): an expert resource for glycogenomics. *Nucleic Acids Res.* 2009. 37(Database issue): D233-D238.
- Carpita, NC, Gibeaut, DM. Structural models of primary-cell walls in flowering plants - consistency of molecular structures with the physical properties of the wall during growth. *Plant J.* 1993. 3: 1-30.
- Carpita, N and McCann, M. Chapter 2: The cell wall, in: B. Buchanan, W. Gruissem, R. Jones (Eds), *Biochemistry & Molecular Biology of Plants*, John Wiley & Sons, Ltd., West Sussex, United Kingdom, 2000 pp. 52-101.
- Charnock, SJ, Spurway, TD, Xie, H, Beylot, M, Virden, R, Warren, RAJ, Hazlewood, GP, and Gilbert, HJ. The topology of the substrate binding clefts of glycosyl hydrolase family 10 xylanases are not conserved. *J. Biol. Chem.* 1998. 273: 32187-32199.

- Christakopoulos, P, Kekos, D, Macris, BJ, Claeysens, M, Bhat, MK. Purification and characterization of a major xylanase with cellulase and transferase activities from *Fusarium oxysporum*. *Carbohydr. Res.* 1996. 289: 91-94.
- Collins, MD, Gibson, GR. Probiotics, prebiotics, and synbiotics: approaches for modulating the microbial ecology of the gut. *Am. J. Clin. Nutr.* 1999. 69(suppl): 1052S-10527S.
- Collins, T, Gerday, C, Feller, G. Xylanases, xylanase families and extremophilic xylanases. *FEMS Microbiol. Rev.* 2005. 29: 3-23.
- Crout, DHG, Vic, G. Glycosidases and glycosyl transferases in glycoside and oligosaccharide synthesis. *Curr. Opin. Chem. Biol.* 1998. 2: 98-111.
- Cummings, JH, Mann, JI, Nishida, C, Vorster, HH. Dietary fibre: an agreed definition. *The Lancet.* 2009. 373: 365-366.
- Davies, G, Henrissat, B. Structures and mechanisms of glycosyl hydrolases, *Structure.* 1995. 3: 853-859.
- Davies, GJ, Wilson, KS, Henrissat, B. Nomenclature for sugar-binding subsites in glycosyl hydrolases. *Biochem. J.* 1997. 321: 557-559.
- Davis, CD, Milner, JA. Gastrointestinal microflora, food components and colon cancer prevention. *J. Nutr. Biochem.* 2009. 20: 743-752.
- de Vries, RP, Visser, J. *Aspergillus* enzymes involved in degradation of plant cell wall polysaccharides. *Microbiol. Mol. Biol. Rev.* 2001. 65: 497-522.
- de Vries, RP, Visser, J. Enzymes releasing L-arabinose and D-galactose from the side chains of pectin, in: J.R. Whitaker, A.G.J. Voragen, D.W.S. Wong (Eds.), *Handbook of Food Enzymology*, Marcel Dekker Inc., Madison Avenue, NY, 2003 pp. 867-877.
- Deschatelets, L, Yu, EKC. A simple pentose assay for biomass conversion studies. *Appl. Microbiol. Biotechnol.* 1986. 24: 379-385.
- Dhawan, S, Kaur, J. Microbial mannanases: An overview of production and applications. *Crit. Rev. Biotechnol.* 2007. 27: 197-216.
- Drouet, P, Mu, Z, Legoy, MD. Enzymatic synthesis of alkyl  $\beta$ -D-xylosides by transxylosylation and reverse hydrolysis. *Biotechnol. Bioeng.* 1994. 43: 1075-1080.
- Dubois, M, Gilles, KA, Hamilton, JK, Rebers, PA, Smith, F. Colorimetric method for determination of sugars and related substances. *Anal. Chem.* 1956. 28: 350-356.
- Duff, SJB, Murray, WD. Bioconversion of forest products industry waste cellulose to fuel ethanol: A review. *Bioresource Technol.* 1996. 55: 1-33.
- Duffaud, GD, McCutchen, CM, Leduc, P, Parker, KN, Kelly, RM. Purification and characterization of extremely thermostable  $\beta$ -mannanase,  $\beta$ -mannosidase, and  $\alpha$ -galactosidase from the hyperthermophilic eubacterium *Thermotoga neapolitana* 5068. *Appl. Environ. Microbiol.* 1997. 63: 169-177.
- Ebringerová, A. Structural diversity and application potential of hemicelluloses. *Macromol. Symp.* 2006. 232: 1-12.
- Emanuelsson, O, Brunak, S, von Heijne, G, Nielsen, H. Locating proteins in the cell using TargetP, SignalP, and related tools. *Nat. Protoc.* 2007. 2: 953-971.
- Eneyskaya, EV, Brumer, H, Backinowsky, LV, Ivanen, DR, Kulminkaya, AA, Shabalin, KA, Neustroev, KN. Enzymatic synthesis of  $\beta$ -xylanase substrates: transglycosylation reaction of the  $\beta$ -xylosidase from *Aspergillus* sp. *Carbohydr. Res.* 2003. 338: 313-325.

- Espinosa-Martos, I, Ruperez, P. Soybean oligosaccharides. Potential as new ingredients in functional food. *Nutr. Hops.* 2006. 21: 92-96.
- Evodia Setati, M, Ademark, P, van Zyl, WH, Hahn-Hagerdal, B, Stålbrand, H. Expression of the *Aspergillus aculeatus* endo- $\beta$ -1,4-mannanase encoding gene (*man1*) in *Saccharomyces cerevisiae* and characterization of the recombinant enzyme. *Protein Expres. Purif.* 2001. 21: 105-114.
- Faijes, M, Pérez, X, Pérez, O, Planas, A. Glycosynthase activity of *Bacillus licheniformis* 1,3-1,4- $\beta$ -glucanase mutants: specificity, kinetics, and mechanism. *Biochemistry.* 2003. 42: 13304-13318.
- FAO. 2001. *Health and Nutritional Properties of Probiotics in Food including Powder Milk with Live Lactic Acid Bacteria*, October 1-4, 2001.
- FAO. 2007. *FAO Technical Meeting on PREBIOTICS. Food Quality and Standards Service (AGNS)*. Food and Agriculture Organization of the United Nations (FAO). September 15-16, 2007.
- Fennema, OR. *Food Chemistry (Food Science and Technology)*. Marcel Dekker, Inc. Madison Avenue, NY, 1996.
- Fernández-Espinar, M, Piñaga, F, de Graaff, L, Visser, J, Ramón, D, Vallés, S. Purification, characterization and regulation of the synthesis of an *Aspergillus nidulans* acidic xylanase. *Appl. Microbiol. Biot.* 1994. 42: 555-562.
- Fernández-Espinar, MT, Ramón, D, Piñaga, F, Vallés, S. Xylanase production by *Aspergillus nidulans*. *FEMS Microbiol. Lett.* 1992. 91: 91-96.
- Ferre, F, Clote, P. DiANNA: a web server for disulfide connectivity prediction. *Nucleic Acids Res.* 2005. 33: W230-232.
- Frederix, SA, Courtin, CM, Delcour, JA. Substrate selectivity and inhibitor sensitivity affect xylanase functionality in wheat flour gluten-starch separation. *J. Cereal Sci.* 2004. 40: 41-49.
- Frederix, SA, van Hoeymissen, KE, Courtin, CM, Delcour, JA. Water-extractable and water-unextractable arabinoxylans affect gluten agglomeration behavior during wheat flour gluten-starch separation. *J. Agr. Food Chem.* 2004b. 52: 7950-7956.
- Galagan, JE, Calvo, SE, Cuomo, C, Ma, LJ, Wortman, JR, Batzoglou, S, Lee, SI, Bastuerkmen, M, Spevak, CC, Clutterbuck, J, Kapitonov, V, Jurka, J, Scazzocchio, C, Farman, ML, Butler, J, Purcell, S, Harris, S, Braus, GH, Draht, O, Busch, S, D'Enfert, C, Bouchier, C, Goldman, GH, Bell-Pedersen, D, Griffiths-Jones, S, Doonan, JH, Yu, J, Vienken, K, Pain, A, Freitag, M, Selker, EU, Archer, DB, Penalva, MA, Oakley, BR, Momany, M, Tanaka, T, Kumagai, T, Asai, K, Machida, M, Nierman, WC, Denning, DW, Caddick, MX, Hynes, M, Paoletti, M, Fischer, R, Miller, BL, Dyer, PS, Sachs, MS, Osmani, SA, Birren, BW. Sequencing of *Aspergillus nidulans* and comparative analysis with *A. fumigatus* and *A. oryzae*. *Nature.* 2005. 438: 1105-1115.
- Ganga, A, Querol, A, Valles, S, Ramon, D, MacCabe, A, Pinaga, F. Heterologous production in *Saccharomyces cerevisiae* of different *Aspergillus nidulans* xylanases of potential interest in oenology. *J. Sci. Food Agric.* 1998. 78: 315-320.
- Gasteiger, E, Hoogland, C, Gattiker, A, Duvaud, S, Wilkins, MR, Appel, RD, Bairoch, A. Protein identification and analysis tools on the ExPASy Server, in: J.M. Walker (Ed.), *The Proteomics Protocols Handbook*, Humana Press, New Jersey, 2005, pp. 571-607.
- Gibson, GR, Roberfroid, MB. Dietary modulation of the human colonic microbiota: Introducing the concept of prebiotics. *J. Nutr.* 1995. 125: 1401-1412.
- Gilbert, HJ, Stålbrand, H, Brumer, H. How the walls come crumbling down: recent structural biochemistry of plant polysaccharide degradation. *Curr. Opin. Plant Biol.* 2008. 11: 338-348.



- Graham, LE, Graham, JM, Wilcok, LW. *Plant Biology*, second ed., Pearson Prentice Hall, Pearson Education Inc., Upper Saddle Rivers, NJ, 2006.
- Gouet, P, Courcelle, E, Stuart, DI, Metoz, F. ESPript: multiple sequence alignments in PostScript. *Bioinformatics*. 1999. 15: 305-308.
- Gübitz, GM, Hayn, M, Sommerauer, M, Steiner, W. Mannan-degrading enzymes from *Sclerotium rolfsii*: Characterisation and synergism of two endo  $\beta$ -mannanases and a  $\beta$ -mannosidase. *Bioresource Technol.* 1996. 58: 127-135.
- Hara, Y, Hinoki, Y, Shimoi, H, Ito, K. Cloning and sequence analysis of endoglucanase genes from an industrial fungus, *Aspergillus kawachii*. *Biosci. Biotechnol. Biochem.* 2003. 67: 2010-2013.
- Harjunpää, V, Helin, J, Koivula, A, Siika-aho, M, Drakenberg, T. A comparative study of two retaining enzymes of *Trichoderma reesei*: transglycosylation of oligosaccharides catalysed by the cellobiohydrolase I, Cel7A, and the  $\beta$ -mannanase, Man5A. *FEBS Lett.* 1999. 443: 149-153.
- Harjunpää, V, Teleman, A, Siikaaho, M, Drakenberg, T. Kinetic and stereochemical studies of manno-oligosaccharide hydrolysis catalysed by  $\beta$ -mannanases from *Trichoderma reesei*. *Eur J Biochem.* 1995. 234: 278-283.
- Harris, PV, Welner, D, McFarland, KC, Re, E, Navarro-Poulsen, JC, Brown, K, Salbo, R, Ding, H, Vlasenko, E, Merino, S, Xu, F, Larsen, S, Cherry, J, Lo Leggio, L. Stimulation of lignocellulosic biomass hydrolysis by proteins of glycoside hydrolase 61: Structure and function of a large, enigmatic family. *Biochemistry*. 2010. 49: 3305-3316.
- Henrissat, B. A classification of glycosyl hydrolases based on amino-acid sequence similarities. *Biochem. J.* 1991. 280: 309-316.
- Henrissat, B, Davies, G. Structural and sequence-based classification of glycoside hydrolases, *Curr. Op. Struct. Biol.* 1997. 7: 637-644.
- Herrmann, MC, Vrsanska, M, Jurickova, M, Hirsch, J, Biely, P, Kubicek, CP. The  $\beta$ -xylosidase of *Trichoderma reesei* is a multifunctional  $\beta$ -D-xylan xylohydrolase. *Biochem. J.* 1997. 321: 375-381.
- Hilge, M, Gloor, SM, Rypniewski, W, Sauer, O, Heightman, TD, Zimmermann, W, Winterhalter, K, Piontek, K. High-resolution native and complex structures of thermostable  $\beta$ -mannanase from *Thermomonospora fusca* - substrate specificity in glycosyl hydrolase family 5. *Struct. Fold Des.* 1998. 6: 1433-1444.
- Hogg, D, Pell, G, Dupree, P, Goubet, F, Martin-Orue, SM, Armand, S, Gilbert, HJ. The modular architecture of *Cellvibrio japonicus* mannanases in glycoside hydrolase families 5 and 26 points to differences in their role in mannan degradation. *Biochem. J.* 2003. 371: 1027-1043.
- Honda, Y, Kitaoka, M. The first glycosynthase derived from an inverting glycoside hydrolase. *J. Biol. Chem.* 2006. 281: 1426-1431.
- Hoshino-Takao, U, Fujii, S, Ishii, A, Han, LK, Okuda, H, Kumao, T. Effects of manno-oligosaccharides from coffee mannan on blood pressure in Dahl salt-sensitive rats. *J. Nutr. Sci. Vitaminol.* 2008. 54: 181-184.
- Howard, RL, Abotsi, E, Jansen Van Rensburg, EL, Howard, S. Lignocellulose biotechnology: issues of bioconversion and enzyme production. *Afr. J. Biotechnol.* 2003. 2: 602-619.
- Hrmova, M, Varghese, JN, De Gori, R, Smith, BJ, Driguez, H, Fincher, GB. Catalytic mechanisms and reaction intermediates along the hydrolytic pathway of a plant  $\beta$ -D-glucan glucohydrolase. *Structure*. 2001. 9: 1005-1016.

- Hrmova, M, Burton, RA, Biely, P, Lahnstein, J, Fincher, GB. Hydrolysis of (1,4)- $\beta$ -D-mannans in barley (*Hordeum vulgare* L.) is mediated by the concerted action of (1,4)- $\beta$ -D-mannan endohydrolase and  $\beta$ -D-mannosidase. *Biochem. J.* 2006. 399: 77-90.
- Hägglund, P, Eriksson, T, Collen, A, Nerinckx, W, Claeysens, M, Stålbrand, H. A cellulose-binding module of the *Trichoderma reesei*  $\beta$ -mannanase Man5A increases the mannan-hydrolysis of complex substrates. *J. Biotechnol.* 2003. 101: 37-48.
- Iiyama, K, Lam, TBT, Stone, BA. Covalent cross-links in the cell wall. *Plant Physiol.* 1994. 104: 315-320.
- IOM. 7. Dietary, Functional, and Total Fiber, in: Institute of Medicine of the National Academies (Eds.), *Dietary Reference Intakes for Energy, Carbohydrate, Fiber, Fat, Fatty Acids, Cholesterol, Protein, and Amino Acids (Macronutrients)*. National Academies Press, Washington, DC, 2005, pp. 339-421.
- Isolauri, E, Kirjavainen, PV, Salminen, S. Probiotics: a role in the treatment of intestinal infection and inflammation? *Gut.* 2002. 50: 50-54.
- Jahn M, Stoll, D, Warren, RAJ, Szabó, L, Singh, P, Gilbert, HJ, Ducros, VMA, Davies, GJ, Withers, SG. Expansion of the glycosynthase repertoire to produce defined manno-oligosaccharides. *Chem. Commun.* 2003a. 12: 1327-1329.
- Jahn, M, Marles, J, Warren, RAJ, and Withers, SG. Thioglycoligases: mutant glycosidases for thioglycoside synthesis. *Angew. Chem. Int. Edit.* 2003b. 42: 352-354.
- Jahn, M, Withers, SG. New approaches to enzymatic oligosaccharide synthesis: glycosynthases and thioglycoligases. *Biocatal. Biotransform.* 2003. 21: 159-166.
- Jakeman, DL, Withers, SG. Glycosynthases: New tools for oligosaccharides synthesis. *Trends Glycosci. Glyc.* 2002a. 14: 13-25.
- Jakeman, DL, Withers, SG. On expanding the repertoire of glycosynthases: mutant  $\beta$ -galactosidases forming  $\beta$ -(1,6)-linkage. *Can. J. Chemistry.* 2002b. 80: 866-870.
- Jiang, ZQ, Deng, W, Zhu, YP, Li, LT, Sheng, YJ, Hayashi, K. The recombinant xylanase B of *Thermotoga maritima* is highly xylan specific and produces exclusively xylobiose from xylans, a unique character for industrial applications. *J. Mol. Catal. B-Enzym.* 2004. 27: 207-213.
- Jones, B. Discovery and development of enzymes, in: W. Aehle (Ed.), *Enzyme in Industry*, WILEY-VCH Verlag GmbH & Co. KGaA, Weinheim, Germany, 2007, pp. 81-90.
- Kadi, N, Belloy, L, Chalier, P, Crouzet, JC. Enzymatic synthesis of aroma compound xylosides using transfer reaction by *Trichoderma longibrachiatum* xylanase. *J. Agr. Food Chem.* 2002. 50: 5552-5557.
- Kadi, N, Crouzet, J. Transglycosylation reaction of endoxylanase from *Trichoderma longibrachiatum*. *Food Chem.* 2008. 106: 466-474.
- Kahl, W, Kuszlik-Jochym, K. N-Glycosyl derivatives of sodium sulfanilate. *Roczniki Chemii.* 1964. 38: 17-21.
- Karkehabadi, S, Hansson, H, Kim, S, Piens, K, Mitchinson, C, Sandgren, M. The first structure of a glycoside hydrolase family 61 member, Cel61B from *Hypocrea jecorina*, at 1.6 Å resolution. *J. Mol. Biol.* 2008. 383: 144-154.
- Karlsson, J, Saloheimo, M, Siika-aho, M, Tenkanen, M, Penttilä, M, Tjerneld, F. Homologous expression and characterization of Cel61A (EG IV) of *Trichoderma reesei*. *Eur. J. Biochem.* 2001. 268: 6498-6507.

- Kasianowicz, JJ, Brandin, E, Branton, D, Deamer, DW. Characterization of individual polynucleotide molecules using a membrane channel. *PNAS*. 1996. 93: 13770-13773.
- Kendall, CWK, Esfahani, A, Jenkins, DJA. The link between dietary fibre and human health. *Food Hydrocolloid*. 2010. 24: 42-48.
- Kim, YW, Fox, DT, Hekmat, O, Kantner, T, McIntosh, LP, Warren, RAJ, Withers, SG. Glycosynthase-based synthesis of xylo-oligosaccharides using an engineered retaining xylanase from *Cellulomonas fimi*. *Org. Biomol Chem*. 2006. 4: 2025-2032.
- Knob, A, Terrasan, CRF, Carmona, EC.  $\beta$ -Xylosidases from filamentous fungi: an overview. *World J. Microbiol. Biotechnol*. 2010. 26: 389-407.
- Kolenová, K, Vrsanská, M, Biely, P. Mode of action of endo- $\beta$ -1,4-xylanases of families 10 and 11 on acidic xylooligosaccharides. *J. Biotechnol*. 2006. 121: 338-345.
- Korf, I. Gene finding in novel genomes. *BMC Bioinformatics*. 2004. 5: 59.
- Koseki, T, Mese, Y, Fushinobu, S, Masak, K, Fujii T, Ito K, Shiono Y, Murayama T, and Iefuji, H. Biochemical characterization of a glycoside hydrolase family 61 endoglucanase from *Aspergillus kawachii*. *Appl. Microbiol. Biot*. 2008. 77: 1279-1285.
- Kubicek, CP. The cellulase proteins of *Trichoderma reesei*: Structure, multiplicity, mode of action and regulation of formation, in: A. Fiechter (Ed.), *Advances in Biochemical Engineering-Biotechnology, Vol. 45. Enzymes and products from bacteria fungi and plant cells*. Springer-Verlag, Berlin, Germany, 1992, 1-27.
- Kumao, T, Fujii, S, Asakawa, A, Takehara, I, Fukuhara, I, Effect of coffee drink containing mannoooligosaccharides on total amount of excreted fat in healthy adults. *J. Health Sci*. 2006. 52: 482-485.
- Kumar, S, Ramon, D. Purification and regulation of the synthesis of a  $\beta$ -xylosidase from *Aspergillus nidulans*. *FEMS Microbiol. Lett*. 1996. 135:287-293.
- Kurakake, M, Fujii, T, Yata, M, Okazaki, T, Komaki, T. Characteristics of transxylosylation by  $\beta$ -xylosidase from *Aspergillus awamori* K4. *Biochem. Biophys. Acta*. 2005. 1726: 272-279.
- Kurakake, M, Komaki, T. Production of  $\beta$ -mannanase and  $\beta$ -mannosidase from *Aspergillus awamori* K4 and their properties. *Curr. Microbiol*. 2001. 42: 377-380.
- Kurakake, M, Osada, S, Komaki, T. Transxylosylation of  $\beta$ -xylosidase from *Aspergillus awamori* K4. *Biosci. Biotech. Biochem*. 1997. 61: 2010-2014.
- Kuriki, T, Yanase, M, Takata, H, Takesada, Y, Imanaka, T, Okada, S. A new way of producing isomalto-oligosaccharide syrup by using the transglycosylation reaction of neopullulanase. *Appl. Environ. Microbiol*. 1993. 59: 953-959.
- Lai, EM, Nair, U, Phadke, ND, Maddock, JR. Proteomic screening and identification of differentially distributed membrane proteins in *Escherichia coli*. *Mol. Microbiol*. 2004. 52: 1029-1044.
- Larsson, AM, Anderson, L, Xu, BZ, Munoz, IG, Uson, I, Janson, JC, Ståhlbrand, H, Stahlberg, J. Three-dimensional crystal structure and enzymic characterization of  $\beta$ -mannanase Man5A from blue mussel *Mytilus edulis*. *J. Mol. Biol*. 2006. 357. 1500-1510.
- Le Nours, J, Anderson, L, Stoll, D, Ståhlbrand, H, Lo Leggio, L. The structure and characterization of a modular endo- $\beta$ -1,4-mannanase from *Cellulomonas fimi*. *Biochemistry*. 2005. 44: 12700-12708.
- Lee, RC, Hrmova, M, Burton, RA, Lahnstein, J, Fincher, GB. Bifunctional family 3 glycoside hydrolases from barley with  $\alpha$ -L-arabinofuranosidase and  $\beta$ -D-xylosidase activity - Characterization, primary structures, and COOH-terminal processing. *J. Biol. Chem*. 2003. 278: 5377-5387.

- Liu, G, Tang, X, Tian, S, Deng, X, and Xing, M. Improvement of the cellulolytic activity of *Trichoderma reesei* endoglucanase IV with an additional catalytic domain. *World J. Microb. Biot.* 2006. 22: 1301-1305.
- Lo Leggio, L. Parry, N.J. Van Beeumen, J. Claeysens, M. Bhat, M.K. Pickersgill, R.W. Crystallization and preliminary X-ray analysis of the major endoglucanase from *Thermoascus aurantiacus*, *Acta Crystallogr D.* 1997. 53: 599-604.
- Lorenz, P, Schleper, C. Metagenome-a challenging source of enzyme discovery. *J. Mol. Catal. B-Enzym.* 2002. 19-20: 13-19.
- MacCabe, AP, Fernández-Espinar, MT, de Graaff, LH, Visser, J, Ramón, D. Identification, isolation and sequence of the *Aspergillus nidulans* xlnC gene encoding the 34-kDa xylanase. *Gene.* 1996. 175: 29-33.
- MacCabe, AP, Ramon, D. Expression of the *Aspergillus nidulans* xlnC gene encoding the X-34 endo-xylanase is subject to carbon catabolite repression and pH control. *World J. Microb. Biot.* 2001. 17: 57-60.
- Mackenzie, LF, Wang, Q, Warren, RAJ, Withers, SG. Glycosynthases: mutant glycosidases for oligosaccharide synthesis. *J. Am. Chem. Soc.* 1998. 120: 5583-5584.
- Manderson, K, Pinart, M, Tuohy, KM, Grace, WE, Hotchkiss, AT, Widmer, W, Yadhav, MP, Gibson, GR, Rastall, RA. In vitro determination of prebiotic properties of oligosaccharides derived from an orange juice manufacturing by-product stream. *Appl. Environ. Microb.* 2005. 71: 8383-8389.
- Margolles-Clark, E, Tenkanen, M, Nakari-Setälä, T, Penttilä, M. Cloning of genes encoding  $\alpha$ -L-arabinofuranosidase and  $\beta$ -xylosidase from *Trichoderma reesei* by expression in *Saccharomyces cerevisiae*. *Appl. Environ. Microbiol.* 1996. 62: 3840-3846.
- Matsumura, S, Sakiyama, K, Toshima, K. Preparation of octyl  $\beta$ -D-xylobioside and xyloside by xylanase-catalyzed direct transglycosylation reaction of xylan and octanol. *Biotechnol. Lett.* 1999. 21: 17-22.
- Matsuo, M, Yasui, T. Purification and some properties of  $\beta$ -xylosidase from *Trichoderma viride*. *Agric. Biol. Chem.* 1984a. 48: 1845-1852.
- Matsuo, M, Yasui, T. Purification and some properties of  $\beta$ -xylosidase from *Emericella nidulans*. *Agric. Biol. Chem.* 1984b. 48: 1853-1860.
- Mayer, C, Jakeman, DL, Mah, M, Karjala, G, Gal, L, Warren, RAJ, Withers, SG. Directed evolution of new glycosynthases from *Agrobacterium*  $\beta$ -glucosidase: a general screen to detect enzymes for oligosaccharide synthesis. *Chem. Biol.* 2001. 8: 437-443.
- Mayer, C, Zechel, DL, Reid, SP, Warren, RAJ, and Withers, SG. The E358S mutant of *Agrobacterium* sp.  $\beta$ -glucosidase is a greatly improved glycosynthase. *FEBS Lett.* 2000. 466: 40-44.
- McFeeters, RF. A manual method for reducing sugar determinations with 2,2'-bichinoninate reagent. *Anal Biochem.* 1980. 103: 302-306.
- Merino, ST, Cherry, J. Progress and challenges in enzyme development for biomass utilization. *Biofuels.* 2007. 108: 95-120.
- Mikkonen, KS, Mathew, AP, Pirkkalainen, K, Serimaa, R, Xu, C, Willför, S, Oksman, K, Tenkanen, M. Glucomannan composite films with cellulose nanowhiskers. *Cellulose.* 2010. 17: 69-81.
- Miller, GL. Use of dinitrosalicylic acid reagent for determination of reducing sugar. *Anal. Chem.* 1959. 31: 426-428.

- Minic, Z, Rihouey, C, Do, CT, Lerouge, P, Jouanin, L. Purification and characterization of enzymes exhibiting  $\beta$ -D-xylosidase activities in stem tissues of Arabidopsis. *Plant Physiol.* 2004. 135: 867-878.
- Moers, K, Celus, I, Brijs, K, Courtin, CM, Delcour, JA. Endoxylanase substrate selectivity determines degradation of wheat water-extractable and water-unextractable arabinoxylan. *Carbohydr. Res.* 2005. 340: 1319-1327.
- Moers, K, Courtin, CM, Brijs, K, Delcour, JA. A screening method for endo- $\beta$ -1,4-xylanase substrate selectivity. *Anal. Biochem.* 2003. 319: 73-77.
- Mohun, AF, Cook, IJY. An improved dinitrosalicylic acid method for determining blood and cerebrospinal fluid sugar levels. *J. Clin. Pathol.* 1962. 15: 169-180.
- Moller, I, Marcus, SE, Haeger, A, Verherbruggen, Y, Verhoef, R, Schols, H, Ulvskov, P, Mikkelsen, JD, Knox, JP, Willats, WGT. High-throughput screening of monoclonal antibodies against plant cell wall glycans by hierarchical clustering of their carbohydrate microarray binding profiles. *Glycoconjugate J.* 2007. 25: 37-48.
- Moreira, LRS, Filho, EXF. An overview of mannan structure and mannan-degrading enzyme systems. *Appl. Microbiol. Biot.* 2008.79: 165-178.
- Mori, H, Sass Bak-Jensen, K, Gottschalk, TE, Saddik Motawia, M, Damager, I, Lindberg Moller, B, Svensson, B. Modulation of activity and substrate binding modes by mutation of single and double subsites+1/+2 and-5/-6 of barley  $\alpha$ -amylase 1. *Eur. J. Biochem.* 2001. 268: 6545-6558.
- Moure, A, Gullón, P, Domínguez, H, Parajó, JC. Advances in the manufacture, purification and applications of xylo-oligosaccharides as food additives and nutraceuticals. *Process Biochem.* 2006. 41: 1913-1923.
- Murata, T, Usui, T. Enzymatic synthesis of oligosaccharides and neoglycoconjugates. *Biosci. Biotech. Bioch.* 2006. 70: 1049-1059.
- Mussatto, SI, Mancilha, IM. Non-digestible oligosaccharides: A review. *Carbohydr. Polym.* 2007. 68: 587-597.
- Muzard, M, Aubry, N, Plantier-Royon, R, O'Donohue, M, Remond, C. Evaluation of the transglycosylation activities of a GH 39  $\beta$ -D-xylosidase for the synthesis of xylose-based glycosides. *J. Mol. Catal. B-Enzym.* 2009. 58: 1-5.
- Müllegger, J, Jahn, M, Chen, H-M, Warren, RAJ, Withers, SG. Engineering of a thioglycoligase: randomized mutagenesis of the acid/base residue leads to the identification of improved catalysts. *PEDS.* 2005. 18: 33-40.
- Nakai, S, Baumann, MJ, Petersen, BO, Westphal, Y, Schols, H, Dilokpimol, A, Abou Hachem, M, Lahtinen, SJ, Duus, JØ, Svensson, B. The maltodextrin transport system and metabolism in *Lactobacillus acidophilus* NCFM and production of novel  $\alpha$ -glucosides through reverse phosphorylation by maltose phosphorylase. *FEBS J.* 2009. 276: 7353-7365.
- Nakakuki, T. Present status and future of functional oligosaccharide development in Japan. *Pure Appl.Chem.* 2002. 74: 1245-1251.
- Nakatani, Y, Cutfield, SM, Cutfield, JF. Crystal Structure of exo-1,3/1,4- $\beta$ -glucanase (ExoP) from *Pseudoalteromonas* sp. BB1. To be published.
- Notredame, C, Higgins, DG, Heringa, J. T-Coffee: A novel method for fast and accurate multiple sequence alignment. *J Mol Biol.* 2000. 302: 205-217.
- O'Neill, MA, York, WS. The composition and structure of plant primary cell walls, in: J.K.C. Rose (Ed.), *The Plant Cell Wall: Annual Plant Reviews Series, Vol. 8*, Blackwell Publishing Ltd, Oxford, UK, pp. 1-54.

- Pastor, FIJ, Gallardo, O, Sanz-Aparicio, J, Diaz, P. Chapter 5. Xylanases: molecular properties and applications, in: J. Polaina, A.P. MacCabe (Eds), *Industrial Enzymes: Structure, Function and Applications*, Springer, The Netherlands, 2007, pp. 65-82.
- Payan, F, Leone, P, Porciero, S, Furniss, C, Tahir, T, Williamson, G, Durand, A, Manzanares, P, Gilbert, HJ, Juge, N, Roussel, A. The dual nature of the wheat xylanase protein inhibitor XIP-I structural basis for the inhibition of family 10 and family 11 xylanases. *J. Biol. Chem.* 2004. 279: 36029-36037.
- Pedersen, M, Lauritzen, HK, Frisvad, JC, Meyer, AS. Identification of thermostable  $\beta$ -xylosidase activities produced by *Aspergillus brasiliensis* and *Aspergillus niger*, *Biotechnol. Lett.* 2007. 29: 743-748.
- Pell, G, Szabo, L, Charnock, SJ, Xie, H, Gloster, TM, Davies, GJ, Gilbert, HJ. Structural and biochemical analysis of *Cellvibrio japonicus* xylanase 10C. *J. Biol. Chem.* 2004. 279: 11777-11788.
- Percy, A, Ono, H, Watt, D, and Hayashi, K. Synthesis of  $\beta$ -D-glucopyranosyl-(1,4)-D-arabinose,  $\beta$ -D-glucopyranosyl-(1,4)-L-fucose,  $\beta$ -D-glucopyranosyl-(1,4)-D-altrose catalysed by cellobiose phosphorylase from *Cellvibrio gilvus*. *Carbohydr. Res.* 1998a. 305: 543-548.
- Percy, A, Ono, H, Watt, D, and Hayashi, K. Acceptor specificity of cellobiose phosphorylase from *Cellvibrio gilvus*: synthesis of three branched trisaccharides. *Carbohydr. Res.* 1998b. 308: 423-429.
- Pérez-González, JA, van Peij, NN, Bezoen, A, MacCabe, AP, Ramón, D, de Graaff, LH. Molecular cloning and transcriptional regulation of the *Aspergillus nidulans* xlnD gene encoding a  $\beta$ -xylosidase. *Appl. Environ. Microbiol.* 1998. 64: 1412-1419.
- Pérez-González, JA, de Graaff, LH, Visser, J, Ramon, D. Molecular cloning and expression in *Saccharomyces cerevisiae* of two *Aspergillus nidulans* xylanase genes. *Appl. Environ. Microbiol.* 1996. 62: 2179-2182.
- Plou, FJ, Gómez de Segura, A, Ballesteros, A. 2007. Chapter 9: Application of glycosidases and transglycosidases in the synthesis of oligosaccharides, in: J. Polaina, A.P. MacCabe (Eds.), *Industrial Enzymes: Structure, Function and Applications*, Springer, Dordrecht, The Netherlands, 2007, pp. 141-159.
- Pohl, NL. Functional proteomics for the discovery of carbohydrate-related enzyme activities. *Curr. Opin. Chem. Biol.* 2004. 9: 76-81.
- Polizeli, MLTM, Rizzatti, ACS, Monti, R, Terenzi, HF, Jorge, JA, Amorim, DS. Xylanases from fungi: properties and industrial applications. *Appl. Microbiol. Biot.* 2005. 67: 577-591.
- Poutanen, K, Puls, J. Characteristics of *Trichoderma reesei*  $\beta$ -xylosidase and its use in the hydrolysis of solubilized xylans. *Appl. Microbiol. Biotechnol.* 1988. 28: 425-432.
- Pozzo, T, Pasten, JL, Karlsson, EN, Logan, DT, Structural and functional analyses of  $\beta$ -glucosidase 3B from *Thermotoga neapolitana*: a thermostable three-domain representative of glycoside hydrolase 3. *J Mol Biol.* 2010. 397: 724-39.
- Puchart, V, Biely, P. A simple enzymatic synthesis of 4-nitrophenyl  $\beta$ -1,4-D-xylobioside, a chromogenic substrate for assay and differentiation of endoxylanases. *J. Biotechnol.* 2007. 128: 576-586.
- Qian, X, Sujino, K, Palcic, MM, Ratchliffe, RM. Glycosyltransferases in oligosaccharide synthesis. *J. Carbohydr. Chem.* 2002. 21: 911-942.
- Rasmussen, LE, Sørensen, HR, Vind, J, Viksø-Nielsen, A. Mode of action and properties of the  $\beta$ -xylosidases from *Talaromyces emersonii* and *Trichoderma reesei*. *Biotechnol. Bioeng.* 2006. 94: 869-876.

Rastall, RA, Hotchkiss, AT. Potential for the development of prebiotic oligosaccharides from biomass, in: G. Eggleston, G.L. Coté (Eds.), *Oligosaccharides in food and agriculture*, Chapter 4, ACS Symposium Series, 849, The American Chemical Society, Washington, 2003. pp. 44-53.

Rodionova NA, Tavobilov IM, Bezborodov AM.  $\beta$ -Xylosidase from *Aspergillus niger* 15: purification and properties. *J. Appl. Biochem.* 1983. 5: 300-312.

Roe, JH, Rice, EW. A photometric method for the determination of free pentoses in animal tissues. *J Biol Chem.* 1984. 173: 507-512.

Rojas, AL, Fischer, H, Eneiskaya, EV, Kulminskaya, AA, Shabalin, KA, Neustroev, KN, Craievich, AF, Golubev, AM, Polikarpov, I. Structural insights into the  $\beta$ -xylosidase from *Trichoderma reesei* obtained by synchrotron small-angle X-ray scattering and circular dichroism spectroscopy. *Biochemistry.* 2005. 44: 15578-15584.

Sabater-Molina, M, Larque, E, Torrella, F, Zamora, S. Dietary fructooligosaccharides and potential benefits on health. *J. Physiol. Biochem.* 2009. 65: 315-328.

Sabini, E, Schubert, H, Murshudov, G, Wilson, KS, Siika-Aho, M, Penttilä, M. The three-dimensional structure of a *Trichoderma reesei*  $\beta$ -mannanase from glycoside hydrolase family 5. *Acta Crystallogr. D.* 2000. 56: 3-13.

Sako, T, Matsumoto, K, Tanaka, R. Recent progress on research and applications of non-digestible galacto-oligosaccharides. *Int. Dairy J.* 1999. 9: 69-80.

Saloheimo, M, Nakari-Setälä, T, Tenkanen, M, Penttilä, M. cDNA cloning of a *Trichoderma reesei* cellulase and demonstration of endoglucanase activity by expression in yeast. *Eur. J. Biochem.* 1997. 249: 584-591.

Saloheimo, M, Paloheimo, M, Hakola, S, Pere, J, Swanson, B, Nyysönen, E, Bhatia, A, Ward, M, Penttilä, M. Swollenin, a *Trichoderma reesei* protein with sequence similarity to the plant expansins, exhibits disruption activity on cellulosic materials. *Eur. J. Biochem.* 2002. 269: 4202-4211.

Sambrook, J, Russell, D. *Molecular Cloning: A Laboratory Manual*, third ed. Cold Spring Harbor Laboratory Press, Cold Spring Harbor, NY. 2001.

Schmidt, A, Gübitz, GM, Kratky, C. Xylan binding subsite mapping in the xylanase from *Penicillium simplicissimum* using xylooligosaccharides as cryo-protectant. *Biochemistry.* 1999. 38: 2403-2412.

Schröder, R, Atkinson, RG, Redgwell, RJ. Re-interpreting the role of endo- $\beta$ -mannanases as mannan endotransglycosylase/hydrolases in the plant cell wall. *Ann. Bot.* 2009. 104: 197-204.

Schröder, R, Wegrzyn, TF, Sharma, NN, Atkinson, RG. LeMAN4 endo- $\beta$ -mannanase from ripe tomato fruit can act as a mannan transglycosylase or hydrolase. *Planta.* 2006. 224: 1091-1102.

Seidle, HF, McKenzie, K, Marten, I, Shoseyov, O, Huber, RE. Trp-262 is a key residue for the hydrolytic and transglucosidic reactivity of the *Aspergillus niger* family 3  $\beta$ -glucosidase: Substitution results in enzymes with mainly transglucosidic activity. *Arch. Biochem. Biophys.* 2005. 444: 66-75.

Selig, MJ, Decker, SR, Knoshaug, EP, Baker, JO, Himmel, ME, Adney, WS. Heterologous expression of *Aspergillus niger*  $\beta$ -D-xylosidase (XlnD): characterization on lignocellulosic substrates. *Appl. Biochem. Biotechnol.* 2008. 146: 57-68.

Shaikh, FA, Withers, SG. Teaching old enzymes new tricks: engineering and evolution of glycosidases and glycosyl transferases for improved glycoside synthesis. *Biochem. Cell. Biol.* 2008. 86: 169-177.

Shallom, D, Shoham, Y. Microbial hemicellulases. *Curr. Opin. Microbiol.* 2003. 6: 219-228.

- Sharkov, VI, Ul'yanovskaya, RI, Bolotova, AK. Glycosides of alditols and glycols as glycerol substitutes. *Sb. Tr., Gos. Mauchn.-Issled. Inst. Gidrolizn. I Sul'fitno-Spirt. Prom.* 1961. 9: 138-152.
- Shimizu, K, Iijima, B, Shimada, N, Onuki, Y. Manufacture of food and beverages containing reduced xylo-oligosaccharides. JP 62278962 A 19871203. 1987.
- Shindyalov, IN, Bourne, PE. Protein structure alignment by incremental combinatorial extension (CE) of the optimal path. *Protein Eng.* 1998. 11: 739-747.
- Shinoyama, H, Kamiyama, Y, Yasui, T. Enzymatic Synthesis of alkyl  $\beta$ -xylosides from xylobiose by application of the transxylosyl reaction of *Aspergillus niger*  $\beta$ -xylosidase. *Agric. Biol. Chem.* 1988. 52: 2197-2202.
- Shintate, K, Kitaoka, M, Kim, YK, Hayashi, K. Enzymatic synthesis of a library of  $\beta$ -(1 $\rightarrow$ 4) hetero-D-glucose and D-xylose-based oligosaccharides employing cellodextrin phosphorylase. *Carbohydr Res.* 2003. 338(19): 1981-1990.
- Singh, S, Scigelova, M, Crout, DHG. Glycosidase-catalysed synthesis of mannobioses by the reverse hydrolysis activity of  $\alpha$ -mannosidase: partial purification of  $\alpha$ -mannosidases from almond meal, limpets and *Aspergillus niger*. *Tetrahedron-Asymmetr.* 2000. 11: 223-229.
- Sinnott, ML. Catalytic mechanisms of enzymatic glycosyl transfer. *Chem. Rev.* 1990. 90: 1171-1202.
- Snart, J, Bibiloni, R, Grayson, T, Lay, C, Zhang, HY, Allison, GE, Laverdiere, JK, Temelli, F, Vasanthan, T, Bell, R, Tannock, GW. Supplementation of the diet with high-viscosity  $\beta$ -glucan results in enrichment for lactobacilli in the rat cecum. *Appl. Environ. Microb.* 2006. 72: 1925-1931.
- Söding, J, Biegert, A, Lupas, AN. The HHpred interactive server for protein homology detection and structure prediction. *Nucleic Acids Res.* 2005. 33: W244-W248.
- Staden, R. A strategy of DNA sequencing employing computer programs. *Nucleic Acids Res.* 1979. 6: 2601-2610.
- Steed, H, Macfarlane, GT, Macfarlane, S. Prebiotics, synbiotics and inflammatory bowel disease. *Mol. Nutr. Food Res.* 2008. 52: 898-905.
- Stick, RV. *Carbohydrates: the sweet molecules of life*. Academic Press, London, UK, 2001.
- Sticklen, MB. 2008. Plant genetic engineering for biofuel production: towards affordable cellulosic ethanol. *Nat. Rev. Genet.* 9: 433-443.
- Stålbrand, H, Siika-Aho, M, Tenkanen, M, Viikari, L. Purification and characterization of two  $\beta$ -mannanases from *Trichoderma reesei*. *J. Biotechnol.* 1993. 20: 229-242.
- Sugimura, M, Nishimoto, M, Kitaoka, M. Characterization of glycosynthase mutants derived from glycoside hydrolase family 10 xylanases. *Biosci. Biotechnol. Biochem.* 2006. 70: 1210-1217.
- Sulistyo, J, Kamiyama, Y, Ito, H, Yasui, T. Enzymatic synthesis of hydroquinone  $\beta$ -xyloside from xylooligosaccharides. *Biosci. Biotechnol. Biochem.* 1994. 58:1311-1313.
- Swennen, K, Courtin, CM, Delcour, JA. Non-digestible oligosaccharides with prebiotic properties. *Crit. Rev. Food. Sci.* 2006. 46: 459-471.
- Tailford, LE, Ducros, VMA, Flint, JE, Roberts, SM, Morland, C, Zechel, DL, Smith, N, Bjornvad, ME, Borchert, TV, Wilson, KS, Davies, GJ, Gilbert HJ. Understanding how diverse  $\beta$ -mannanases recognize heterogeneous substrates. *Biochemistry.* 2009. 48: 7009-7018.
- Taiz, L, Zeiger, E. *Plant Physiology*. The Benjamin/Cummings Publishing Company, Inc. Redwood City, CA, 1991.



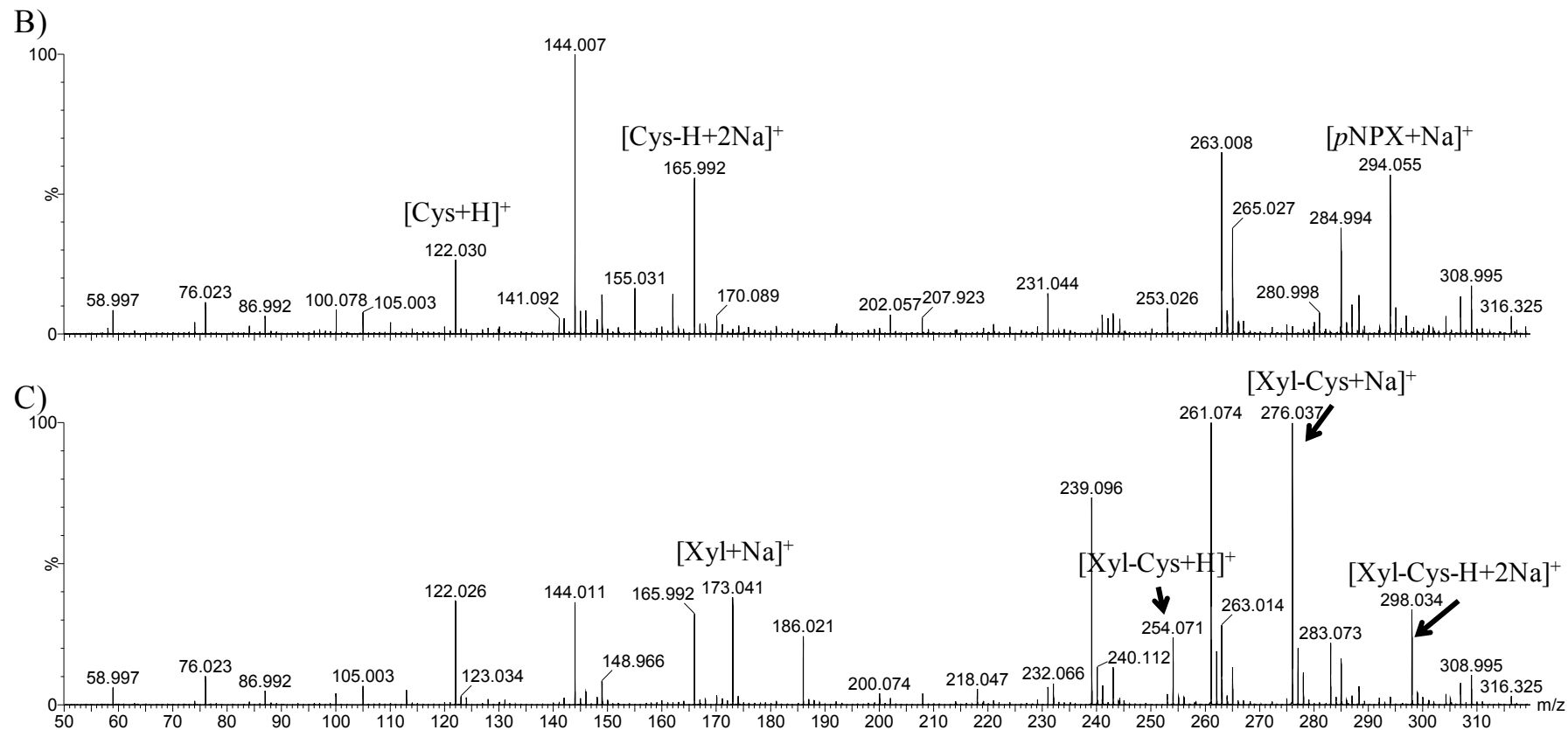
- Tenkanen, M, Puls, J, Poutanen, K. Two major xylanases of *Trichoderma reesei*. *Enzyme Microb. Tech.* 1992. 14: 566-574.
- Tomme, P, Warren, RA, Miller, RC, Kilburn, DG, Gilkes, NR, in: J.N. Saddler, M. Penner (Eds.), *Enzymatic Degradation of Insoluble Polysaccharides, Cellulose-binding domains: classification and properties*, American Chemical Society, Washington, 1995, pp. 142-163.
- Topping, DL, Fukushima, M, Bird, AR. Resistant starch as a prebiotic and synbiotic: state of the art. *P. Nutr. Soc.* 2003. 62: 171-176.
- Törrönen, A, Rouvinen, J. Structural and functional properties of low molecular weight endo-1,4- $\beta$ -xylanases. *J. Biotechnol.* 1997. 57: 137-149.
- Tsumuraya, Y, Brewer, CF, Hehre, EJ. Substrate-induced activation of maltose phosphorylase: interaction with the anomeric hydroxyl group of  $\alpha$ -maltose and  $\alpha$ -D-glucose controls the enzyme's glucosyltransferase activity. *Arch. Biochem. Biophys.* 1990. 281: 58-65.
- Uttamchandani, M, Lu, CHS, Yao, SQ. Next generation chemical proteomic tools for rapid enzyme profiling. *Accounts Chem. Res.* 2009. 42: 1183-1192.
- Van Loo, J, Franck, A, Roberfroid, M. Functional food properties of non-digestible oligosaccharides – reply. *Brit. J. Nutr.* 1999. 82: 329-329.
- van Peij, NN, Brinkmann, J, Vrsanská, M, Visser, J, de Graaff, LH.  $\beta$ -Xylosidase activity, encoded by *xlnD*, is essential for complete hydrolysis of xylan by *Aspergillus niger* but not for induction of the xylanolytic enzyme spectrum. *Eur. J. Biochem.* 1997. 245: 164-173.
- Vardakou, M, Dumon, C, Murray, JW, Christakopoulos, P, Weiner, DP, Juge, N, Lewis, RJ, Gilbert, HJ, Flint, JE. Understanding the structural basis for substrate and inhibitor recognition in eukaryotic GH11 xylanases. *J. Mol. Biol.* 2008. 375: 1293-1300.
- Varghese, JN, Hrmova, M, Fincher, GB. Three-dimensional structure of a barley  $\beta$ -D-glucan exohydrolase, a family 3 glycosyl hydrolase. *Structure.* 1999. 7: 179-190.
- Vázquez, MJ, Alonso, JL, Domínguez, H, Parajó, JC. Xylooligosaccharides: manufacture and applications. *Trends Food Sci. Technol.* 2000. 11: 387-393
- Vincken, JP, York, WS, Beldman, G, Voragen, AG. Two general branching patterns of xyloglucan, XXXG and XXGG. *Plant Physiol.* 1997. 114: 9-13.
- Vogel, J. Unique aspects of the grass cell wall. *Curr. Opin. Plant Biol.* 2008. 11: 301-307.
- Vroemen, S, Heldens, J, Boyd, C, Henrissat, B, Keen, NT. Cloning and characterization of the *bgxA* gene from *Erwinia Chrysanthemi* D1 which encodes a  $\beta$ -glucosidase/xylosidase enzyme. *Mol. Gen. Genet.* 1995. 246: 465-477.
- Wakiyama, M, Yoshihara, K, Hayashi, S, Ohta, K. Purification and properties of an extracellular  $\beta$ -xylosidase from *Aspergillus japonicus* and sequence analysis of the encoding gene. *J. BioSci. Bioeng.* 2008. 106: 398-404.
- Waldron, KW, Faulds, CB. Cell wall polysaccharides: composition and structure, in: J. P. Kamerling, G-J. Boons, Y.C. Lee, A. Suzuki, N. Taniguchi, A.G.J. Voragen (Eds.), *Comprehensive glycoscience: Introduction to Glycoscience Synthesis of Carbohydrates, Vol. 1*, Elsevier, Oxford, United Kingdom, 2007, pp 181-201.
- Wallner, B, Elofsson, A. Can correct protein models be identified? *Protein Sci.* 2003. 12: 1073-1086.
- Wang, LX. Chemoenzymatic synthesis of glycopeptides and glycoproteins through endoglycosidase-catalyzed transglycosylation. *Carbohydr. Res.* 2008. 343: 1509-1522.

- Wang, LX. Expanding the repertoire of glycosynthases. *Chem. Biol.* 2009. 16: 1026-1027.
- Webb, EC. 1992. *Enzyme nomenclature: Recommendations of the Nomenclature Committee of the International Union of Biochemistry and Molecular Biology on the nomenclature and classification of enzymes*. Academic Press, San Diego, CA. 1992.
- Westphal, Y, Schols, HA, Voragen, AGJ, Gruppen, H. Introducing porous graphitized carbon liquid chromatography with evaporative light scattering and mass spectrometry detection into cell wall oligosaccharide analysis. *J. Chromatogr. A.* 2010. 1217: 689-695.
- Whitaker, JR. *Principles of Enzymology for the Food Sciences*, 2<sup>nd</sup> ed. Marcel Dekker, Inc., Madison Avenue, NY. 1994.
- Wilkinson, S, Liew, C, Mackay, J, Salleh, H, Withers, S, McLeod, M. *Escherichia coli* glucuronylsynthase: an engineered enzyme for the synthesis of  $\beta$ -glucuronides. *Org. Lett.* 2008. 10: 1585-1588.
- Williams, SJ, Withers, SG. Glycosyl fluorides in enzymatic reactions. *Carbohydr. Res.* 2000. 327: 27-46.
- Win, M, Kamiyama, Y, Matsuo, M, Yasui, T. Transxylosylation products of xylobiose by  $\beta$ -xylosidase from *Penicillium wortmanni* IFO 7237. *Agric. Biol. Chem.* 1988. 52: 1151-1158.
- Withers, SG, Rupitz, K, Trimbur, D, Warren, RAJ. Mechanistic consequences of mutation of the active-site nucleophile Glu-358 in *Agrobacterium*  $\beta$ -glucosidase. *J. Biochem.* 1992. 31: 9979-9985.
- Wood, BJB, Rainbow, C. The maltophosphorylase of beer *Lactobacilli*. *Biochem. J.* 1961. 78: 204-209
- Wong, D. Enzymatic deconstruction of backbone structures of the ramified regions in pectins. *Protein J.* 2008. 27: 30-42.
- Wong, KKY, Tan, LUL, Saddler, JN. Multiplicity of  $\beta$ -1,4-xylanase in microorganisms: functions and applications. *Microbiol. Rev.* 1988. 52(3): 305-317.
- Xiong, JS, Balland-Vaney, M, Xie, ZP, Schultze, M, Kondorosi, A, Kondorosi, E, Staehelin, C. Molecular cloning of a bifunctional  $\beta$ -xylosidase/ $\alpha$ -L-arabinosidase from alfalfa roots: heterologous expression in *Medicago truncatula* and substrate specificity of the purified enzyme. *J. Exp. Bot.* 2007. 58: 2799-2810.
- Xu, BZ, Häggglund, P, Stålbrand, H, Janson, JC. Endo- $\beta$ -1,4-mannanases from blue mussel, *Mytilus edulis*: purification, characterization, and mode of action. *J. Biotechnol.* 2002. 92: 267-277.
- Yan, Q, Hao, S, Jiang, Z, Zhai, Q, Chen, W. Properties of a xylanase from *Streptomyces matensis* being suitable for xylooligosaccharides production. *J. Mol. Catal. B-Enzym.* 2009. 58: 72-77.
- Zeng, H, Xue, Y, Peng, T, Shao, W. Properties of xylanolytic enzyme system in bifidobacteria and their effects on utilization of xylooligosaccharides. *Food Chem.* 2007. 101: 1172-1177.
- Zhang, YL, Ju, JS, Peng, H, Gao, F, Zhou, C, Zeng, Y, Xue, YF, Li, Y, Henrissat, B, Gao, GF, Ma, YH. Biochemical and structural characterization of the intracellular mannanase AaManA of *Alicyclobacillus acidocaldarius* reveals a novel glycoside hydrolase family belonging to clan GH-A. *J. Biol. Chem.* 2008. 283: 31551-31558.
- Ziemer, CJ, Gibson, GR. An overview of probiotics, prebiotics and synbiotics in the functional food concept: Perspectives and future strategies. *Int. Dairy J.* 1998. 8: 473-479.
- Øbro, J, Sørensen, I, Derkx, P, Madsen, CT, Drews, M, Willer, M, Mikkelsen, JD, Willats, WG. High-throughput screening of *Erwinia chrysanthemi* pectin methylesterase variants using carbohydrate microarrays. *Proteomics.* 2009. 9: 1861-1868.

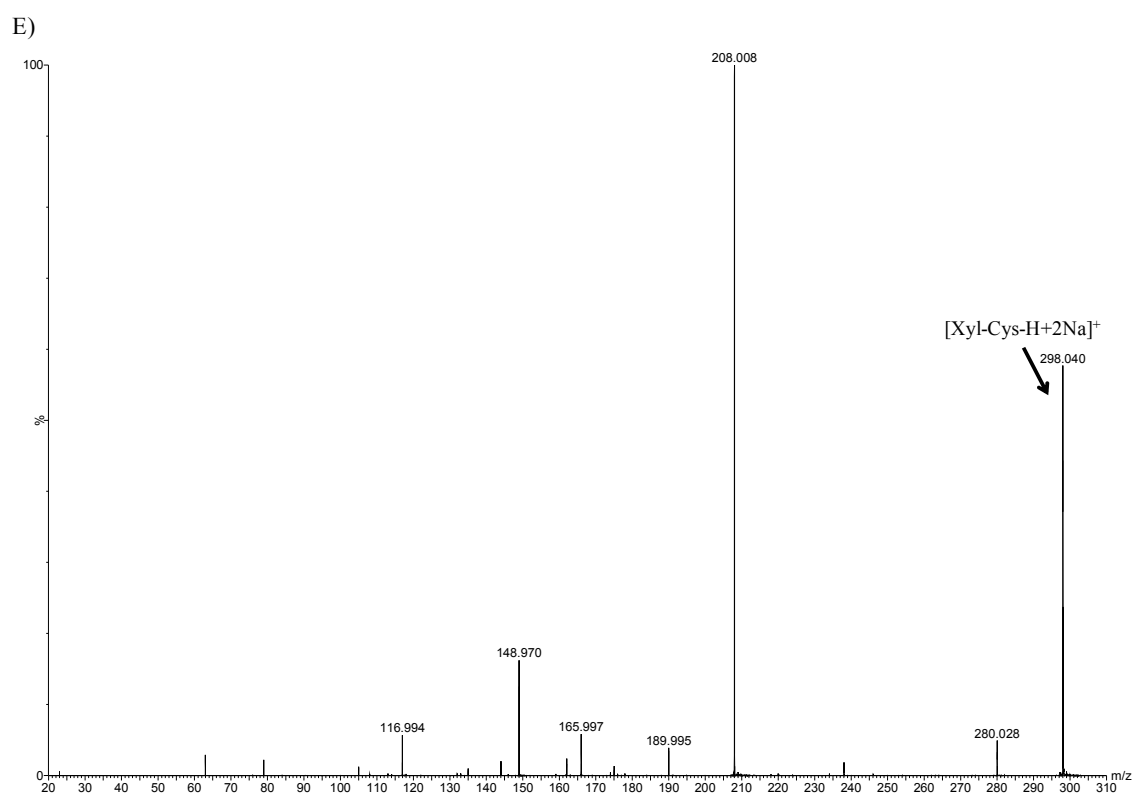
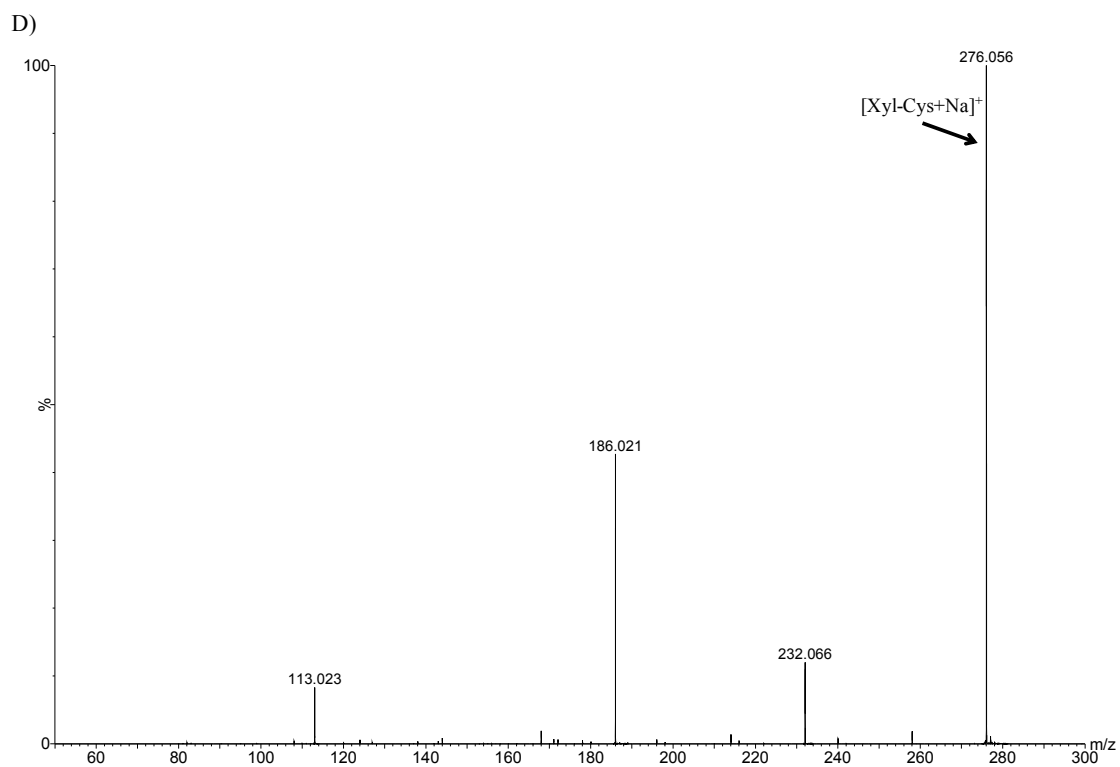
Øbro, J, Sørensen, I, Møller, I, Skjøt, M, Mikkelsen, JD, Willats, WGT. High-throughput microarray analysis of pectic polymers by enzymatic epitope deletion. *Carbohydr. Polym.* 2007. 70: 77-81.

## 10. Appendix

### 10.1 Supplementary Figures



**Supplementary Fig. 1** ESI-Q-TOF mass spectra ( $m/z$  50-320) of Xyl-Cys transglycosylation reaction mixture containing 200 nM BxlA, 30 mM *p*NPX, and 200 mM L-cysteine in 10 mM sodium acetate pH 5.0 at 40°C. B) reaction with L-cysteine at 0 min. C) reaction with L-cysteine at 60 min reaction time (from Figure 17).



**Supplementary Fig. 1** (cont.) ESI-Q-TOF mass spectra of Xyl-Cys transglycosylation reaction mixture. D) ESI-Q-TOF MS/MS spectrum of Xyl-Cys at  $m/z$  276. E) ESI-Q-TOF MS/MS spectrum of Xyl-Cys at  $m/z$  298 (from Figure 17).









EAA64470\_ASPNI\_Bx1A

α14 β6 β7

530 540 550 560 570 580

EAA64470\_ASPNI\_Bx1A ISKLS...EL.GKPLVVLQMGGGQVDSSSLKNDNVNALIWGGYPGQSGGHALA...DIITGK..  
 ABA40420\_ASPFU\_X1d IDQLS...QL.GKPLIVLQMGGGQVDSSSLKSNKNVNSLIWGGYPGQSGGQALL...DIITGK..  
 EED57542\_ASPFL\_Xy1A ITKLA...DL.GKPLIVLQMGGGQVDSSSLKNNKNVNALIWGGYPGQSGGQALL...DIITGK..  
 EAA67023\_ASPNI\_Bx1B ILELA...EL.GRPLTVVQFGGGQVDSSSLASAGVGAIVWAGYPSQAGGAVF...DVLTKG..  
 BAE65591\_ASPOR IEQLS...DL.EKPLIVVQFGGGQVDSSSLANAGVGAIVWAGYPSQAGGAAVF...DILTKG..  
 EED45224\_ASPFL IEQLS...DL.EKPLIVVQFGGGQVDSSSLANAGVGAIVWAGYPSQAGGAAVF...DILTKG..  
 CAA93248\_HYPJE\_Bx11 IQKLS...EV.GKPLVVLQMGGGQVDSSSLKSNKKVNSLVWGGYPGQSGGVALF...DILSGK..  
 CAB89357\_ARATH\_AtBX3 VTRVA...MAARGPVVLMVIMSGGFDITFAKNDKKITSIMVVGYPGEAGGLAIA...DVFVGR..  
 AAK38482\_HORVU VNSVA...DAAKKPVILVLLCGGFPVDTFAKNNPKIGAIWAGYPSQAGGAI...DVLFGD..  
 CAW52613\_ZEAMA INAVA...MASPTIVLVMISAGGVVDSFAHNNTKIGAIWAGYPSQAGGTAIA...DVLFGK..  
 ABI29899\_THENE\_Bg13B IKTVSRBFHEQ.GKKVIVLLNIGSPVEVVSWRD..LVDGILLVWQAGQETGRIVA...DVLTKG..  
 BAA10968\_ASPAC IEAVA...EV.QSNIVVLLNIGSPVEVVPWI..D..KVKSVLEAYLGGQALGGR.W...RMCYSV..  
 ABC88234\_PSEBB\_ExoP IKAAA...NN.CNNTIVVHLSVGFVLDVWEDYDHPNVTAILWAGLPGQESGNSLA...DVLTKG..  
 AAD23382\_HORVU\_ExoI LKQLK...A.DNIPVTVFLSAGRPFLVWELNA..SDAFVAAWLPGSE.GEGVA...DVLTKG..  
 AAA64351\_BACSU\_YbbD VQAVC...G.GVR.CATVLISGRFVWVQPLAA..SDALVAAWLPGSE.GGGVT...DALFGD..  
 AAF93857\_VIBCH\_NagZ MKAAL...Q.HNKPFVLMSLR.NPYDAANFEEA..KALIAVYGFKGYANGRYLQPNIPAGVMAIFGQ..  
 AAQ05801\_CELFI ..YLA...NL.....STRNQTVVRIEWAEPMG.....  
 ABU76375\_ENTSA ISALK...AT.GKPLVVLQMGGGQVDSSSLKNDNVNALIWGGYPGQSGGHALA...DIITGK..

EAA64470\_ASPNI\_Bx1A

590 600 610 620

EAA64470\_ASPNI\_Bx1A ...RAPAGRLVTTQYP..AEYAEVFPFAI.DMN...LRPNET.SGNPQG...TYMWWY...T  
 ABA40420\_ASPFU\_X1d ...RAPAGRLVTTQYP..AEYATQFPAT.DMS...LRPHG...NNPQG...TYMWWY...T  
 EED57542\_ASPFL\_Xy1A ...RAPAARLVTTQYP..AEYAEVFPFAI.DMN...LRPNG...SNPQG...TYMWWY...T  
 EAA67023\_ASPNI\_Bx1B ...AAPAGRLVTTQYP..KSYVDEVPMT.DMN...LQPGT...DNPGR...TYRWY...E  
 BAE65591\_ASPOR ...SAPAGRLVTTQYP..ASYVDEVPMT.DMT...LRPGS...NNPGR...TYRWY...D  
 EED45224\_ASPFL ...SAPAGRLVTTQYP..ASYVDEVPMT.DMT...LRPGS...NNPGR...TYRWY...D  
 CAA93248\_HYPJE\_Bx11 ...RAPAGRLVTTQYP..AEYVHQFPQN.DMN...LRPDG...KSNPQG...TYRWY...T  
 CAB89357\_ARATH\_AtBX3 ...HNPSSGLVPTWYF..QSYVEKVPMS.NMN...MRPDKS.KGYPGR...SYRFY...T  
 AAK38482\_HORVU ...HNPSSGLVPTWYF..KEFT.AVPMT.DMR...MRADPS.TGYPGR...TYRFY...K  
 CAW52613\_ZEAMA ...YNPSSGLVPTWYF..NEYVNIQIPMT.SMA...LRPDA.LGYPGR...TYKFY...G  
 ABI29899\_THENE\_Bg13B ...INPSGKLVPTT.FP.RDYS.DVPSW.TF..P..GEPK...DNPQKVVVEEDIVVGYRYDTPG  
 CAA33665\_CLOTH ...KSIIVGKLVPTT.FP.VKLS.HNPSYLN.F..P..GEDD...R...VEYKEGLFVGYRYDTPG  
 BAA10968\_ASPAC ...VNPAGKLVPTT.FP.VKLS.HNPSYLN.F..P..GEDD...R...VEYKEGLFVGYRYDTPG  
 ABC88234\_PSEBB\_ExoP ...GKTQDFDFTGKLVPTT.FP.VKLS.HNPSYLN.F..P..GEDD...R...VEYKEGLFVGYRYDTPG  
 AAD23382\_HORVU\_ExoI ...FGFTGRVPTT.FP.VKLS.HNPSYLN.F..P..GEDD...R...VEYKEGLFVGYRYDTPG  
 AAA64351\_BACSU\_YbbD ...AKPKGTLVPTT.FP.VKLS.HNPSYLN.F..P..GEDD...R...VEYKEGLFVGYRYDTPG  
 AAF93857\_VIBCH\_NagZ ...D...N...PIM...EVVQA.EA...L  
 AAQ05801\_CELFI ...D...N...ANVPA..YVHSVPTV.FVS..FEN..P...L  
 ABU76375\_ENTSA ...YNPSSGLVPTT.FP.VKLS.HNPSYLN.F..P..GEDD...R...VEYKEGLFVGYRYDTPG

EAA64470\_ASPNI\_Bx1A

630 640 650

EAA64470\_ASPNI\_Bx1A GTP.VYEFHGHLFVTTTFE.ESTETTD...AGSFNI...  
 ABA40420\_ASPFU\_X1d GTP.VYEFHGHLFVTTTFH.ASLPGTG..KD.KTSFNI...  
 EED57542\_ASPFL\_Xy1A GTP.VYEFHGHLFVTTNFT.ASASAGSGTKN.RTSFNI...  
 EAA67023\_ASPNI\_Bx1B ...DA.VLPPFGFGLHYTTFN.VSWAKKA...FGPYDA...  
 BAE65591\_ASPOR ...KA.VLPPFGFGLHYTTFN.VSWNHAE...YGPYNT...  
 EED45224\_ASPFL ...KA.VLPPFGFGLHYTTFN.VSWNHAE...YGPYNT...  
 CAA93248\_HYPJE\_Bx11 GKP.VYEFHGSLFVTTTFK.ETLASHP..K..SLKFNT...  
 CAB89357\_ARATH\_AtBX3 GET.VYAFADALTYTKFD.HQLIKAP..R..LVLSL...  
 AAK38482\_HORVU GKT.VYNFGYGLSYTKYS.HRFASKG..TK.PPSMSGI...  
 CAW52613\_ZEAMA GPAVLVPPFGHGLSYTNFS.YASGTG..A..TVTIHIGA...WEHC...  
 ABI29899\_THENE\_Bg13B VEP.AYEFHGGLSYTTTFE.YSDLVSD..F...  
 CAA33665\_CLOTH IEP.LFPFGHGLSYTKFE.YSDISVD..KK...D...  
 BAA10968\_ASPAC ETP.IYEFHGGLSYTTFN.YSGLHIQ..VL.NASSNAQVATETGAAPTFGQVGNASDYVYPEGLTRISKF  
 ABC88234\_PSEBB\_ExoP YDP.LFAYGYGLTYQDNINVPVLEK..TSPKKTVNS...  
 AAD23382\_HORVU\_ExoI YDP.LFRLGYGLTY...  
 AAA64351\_BACSU\_YbbD GNT.LYPLGYGLNI...  
 AAF93857\_VIBCH\_NagZ LK...KQQF.S...  
 AAQ05801\_CELFI ...YHLFD.VPRVRT...  
 ABU76375\_ENTSA NGP.LYPPFGYGLSYTTFS.VSDVKLS..AP...T

EAA64470\_ASPNI\_Bx1A

660 670

EAA64470\_ASPNI\_Bx1A ...QT..V.LTTPHS...GYEHAQQKT  
 ABA40420\_ASPFU\_X1d ...QD..L.LTQPH...GFANVEQMP  
 EED57542\_ASPFL\_Xy1A ...DE..V.LGRPH...GKLVQEMMP  
 EAA67023\_ASPNI\_Bx1B ...AT..L.ARGKN...P.SSNI  
 BAE65591\_ASPOR ...DS..V.ASGTTN...APVDTEL  
 EED45224\_ASPFL ...DS..V.ASGTTN...APVDTEL  
 CAA93248\_HYPJE\_Bx11 ...SS..I.LSAPH...GYTYSEIQP  
 CAB89357\_ARATH\_AtBX3 ...LDENHPCRSSE..CQSL..DAIG..PH...CENAVEGGS  
 AAK38482\_HORVU ...EG..LKATARASAAG..TVSY..DVE..EM...GAEA.CDRL  
 CAW52613\_ZEAMA ...KMLTYKMGAPSPSPA..CPAL..N...VASH.MCSE  
 ABI29899\_THENE\_Bg13B ...DGE  
 CAA33665\_CLOTH ...VSDNS  
 BAA10968\_ASPAC IYPWLNSTDLKASSGDPPY..G..VDTA...EHVP..EGATDGSQPVPVLPAGGSGGPNRLYDE  
 ABC88234\_PSEBB\_ExoP ...D...SHPLFVRSLLAKNMTWQLADTSTQKVLASGAS..A.TSGDKQS  
 AAD23382\_HORVU\_ExoI ...  
 AAA64351\_BACSU\_YbbD ...  
 AAF93857\_VIBCH\_NagZ ...  
 AAQ05801\_CELFI ...  
 ABU76375\_ENTSA ...MKRDS

Supplementary Fig. 2 (cont.)





```

ManC
ManA
HjMan5A_1qnr SPLYGQCGGSGYTGFTCCAQGTCTIYSNYWYSQCLNT
SlMan4_1rh9 .....LLQSLAL
CmMan5A_1uuq .....
MeMan5A_2c0h .....
TfMan_1bqc .....

```

**Supplementary Fig. 3** Amino acid sequence alignment of ManC and ManA from *A. nidulans* FGSC A4 with reported crystal structures of GH5 mannanases: *Trichoderma reesei* (Teleomorph: *H. jecorina*; UniProt ID: Q99036), *Solanum lycopersicum* (UniProt ID: Q8L5J1), *Mytilus edulis* (UniProt ID: Q8WPI2), *Thermobifida fusca* KW3 (UniProt ID: Q9ZF13), and *Bacillus* sp. JAMB-602 (UniProt ID: Q4W8M3). ▼), possible subsite -2; ▼), possible subsite +1 and +2; ▼), possible subsite +3; ▼), mutation position (subsite +1).

## 10.2 List of publications

### 10.2.1 Oral presentations

20 Nov 2007. Xylooligosaccharides, xylanases, and xylosidases as tools for novel prebiotics production. Protein and Enzyme Engineering Workshop, EPC, BioCentrum-DTU.

07 Jan 2007. Chemo-enzymatic synthesis of prebiotics: xylooligosaccharides, xylanases, and xylosidases: as tools for novel prebiotics production. 07-annual meeting, Center for Biological Production of Dietary Fibres and Prebiotics, Department of Chemical Engineering, DTU.

07 Apr 2007. Chemo-enzymatic synthesis of prebiotics: xylooligosaccharides, xylanases, and xylosidases: as tools for novel prebiotics production, an update status. Seminar at Danisco, Langebrogade, Copenhagen.

14 May 2008. The mutation plan for xylosidase (GH3) and xylanase (GH10). Protein and Enzyme Engineering Workshop, EPC, Department of Systems Biology, DTU.

22 Jul 2008. Production of xylooligosaccharides by transglycosylation of  $\beta$ -xylosidase and xylanase. Protein and Enzyme Engineering Workshop, EPC, Department of Systems Biology, DTU.

29 Oct 2008. Production of xylooligosaccharides by transglycosylation of  $\beta$ -xylosidase and xylanase. Center for Biological Production of Dietary Fibres and Prebiotics, Department of Chemical Engineering, DTU.

23 Jun 2009. GH3  $\beta$ -xylosidases characterization and transglycosylation & update status of GH61 putative endoglucanase. Center for Biological Production of Dietary Fibres and Prebiotics Workshop, Comwell Holte Hotel, Holte.

As well as, nine EPC group meetings, EPC, Department of Systems Biology, DTU.

### 10.2.2 Poster presentations

**Dilokpimol A.**, H. Nakai., M.J. Baumann, M. Abou Hachem & B. Svensson: The production of xylanases and xylosidase from *Aspergillus nidulans*. 27818 Enzyme Technology, Lignocellulose, and Non-Starch Polysaccharides, Lyngby, Denmark, May 2008.

**Dilokpimol A.**, H. Nakai., M.J. Baumann, M. Abou Hachem & B. Svensson: Recombinant production of xylanases and xylosidase from *Aspergillus nidulans*. Protein Science Meeting, Tisvildeleje, Denmark, Nov 2008.

#### Posters and conference talks (given by others):

Nakai, H., A. Majumder, **A. Dilokpimol**, M. Ejby, M. Abou Hachem, S. Lahtinen, S. Jacobsen & B. Svensson: The relationship between probiotics and prebiotic carbohydrates. Chemoenzymatic synthesis and differential proteome analysis. 4<sup>th</sup> Conference on Biocatalysis in the Food and Drink Industries, Toulouse, France, April 2010.

Seo, E.-S., M.M. Nielsen, J.M. Andersen, M.B. Vester-Christensen, J.M. Jensen, C. Christiansen, **A. Dilokpimol**, M. Abou Hachem, P. Hägglund, K. Maeda, C. Finnie, A. Blennow & B. Svensson:  $\alpha$ -amylases. Interaction with polysaccharide substrates, proteinaceous inhibitors and regulatory proteins. Agricultural Biotechnology Symposium, Seoul, Korea, September 2008.

Svensson, B., M.M. Nielsen, E.-S. Seo, J. Andersen, **A. Dilokpimol**, C. Christiansen, S. Bozonnet, M. Abou Hachem, A. Blennow, R. Haser & N. Aghajari: The many facets of the molecular interactions and mechanisms involved in carbohydrate recognition and processing by barley  $\alpha$ -amylase. AACC International Annual Meeting, Honolulu, Hawaii, September 2008.

Svensson, B., E.-S. Seo, M.M. Nielsen, L. Kandra, J. Andersen, **A. Dilokpimol**, M. Abou Hachem, G. Gyémánt, R. Haser, N. Aghajari, S. Bozonnet & A. Blennow: Polysaccharide multi-site interactions in  $\alpha$ -amylase: From surface site-active site cross-talk to starch granule recognition. Plant Polysaccharide Workshop, Sigtuna, Sweden, August 2008.

Svensson, B., M.M. Nielsen, E.-S. Seo, J.M. Andersen, **A. Dilokpimol**, S. Bozonnet, M. Abou Hachem, A. Blennow, R. Haser & N. Aghajari: Roles of individual carbohydrate binding surface sites in barley  $\alpha$ -amylase. 24<sup>th</sup> International Carbohydrate Symposium, Oslo, Norway, July 2008.

Andersen, J., M.M. Nielsen, **A. Dilokpimol**, S. Bozonnet, M. Abou Hachem, A. Blennow & B. Svensson: Structure-function relationship investigations and protein engineering of carbohydrate binding surface sites of barley  $\alpha$ -amylase 1. Plant Biotech Denmark Annual Meeting, Frederiksberg, Denmark, January 2008.

Nielsen, M.M., E.-S. Seo, J. Andersen, **A. Dilokpimol**, S. Bozonnet, M. Abou Hachem, H. Naested, A. Blennow & B. Svensson: Mutational analysis of individual roles of carbohydrate binding surface sites in barley  $\alpha$ -amylase 1. ALAMY-3, Smolenice, Slovakia, September 2007.

Seo, E.-S., M. Abou Hachem, M.M. Nielsen, **A. Dilokpimol**, K. Fukuda & B. Svensson: Mutational analysis of sugar tongs in barley  $\alpha$ -amylase 2. ALAMY-3, Smolenice, Slovakia, September 2007.

Abou Hachem, M., W.-F. Xue, **A. Dilokpimol**, B.W. Sigurskjold & B. Svensson: Calcium binding to barley  $\alpha$ -amylase isozymes and its implications on stability and activity. ALAMY-3, Smolenice, Slovakia, September 2007.

Nielsen, M.M., E. S. Seo, **A. Dilokpimol**, M. Abou Hachem, S. Bozonnet, H. Naested & B. Svensson: Mutational analysis of the function of surface binding sites in barley  $\alpha$ -amylase. VII<sup>th</sup> European Symposium of the Protein Society, Stockholm/Uppsala, Sweden, May 2007.

Nielsen, M. M., E.-S. Seo, J. Andersen, **A. Dilokpimol**, S. Bozonnet, M. Abou Hachem, H. Naested, A. Blennow & B. Svenson: Site-directed mutagenesis of secondary carbohydrate binding sites in barley  $\alpha$ -amylase 1. 7<sup>th</sup> Carbohydrate Bioengineering Meeting, Braunschweig, Germany, April 2007.

Svensson, B., M.M. Nielsen, E.-S. Seo, **A. Dilokpimol**, J. Andersen, M. Abou Hachem, H. Naested, M., Willemoës, S. Bozonnet, L. Kandra, G. Gyémánt, N. Aghajari & R. Haser: Roles of multiple surface sites, long substrate binding clefts, and carbohydrate binding modules in the action of amylolytic enzymes on polysaccharide substrates. 7<sup>th</sup> Carbohydrate Bioengineering Meeting, Braunschweig, Germany, April 2007.

Nielsen, M.M., E.-S. Seo, M. Abou Hachem, **A. Dilokpimol** & B.Svensson: Molecular enzymology of starch degradation: Workshop on Food and Feed – Nutrition, Safety and Improved Use of Raw Material, Hyderabad, India, January 2007.

Nielsen, M.M., E.-S. Seo, J. Andersen, **A. Dilokpimol**, S. Bozonnet, M. Abou Hachem, H. Naested, V. Barkholt & B. Svensson: Site-directed mutagenesis of secondary sugar binding site in barley  $\alpha$ -amylase 1. 23<sup>rd</sup> International Carbohydrate Symposium, Whistler, Canada, July 2006.

Nielsen, M.M., E.-S. Seo, J. Andersen, **A. Dilokpimol**, S. Bozonnet, B. Kramhøft, M. Abou Hachem, H. Naested, V. Barkholt & B. Svensson: Site-directed mutagenesis of secondary sugar binding site in barley  $\alpha$ -amylase 1. INPEC Annual Meeting, Elsinore, Denmark, 2006.

### 10.2.3 Manuscripts and publications

**Dilokpimol, A.**, Nakai, H., Gotfredsen, C. H., Appeldoorn, M., Baumann, M. J., Nakai, N., Schols, H. A., Abou Hachem, M., Svensson, B. Enzymatic synthesis of  $\beta$ -xylosyl-oligosaccharides by transxylosylation using two  $\beta$ -xylosidases of glycoside hydrolase family 3 from *Aspergillus nidulans* FGSC A4, submitted to *Carbohydrate Research* (see 10.2.3.1)

**Dilokpimol, A.**, Nakai, H., Gotfredsen, C. H., Baumann, M. J., Nakai, N., Abou Hachem, M., Svensson, B. GH5 endo- $\beta$ -1,4-mannanases from *Aspergillus nidulans* FGSC A4 producing hetero manno-oligosaccharides by transglycosylation, to be submitted to *Biochimica et Biophysica Acta, Proteins and Proteomics* (see 10.2.3.2)

Nakai, H., **Dilokpimol, A.**, Abou Hachem, M., Svensson, B. Efficient one-pot enzymatic synthesis of  $\alpha$ -(1 $\rightarrow$ 4)-glucosidic disaccharides through a coupled reaction catalysed by *Lactobacillus acidophilus* NCFM maltose phosphorylase. *Carbohydr. Res.* 2010. 345: 1061-1064.

Nakai, H., Baumann, M.J., Petersen, B.O., Westphal, Y., Schols, H.A., **Dilokpimol, A.**, Abou Hachem, M., Lahtinen, S.J., Duus, J.Ø., Svensson, B. The maltodextrin transport system and metabolism in *Lactobacillus acidophilus* NCFM and production of novel  $\alpha$ -glucosides through reverse phosphorolysis by maltose phosphorylase. *FEBS J.* 2009. 276: 7353-7365.

Nakai, H., Nakai, N., Petersen, B.O., Westphal, Y., **Dilokpimol, A.**, Abou Hachem, M., Lahtinen, S.J., Duus, J.Ø., Schols, H.A., Svensson, B. Substrate recognition by two members of glycoside hydrolase family 32 involved in fructo-oligosaccharide metabolism in *Lactobacillus acidophilus* NCFM. *In preparation.*

Nakai, H., Baumann, M.J., Petersen, B.O., Westphal, Y., Abou Hachem, M., **Dilokpimol, A.**, Duus, J.Ø., Schols, H.A., Svensson, B. *Aspergillus nidulans*  $\alpha$ -galactosidase of glycoside hydrolase family 36 catalyses formation of  $\alpha$ -galacto-oligosaccharides by transglycosylation. *FEBS J.* Submitted.

Nakai, H., Abou Hachem, M., Petersen, B.O., Westphal, Y., Mannerstedt, K., Baumann, M.J., **Dilokpimol, A.**, Schols, H.A., Duus, J.Ø., Svensson, B. Efficient chemoenzymatic oligosaccharide synthesis by reverse phosphorolysis using cellobiose phosphorylase and cellodextrin phosphorylase from *Clostridium thermocellum*. *Biochimie.* Submitted.

Nakai, H., Petersen, B.O., Westphal, Y., **Dilokpimol, A.**, Abou Hachem, M., Duus, J.Ø., Schols, H.A., Svensson, B. Rational engineering of *Lactobacillus acidophilus* NCFM maltose phosphorylase into either trehalose or kojibiose dual specificity phosphorylase. *Protein Eng. Des. Sel.* *In preparation.*

#### Publications (with other projects)

Nielsen, M.M., Bozonnet, S., Seo, E.-S., Motyan, J.A., Andersen, J.M., **Dilokpimol, A.**, Abou Hachem, M., Gyemant, G., Næsted, H., Kandra, L., Sigurskjold, B.W., Svensson, B. Two secondary

carbohydrate binding sites on the surface of barley  $\alpha$ -amylase 1 have distinct functions and display synergy in hydrolysis of starch granules. *Biochemistry*. 2009. 48: 7686-7697.

Nielsen, M.M., Seo, E.-S., **Dilokpimol, A.**, Andersen, J.M., Abou Hachem, M., Naested, H., Willemoës, M., Bozonnet, S., Kandra, L., Gyémánt, G., Haser, R., Aghajari N., Svensson, B. Roles of multiple surface sites, long substrate binding clefts, and carbohydrate binding modules in the action of amylolytic enzymes on polysaccharide substrates. *Biocatal. Biotransform.* 2008. 26: 59-67.

Seo, E.-S., Nielsen, M.M., Andersen, J.M., Vester-Christensen, M.B., Jensen, J.M., Christiansen, C., **Dilokpimol, A.**, Abou Hachem, M., Hägglund, P., Maeda, K., Finnie, C., Blennow, A., Svensson, B.  $\alpha$ -amylases. Interaction with polysaccharide substrates, proteinaceous inhibitors and regulatory proteins, in: H.-K. Park (Ed), *Carbohydrate-active enzymes: Structure, function and applications*, Woodhead Publishing Ltd., Cambridge, United Kingdom, 2008, pp 20-36.



# **Manuscript I**

**Enzymatic synthesis of  $\beta$ -xylosyl-oligosaccharides by transxylosylation using  
two  $\beta$ -xylosidases of glycoside hydrolase family 3  
from *Aspergillus nidulans* FGSC A4**

Adiphol Dilokpimol<sup>a</sup>, Hiroyuki Nakai<sup>a</sup>, Charlotte H. Gotfredsen<sup>b</sup>, Maaïke Appeldoorn<sup>c</sup>, Martin J. Baumann<sup>a</sup>, Natsuko Nakai<sup>a</sup>, Henk A. Schols<sup>c</sup>, Maher Abou Hachem<sup>a</sup>, Birte Svensson<sup>a\*</sup>

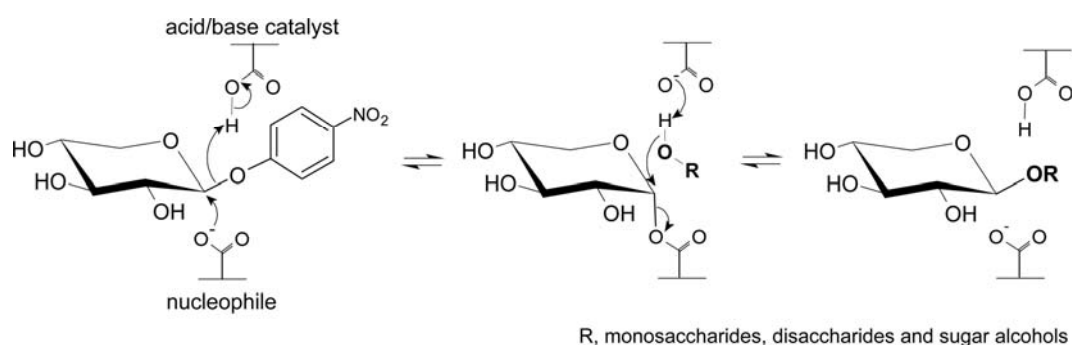
<sup>a</sup>Enzyme and Protein Chemistry, Department of Systems Biology, Technical University of Denmark, Søtofts Plads, Building 224, DK-2800 Kgs. Lyngby, Denmark

<sup>b</sup>Department of Chemistry, Technical University of Denmark, Kemitorvet, Building 201, DK-2800 Kgs. Lyngby, Denmark

<sup>c</sup>Laboratory of Food Chemistry, Wageningen University, Bomenweg 2, 6703 HD Wageningen, The Netherlands

**Graphical abstract**

Enzymatic synthesis of novel  $\beta$ -xylosyl-oligosaccharides catalysed by transglycosylation of two recombinant *Aspergillus nidulans* FGSC A4  $\beta$ -xylosidases of glycoside hydrolase family 3.



# Enzymatic synthesis of $\beta$ -xylosyl-oligosaccharides by transxylosylation using two $\beta$ -xylosidases of glycoside hydrolase family 3 from *Aspergillus nidulans* FGSC A4

Adiphol Dilokpimol<sup>a</sup>, Hiroyuki Nakai<sup>a</sup>, Charlotte H. Gotfredsen<sup>b</sup>, Maaike Appeldoorn<sup>c</sup>, Martin J. Baumann<sup>a</sup>, Natsuko Nakai<sup>a</sup>, Henk A. Schols<sup>c</sup>, Maher Abou Hachem<sup>a</sup>, Birte Svensson<sup>a\*</sup>

<sup>a</sup>Enzyme and Protein Chemistry, Department of Systems Biology, Technical University of Denmark, Søltofts Plads, Building 224, DK-2800 Kgs. Lyngby, Denmark

<sup>b</sup>Department of Chemistry, Technical University of Denmark, Kemitorvet, Building 201, DK-2800 Kgs. Lyngby, Denmark

<sup>c</sup>Laboratory of Food Chemistry, Wageningen University, Bomenweg 2, 6703 HD Wageningen, The Netherlands

\*Corresponding author. Tel.: +45 4525 2740; fax: +45 4588 6307 *E-mail address*: bis@bio.dtu.dk (B. Svensson).

## Abstract

Two  $\beta$ -xylosidases of glycoside hydrolase family 3 (GH 3) from *Aspergillus nidulans* FGSC A4, BxlA and BxlB were produced recombinantly in *Pichia pastoris* and secreted to the culture supernatants in yields of 16 and 118 mg/L, respectively. BxlA showed about 6 fold higher catalytic efficiency ( $k_{cat}/K_m$ ) than BxlB towards *para*-nitrophenyl  $\beta$ -D-xylopyranoside (*p*NPX) and  $\beta$ -1,4-xylo-oligosaccharides (degree of polymerisation 2–6). For both enzymes  $k_{cat}/K_m$  decreased with increasing  $\beta$ -1,4-xylo-oligosaccharide chain length. Using *p*NPX as donor with 9 monosaccharides, 7 disaccharides, and two sugar alcohols as acceptors 18 different  $\beta$ -xylosyl-oligosaccharides were synthesised in 2–36% (BxlA) and 6–66% (BxlB) yields by transxylosylation. BxlA utilised the monosaccharides D-mannose, D-lyxose, D-talose, D-xylose, D-arabinose, L-fucose, D-glucose, D-galactose, and D-fructose as acceptors, whereas BxlB used the same except for D-lyxose, D-arabinose, and L-fucose. BxlB transxylosylated the disaccharides xylobiose, lactulose, sucrose, lactose, and turanose in up to 35% yield, while BxlA gave inferior yields. The regioselectivity was acceptor dependent and primarily involved  $\beta$ -1,4 or 1,6 product linkage formation although minor products with different linkages were also obtained. Five of the 18 transxylosylation products obtained from D-lyxose, D-galactose, turanose and sucrose (two products) as acceptors were novel xylosyl-oligosaccharides,  $\beta$ -D-Xylp-(1 $\rightarrow$ 4)-D-Lyxp,  $\beta$ -D-Xylp-(1 $\rightarrow$ 6)-D-Galp,  $\beta$ -D-Xylp-(1 $\rightarrow$ 4)- $\alpha$ -D-Glcp-(1 $\rightarrow$ 3)- $\beta$ -D-Fruf,  $\beta$ -D-Xylp-(1 $\rightarrow$ 4)- $\alpha$ -D-Glcp-(1 $\rightarrow$ 2)- $\beta$ -D-Fruf, and  $\beta$ -D-Xylp-(1 $\rightarrow$ 6)- $\beta$ -D-Fruf-(2 $\rightarrow$ 1)- $\alpha$ -D-Glcp, as structure-determined by 2D NMR, indicating that GH3  $\beta$ -xylosidases are able to transxylosylate a larger variety of carbohydrate acceptors than earlier reported. Furthermore, transxylosylation of certain acceptors resulted in mixtures of products of which the individual structures have not been determined. Some of these products are also novel.

**Keywords:** Glycoside hydrolase family 3; Transglycosylation;  $\beta$ -Xylosyl-oligosaccharides;  $\beta$ -Xylosidase; Regioselectivity; NMR.

**Abbreviations:** BxlA and BxlB, *Aspergillus nidulans* FGSC A4 GH3  $\beta$ -xylosidases, encoded by *bxlA* (GenBank EAA64470.1) and *bxlB* (GenBank EAA67023.1); DP, degree of polymerisation; ESI-MS, electrospray ionization mass spectrometry; GH, glycoside hydrolase family; HPAEC-PAD, high performance anion exchange chromatography with pulsed amperometric detection; HPLC, high performance liquid chromatography; IMAC, immobilized metal ion affinity chromatography; NMR, nuclear magnetic resonance spectroscopy; NMWL, nominal molecular weight limit; NOE, nuclear Overhauser effect; *p*NP, *para*-nitrophenol; *p*NPA, *para*-nitrophenyl  $\alpha$ -L-arabinofuranoside; *p*NPX, *para*-nitrophenyl  $\beta$ -D-xylopyranoside; X2, xylobiose; X3, xylotriose; X4, xylotetraose; X5, xylopentaose; X6, xylohexaose; XOS,  $\beta$ -xylo-oligosaccharides.

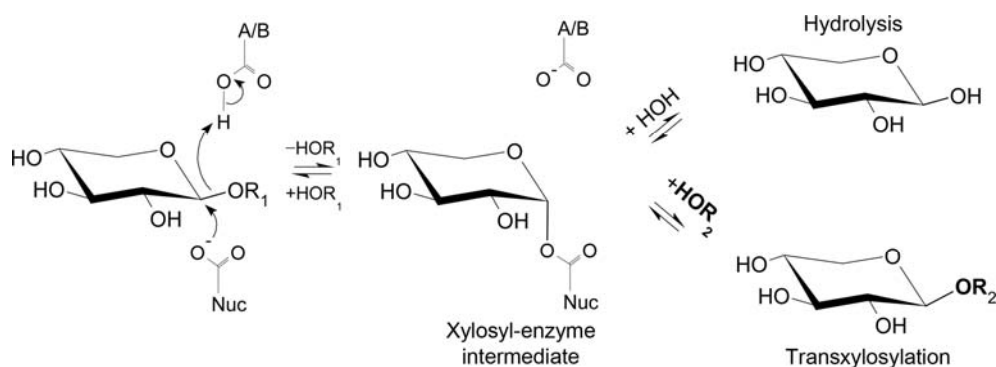
## 1. Introduction

$\beta$ -Xylo-oligosaccharides (often referred to as XOS) are oligomers of  $\beta$ -1,4 linked xylose which act as prebiotics and have important applications in the food industry as functional ingredients promoting growth of probiotic bacteria in the human gut.<sup>1-3</sup> XOS occur naturally in fruits and vegetables and are produced commercially by enzymatic and/or chemical hydrolysis of xylan for example from barley hulls, brewery spent grains, corn cobs, corn stover, rice hulls, wheat straw, and bamboo.<sup>2,3</sup> Most xylans are heteropolysaccharides containing different substituents such as (4-*O*-methyl)- $\alpha$ -D-glucuronopyranosyl,  $\alpha$ -L-arabinofuranosyl, acetyl, feruloyl and coumaroyl residues.<sup>2,3</sup> Complete degradation of xylans therefore requires a battery of glycoside hydrolases and esterases including endo- $\beta$ -1,4-xylanases (EC 3.2.1.8), exo- $\beta$ -1,4-xylosidases (EC 3.2.1.37),  $\alpha$ -glucuronosidases (EC 3.2.1.139),  $\alpha$ -L-arabinofuranosidases (EC 3.2.1.55), acetylxylan esterases (EC 3.1.1.72), ferulic acid esterases (EC 3.1.1.73), and *p*-coumaric acid esterases (EC 3.1.1.-).<sup>4-8</sup> Synergistic action of such xylanolytic enzymes accomplishes the degradation of xylan,<sup>5,8-10</sup> which is central *e.g.* in production of second generation biofuels from lignocellulosic biomass.<sup>8,9,11</sup>

The exo- $\beta$ -1,4-xylosidases ( $\beta$ -xylosidases) catalyse hydrolysis of  $\beta$ -xylo-oligosaccharides to release xylose from the non-reducing end and are classified into five glycoside hydrolase families GH3, 30, 39, 43 and 52, based on sequence similarity (<http://www.cazy.org>).<sup>8,9,12</sup> Except for GH43, these families use the double-displacement (retaining) mechanism where the substrate glycone part forms a covalent glycosyl-enzyme intermediate that is attacked by water in case of hydrolysis and by a carbohydrate leading to formation of a new glycosidic linkage in the case of transglycosylation (Fig. 1).<sup>13-15</sup> Retaining GH3  $\beta$ -xylosidases have been reported to use *para*-nitrophenyl  $\beta$ -D-xylopyranoside (*p*NPX) or  $\beta$ -xylo-oligosaccharides of degree of polymerisation (DP) 2 and 3 in transxylosylations resulting in *p*NP  $\beta$ -xylo-

oligosaccharides or longer  $\beta$ -xylo-oligosaccharides with mainly  $\beta$ -1,4 linkages.<sup>16-19</sup>  $\beta$ -1,6 linkages, however, were formed predominantly when using hexose-containing acceptors.<sup>20,21</sup> There are a few studies addressing GH3  $\beta$ -xylosidase transxylosylation with acceptors other than xylose or  $\beta$ -xylo-oligosaccharide, *i.e.*, different monosaccharides,<sup>20</sup> disaccharides,<sup>20,21</sup> sugar alcohols,<sup>20,21</sup> aliphatic or aromatic alcohols,<sup>21-23</sup> and hydroquinones.<sup>24</sup> Although this seems to indicate a broad acceptor specificity, the transglycosylation capacity of GH3  $\beta$ -xylosidases was in fact previously only tested with a few carbohydrate (three mono- and five disaccharide) acceptors.<sup>20,21</sup> Indeed insight lags behind as in the diversity of acceptor preference of GH3  $\beta$ -xylosidases and this motivated the present screening of acceptor specificity.

GH3  $\beta$ -xylosidases are found in prokaryotes and eukaryotes, but have been purified and characterised mostly from fungi such as *Aspergillus* spp.<sup>13,20,25</sup> and *Hypocrea jecorina* (anamorph *Trichoderma reesei*);<sup>13,18,26</sup> some recombinant GH3  $\beta$ -xylosidases have been obtained previously.<sup>10,11,27-29</sup> Two GH3 *A. nidulans* FGSC A4  $\beta$ -xylosidases, Bx1A and Bx1B, has of 45% sequence identity of which hydrolytic activity and biochemical properties of native Bx1A (previously called XlnD; from *A. nidulans* CECT2544) were subjected to limited characterisation,<sup>25</sup> whereas Bx1B was not isolated. Bx1A and Bx1B were previously produced recombinantly, but characterised very superficially.<sup>27,30</sup> However, in the present work, Bx1A and Bx1B were efficiently produced in *Pichia pastoris* and using a large variety of acceptors, enzymatic synthesis was achieved of 18 hetero  $\beta$ -xylosyl-oligosaccharides having a  $\beta$ -xylosyl residue at the non-reducing end, which may be prebiotic candidates. The present comparative transxylosylation reveals that isozymes can vary considerably in transxylosylation capacity and acceptor preference, which has a direct impact on their potential as synthetic tools.



**Figure 1.** Schematic diagram of hydrolysis and transxylosylation reactions catalysed by GH3  $\beta$ -xylosidases. A/B, acid/base catalyst; Nuc, catalytic nucleophile; R<sub>1</sub>, R<sub>2</sub>, carbohydrate residues.

## 2. Results and discussion

### 2.1. Production and purification of recombinant BxlA and BxlB

*A. nidulans* FGSC A4 BxlA and BxlB were obtained as His-tag fusion proteins by secretory expression in *P. pastoris* in yields of 16 and 118 mg/L culture supernatant, respectively. BxlB was purified by immobilized metal ion affinity chromatography (IMAC) followed by gel filtration. BxlA, however, had to be purified by anion exchange chromatography and gel filtration due to its instability at pH 7.5 (see 2.2, Fig. 2B) used for IMAC purification. IMAC purification was tried at pH 5.5, but gave poor purification yield. In comparison approximately 0.5 mg/L native BxlA (called XlnD) was purified from an *A. nidulans* CECT2544 culture.<sup>25</sup>

The isoelectric point (pI) of BxlA and BxlB was 3.0 (Supplementary Fig. S1A), similar to pI = 3.4 of native BxlA purified from *A. nidulans* CECT2544.<sup>25</sup> BxlA and BxlB gave single bands in SDS-PAGE with apparent molecular masses of 110 and 106 kDa, respectively (Supplementary Fig. S1B). These are higher than the theoretical values of 86045.2 and 92402.0 Da, respectively. Endoglycosidase H treatment of BxlA and BxlB reduced the size to 86 and 92 kDa, respectively (Supplementary Fig. S1B) suggesting some of the 10 and 8 putative sites predicted in BxlA and BxlB

to be *N*-glycosylated, respectively. The total carbohydrate content was estimated to 18% and 29% (w/w) for BxlA and 10% and 17% for BxlB with mannose and glucose as standards, respectively. Such native BxlA secreted from *A. nidulans* CECT2544<sup>25</sup> was not glycosylated, the glycosylation of recombinant BxlA was expression host-related.<sup>31</sup> Gel filtration indicated that BxlA is a dimer of 220 kDa, similarly to native BxlA from *A. nidulans* CECT2544<sup>25</sup> and *A. awamori* GH3  $\beta$ -xylosidase,<sup>19</sup> and that BxlB is a monomer of 135 kDa, as previously found for a GH3  $\beta$ -xylosidase from *A. japonica*.<sup>32</sup>

### 2.2. Biochemical properties and substrate specificity

BxlA and BxlB hydrolysed *p*NPX with pH optimum of 5.0 and 5.2 (Fig. 2A) and were stable at pH 4.0–6.0 and 4.0–8.0, respectively (Fig. 2B). Maximum activity of BxlA was at 50°C and of BxlB was at 60°C (Fig. 2C) and both enzymes retained >95% activity after 5 h at up to 40°C and 55°C, respectively (Fig. 2D). Other GH3  $\beta$ -xylosidases show pH and temperature optima in the ranges of pH 4–6 and 50–70°C.<sup>13,18,20,25,26</sup> BxlB displayed broader pH and temperature stabilities than BxlA. pH and temperature stabilities of GH3  $\beta$ -xylosidases from *A. nidulans* CECT2544<sup>25</sup> and *A. awamori*<sup>20</sup> were similar to BxlA, thus glycosylation of BxlA by *P. pastoris* did not confer extra stability.

*p*NPX and xylobiose were the best substrates for BxlA and BxlB (Table 1). The  $k_{\text{cat}}/K_{\text{m}}$  values gradually decreased with the size of  $\beta$ -1,4-xylo-oligosaccharides (DP 3–6). Activity ( $k_{\text{cat}}/K_{\text{m}}$ ) towards *para*-nitrophenyl  $\alpha$ -L-arabinofuranoside (*p*NPA) was essentially the same for BxlA and BxlB and was 100 and 13 fold lower than the activity of these two enzymes towards *p*NPX. *H. jecorina*<sup>18</sup> and *Hordeum vulgare*<sup>34</sup> GH3  $\beta$ -xylosidases also showed low activity towards *p*NPA.  $\beta$ -D-Xylopyranose preferably adopts a pyranose ring conformation having equatorial hydroxyl groups, which resemble the conformation of  $\alpha$ -L-arabinofuranose (Fig. 3).<sup>35</sup> The structural similarity of the energetically favourable conformations may explain the  $\alpha$ -L-arabinofuranosidase side-activity displayed by  $\beta$ -xylosidases.

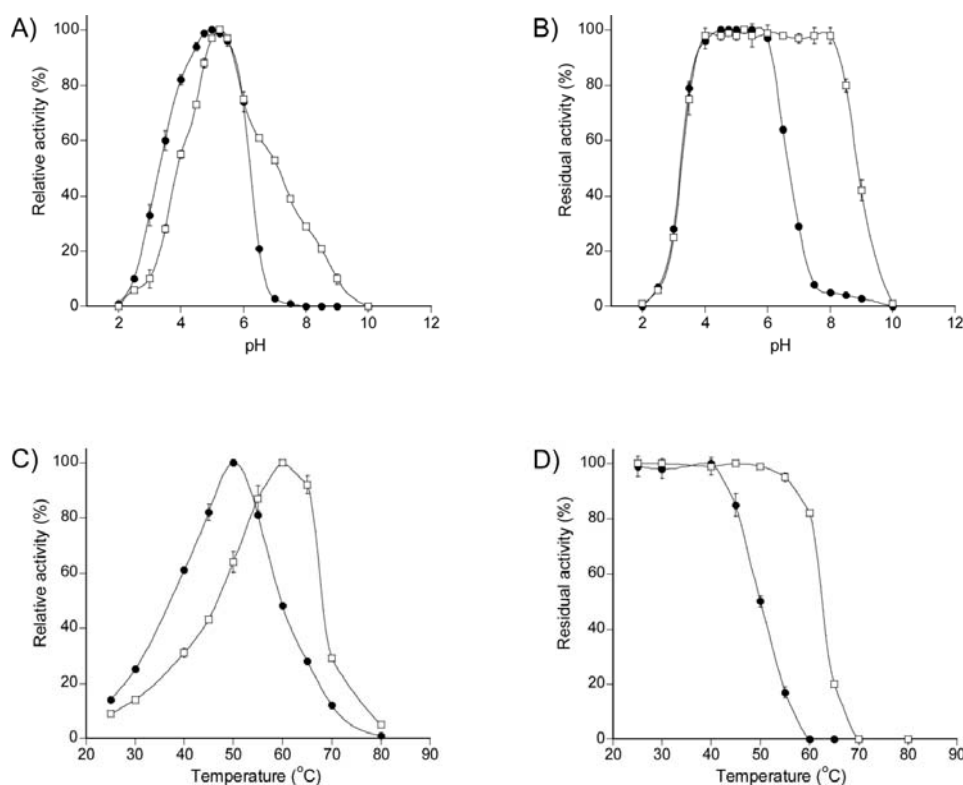
BxlA produced by *P. pastoris* had three fold higher  $k_{\text{cat}}$  (112 s<sup>-1</sup>) towards *p*NPX (Table 1) but the same  $K_{\text{m}}$  (1.3 mM) as native BxlA purified from *A. nidulans* CECT2544,<sup>25</sup> while BxlB had the same  $K_{\text{m}}$ , but 6 fold lower  $k_{\text{cat}}$  (18 s<sup>-1</sup>; Table 1). These values are comparable to those of GH3  $\beta$ -xylosidases from *A. awamori*,<sup>19,33</sup> *H. jecorina*<sup>18</sup> and *H. vulgare*,<sup>34</sup> which have  $K_{\text{m}}$  and  $k_{\text{cat}}$  for *p*NPX ranging from 0.23 to 4.1 mM and from 11 to 176 s<sup>-1</sup>, respectively. BxlA showed 5–7 fold higher  $k_{\text{cat}}/K_{\text{m}}$  towards  $\beta$ -xylo-oligosaccharides than BxlB (Table 1). The shared preference for shorter xylooligosaccharides of BxlA and BxlB is in accordance with other GH3  $\beta$ -xylosidases.<sup>9,11,18</sup>

### 2.3. Transxylosylation catalysed by BxlA and BxlB

The transxylosylation ability was investigated using *p*NPX as donor with 10 monosaccharides, six disaccharides, and two sugar alcohols as acceptor candidates for BxlA, and 12 monosaccharides and 13 disaccharides in case of BxlB (Table 2). The progress of transxylosylation was monitored over 5 h (Fig. 4). Mostly more than one product was detected by HPAEC-PAD (not shown). Total product yields (products/donor mM/mM) were

calculated for each acceptor based on the sum of all oligosaccharide products. As monitored here, the reaction yields in most cases showed a maximum after which they decreased. The obtained maximum yields are listed in Table 2. Noticeably, the extent of product decrease differed for the individual acceptors (Fig. 4A–F), reflecting variation in hydrolysis of transxylosylation products or their participation as acceptors in subsequent transxylosylations or both. From these two possibilities, hydrolysis is the most probable, as activities are lower on longer substrates as judged from catalytic efficiencies on xylooligosaccharides (Table 1), and transxylosylation yields are lower on disaccharides compared to monosaccharides (Table 2). Noticeably, transxylosylation products of D-galactose (for both BxlA and BxlB; Fig. 4B,E), D-fructose (for BxlB; Fig. 4E), sorbitol (for BxlA; Fig. 4A) and lactose (for BxlB; Fig. 4F) remained at the maximum level without subsequent decline suggesting a much slower hydrolysis rate than of products formed with other acceptors.

BxlA and BxlB both possess broad acceptor specificity (Table 2). For BxlA the highest yield was with xylitol (36%), while D-mannose, D-lyxose and D-talose were transxylosylated with a similar maximum yield compared to as D-xylose (>20%). Transxylosylation of D-arabinose, L-fucose, D-glucose, D-galactose and D-fructose was less efficient and L-rhamnose seemed not to act as acceptor (Table 2). Among 12 monosaccharides, BxlB preferred D-mannose, D-xylose, D-glucose and D-talose as acceptors as judged by high product yields (43–66%), while yields with D-galactose and D-fructose were only 16%. Transxylosylation yields for BxlB were in general higher than for BxlA. Noticeably except for D-xylose, BxlB did not accommodate pentoses (D-arabinose, L-arabinose, D-lyxose, L-lyxose). Also the deoxy sugars L-fucose and L-rhamnose were not acceptors for BxlB. BxlA in contrast used arabinose, lyxose and L-fucose as acceptors. BxlB efficiently transxylosylated lactulose, sucrose and turanose, and gave lower yields with lactose and xylobiose (Table 2), whereas disaccharides were poor acceptors for BxlA (Table 2, Fig. 4C).



**Figure 2.** Effect of pH and temperature on activity and stability of BxlA and BxlB. A) pH-dependence for activity towards 2 mM *p*NPX by 71 nM BxlA (●) and 179 nM BxlB (□) in 40 mM Britton-Robinson buffer. B) pH-stability of 355 nM BxlA (●) and 895 nM BxlB (□) in 40 mM Britton-Robinson buffer after 5 h incubation at 40°C. C) Temperature-activity dependence for 71 nM BxlA (●) and 179 nM BxlB (□) at 25–80°C with 10 min reaction time. D) Thermal stability of 355 nM BxlA (●) and 895 nM BxlB (□) incubated 5 h at 25–80°C in 50 mM sodium acetate pH 5.0. Each experiment was made in triplicate. Standard deviations are shown as error bars.

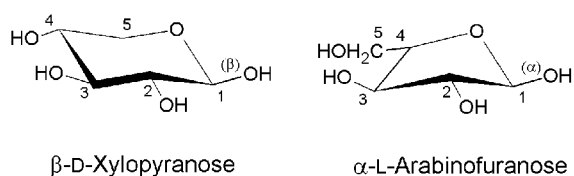
**Table 1.** Kinetic parameters of BxlA and BxlB for hydrolysis of  $\beta$ -xylo-oligosaccharides, *p*NPX and *p*NPA.

Substrate	BxlA			BxlB		
	$k_{cat}$ $s^{-1}$	$K_m$ mM	$k_{cat}/K_m$ $s^{-1}\cdot mM^{-1}$	$k_{cat}$ $s^{-1}$	$K_m$ mM	$k_{cat}/K_m$ $s^{-1}\cdot mM^{-1}$
Xylobiose	$139 \pm 7.8$	$2.0 \pm 0.07$	70	$36 \pm 0.7$	$2.5 \pm 0.40$	14
Xylotriose	$122 \pm 7.8$	$2.1 \pm 0.14$	58	$28 \pm 0.1$	$3.0 \pm 0.06$	9
Xylo-tetraose	$104 \pm 1.1$	$2.5 \pm 0.11$	42	$25 \pm 0.2$	$3.2 \pm 0.15$	8
Xylopentaose	$93 \pm 4.7$	$2.8 \pm 0.15$	33	$23 \pm 0.2$	$4.3 \pm 0.15$	5
Xylohexaose	$65 \pm 1.5$	$3.0 \pm 0.14$	22	$22 \pm 0.5$	$5.2 \pm 0.58$	4
<i>p</i> NPX	$112 \pm 1.3$	$1.3 \pm 0.16$	90	$18 \pm 0.4$	$1.3 \pm 0.11$	14
<i>p</i> NPA	–	–	0.9	–	–	1.1

<sup>a</sup> BxlA secreted from *A. nidulans* CECT2544 gave  $k_{cat} = 37 s^{-1}$  and  $K_m = 1.1 mM^{25}$

<sup>b</sup> Low affinity precludes determination of  $K_m$  and  $k_{cat}$

Standard deviations are calculated from triplicate experiments.



**Figure 3.** Preferred conformational structures of  $\beta$ -D-xylopyranose and  $\alpha$ -L-arabinofuranose.

**Table 2.** Maximum transxylosylation yields with different acceptors

Acceptor	Total yield (%)		Acceptor	Total yield (%)	
	BxlA	BxlB		BxlA	BxlB
<u>Monosaccharides</u>			<u>Disaccharides</u>		
D-Xylose	<b>21<sup>b</sup></b>	<b>64<sup>b</sup></b>	Xylobiose	–	6
D-Arabinose	<b>17<sup>b</sup></b>	n.d.	Maltose	2	n.d.
L-Arabinose	–	n.d.	Sucrose	<b>6<sup>c</sup></b>	<b>33<sup>c</sup></b>
D-Lyxose	<b>23<sup>c</sup></b>	n.d.	Lactose	n.d.	<b>9<sup>d</sup></b>
L-Lyxose	–	n.d.	Cellobiose	2	n.d.
L-Fucose	<b>14<sup>d</sup></b>	n.d.	Turanose	<b>7<sup>c</sup></b>	<b>30<sup>c</sup></b>
L-Rhamnose	n.d.	n.d.	Lactulose	3	<b>35<sup>d</sup></b>
D-Glucose	<b>10<sup>b</sup></b>	<b>50<sup>b</sup></b>	Isomaltose	–	n.d.
D-Galactose	9	<b>16<sup>c</sup></b>	Trehalose	–	n.d.
D-Mannose	<b>25<sup>b</sup></b>	<b>66<sup>b</sup></b>	Palatinose	–	n.d.
D-Talose	<b>22<sup>d</sup></b>	<b>43<sup>d</sup></b>	Melibiose	–	n.d.
D-Fructose	8	<b>16</b>	Sorbose	–	n.d.
Xylitol <sup>a</sup>	36	–	Gentibiose	–	n.d.
Sorbitol <sup>a</sup>	20	–			

<sup>a</sup> sugar alcohol; <sup>b</sup> known compound (structure-confirmed, see Supplementary Table S1); <sup>c</sup> novel compound (structure-determined, see Table 3 and Fig. 5); <sup>d</sup> novel compound (not structure-determined, due to complex reaction mixture). Products were quantified by HPAEC-PAD using xylobiose and xylotriose as standards for di- and trisaccharides, respectively. The total yield was estimated including all products and calculated as a percentage of products/donor concentration; n.d., not detected; –, product was not tested. Products in bold were purified for structural analysis and showed no difference in structure from BxlA and BxlB.

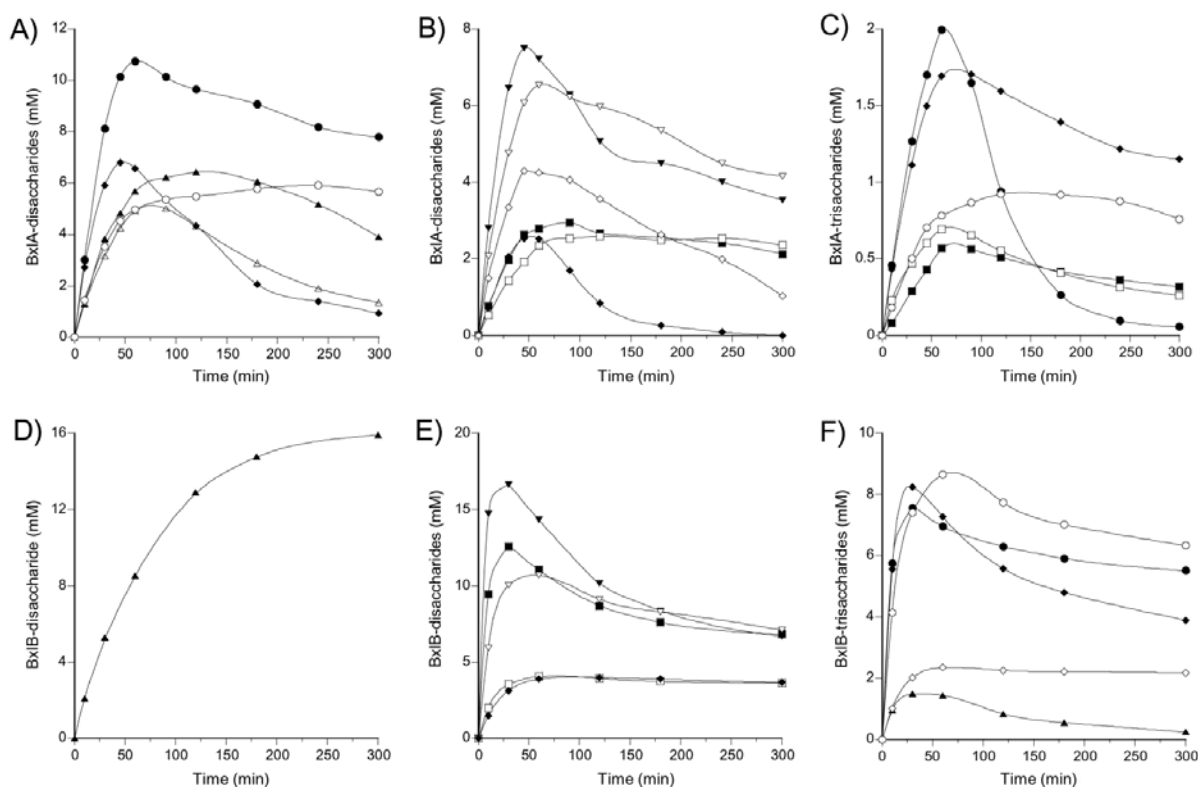
In total BxlA and BxlB formed 14 and 11  $\beta$ -xylosyl oligosaccharides from 18 and 25 acceptor candidates, respectively. The new oligosaccharides were prepared at the maximum production conditions (Fig. 4) for structure determination by NMR. Five such structure-determined oligosaccharides, which were obtained with D-lyxose, D-galactose, sucrose (two different products) and turanose as acceptors, were not reported before. BxlA and BxlB displayed different transglycosylation capacity with respect to both yield and preferred acceptors. In comparison, a homologous GH3  $\beta$ -xylosidase from *A. awamori*<sup>20,21</sup> (having 65% sequence identity with BxlA and 46% with BxlB) showed different acceptor preference and transglycosylation yield, except for that all three enzymes transxylosylate D-mannose with highest yield. The variations among related enzymes emphasise the importance of screening many

different acceptor candidates to evaluate the transxylosylation capacity.

#### 2.4. Structure determination of novel $\beta$ -transxylosylation oligosaccharide products

Generally BxlA and BxlB formed more than one transxylosylation product with a given acceptor as reported also for other enzymatic transxylosylations.<sup>20,21,36,37</sup> This product heterogeneity, as observed on the NMR chemical shifts (data not shown), reflects variation in regioselectivity due to several acceptor binding modes and possibly reaction with different forms (*e.g.*  $\alpha$ ,  $\beta$ , pyranosyl and furanosyl forms) of an acceptor. Such product mixtures complicate structural analysis and hamper NMR based assignments, thus precluding identification of some of the obtained products.



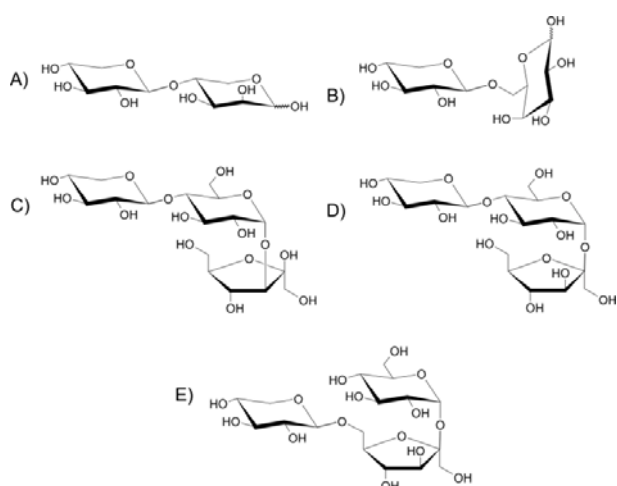


**Figure 4.** Progress of di- and trisaccharide formation by transxylosylation with *pNPX* as donor and different acceptors as catalysed by BxlA (A–C) and BxlB (D–F). A) D-Xylose (▲), D-arabinose, (△), D-lyxose (◆), xylitol (●) and sorbitol (○). B) D-Glucose (■), D-galactose (□), D-mannose (▼), D-talose (▽), D-fructose (◆) and L-fucose (◇). C) Maltose (■), sucrose (◆), cellobiose (□), turanose (●) and lactulose (○). D) D-Xylose (▲). E) D-Glucose (■), D-galactose (□), D-mannose (▼), D-talose (▽) and D-fructose (◆). F) Xylobiose (▲), sucrose (◆), lactose (◇), turanose (●) and lactulose (○). Product concentrations were calculated from peak areas of HPAEC-PAD chromatograms using xylobiose and xylotriose as standards for di- and trisaccharides, respectively (see 3.6 for details).

Oligosaccharides were purified by HPLC from BxlA- (9) and BxlB- (11) reaction mixtures (Table 2) and subjected to structure determination by 2D NMR and ESI-MS. The molecular mass of each product was in agreement with the calculated molecular mass of the  $\text{Li}^+$  adduct of the corresponding acceptor conjugate of D-xylose (Table 3) and also supported the presence of product mixtures. Linkage analysis by NMR was based on chemical shifts of the products using 2D NMR (Table 3 and Supplementary Table S1) and showed that both BxlA and BxlB produced mainly  $\beta$ -1,4 linked products with D-xylose, D-lyxose and D-arabinose as acceptors as identified by long range proton-carbon bond correlations between the non-reducing anomeric proton and C-4 of the substituted position and confirmed by inter-residue nuclear Overhauser effect (NOE) correlations. This

corresponds to mainly  $\beta$ -1,4 regioselective formation of *pNP*  $\beta$ -xylo-oligosaccharides and  $\beta$ -xylo-oligosaccharides reported for GH3  $\beta$ -xylosidases from *A. awamori*,<sup>19</sup> *A. niger*,<sup>36</sup> *H. jecorina*<sup>18</sup> and *Penicillium wortmanni*,<sup>37</sup> although small amounts of products with different linkages were also found. In contrast transxylosylation of D-mannose, D-glucose and D-galactose occurred with predominant  $\beta$ -1,6 regioselectivity, as identified by the downfield shift of the C6 or by inter NOE correlation across the glycosidic bond. Obviously these monosaccharides are accommodated at subsite +1 of the active site in a different way possibly due to specific protein-carbohydrate interactions rendering the primary alcohol group (6-OH) best positioned to perform a nucleophilic attack on the covalent xylosyl-enzyme intermediate. Preference

for the primary alcohol group in hexose-containing acceptors was also reported for  $\beta$ -xylosidase from *A. awamori*.<sup>20,21</sup> In case of disaccharide acceptors,  $\beta$ -1,4 or  $\beta$ -1,6 xylosyl linkage was formed with either of the disaccharide moieties reflecting variation in binding mode indicative of rather loose acceptor recognition at subsite +1 in BxlA and BxlB. Noticeably five novel oligosaccharides were generated with D-lyxose, D-galactose, turanose and sucrose (two products) as acceptors:  $\beta$ -D-xylopyranosyl-(1 $\rightarrow$ 4)-D-lyxopyranoside;  $\beta$ -D-xylopyranosyl-(1 $\rightarrow$ 6)-D-galactopyranoside;  $\beta$ -D-xylopyranosyl-(1 $\rightarrow$ 4)- $\alpha$ -D-glucopyranosyl-(1 $\rightarrow$ 3)- $\beta$ -D-fructofuranoside;  $\beta$ -D-xylopyranosyl-(1 $\rightarrow$ 4)- $\alpha$ -D-glucopyranosyl-(1 $\rightarrow$ 2)- $\beta$ -D-fructofuranoside; and  $\beta$ -D-xylopyranosyl-(1 $\rightarrow$ 6)- $\beta$ -D-fructofuranosyl-(2 $\rightarrow$ 1)- $\alpha$ -D-glucopyranoside as identified by 2D NMR (Table 3; Fig. 5). In contrast, structures of the transxylosylation products obtained with the other novel acceptors L-fucose, D-talose, lactose and lactulose were not solved due to the formation of product mixtures, which could not be separated and purified in sufficient amounts enabling an NMR analysis. ESI-MS, however, identified that these products, as expected, were Li-adducts of di- and trisaccharides with molecular masses of  $m/z$  303, 319, 481 and 481, respectively.



**Figure 5** Structures determined by 2D-NMR of five novel  $\beta$ -xylosyl-oligosaccharides produced by transxylosylation using BxlA or BxlB. A)  $\beta$ -D-Xylp-(1 $\rightarrow$ 4)-D-Lyxp; B)  $\beta$ -D-Xylp-(1 $\rightarrow$ 6)-D-Galp; C)  $\beta$ -D-Xylp-(1 $\rightarrow$ 4)- $\alpha$ -D-Glcp-(1 $\rightarrow$ 3)- $\alpha$ -D-Fruf; D)  $\beta$ -D-Xylp-(1 $\rightarrow$ 4)- $\alpha$ -D-Glcp-(1 $\rightarrow$ 2)- $\beta$ -D-Fruf; E)  $\beta$ -D-Xylp-(1 $\rightarrow$ 6)- $\beta$ -D-Fruf-(2 $\rightarrow$ 1)- $\alpha$ -D-Glcp.

## 2.5. Conclusion

GH3  $\beta$ -xylosidases BxlA and BxlB from *A. nidulans* FGSC A4 showed remarkably different hydrolytic and transglycosylation activities. Whereas BxlA had about 6 fold higher catalytic efficiency than BxlB in hydrolysis of *p*NPX and  $\beta$ -1,4-xylo-oligosaccharides, BxlB was more efficient in transxylosylation, the highest yield being 66% obtained with mannose. BxlA and BxlB showed broad acceptor specificity, however the results cannot be interpreted on the basis of a 3D structural model, since no GH3  $\beta$ -xylosidase structure has been solved and the other solved GH3 structures are too taxonomically distant to allow reliable modelling. All together BxlA or BxlB were found to form  $\beta$ -xylosyl-oligosaccharides with 18 different acceptors and five not previously described oligosaccharides were identified. Although some of the transxylosylation reactions resulted in several products reflecting multiple acceptor accommodation modes, some of these products are also novel and together with the five novel  $\beta$ -xylosyl oligosaccharides represent new candidates for evaluation as prebiotics.

## 3. Experimental

### 3.1. Materials

*p*NP, *p*NPX, *p*NPA, D-arabinose, L-arabinose, D-lyxose, L-lyxose, L-fucose, L-rhamnose, D-galactose, D-mannose, D-talose, D-fructose, xylitol, sorbitol, maltose, sucrose, lactose, cellobiose, turanose, lactulose, isomaltose, trehalose, palatinose, melibiose, sophorose, and gentibiose were purchased from Sigma Aldrich (St. Louis, MO). D-Xylose was from Carl Roth (Karlsruhe, Germany). D-Glucose was from Merck (Darmstadt, Germany). Xylobiose, xylotriose, xylo-tetraose, xylopentaose, and xylohexaose were purchased from Megazyme (Wicklow, Ireland).

**Table 3.** <sup>1</sup>H and <sup>13</sup>C NMR spectra assignment and ESI-MS *m/z* values of novel β-xylosyl-oligosaccharides produced by transxylosylation with *p*NPX as donor and suitable acceptors.

Compound (molecular mass) <sup>a</sup>	Chemical shifts (δ, p.p.m.)					
	H-1 C-1	H-2 C-2	H-3 C-3	H-4 C-4	H-5a/H-5b C-5	H-6a/H-6b C-6
β-D-Xylp-(1,4)-	4.47 103.6	3.26 73.7	3.42 76.6	3.60 70.2	3.30/3.94 66.1 <sup>b</sup>	
α-D-Lyxp	4.95 94.9	3.74 70.8	4.03 ~70.2	3.91 77.0	3.80/3.88 62.4	
β-D-Lyxp ( <i>m/z</i> 289)	4.88 95.2	3.92 n.d.	n.d. n.d.	n.d. n.d.	n.d. n.d.	
β-D-Xylp-(1,6)-	4.42 104.4	3.25 74.1	3.40 76.6	3.58 n.d.	3.28/3.92 66.1 <sup>b</sup>	
α-D-Galp	5.22 93.3	3.76 n.d.	3.81 n.d.	3.95 n.d.	n.d. n.d.	n.d. n.d.
β-D-Galp ( <i>m/z</i> 319)	4.54 97.4	3.44 n.d.	3.60 n.d.	3.88 n.d.	3.85 n.d.	3.78/3.95 70.3
β-D-Xylp-(1,4)-	4.43 102.1	3.33 73.6	3.42 70.2	3.63 70.1	3.93/3.26 66.1 <sup>b</sup>	
α-D-Glcp-(1,3)-	5.31 101.5	3.56 73.0	3.72 73.7	3.40 76.5	3.71 73.7	3.83/3.77 61.4
β-D-Fruf ( <i>m/z</i> 481)	3.48/3.73 64.7	– n.d.	3.97 77.0	4.16 70.2	4.12 70.2	3.84/3.97 61.8
β-D-Xylp-(1,4)-	4.41 104.2	3.27 74.0	3.41 76.6	3.61 70.1	3.96/3.28 66.1 <sup>b</sup>	
α-D-Glcp-(1,2)-	5.37 92.9	3.55 71.9	3.81 71.9	3.62 78.8	3.93 72.1	3.82/3.88 60.3
β-D-Fruf ( <i>m/z</i> 289)	3.66/3.59 62.1	– 104.6	4.18 77.3	3.99 74.9	3.85 82.2	3.75/3.80 63.4
β-D-Xylp-(1,6)-	4.47 104.3	3.27 74.0	3.42 76.5	3.59 70.1	3.94/3.29 66.1 <sup>b</sup>	
β-D-Fruf <sup>2</sup> -(2,1)-	n.d. n.d.	– 104.9	4.18 77.0	4.03 75.4	4.02 81.0	3.95 n.d.
α-D-Glcp ( <i>m/z</i> 481)	5.37 93.2	3.52 72.0	3.73 n.d.	3.44 n.d.	3.81 n.d.	3.78/3.82 n.d.

<sup>a</sup> Molecular mass as Li<sup>+</sup> adduct (estimated mass + *m/z* 7) determined by ESI-MS shown in parenthesis; <sup>b</sup> Reference carbon shifts according to C5 ; n.d., not detected

### 3.2. Cloning of *bxlA* and *bxlB* encoding GH3 $\beta$ -xylosidases

*P. pastoris* X-33 (FGSC database accession no. 10077 and 10125; [www.fgsc.net](http://www.fgsc.net)) harbouring *A. nidulans* FGSC A4 full-length *bxlA* (GenBank ID: EAA64470.1) and *bxlB* (GenBank ID: EAA67023.1)<sup>30</sup> were purchased from Fungal Genetics Stock Center, School of Biological Sciences, University of Missouri, (Kansas City, MO). The two genes were recloned to encode mature polypeptides lacking Met1–Ser18 (BxlA) and Met1–Ser23 (BxlB) (<http://www.cbs.dtu.dk/services/SignalP/>).<sup>38</sup> Expand High Fidelity DNA polymerase (Roche Diagnostics GmbH, Mannheim, Germany) was used for DNA amplification with oligonucleotide primers (Supplementary Table S1) based on the genomic sequence.<sup>39</sup> A silent mutation (1374T→C) in the *bxlB* EcoRI site was introduced by overlap PCR<sup>40</sup> using appropriate primers (Supplementary Table S2). PCR products were digested for *bxlA* by XhoI and XbaI and for *bxlB* by EcoRI and NotI (New England BioLabs, Ipswich, MA) and cloned in frame with the  $\alpha$ -mating factor secretion signal in pPICZ $\alpha$ A (Invitrogen, Carlsbad, CA). The plasmids were transformed into *Escherichia coli* DH5 $\alpha$  (Invitrogen) and selected on low salt Luria Bertani medium supplemented with 25  $\mu$ g/mL Zeocin. Fully sequenced plasmids (Eurofins MWG Operon, Ebersberg, Germany) were linearised by PmeI (New England BioLabs), transformed into *P. pastoris* X-33 (Invitrogen) by electroporation (Micropulser; Bio-Rad Laboratories Inc, Hercules, CA), and selected at 30°C for 3 days on yeast peptone dextrose plates (1% yeast extract, 2% peptone, 2% dextrose) containing 1 M sorbitol and 100  $\mu$ g/mL Zeocin.

### 3.3. Production and purification of BxlA and BxlB

*P. pastoris* transformants were grown in 3 L (BxlA) or 4 L (BxlB) buffered glycerol-complex medium (1% yeast extract, 2% peptone, 100 mM potassium phosphate pH 6.0, 1.34% yeast nitrogen

base with ammonium sulfate,  $4 \times 10^{-5}$ % biotin, and 1% glycerol) at 30°C for 24 h to OD<sub>600</sub> of 25 (BxlA) and 52 (BxlB). Cells were harvested (3000g, 5 min, 4°C) and resuspended for induction in 1 L buffered minimal methanol medium (BxlA; 100 mM potassium phosphate pH 6.0, 1.34% yeast nitrogen base with ammonium sulfate,  $4 \times 10^{-5}$ % biotin, 1% methanol, 1% casamino acid) or in 1 L of buffered methanol-complex medium (BxlB; 0.5% methanol, 1% yeast extract, 2% peptone, 100 mM potassium phosphate pH 6.0, 1.34% yeast nitrogen base with ammonium sulfate,  $4 \times 10^{-5}$ % biotin) at 22°C for 72 (BxlA) and 120 h (BxlB). Methanol was supplemented every 24 h to a final concentration (v/v) of 1% (BxlA) and 0.5% (BxlB), until harvest (13,500g, 4°C, 1 h).

The BxlA culture supernatant was concentrated with buffer-exchange to 10 mM MES pH 6.0 (Pellicon tangential flow filtration systems, nominal molecular weight limit (NMWL) 10 kDa; Millipore, Billerica, MA) and applied to a 6 mL Resource Q column (GE Healthcare, Uppsala, Sweden) equilibrated in the same buffer. After wash with 37.5 mM NaCl in the same buffer, protein was eluted by a linear 37.5–325 mM NaCl gradient (flow rate: 2 mL/min). Fractions containing BxlA were pooled, concentrated (Amicon Ultra-15, NMWL 30 kDa, Millipore), and applied to a Hiload 26/60 Superdex 200 column (GE Healthcare) equilibrated with 20 mM MES, 0.25 M NaCl pH 6.0 (flow rate: 1 mL/min). BxlA-containing fractions were pooled, concentrated, and buffer-exchanged to 10 mM MES pH 6.0. The BxlB culture supernatant was adjusted to pH 7.5 by 1 M K<sub>2</sub>HPO<sub>4</sub>, filtered (0.22  $\mu$ m; TPP, Trasadingen, Switzerland) and applied to 5 mL HisTrap HP column (GE Healthcare) equilibrated with 20 mM HEPES, 0.5 M NaCl, 10 mM imidazole pH 7.5. Following wash with the above buffer containing 22 mM imidazole, BxlB was eluted by a linear 22–400 mM imidazole gradient (flow rate: 1.0 mL/min). BxlB-containing fractions were pooled, concentrated (Centriprep YM30, Millipore), and applied to a Hiload 26/60 Superdex 200 column (GE Healthcare) equilibrated with 20 mM MES, 0.15 M NaCl pH 6.8 (flow rate: 0.5 mL/min). Fractions containing BxlB were

pooled, concentrated, and buffer exchanged to 20 mM HEPES pH 7.0. All purification steps were performed using an ÄKTAexplorer chromatograph (GE Healthcare) at 4°C.

### 3.4. Properties of BxlA and BxlB

Protein concentration was determined spectrophotometrically at 280 nm using  $E^{0.1\%} = 1.79$  and 0.97 for BxlA and BxlB, respectively, determined by aid of amino acid analysis. Molecular masses were estimated by SDS-PAGE (NuPAGE Novex Bis-Tris gels; Invitrogen) and gel filtration (precalibrated Hiload 16/60 Superdex 200 column; flow rate: 1 mL/min; Gel Filtration Calibration Kits; GE Healthcare). Theoretical molecular masses were calculated using ExPASy-ProtParam tool (<http://www.expasy.ch/tools/protparam.html>).<sup>41</sup> *N*-glycosylation was predicted using NetNGlyc 1.0 Server (<http://www.cbs.dtu.dk/services/NetNGlyc/>).<sup>42</sup> Endoglycosidase H (New England BioLabs) deglycosylation of BxlA (7 µg) and BxlB (5 µg) was performed according to the manufacturer's protocol. Carbohydrate contents were determined on 400 µg enzyme using the phenol-sulfuric acid method<sup>43</sup> with either glucose or mannose as standard. Isoelectric focusing of 600 ng BxlA and 400 ng BxlB was carried out (Pharmacia PhastSystem; GE Healthcare) at pH 4.0–6.5 (4 cm polyacrylamide PhastGel IEF) using the low range pI (pH 2.5–6.5) calibration kit and PlusOne Silver Stain Kit, Protein (GE Healthcare).

### 3.5. Enzyme activity assays of BxlA and BxlB

*p*NPX (2 mM) was hydrolysed at 40°C for 10 min by BxlA (20–150 nM; 50 mM sodium acetate pH 5.0) or BxlB (25–250 nM; 50 mM sodium acetate pH 5.2) in 50 µL reaction mixtures. The reaction was stopped by 1 M Na<sub>2</sub>CO<sub>3</sub> (100 µL) and *p*NP was quantified spectrophotometrically at 410 nm using 0.05–0.5 mM *p*NP as standard. One unit was defined as the amount of enzyme liberating 1 µmol of *p*NP per min under the assay conditions.

pH activity optima of BxlA (71 nM) and BxlB (179 nM) were determined for the pH range 2.0–10.0 towards *p*NPX (2 mM) in 40 mM Britton-Robinson buffer.<sup>44</sup> Activity was determined in the temperature range of 25–80°C using the above BxlA and BxlB concentrations in 50 mM sodium acetate pH 5.0 and 5.2, respectively. The stability at 40°C in the range pH 2.0–10.0 (40 mM Britton-Robinson buffers) and at 25–80°C was deduced from residual activity towards *p*NPX of 355 nM BxlA and 895 nM BxlB after 5 h incubation.

Initial rates of hydrolysis at 8 concentrations of *p*NPX (0.1–8.0 mM), *p*NPA (0.2–2 mM), and β-xylo-oligosaccharides (X2–X6, 0.4–6.0 mM) were measured using 40 nM (for *p*NPX), 465 nM (for *p*NPA), 32 nM (for X2–X6) BxlA, and at 11 different concentrations of *p*NPX (0.1–8.0 mM), *p*NPA (0.1–8.0 mM), X2–X6 (1.0–8.0 mM) using 66 nM (for *p*NPX and X2–X6) and 328 nM (for *p*NPA) BxlB. Hydrolysis of X2–X6 was assayed in 50 mM sodium acetate pH 5.0 for BxlA and pH 5.2 for BxlB (100 µL reaction mixture) and stopped by addition of 2% *p*-bromoaniline and 4% thiourea in glacial acetic acid (500 µL) and incubated in the dark at 70°C for 10 min, followed by 60 min at 37°C and quantified from the absorbance at 520 nm using 0.25–5.0 mM xylose as standard.<sup>45,46</sup> Kinetic parameters,  $K_m$  and  $k_{cat}$ , were determined by fitting the Michaelis-Menten equation to initial rates using SigmaPlot v. 9.0.1 (Systat Software Inc. San Jose, CA). Due to poor affinity ( $K_m > 8$  mM),  $k_{cat}/K_m$  of *p*NPA was obtained from the slope of the plot of initial rate ( $v/[E]$ ) vs substrate concentration.

### 3.6. Transxylosylation by BxlA and BxlB

Transxylosylation with 1) 200 nM BxlA, 30 mM *p*NPX and 200 mM acceptor (D-xylose, D-arabinose, D-lyxose, L-fucose, L-rhamnose, D-glucose, D-galactose, D-mannose, D-talose, D-fructose, xylitol, sorbitol, maltose, sucrose, lactose, cellobiose, turanose, or lactulose) in 50 mM sodium acetate pH 5.0 (1 mL) or 2) 1.7 µM BxlB, 25 mM *p*NPX and 400 mM acceptor as above except for

sugar alcohols and including also (L-arabinose, L-lyxose, xylobiose, isomaltose, trehalose, palatinose, melibiose, sophorose, or gentibiose) in 40 mM sodium acetate pH 5.2 (1 mL) occurred at 40°C during 5 h. Aliquots (5  $\mu$ L for Bx1A; 10  $\mu$ L for Bx1B) were removed at time intervals and added to 100 mM NaOH (195  $\mu$ L for Bx1A) and 500 mM NaOH (90  $\mu$ L for Bx1B). The Bx1B samples were diluted to a suitable concentration level before analysis. Products were quantified based on peak areas in HPAEC-PAD (ICS-3000 IC system; Dionex Corporation, Sunnyvale, CA) equipped with CarboPac PA200 anion exchange column (3  $\times$  250 mm and 3  $\times$  50 mm guard column; Dionex) using a linear 0–75 mM sodium acetate gradient in 100 mM NaOH (35 min; 25°C; flow rate: 0.35 mL/min) calibrated with xylobiose and xylotriose for di- and trisaccharide products, respectively. Transxylosylation yields were calculated based on the *p*NPX concentration.

### 3.7. Xylosyl-oligosaccharide purification

For structural analysis of tranxylosylation products reactions in 50 mM sodium acetate pH 5.0 (1 mL) were performed as described in 3.6 with 1) Bx1A and D-xylose, D-arabinose, D-lyxose, L-fucose, D-glucose, D-mannose, D-talose, sucrose, or turanose and 2) Bx1B and D-xylose, D-glucose, D-galactose, D-mannose, D-talose, D-fructose, xylobiose, sucrose, lactose, turanose, or lactulose at 40°C for optimal reaction times (Fig. 4). Reactions were terminated by heat inactivation (95°C, 10 min) followed by centrifugation (18,000g, 4°C, 5 min), desalting (Amberlite MB-20; Fluka, Sigma Aldrich), and filtration (0.45  $\mu$ m nylon filter; Frientte Aps, Kenbel, Denmark). Oligosaccharides were purified by HPLC (UltiMate 3000 Standard LC system; Dionex) equipped with a TSKgel Amide-80 column (5  $\mu$ m, 4.6  $\times$  250 mm and 4.6  $\times$  10 mm guard column; TOSOH, Tokyo, Japan) and refractive index detector (RI-101; Showa Denko, Kanagawa, Japan) at 1 mL/min (for mobile phase composition and column temperature see Supplementary Table S3). The purity was assessed by thin layer

chromatography (TLC; aluminium-coated silica gel 60 F<sub>254</sub>, Merck) developed by acetonitrile/water (80:20, v/v), sprayed with orcinol/sulphuric acid/water/ethanol, (2:10:10:80, w/v/v/v) or with  $\alpha$ -naphthol/sulphuric acid/methanol (0.03:15:85, w/v/v) and tarred at 120°C.

### 3.8. Nuclear Magnetic Resonance spectroscopy

Purified oligosaccharide products (500  $\mu$ L, 1–2 mM) were vacuum dried (from Bx1A; Savant SVC100 SpeedVac Concentrator; Savant Instruments, Inc. Farmingdale, NY) or freeze dried (from Bx1B; CoolSafe –55°C; ScanLaf A/S, Lynge, Denmark) and dissolved in deuterium oxide. Structures were determined by <sup>1</sup>H- and <sup>13</sup>C-NMR analysis. The majority of the spectra were recorded on a Varian Unity Inova 500 MHz NMR spectrometer and a few on a Bruker Avance 800 MHz spectrometer. A series of 2D homo- and heteronuclear correlated DQF-COSY, NOESY, gHSQC, and gHMBC spectra were obtained using standard pulse sequences. The proton chemical shifts were referenced to the solvent  $\delta_H$  4.78 ppm and the carbon shifts were referenced according to C5 of xylose at 66.1 ppm.

### 3.9. Electrospray ionization mass spectrometry

ESI-MS was performed (LTQ XL ion trap MS; Thermo Scientific, San Jose, CA) on vacuum dried or lyophilised samples (see 3.8). Samples were dissolved in milliQ water (100  $\mu$ g/mL) and applied to a Thermo Accela UHPLC system equipped with a Hypercarb (100  $\times$  2.1 mm, 3  $\mu$ m) column (Thermo Scientific). Elution was performed with a gradient of deionized water/acetonitrile and 0.2% trifluoroacetic acid (0.4 mL/min; 70°C). MS detection was performed in the positive mode using a spray voltage of 4.5 kV and a capillary temperature of 260°C and auto-tuned on glucohexaose.<sup>47</sup>

## Acknowledgements

The authors wish to thank Anne Blicher for amino acid analysis, Yvonne Westphal for assisting with ESI-MS, Louise Enggaard Rasmussen for maintaining the *Pichia pastoris* transformant strains, and Jørn Dalgaard Mikkelsen and Anne Meyer for discussions on the enzymes. This study was supported by the Danish Strategic Research Council's Committee on Food and Health (FøSu, to the project 'Biological Production of Dietary Fibres and Prebiotics' no. 2101-06-0067), the Carlsberg Foundation, the Danish Research Council for Natural Sciences, and an H.C. Ørsted postdoctoral fellowship from DTU (M.J.B.). The spectra at 800 MHz were obtained on the Bruker Avance 800 spectrometer of the Danish Instrument Center for NMR Spectroscopy of Biological Macromolecules.

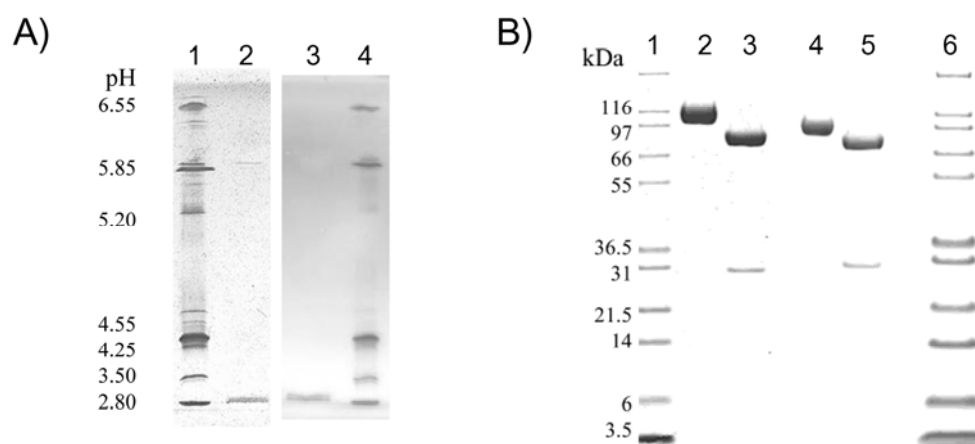
## References

1. Isolauri, E.; Kirjavainen, P. V.; Salminen, S. *Gut*, **2002**, *50*, 50–54.
2. Vázquez, M. J.; Alonso, J. L.; Domínguez, H.; Parajó, J.C. *Trends Food Sci. Technol.*, **2000**, *11*, 387–393.
3. Moure, A.; Gullón, P.; Domínguez, H.; Parajó, J.C. *Process Biochem.*, **2006**, *41*, 1913–1923.
4. Collins, T.; Gerday, C.; Feller, G. *FEMS Microbiol. Rev.*, **2005**, *29*, 3–23.
5. de Vries, R. P.; Visser, J. *Microbiol. Mol. Biol. Rev.*, **2001**, *65*, 497–522.
6. Ebringerova, A. *Macromol. Symp.*, **2006**, *232*, 1–12.
7. Beg, Q. K.; Kapoor, M.; Mahajan, L.; Hoondal, G. S. *Appl. Microbiol. Biot.*, **2001**, *56*, 326–338.
8. Pastor, F. I. J.; Gallardo, O.; Sanz-Aparicio, J.; Diaz, P. Xylanases: molecular properties and applications, C.5. In *Industrial Enzymes: Structure, Function and Applications*; Polaina, J., MacCabe, A.P., Eds; Springer: The Netherlands, 2007; pp. 65–82.
9. Biely, P. Xylanolytic enzymes. In *Handbook of Food Enzymology*; Whitaker, J. R., Voragen, A. G. J., Wong, D. W. S., Eds; Marcel Dekker Inc.: New York, 2003; pp. 879–916.
10. Margolles-Clark, E.; Tenkanen, M.; Nakari-Setälä, T.; Penttilä, M. *Appl. Environ. Microbiol.*, **1996**, *62*, 3840–3846.
11. Rasmussen, L. E.; Sørensen, H. R.; Vind, J.; Viksø-Nielsen, A. *Biotechnol. Bioeng.*, **2006**, *94*, 869–876.
12. Cantarel, B. L.; Coutinho, P. M.; Rancurel, C.; Bernard, T.; Lombard, V.; Henrissat, B. *Nucleic Acids Res.*, **2009**, *37*, D233–D238.
13. Knob, A.; Terrasan, C. R. F.; Carmona, E. C. *World J. Microbiol. Biotechnol.*, **2010**, *26*, 389–407.
14. Davies, G.; Henrissat, B. *Structure*, **1995**, *3*, 853–859.
15. Henrissat, B.; Davies, G. *Curr. Op. Struct. Biol.*, **1997**, *7*, 637–644.
16. Matsuo, M.; Yasui, T. *Agric. Biol. Chem.*, **1984**, *48*, 1853–1860.
17. Rodionova, N. A.; Tavobilov, I. M.; Bezborodov, A. M. *J. Appl. Biochem.*, **1983**, *5*, 300–312.
18. Herrmann, M. C.; Vrsanska, M.; Jurickova, M.; Hirsch, J.; Biely, P.; Kubicek, C. P. *Biochem. J.*, **1997**, *321*, 375–381.
19. Eneyskaya, E. V.; Brumer, H.; Backinowsky, L. V.; Ivanen, D. R.; Kulminskaya, A. A.; Shabalin, K. A.; Neustroev, K. N. *Carbohydr. Res.*, **2003**, *338*, 313–325.
20. Kurakake, M.; Osada, S.; Komaki, T. *Biosci. Biotech. Biochem.*, **1997**, *61*, 2010–2014.
21. Kurakake, M.; Fujii, T.; Yata, M.; Okazaki, T.; Komaki, T. *Biochim. Biophys. Acta*, **2005**, *1726*, 272–279.
22. Shinoyama, H.; Kamiyama, Y.; Yasui, T. *Agric. Biol. Chem.*, **1988**, *52*, 2197–2202.
23. Drouet, P.; Mu, Z.; Legoy, M. D. *Biotechnol. Bioeng.*, **1994**, *43*, 1075–1080.
24. Sulistyo, J.; Kamiyama, Y.; Ito, H.; Yasui, T. *Biosci. Biotechnol. Biochem.*, **1994**, *58*, 1311–1313.
25. Kumar, S.; Ramón, D. *FEMS Microbiol. Lett.*, **1996**, *135*, 287–293.
26. Poutanen, K.; Puls, J. *Appl. Microbiol. Biotechnol.*, **1988**, *28*, 425–432.
27. Pérez-González, J. A.; van Peij, N. N.; Bezoen, A.; MacCabe, A. P.; Ramón, D.; de Graaff, L. H. *Appl. Environ. Microbiol.*, **1998**, *64*, 1412–1419.
28. van Peij, N. N.; Brinkmann, J.; Vrsanská, M.; Visser, J.; de Graaff, L. H. *Eur. J. Biochem.*, **1997**, *245*, 164–173.
29. Selig, M. J.; Decker, S. R.; Knoshaug, E. P.; Baker, J. O.; Himmel, M. E.; Adney, W. S. *Appl. Biochem. Biotechnol.*, **2008**, *146*, 57–68.
30. Bauer, S.; Vasu, P.; Persson, S.; Mort, A. J.; Somerville, C. R. *PNAS*, **2006**, *130*, 11417–11422.
31. Daly, R.; Hearn, M. T. J. *Mol. Recognit.*, **2005**, *18*, 119–138.
32. Wakiyama, M.; Yoshihara, K.; Hayashi, S.; Ohta, K. *J. BioSci. Bioeng.*, **2008**, *106*, 398–404.
33. Eneyskaya, E. V.; Ivanen, D. R.; Bobrov, K. S.; Isaeva-Ivanova, L. S.; Shabalin, K. A.; Savell'ev, A. N.;

- Golubev, A. M.; Kulminskaya, A. A. *Arch. Biochem. Biophys.*, **2007**, *457*, 225–234.
34. Lee, R. C.; Hrmova, M.; Burton, R. A.; Lahnstein, J.; Fincher, G. B. *J. Biol. Chem.*, **2003**, *278*, 5377–5387.
35. Carpita, N.; McCann, M. Chapter 2: The cell wall. In *Biochemistry & Molecular Biology of Plants*; Buchanan, B., Gruissem, W., Jones, R., Eds; John Wiley & Sons, Ltd: United Kingdom, 2000; pp. 52–101.
36. Puchart, V.; Biely, P. *J. Biotechnol.*, **2007**, *128*, 576–586.
37. Win, M.; Kamiyama, Y.; Matsuo M.; Yasui, T. *Agric. Biol. Chem.*, **1988**, *52*, 1151–1158.
38. Emanuelsson, O.; Brunak, S.; von Heijne, G.; Nielsen, H. *Nat. Protoc.*, **2007**, *2*, 953–971.
39. Galagan, J. E.; Calvo, S. E.; Cuomo, C.; Ma, L. J.; Wortman, J. R.; Batzoglou, S.; Lee, S. I.; Bastuerkmen, M.; Spevak, C. C.; Clutterbuck, J.; Kapitonov, V.; Jurka, J.; Scazzocchio, C.; Farman, M. L.; Butler, J.; Purcell, S.; Harris, S.; Braus, G. H.; Draht, O.; Busch, S.; D'Enfert, C.; Bouchier, C.; Goldman, G. H.; Bell-Pedersen, D.; Griffiths-Jones, S.; Doonan, J. H.; Yu, J.; Vienken, K.; Pain, A.; Freitag, M.; Selker, E. U.; Archer, D. B.; Penalva, M. A.; Oakley, B. R.; Momany, M.; Tanaka, T.; Kumagai, T.; Asai, K.; Machida, M.; Nierman, W. C.; Denning, D. W.; Caddick, M. X.; Hynes, M.; Paoletti, M.; Fischer, R.; Miller, B. L.; Dyer, P. S.; Sachs, M. S.; Osmani, S. A.; Birren, B. W. *Nature*, **2005**, *438*, 1105–1115.
40. Sambrook, J.; Fritsch, E. F.; Maniatis, T. *Molecular Cloning: A Laboratory Manual*, 2nd ed; Cold Spring Harbor Laboratory Press: New York, 1989.
41. Gasteiger, E.; Hoogland, C.; Gattiker, A.; Duvaud, S.; Wilkins, M. R.; Appel, R. D.; Bairoch, A. Protein identification and analysis tools on the ExPASy Server. In *The Proteomics Protocols Handbook*; Walker J.M., Ed; Humana Press: New Jersey, 2005; pp. 571–607.
42. Blom, N.; Sicheritz-Ponten, T.; Gupta, R.; Gammeltoft, S.; Brunak, S. *Proteomics*, **2004**, *4*, 1633–1649.
43. Dubois, M.; Gilles, K. A.; Hamilton, J. K.; Rebers, P. A.; Smith, F. *Anal. Chem.*, **1956**, *28*, 350–356.
44. Britton, H. T. K.; Robinson, R. A. *J. Chem. Soc.*, **1931**, 1456–1462.
45. Deschatelets, L.; Yu, E. K. C. *Appl. Microbiol. Biotechnol.*, **1986**, *24*, 379–385.
46. Roe, J. H.; Rice, E. W. *J Biol. Chem.*, **1984**, *173*, 507–512.
47. Westphal, Y.; Kühnel, S.; Schols, H.A.; Voragen, A.G.J.; Gruppen, H. *Carbohydr. Res.*, 2010, *345*, 2239–2251.



## Supplementary Documents



**Supplementary Figure S1.** Isoelectric focusing (A) and endoglycosidase H treatment monitored by SDS-PAGE (B) of purified BxlA and BxlB. A) Lane 1 and 4, low range pI (pH 2.5–6.5) calibration standard (GE Healthcare); lane 2, 600 ng BxlA; lane 3, 400 ng BxlB. B) Lane 1 and 6, Mark12 unstained protein standard marker (Invitrogen). Lane 2, 7  $\mu$ g BxlA; lane 3, 7  $\mu$ g deglycosylated BxlA; lane 4, 5  $\mu$ g BxlB; lane 5, 5  $\mu$ g deglycosylated BxlB. Endoglycosidase H is seen as the 29 kDa band in lanes 3 and 5.

**Supplementary Table S1**  $^1\text{H}$  and  $^{13}\text{C}$  NMR spectra assignment and ESI-MS  $m/z$  values of known  $\beta$ -xylosyl-oligosaccharides produced by transxylosylation with *p*NPX as donor and suitable acceptors.

Compound (molecular mass) <sup>a</sup>	Chemical shifts ( $\delta$ , p.p.m.)					
	H-1 C-1	H-2 C-2	H-3 C-3	H-4 C-4	H-5a/H-5b C-5	H-6a/H-6b C-6
$\beta$ -D-Xylp-(1,4)-	4.43 102.7	3.23 73.6	3.40 76.4	3.60 70.1	3.95/3.28 66.1 <sup>b</sup>	
$\alpha$ -D-Xylp	5.16 92.9	3.52 72.2	n.d. 72.0	n.d. 74.3	3.80/3.73 59.7	
$\beta$ -D-Xylp ( $m/z$ 289)	4.56 97.3	3.22 ~74.9	3.52 ~74.9	3.76 77.3	3.35/4.04 63.8	
$\beta$ -D-Xylp-(1,4)-	4.43 102.3	3.32 73.8	3.42 76.6	3.62 70.2	3.26/3.93 66.1 <sup>b</sup>	
$\alpha$ -D-Arap	5.22 93.4	3.79 n.d.	3.91 n.d.	4.10 77.2	3.78/3.96 61.0	
$\beta$ -D-Arap ( $m/z$ 289)	4.53 97.3	3.48 73.0	3.68 72.5	4.05 76.8	3.60/4.00 64.6	
$\beta$ -D-Xylp-(1,6)-	4.43 104.4	3.28 73.9	3.42 76.4	3.60 70.2	3.31/3.94 66.1 <sup>b</sup>	
$\alpha$ -D-Manp	5.14 95.0	3.91 ~72.1	3.81 ~71	3.69 ~67.6	3.93 ~72.2	3.85/4.09 ~69.9
$\beta$ -D-Manp ( $m/z$ 319)	4.87 94.6	3.92 71.8	3.63 ~73.8	3.59 70.1	3.49 ~76	3.82/4.13 ~69.9
$\beta$ -D-Xylp-(1,6)-	4.42 104.2	3.27 73.9	3.43 76.6	3.60 70.0	3.29/3.93 66.1 <sup>b</sup>	
$\alpha$ -D-Glcp	5.19 92.9	3.50 72.3	3.68 73.3	3.4 70.5	3.93 71.1	3.84/4.10 ~69.8
$\beta$ -D-Glcp ( $m/z$ 319)	4.61 96.9	3.22 75.0	3.45 76.5	3.94 71.3	3.58 76.0	3.80/4.12 ~69.9

<sup>a</sup> Molecular mass as  $\text{Li}^+$  adduct (estimated mass +  $m/z$  7) determined by ESI-MS shown in parenthesis; <sup>b</sup> Reference carbon shifts according to C5 ; n.d., not detected

**Supplementary Table S2** Primers for construction of expression plasmids encoding *bxlA* and *bxlB*

Primer	Primer sequence	Restriction site
<i>bxlA</i>		
Sense	ATT <u>CTCGAG</u> AAAAGAGAGGCTGAAGCTGCGAACACCAGCTACAC <sup>a</sup>	XhoI
Antisense	ACT <u>CTAGAT</u> TAATGATGATGATGATGATGAGCAATAACATCCTGC <sup>a</sup>	XbaI
<i>bxlB</i>		
Sense	GGG <u>GAA</u> TTCAACTACCCGGACTGCACAACGGGCCCTC <sup>a</sup>	EcoRI
Antisense	CCCGGCGGCCGCATCACTGTCGTTACCTGACAACGG <sup>a</sup>	NotI
1374T→C-sense	GGACAGAGGT <u>GAACT</u> CGACAAGCACAGAC <sup>b</sup>	
1374T→C-antisense	GTCTGTGCTTGTC <u>GAGTT</u> CACCTCTGTCC <sup>b</sup>	

<sup>a</sup> Restriction sites are underlined

<sup>b</sup> Silent mutation position is double underlined

**Supplementary Table S3** HPLC purification conditions of  $\beta$ -xylosyl-oligosaccharides

Acceptor	BxIA		BxIB	
	Mobile phase (ACN <sup>a</sup> /water, v/v)	Column temp. (°C)	Mobile phase (ACN <sup>a</sup> /water, v/v)	Column temp. (°C)
<u>Monosaccharides</u>				
D-Xylose	85/15	70	80/20	70
D-Lyxose	85/15	70	–	–
D-Arabinose	80/20	70	–	–
L-Fucose	80/20	70	–	–
D-Glucose	80/20	70	80/20	65
D-Galactose	–	–	80/20	50
D-Mannose	85/15	70	80/20	70
D-Talose	85/15	70	80/20	55
D-Fructose	–	–	80/20	55
<u>Disaccharides</u>				
Xylobiose	–	–	80/20	65
Turanose	85/15	70	80/20	65
Lactose	–	–	85/15	70
Lactulose	–	–	85/15	70
Sucrose	85/15	70	85/15	70

<sup>a</sup> ACN: Acetonitrile

–, not tested

## **Manuscript II**

# **GH5 endo- $\beta$ -1,4-mannanases from *Aspergillus nidulans* FGSC A4 producing hetero manno-oligosaccharides by transglycosylation**

Adiphol Dilokpimol<sup>a</sup>, Hiroyuki Nakai<sup>a</sup>, Charlotte H. Gotfredsen<sup>b</sup>, Martin J. Baumann<sup>a</sup>, Natsuko Nakai<sup>a</sup>,

Maher Abou Hachem<sup>a</sup>, Birte Svensson<sup>a\*</sup>

<sup>a</sup>Enzyme and Protein Chemistry, Department of Systems Biology, Technical University of Denmark, Søtofts Plads, Building 224, DK-2800 Kgs. Lyngby, Denmark

<sup>b</sup>Department of Chemistry, Technical University of Denmark, Kemitorvet, Building 201, DK-2800 Kgs. Lyngby, Denmark

\*Corresponding author. Tel.: +45 4525 2740; fax: +45 4588 6307; *E-mail address*: bis@bio.dtu.dk (B. Svensson).

## **Abstract**

Two *Aspergillus nidulans* FGSC A4 endo- $\beta$ -1,4-mannanases, ManA and ManC, of glycoside hydrolase family 5 were secretory expressed by *Pichia pastoris* in high yields. 120 and 145 mg/L were purified from culture supernatant, respectively, by His-tag affinity and gel filtration chromatography. Both enzymes hydrolysed  $\beta$ -1,4 linked manno-oligosaccharides with increase in catalytic efficiency ( $k_{cat}/K_M$ ) from degree of polymerisation (DP) 4 through 6. Both enzymes hydrolysed konjac glucomannan, guar gum and locust bean gum galactomannans. ManC showed two fold higher  $k_{cat}/K_M$  towards manno-oligosaccharides of DP 5 and 6, and 30–80% higher activity towards the mannans than ManA. By transglycosylation ManC formed  $\beta$ -1,4 manno-oligosaccharides in eight fold higher yield than ManA and used mannotriose, isomaltotriose and melezitose as acceptors, whereas ManA only used mannotriose. Two novel penta- and two novel hexasaccharides were obtained with isomaltotriose and melezitose acceptors. ManA and ManC share 39% sequence identity and homology modelling indicated very similar substrate interactions at subsites +1 and +2 except that Trp283 in ManC (subsite +1) corresponds to Ser289 in ManA. The ManAS289W mutant decreased 30–45%  $K_M$  towards manno-oligosaccharides of DP 5 and 6 and increased transglycosylation yield by 50% as compared with wild-type ManA. ManCW283S in contrast increased 40%  $K_M$  for manno-oligosaccharides and decreased transglycosylation yields by 30–45%. This mutation also lowered the higher activity found for ManC towards different mannans to the level found for ManA. This first mutational analysis at subsite +1 of GH5 endo- $\beta$ -1,4-mannanases identifies Trp283 as a residue that discriminates between mannans with different degree of branching and has impact on transglycosylation and binding affinity.

**Keywords:** Endo- $\beta$ -1,4-mannanase, Glycoside hydrolase family 5, Transglycosylation, Manno-oligosaccharide action pattern, Mannans, Subsite +1 mutagenesis

**Abbreviations:** DP, degree of polymerisation; GH, glycoside hydrolase family; *HjMan5A*, endo- $\beta$ -1,4-mannanase from *Hycocrea jecorina* RUTC-30 (GenBank AAA34208.1); HPAEC-PAD, high performance anion exchange chromatography with pulsed amperometric detection; HPLC, high performance liquid chromatography; IMAC, immobilized metal ion affinity chromatography; M1, mannose; M2, mannobiose; M3, mannotriose; M4, mannotetraose; M5, mannopentaose; M6, mannohexaose; M7, mannoheptaose; MALDI-TOF MS, matrix-assisted laser desorption/ionisation time-of-flight mass spectrometry; ManA and ManC, GH5 endo- $\beta$ -1,4-mannanase from *A. nidulans* FGSC A4 (GenBank EAA63326.1 and EAA58449.1, respectively); *TfMan*, GH5 endo- $\beta$ -1,4-mannanase from *Thermobifida fusca* KW3 (GenBank CAA06924.1).

## 1. Introduction

Mannans are found as structural constituents in plant cell walls being the dominant hemicelluloses in softwood and are also major storage polysaccharides [1]. Based on the backbone composition and galactose side chain substitution mannans are classified into four groups; unsubstituted mannans; galactomannans; glucomannans; and galactoglucomannans, [1,2]. Unsubstituted mannans and galactomannans (with  $\alpha$ -1,6 D-galactosyl substituents) have 1,4 linked  $\beta$ -D-mannopyranosyl backbones and are mainly storage polysaccharides in legume seed endosperm. Glucomannans and galactoglucomannans contain randomly distributed 1,4 linked  $\beta$ -D-mannopyranosyl and  $\beta$ -D-glucopyranosyl residues and are the major hemicelluloses in secondary cell walls of softwood. Galactose substitution occurs mainly at the O6 position while *O*-acetylation is found at the O2 or O3 position of main chain mannosyl residues [1–4]. Mannans are used in the food industry as gelling agents and thickeners and are also reported to function as dietary fibres [1].  $\beta$ -manno-oligosaccharides are mostly produced by steam treatment at high pressure from natural sources such as coffee beans [5]. They are used in food and feed industries as prebiotics promoting gastrointestinal health as well as increasing the amount of excreted fat and reducing blood pressure [5–7].

Depending on the mannan type a consortium of endo- $\beta$ -1,4-mannanases (EC 3.2.1.78), exo- $\beta$ -1,4-mannosidases (EC 3.2.1.25),  $\alpha$ -galactosidases (EC 3.2.1.22),  $\beta$ -glucosidases (EC 3.2.1.21) and acetyl mannan esterases (EC 3.1.1.6) is needed for complete depolymerisation [1,2,8]. Hydrolysis of backbone linkages by endo- $\beta$ -1,4-mannanases is influenced by the extent and pattern of galactose substitution and the distribution of glucose in the polysaccharide main chain [1,2,8]. Endo- $\beta$ -1,4-mannanases are classified into three glycoside hydrolase families (GH5, 26 and 113) based on amino acid sequence similarities (<http://www.cazy.org>) [9]. GH5 contains bacterial

and eukaryotic endo- $\beta$ -1,4-mannanases, whereas GH26 and GH113 endo- $\beta$ -1,4-mannanases are mainly from prokaryotes [10]. Endo- $\beta$ -1,4-mannanases hydrolyse mannans to mainly mannobiose and mannotriose [11–14]. The active sites in GH5 endo- $\beta$ -1,4-mannanases are reported to possess at least five subsites able to accommodate substrate backbone carbohydrate residues [15–18]. Hydrolysis seems to require binding involving at least four subsites (mostly –2 through +2); hence degradation of mannotriose is extremely slow [2,10,13,19].

The three endo- $\beta$ -1,4-mannanase-containing GHs belong to clan GH-A and sharing a common fold and the general acid/base catalysis proceeding *via* a double displacement mechanism resulting in retention of the anomeric configuration [9]. The acid/base and nucleophile catalysts are two glutamic acid residues [1,20]. First the catalytic nucleophile attacks the anomeric carbon center and forms a covalent glycosyl-enzyme intermediate aided by the acid catalyst protonation of the glycosidic bond to be cleaved. Subsequently water (in hydrolysis) or a carbohydrate hydroxyl group (in transglycosylation) is activated by the base catalyst and performs a nucleophilic attack at the anomeric centre of the covalent intermediate to release products with retention of the anomeric configuration of the substrate [21–22]. In transglycosylation, the substrate glycone that forms the glycosyl-enzyme intermediate and the incoming carbohydrate are referred to as donor and acceptor, respectively. Previously manno-oligosaccharides (DP 4–6) were used as donors for transglycosylation to produce longer manno-oligosaccharides catalysed by GH5 and GH113 endo- $\beta$ -1,4-mannanases [19,20,23–25], whereas GH26 had poor transglycosylation activity [15,26,27]. Previously no heterogeneous transglycosylation, however, using non-manno-oligosaccharide acceptors has been reported and insight moreover is lagging behind on how structural features of the active sites in different endo- $\beta$ -1,4-mannanases influence enzymatic properties, including the transglycosylation ability. Two 39% sequence identical GH5 mannan degrading enzymes,

ManA and ManC, were identified in the genome of the cell-wall degrading fungus *Aspergillus nidulans* FGSC A4 [28] and showed mannanolytic activity after heterologous expression in *Pichia pastoris* of the full-length enzymes including signal peptides [29]. In the present study, high amounts of ManA and ManC were obtained by secretion of *P. pastoris* after recloning without signal peptides. The substrate specificity as well as transglycosylation potential were characterised and homology modelling suggested that an important difference was Trp283 at subsite +1 of ManC, which corresponded to Ser289 in ManA of the otherwise very similar substrate binding subsites +1 and +2. This motivated site-directed mutagenesis to discern the contribution of this position to hydrolytic and transglycosylation activities, representing the first subsite +1 engineering in GH5 endo- $\beta$ -1,4-mannanases.

## 2. Material and methods

### 2.1 Materials

N-Acetyl-glucosamine, arabinose, L-arabinose, fructose, L-fucose, galactose, glucosamine, glucose, mannose (M1), L-rhamnose, talose, cellobiose, gentibiose, isomaltose, lactose, lactulose, laminaribiose, maltose, melibiose, sophorose, sucrose, trehalose, turanose, laminaritriose, maltotriose, melezitose, panose, raffinose and locust bean gum galactomannan were purchased from Sigma Aldrich (St. Louis, MO); xylose and guar gum galactomannan were from Carl Roth (Karlsruhe, Germany); arabinobiose, arabinotriose, mannobiose (M2), mannotriose (M3), mannotetraose (M4), mannopentaose (M5), mannohexaose (M6), xylobiose, xylotriase and konjac glucomannan were from Megazyme (Wicklow, Ireland); and isomaltotriose was from Tokyo Chemical Industry (Tokyo, Japan).

### 2.2 Sequence comparison and homology modelling

The BLAST tool was used for homology search of protein sequences ([http://blast.ncbi.nlm.](http://blast.ncbi.nlm.nih.gov/Blast.cgi)

<http://blast.ncbi.nlm.nih.gov/Blast.cgi>) [30]. Homology models of ManA and ManC were generated using the HHpred–Homology server (<http://toolkit.tuebingen.mpg.de/hhpred>) [31] with the template endo- $\beta$ -1,4-mannanase from *Hypocrea jecorina* RUTC-30 (*HjMan5A*) in complex with mannobiose accommodated at subsites +1 and +2 (PDB ID: 1QNR [17]), which has 56% and 37% sequence identity to ManA and ManC, respectively. The homology models were validated by the combinatorial extension method (<http://cl.sdsc.edu/ce.html>) [32] giving an RMSD of 0.3 Å for 343 equivalent C $^{\alpha}$  positions (of 372 in ManA and 381 in ManC) compared to 1QNR with 7.9 and 7.7 Z-score for ManA and ManC, respectively, whereas ProQ-Protein Quality Predictor (<http://www.sbc.su.se/~bjornw/ProQ/ProQ.html>) [33] gave LGScore/MaxSub of 5.337/0.627 and 5.468/0.567 for ManA and ManC, respectively, indicating good to very good quality of both models. Models were rendered and analysed using Pymol v0.99 (DeLano Scientific LLC, San Carlos, CA) and superimposed with  $\beta$ -mannanase from *Thermobifida fusca* KW3 (*TfMan*; PDB ID: 2MAN) [34] having 23% and 37% sequence identity to ManA and ManC, respectively, in complex with mannobiose bound at subsites –3 through –2, to illustrate possible carbohydrate-protein interactions at the substrate glycone binding area.

### 2.3 Cloning of $\beta$ -mannanase genes *manA* and *manC* and site-directed mutagenesis of subsite +1 residues Trp283 and Ser289

*P. pastoris* strain X-33 transformants (FGSC database accession no. 10088 and 10106; [www.fgsc.net](http://www.fgsc.net)) harbouring *A. nidulans* FGSC A4  $\beta$ -mannanase genes (*manA*; GenBank EAA63326.1 and *manC*; GenBank EAA58449.1) [29] were purchased from Fungal Genetics Stock Center, School of Biological Sciences, University of Missouri, (Kansas City, MO). These clones encoded the full-length enzymes, signal peptides inclusive, predicted as Met1–Ala18 for both genes (SignalP 3.0; <http://www.cbs.dtu.dk/services/SignalP>) [35]



and were recloned to encode the mature polypeptides with the C-terminal hexa His-tag. Expand High Fidelity DNA polymerase (Roche Diagnostics GmbH, Mannheim, Germany) was used for DNA amplification with oligonucleotide primers (Supplementary Table S1) constructed based on the genomic sequence [28]. The PCR products were digested by EcoRI and NotI for *manA* and *manC* (New England BioLabs, Ipswich, MA) and cloned downstream in frame with *Saccharomyces cerevisiae*  $\alpha$ -mating factor secretion signal in pPICZ $\alpha$ A (Invitrogen, Carlsbad, CA). The obtained plasmids pPICZ $\alpha$ A-ManA and pPICZ $\alpha$ A-ManC were purified from *Escherichia coli* DH5 $\alpha$  (Invitrogen) transformants selected on low salt Luria Bertani medium supplemented with 25  $\mu$ g/mL zeocin, fully sequenced (Eurofins MWG Operon, Ebersberg, Germany), linearised by PmeI (New England BioLabs), and transformed into *P. pastoris* strain X-33 according to the manufacturer's recommendation.

Site-directed mutagenesis (QuikChange Lightning Site-Directed Mutagenesis kit; Stratagene, La Jolla, CA) was performed using ManAS289W and ManCW283S primer pairs (Supplementary Table S1) and pPICZ $\alpha$ A-ManA and pPICZ $\alpha$ A-ManC as templates. Mutant plasmids were transformed in *E. coli* DH5 $\alpha$ , verified by sequencing, and used for transformation of *P. pastoris* X-33 (as above).

#### 2.4 Production and purification of recombinant ManA and ManC

*P. pastoris* transformants were grown in 4  $\times$  1 L (ManA; ManC) and 3  $\times$  1 L (ManAS289W; ManCW283S) buffered glycerol-complex medium (1% yeast extract, 2% peptone, 100 mM potassium phosphate pH 6.0, 1.34% yeast nitrogen base with ammonium sulfate, 4  $\times$  10<sup>-5</sup>% biotin, 1% glycerol) in 2.5 L plastic baffled shake flasks at 30°C for 24 h to OD<sub>600</sub> of 34 (ManA), 39 (ManC), 34 (ManAS289W), and 28 (ManCW283S). The cells were harvested (3000g, 5 min, 4°C) and resuspended in 1 L buffered methanol-complex medium for

ManA and ManC (100 mM potassium phosphate pH 6.0, 1% yeast extract, 2% peptone, 1.34% yeast nitrogen base with ammonium sulfate, 4  $\times$  10<sup>-5</sup>% biotin, 0.5% methanol) or 1 L buffered minimal methanol medium for ManAS289W and ManCW283S (100 mM potassium phosphate pH 6.0, 1.34% yeast nitrogen base with ammonium sulfate, 4  $\times$  10<sup>-5</sup>% biotin, 0.5% methanol, 1% casamino acid). The induction continued at 22°C for 120 h (ManA; ManC) and 72 h (ManAS289W; ManCW283S) with methanol supplemented to the culture to a final concentration of 0.5% (v/v) every 24 h. Culture supernatants were harvested (13,500g, 4°C, 1 h), adjusted to pH 7.5 with 1 M K<sub>2</sub>HPO<sub>4</sub>, filtered (0.22  $\mu$ m; TPP, Trasadingen, Switzerland), and applied to a 5 mL HisTrap HP column (GE Healthcare, Uppsala, Sweden) equilibrated with 20 mM HEPES, 0.5 M NaCl, 10 mM imidazole, pH 7.5. After wash with 20 mM HEPES, 0.5 M NaCl, 22 mM imidazole, pH 7.5, protein was eluted by a linear 22–400 mM imidazole gradient in the same buffer (25 mL; flow rate 1.0 mL/min). Fractions containing enzyme were pooled, concentrated (Centriprep YM30, Millipore), and applied to a Hiload 26/60 Superdex G75 column (GE Healthcare) equilibrated with 20 mM MES, 0.15 M NaCl, pH 6.8 for ManA and ManC or pH 7.0 for ManAS289W and ManCW283S (flow rate 0.5 mL/min). Enzyme-containing fractions were pooled, concentrated, and the buffer was exchanged to 20 mM HEPES pH 7.0 (Centriprep YM30, Millipore). All purification steps were performed at 4°C.

#### 2.5 Protein characterisation

Protein concentration was determined spectrophotometrically at 280 nm using  $E^{0.1\%} = 2.26, 2.57, 2.33$  and  $2.51$  for ManA, ManC, ManAS289W and ManCW283S, respectively, as determined by aid of amino acid analysis. Molecular masses were estimated by SDS-PAGE (NuPAGE Novex Bis-Tris gels; Invitrogen) and by analytical gel filtration using a precalibrated Hiload 16/60 Superdex G75 column (flow rate: 1 mL/min; GE Healthcare). Theoretical molecular masses were calculated by ExPASy–ProtParam tool (<http://www.expasy.ch/>)

tools/protparam.html) [36]. *N*-glycosylation was predicted using NetNGlyc 1.0 Server (<http://www.cbs.dtu.dk/services/NetNGlyc>) [37]. Purified enzymes (7  $\mu$ g) were treated with endoglycosidase H (New England BioLabs) as recommended by the manufacturer. Carbohydrate content of purified enzymes (400  $\mu$ g) was quantified by the phenol-sulfuric acid procedure [38] using glucose and mannose as standards.

## 2.6 Enzyme stability and activity

$\beta$ -Mannanase activity towards 0.5% (w/v) konjac glucomannan, locust bean gum or guar gum galactomannan was measured at 37°C for 5 min in 100 mM sodium acetate, 0.005% BSA, pH 5.5 (400  $\mu$ L). Substrate (1 g) was dissolved in 95% ethanol (6 mL), added Milli-Q water (90 mL) with stirring and heated until boiling. Stirring continued until the mixture cooled down to room temperature and the volume was adjusted to 100 mL with Milli-Q water. Released reducing sugars were determined by adding 3,5-dinitrosalicylic acid solution (600  $\mu$ L), incubating at 95°C (15 min), cooling on ice (10 min), and measuring absorbance at 540 nm [39,40] using a microtiter plate reader (Bio-Tek Instrument Inc., Winooski, VT). One unit (U) was defined as the amount of enzyme liberating 1  $\mu$ mol/min reducing sugar equivalents under the assay condition, using mannose as standard.

The activity of 213 nM ManA, 104 nM ManC, 276 nM ManAS289W and 249 nM ManCW283S was measured using 0.5% locust bean gum galactomannan (as above) in 40 mM Britton-Robinson buffers pH 2.0–12.0 [41] and at 20–80°C in 50 mM sodium acetate pH 5.5. The dependence of stability on pH and temperature was deduced from residual activity measured as above after 3 h at 37°C in 40 mM Britton-Robinson buffers pH 2.0–10.0 or at 25–80°C in 50 mM sodium acetate pH 5.5 for 2130 nM ManA, 1040 nM ManC, 2760 nM ManAS289W, and 2490 nM ManCW283S.

## 2.7 Enzyme kinetics and action pattern towards manno-oligosaccharides

Initial rates of hydrolysis of M4–M6 (0.2–6.0 mM) were determined for ManA (60 nM with M4; 30 nM with M5; 10 nM with M6); ManC (75 nM with M4; 15 nM with M5; 12 nM with M6); ManAS289W (50 nM with M4; 28 nM with M5; 12 nM with M6); and ManCW283S (120 nM with M4; 32 nM with M5; 20 nM with M6) in 100 mM sodium acetate, 0.005% BSA, pH 5.5 (300  $\mu$ L) from released reducing sugars quantified after 2.5, 5.0, 7.5, 10.0, 12.5 and 15.0 min reaction by copper bicinchoninate measuring the absorbance at 540 nm [42,43] and using mannose as standard. Kinetic parameters,  $K_M$  and  $k_{cat}$ , were determined by fitting the Michaelis-Menten equation to initial rate data using SigmaPlot v. 9.0.1 (Systat Software Inc. San Jose, CA).

Action patterns on 0.5 mM M4–M6 were analysed using the same enzyme concentrations as above in 100 mM sodium acetate pH 5.5 at 37°C. Aliquots (6  $\mu$ L) were removed at appropriate intervals up to 30 min for M4–M6, and added to 100 mM NaOH (294  $\mu$ L) to stop the reaction. Manno-oligosaccharides were quantified from peak areas in HPAEC-PAD (ICS3000 system; Dionex Corporation, Sunnyvale, CA) equipped with CarboPac PA200 anion exchange column (3  $\times$  250 mm with 3  $\times$  50 mm guard column; Dionex) using isocratic elution with 37.5 mM NaOH for 35 min at 25°C; flow rate: 0.35 mL/min) calibrated with M1–M6.

## 2.8 Transglycosylation

ManA and ManC (91 nM) reacted with 14 mM M4 as donor and 400 mM of 36 potential acceptors (arabinose, L-arabinose, xylose, L-fucose, L-rhamnose, glucose, galactose, mannose, talose, fructose, glucosamine, *N*-acetylglucosamine, arabinobiose, cellobiose, gentibiose, isomaltose, lactose, lactulose, laminaribiose, maltose, mannobiose, melibiose, sophorose, sucrose, trehalose, turanose, xylobiose, arabinotriose, isomaltotriose, laminaritriose, mannotriose, maltotriose, melezitose, panose, raffinose and

xylotriose) in 100 mM sodium acetate pH 5.5 at 37°C for 30 min (1 mL). The reaction products were quantified using HPAEC-PAD (see 2.7) and isocratic elution with 50 mM NaOH, 35 min at 25°C (flow rate: 0.35 mL/min) using M5 and M6 as standards for penta- and hexasaccharide products. Transglycosylation yield was calculated based on the donor concentration.

ManA or ManAS289W (330 nM) and ManC or ManCW283S (145 nM) reacted either with 30 mM M4 (without acceptor) or with 24 mM M4 and 100 mM M3, in 100 mM sodium acetate pH 5.5 at 37°C for 150–300 min (1 mL). For ManA and ManC aliquots (5 µL) removed at 0, 2.5, 5, 10, 15, 20, 25, 30, 35, 40, 45, 60, 80, 100, 120 and 150 min, and for ManAS289W and ManCW283S aliquots removed at 0, 2.5, 5, 10, 20, 30, 45, 60, 90, 120, 150, 180, 210, 240, 270 and 300 min were added to 100 mM NaOH (245 µL) to stop the reaction. To optimize transglycosylation yields, the time course of 145 nM ManC with 24 mM M4 and 200 mM isomaltotriose or melezitose in 100 mM sodium acetate pH 5.5 (1 mL) at 37°C was determined from aliquots (5 µL) removed at 0, 2.5, 5, 10, 15, 20, 25, 30, 35, 40, 45, 60, 80, 100, 120, 140, 160 and 180 min and stopping the reaction as above. A minor product M7 appeared in HPAEC-PAD and was estimated using M6 as standard as M7 is not available and too small amounts of M7 were produced to establish a standard curve using purified M7.

## 2.9 Manno-oligosaccharide purification

For structural analysis of transglycosylation products reaction mixtures of ManC (145 nM), 24 mM M4 and 100 mM M3, 200 mM isomaltotriose or 200 mM melezitose were incubated at 37°C (60, 120 and 180 min for M3, isomaltotriose and melezitose, respectively, as guided by time course experiments in 2.8) in 100 mM sodium acetate, pH 5.5 (1 mL) and heated (95°C, 10 min), centrifuged (18,000g, 4°C, 5 min), desalted (Amberlite MB-20; Fluka, Sigma Aldrich), filtered (0.45 µm nylon filter; Frisette Aps, Knebel, Denmark), and purified by HPLC (UltiMate 3000 Standard LC

system; Dionex) equipped with a TSKgel Amide-80 column (5 µm, 4.6 × 250 mm and 4.6 × 10 mm guard column; TOSOH, Tokyo, Japan) and refractive index detector (RI-101; Showa Denko, Kanagawa, Japan) at constant flow rate (1 mL/min) of mobile phase (acetonitrile/water 70:30, v/v) at 70°C. Purity was confirmed by thin layer chromatography (aluminium-coated silica gel 60 F<sub>254</sub>, Merck) developed twice by acetonitrile/water (70:30, v/v), sprayed with 2% orcinol in sulphuric acid/water/ethanol (10:10:80, v/v/v) [44] and tarred at 120°C.

## 2.10 Nuclear Magnetic Resonance spectroscopy (NMR)

Purified oligosaccharides (500 µL, 1–2 mM) were freeze dried (CoolSafe –55°C; ScanLaf A/S, Lyngø, Denmark) and dissolved in deuterium oxide prior to recording of spectra on a Varian Unity Inova 500 MHz NMR spectrometer or a Bruker Avance 800 MHz spectrometer. A series of 2D homo- and heteronuclear correlated spectra: DQF-COSY, NOESY, gHSQC and gHMBC, were acquired using standard pulse sequences. The NMR data for structural assignment were acquired in D<sub>2</sub>O.

## 2.11 Matrix-assisted laser desorption/ionisation-time of flight mass spectrometry (MALDI-TOF MS)

MALDI-TOF MS was made using an Ultraflex II TOF/TOF instrument (Bruker Daltonics GmbH, Bremen, Germany) selected for positive ions and analysed at 25040 V and detected using reflector mode. High (75%) laser power was required to obtain good spectra and >100 spectra were collected. Calibration was done with M5 and M6 (as Na<sup>+</sup> adducts) and trypsin-digested β-lactoglobulin (mass range *m/z* 851–2313.3). The matrix solution was prepared by dissolving 10 mg 2,5-dihydroxybenzoic acid in 1 mL acetonitrile/water (30:70, v/v) containing 10 mM NaCl. Purified samples of 0.2 mM M5 or manno-isomaltotrioses and 0.1 mM M6 or manno-melezitoses (1 µL) and matrix (1 µL) were pipetted onto a MALDI-TOF-

target plate (Bruker Daltonics) and air-dried prior to analysis [44].

### 3. Results and discussion

#### 3.1 Production and purification of recombinant ManA, ManC, ManAS289W and ManCW283S

His-tag fusions of ManA and ManC were secreted by *P. pastoris* and 120 and 145 mg/L, respectively, were purified from culture supernatants. These yields are very high compared to native GH5 endo- $\beta$ -1,4-mannanases secreted by *A. niger* (1.6 mg/L) [11] or *H. jecorina* (0.8 mg/L [13]; 2 mg/L [45]) and to recombinant *A. aculeatus* GH5 endo- $\beta$ -1,4-mannanase produced in *S. cerevisiae* (1.8 mg/L) [12].

ManC migrated in SDS-PAGE as a single band of 56 kDa, whereas ManA gave a smear with the lower band corresponding to 56 kDa (Supplementary Fig. S1); the calculated values are 43847.1 and 46643.8 Da, respectively, and endoglycosidase H treatment reduced the apparent molecular mass of ManA and ManC by 10 and 5 kDa, respectively, and the deglycosylated ManA migrated as sharp band of 45 kDa (Supplementary Fig. S1). The effect of endoglycosidase H confirmed that ManA and ManC were glycosylated in agreement with a content of four and two predicted *N*-glycosylation sites and carbohydrate contents were estimated to 19% and 15% using glucose, and 13% and 9% using mannose as standard, respectively. Glycosylation is not uncommon for fungal secreted GH5 endo- $\beta$ -1,4-mannanases as found *e.g.* for *H. jecorina* mannanase [45] that shares one site with ManA. Gel filtration indicated that both ManA and ManC are monomers of approximately 58 kDa (data not shown).

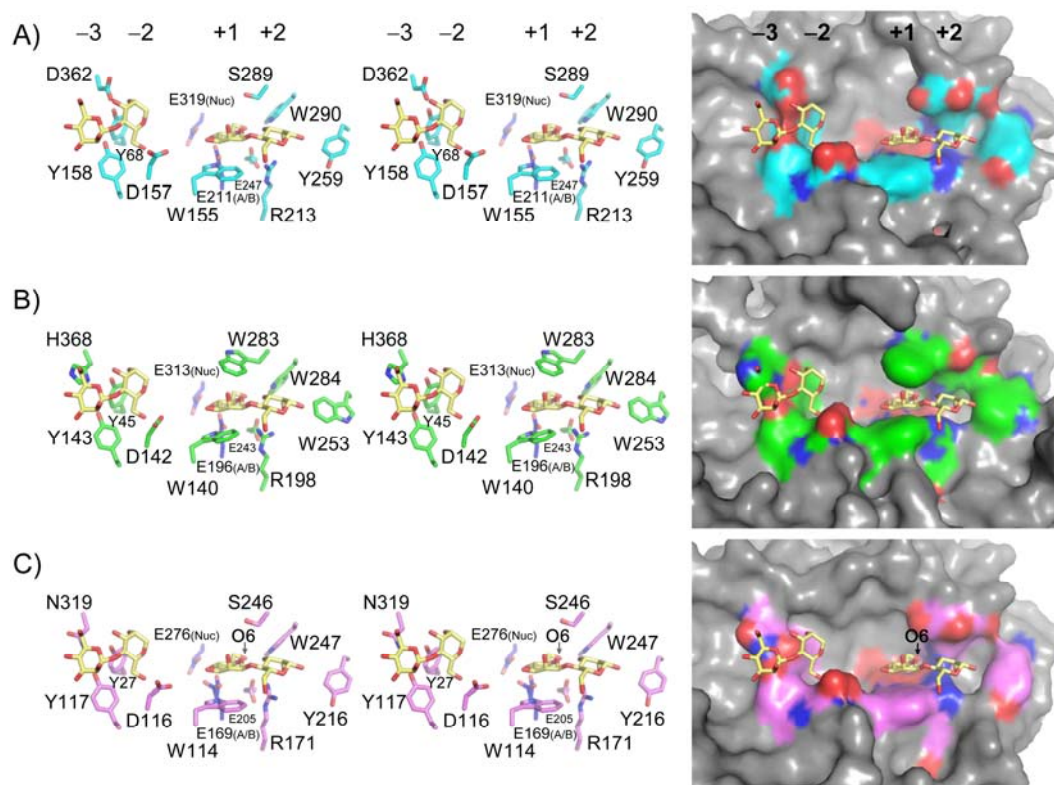
The crystal structure of *H. jecorina* GH5 endo- $\beta$ -1,4-mannanase (*HjMan5A*) with bound manno-oligosaccharide [17] (see 2.2) showed Trp114, Arg171, Glu205 and Trp247 are involved in substrate binding at subsites +1 and +2 (Fig. 1C). These residues are well conserved in ManA (Trp155, Arg213, Glu247, and Trp290) and ManC (Trp140, Arg198, Glu243, and Trp284) (Fig. 1;

Supplementary Fig. S2). According to the ManC homology model, Trp283 is close enough to interact with a mannosyl residues bound at subsite +1, together with Trp140 (Fig. 1B). Trp283 corresponds to Ser289 in ManA (Fig. 1A) and *HjMan5A* Ser246, both located about 5 Å from the sugar ring and thus unlikely to interact with the mannosyl moiety at subsite +1. To investigate the impact of ManC Trp283 in hydrolysis and transglycosylation, ManAS289W and ManCW283S mimicking Trp283 and Ser289 in ManC and ManA, were made by site-directed mutagenesis and obtained in yields of 12 and 24 mg/L culture, respectively. ManAS289W and ManCW283S were monomers of 59 and 56 kDa as determined by gel filtration and migrated in SDS-PAGE as the parent enzymes (Supplementary Fig. S1).

#### 3.2 Hydrolytic activity of ManA, ManC, ManAS289W and ManCW283S

ManA and ManC showed increasing catalytic efficiency ( $k_{cat}/K_M$ ) with increasing DP of manno-oligosaccharides (M4–M6) (Table 1) as is characteristic of endo-acting mannanases, suggesting that ManA and ManC possess with 5–6 substrate binding subsites [15–18]. Both enzymes exhibited low affinity for M4 similarly to GH5 endo- $\beta$ -1,4-mannanases from *Cellvibrio japonicus* [10] and *Mytilus edulis* [16]. ManC moreover showed about twice as high  $k_{cat}/K_M$  towards M5 and M6 as ManA, in part due to a lower  $K_M$  tentatively attributed to the presence of Trp283 in ManC (see Fig. 1). The  $k_{cat}/K_M$  of the subsite +1 mutants, ManCW283S and ManAS289W, increased with DP of manno-oligosaccharides as for the wild-type enzymes. While  $k_{cat}/K_M$  of ManCW283S decreased by 50% compared to ManC, ManAS289W and ManA gave similar  $k_{cat}/K_M$  values, although  $K_M$  of the mutant decreased and more so for M5 than for M6. Hence, the differences in  $k_{cat}/K_M$  towards M5 and M6 for subsite +1 mutants as compared to wild-type enzymes, stemmed mainly from changes in  $K_M$ , which decreased for ManAS289W and increased for ManCW283S. These observations are in accordance

with contribution of ManC Trp283 to binding at subsite +1. The modest effect, however, suggests that the Trp is not critical for activity.



**Figure 1.** 3D cartoons representing the key active site residues of the homology models of ManA (A) and ManC (B), and the crystal structure of endo- $\beta$ -1,4-mannanase from *H. jecorina* RUTC-30 (C) with mannobiose bound at subsites +1 and +2 (PDB ID: 1QNR) [17]; mannobiose is superimposed at subsites –2 and –3 from the structure of the complex with *T. fusca* KW3 mannanase (PDB ID: 2MAN) [34] (see 2.2). Nuc, catalytic nucleophile; A/B, catalytic acid/base; Nuc and A/B residues of ManA and ManC were predicted according to sequence alignment and 3D-models. The same color coding is residues as used on the stereo view panels (to the left) and the surface presentations (to the right).

**Table 1.** Hydrolysis kinetic parameters of ManA, ManAS289W, ManC and ManCW283S towards manno-oligosaccharides (M4–M6)

Enzyme	Substrate	$k_{cat}$ $s^{-1}$	$K_M$ mM	$k_{cat}/K_M$ $s^{-1} mM^{-1}$
ManA	M4	–	–	6
	M5	$67 \pm 2.8$	$2.9 \pm 0.03$	23
	M6	$193 \pm 5.8$	$1.8 \pm 0.08$	109
ManAS289W	M4	–	–	10
	M5	$42 \pm 2.5$	$1.6 \pm 0.16$	27
	M6	$148 \pm 1.7$	$1.3 \pm 0.05$	115
ManC	M4	–	–	7
	M5	$112 \pm 8.1$	$1.8 \pm 0.13$	61
	M6	$134 \pm 5.2$	$0.6 \pm 0.04$	215
ManCW283S	M4	–	–	3
	M5	$98 \pm 3.1$	$2.8 \pm 0.13$	36
	M6	$117 \pm 3.3$	$1.0 \pm 0.03$	118

Standard deviations were calculated from triplicate experiments

The activity towards locust bean gum galactomannan, guar gum galactomannan, and konjac glucomannan was 30–80% higher for ManC than ManA (Table 2), which has activity towards locust bean gum galactomannan comparable to other fungal GH5 endo- $\beta$ -1,4-mannanases from *H. jecorina* [46], *A. fumigatus* [47], *A. niger* [11], *A. culeatus* [12] of 230–630 U/mg. ManC has the highest reported activity (730 U/mg) and prefers locust bean gum galactomannan (Table 2), possibly due to its lower content of  $\alpha$ -1,6-galactosyl substituents (galactose:mannose, 1:4) compared to guar gum galactomannan (galactose:mannose, 1:2) [1–2]. ManC has also higher activity for galactomannan than glucomannan (Table 2), whereas ManA appears almost insensitive to the side chain substitution and backbone composition as the activity was 340–400 U/mg for all three polysaccharides (Table 2). Currently no structural basis has been identified for the discriminate action of GH5 endo- $\beta$ -1,4-mannanases towards polysaccharides with varying extent of side chain substitution or backbone composition. *A. nidulans* FGSC A4 produces at least three homologous GH5 endo- $\beta$ -1,4-mannanases [47] differing with regard to substrate specificity, and these may confer synergy required for depolymerisation of mannans [2,10]. In fact the subsite +1 ManCW283S mutant in contrast to wild-type ManC had essentially the same activity towards all three polysaccharides, suggesting that Trp283 (Fig. 1B) contributes to the specificity differences between ManC and ManA (Table 2). Interestingly, the mutations seemed to modulate specificity with respect to degree of branching and backbone composition. Hence the ratio of specific activities of guar/locust bean gum galactomannan and konjac glucomannan/locust bean gum galactomannan of ManCW283S resembles those of ManA and *vice versa* (Table 2). Both ManCW283S and ManAS289W lost 25–60% activity towards all three mannans indicating higher catalytic efficiency of the wild-type enzymes, although ManAS289W has comparable activity to wild-type towards manno-oligosaccharides (Table 1). Interrogating the structure of *H. jecorina* in complex with

mannobiose (Fig. 1C) and the homology models of ManA and ManC (Fig. 1A,B) suggested that galactose substitution at the mannosyl ring at subsite +1 is not tolerated as the 6-OH group points into the active site (Fig. 1C). An O6 galactosyl substituted mannosyl, however, seems more readily accommodated at subsite –1 this can also be affected by the Trp→Ser substitution at the neighbouring subsite +1. Lack of structural data prevents detailed insight, but Trp283 in ManC inevitably makes the active site cleft narrower and more restrained than the Ser in ManA (Fig. 1).

ManA and ManC have activity optimum at pH 5.5 (Fig. 2A) and stable (>95 % residual activity) at pH 4.5–7.0 and 4.0–8.0, respectively (Fig. 2B). Both enzymes showed maximum activity at 50°C (Fig. 2C) and retained >95% activity after 3h incubation up to 40°C (Fig. 2D). ManCW283S showed slightly reduced stability in the alkaline pH range compared to the parent enzyme, but otherwise the subsite +1 mutation had little effect on the dependence of activity stability of pH and temperature (Fig. 2). This behaviour resembled that of other fungal GH5  $\beta$ -1,4-mannanases showed having reported activity optima at pH 3.0–7.5 and 45–70°C [2,11–13,45–47].

To gain further insight into the mode of substrate interaction, the time course of hydrolysis of M4–M6 was monitored by HPAEC-PAD (Fig. 3), and the products were quantified towards the end of the reaction (Fig. 4). ManA and ManC both formed M2 as main hydrolysis product from M4, and M2 together with M3 and M4 from M5 and M6. These action patterns suggest higher-affinity substrate binding at subsite(s) –2 and/or +2, even though the hydrolysis of M4 was not fully complete (>65% hydrolysed). Noticeably, ManA produced more M1 and M3 from M4 than ManC (Fig. 4), suggesting relatively more important affinity at subsite(s) –3 and/or +3 or lower affinity at subsite(s) –2 and/or +2 for ManA. However, ManA has a relatively lower affinity at the –2 and/or +2 subsites since ManA and ManC produced 12% and 8% M3 from M6, reflecting a similar relative affinity for their subsite(s) –3 and/or +3. The 0.5 mM of manno-

oligosaccharides was used for hydrolysis action pattern analysis to prevent transglycosylation at higher substrate concentration.

Sequence alignment and homology models of ManA and ManC superimposed onto the mannobiose complex of *T. fusca* GH5 mannanase (*TfMan*; see 2.2) identify ManA Tyr68, Asp157, Tyr158, Asp362 and ManC Tyr45, Asp142, Tyr143, His368 to interact with substrate at subsites -2 and -3 (Fig 1A,B). Moreover ManA Trp155, Arg213, Glu247, Trp290 and ManC Trp140, Arg198, Glu243, Trp283, Trp284 appear to be involved in substrate binding at subsites +1 and +2 (see 3.1). These proposed interactions can agree with ManA and ManC producing mostly M2 in hydrolysis of M4–M6. Moreover, ManC His368 is solvent exposed and may obscure substrate binding at subsite -3, possibly resulting in the higher formation of M2 in hydrolysis of M4 than in ManA. In case of the subsite +1 mutants, ManAS289W and ManCW283S also formed M2 as main hydrolysis product from M4–M6 and the action patterns showed no obvious difference from their wild-type enzymes (Fig. 3D–F,J–L and Fig. 4). Hence ManC Trp283 has no effect on substrate binding pattern.

### 3.3 Transglycosylation by *ManA*, *ManC*, *ManAS289W* and *ManCW283S*

Transglycosylation catalysed by ManA and ManC was monitored using 30 mM M4 (Fig. 5; Supplementary Fig. S3) and M5–M7 were produced by ManA (Fig. 5A), whereas ManC produced only M5 and M6 (Fig. 5C). Maximum product yields (M5+M6) of ManA and ManC obtained after 25 and 100 min, were 2% and 16% (Fig 5A,C), respectively. ManC transglycosylation was thus 8

times more efficient than by ManA. The major transglycosylation product M6 reflected transfer of mannobiosyl to M4 as acceptor in agreement with the action pattern analysis (Fig. 4) showing M2 as the main hydrolysis product from M4, and M2 and M4 as main products from M6. Clearly subsite -2 governs binding of the glycone part of the active site. Using 24 mM M4 as donor and 100 mM M3 as acceptor resulted in approximately 50% increased transglycosylation yields (M5+M6) of 4% and 35% for ManA (at 40 min) and ManC (at 120 min), respectively (Fig, 5E,G). M5 was the major product confirming preferred transfer of mannobiosyl to M3.

The subsite +1 mutant ManAS289W produced M5–M7 (Fig. 5B) while ManCW283S produced only M5 and M6 (Fig. 5D) from 30 mM M4, thus the mutants caused no real difference from the parent ManA and ManC enzymes although the M5+M6 yield of ManAS289W was 5% (at 30 min), which is 2.5 fold higher than for ManA, whereas the yield of ManCW283S was reduced to 9% (at 90 min) compared to ManC (16%). Thus somehow the Trp283 and Ser289 determine the fine-specificity of the enzymes. This is also supported when using 24 mM M4 and 100 mM M3, resulting in yields of 8% (at 90 min) and 24% (at 150 min) for ManAS289W and ManCW283S (Fig. 5F,H), respectively, representing doubling the yield for ManAS289W compared to ManA (4%), whereas yield decreased 1.5 fold with ManCW283S compared to wild-type (35%). ManC Trp283 has a role in transglycosylation possibly increasing acceptor affinity at subsite +1, which is reminiscent of the decrease and increase of  $K_M$  found for ManAS289W and ManCW283S, respectively (see 3.2).

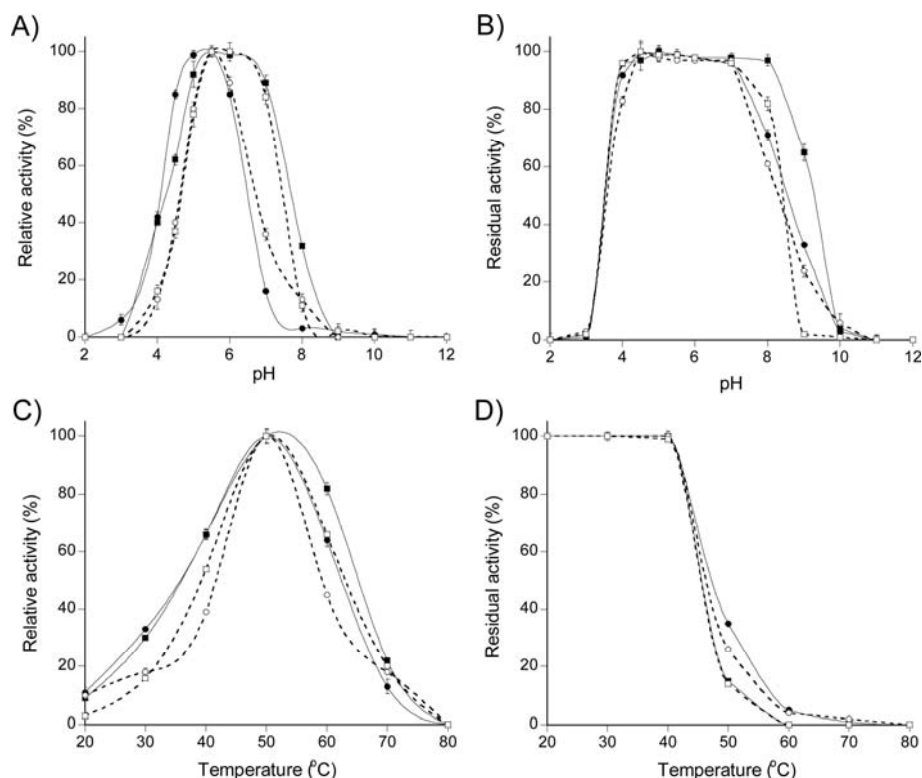
**Table 2.** Specific activities of purified ManA, ManAS289W, ManC, and ManCW283S towards mannans

Enzyme	Substrate <sup>a</sup>	Specific activity <sup>b</sup>	
		U/mg	Ratio <sup>c</sup>
ManA	Locust bean gum galactomannan	400 ± 4	1
	Guar gum galactomannan	390 ± 6	0.98
	Konjac glucomannan	340 ± 2	0.85
ManAS289W	Locust bean gum galactomannan	300 ± 1	1
	Guar gum galactomannan	250 ± 1	0.83
	Konjac glucomannan	220 ± 1	0.73
ManC	Locust bean gum galactomannan	730 ± 2	1
	Guar gum galactomannan	600 ± 2	0.82
	Konjac glucomannan	430 ± 4	0.59
ManCW283S	Locust bean gum galactomannan	320 ± 4	1
	Guar gum galactomannan	300 ± 1	0.94
	Konjac glucomannan	270 ± 1	0.84

<sup>a</sup> 0.5% mannan substrates

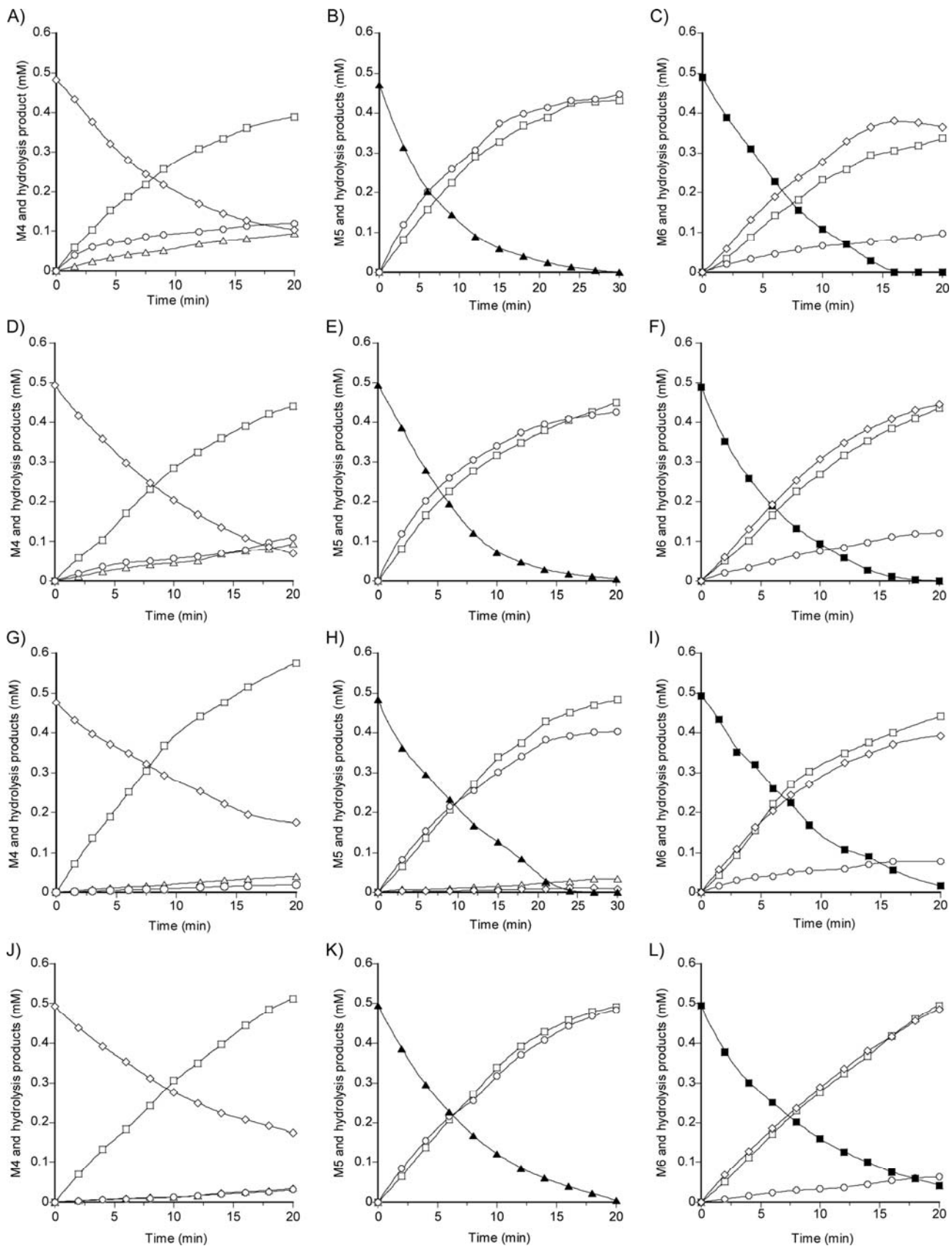
<sup>b</sup> Standard deviations were calculated from triplicate experiments

<sup>c</sup> Normalized by specificity activity towards locust bean gum galactomannan

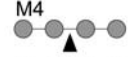

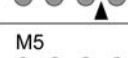
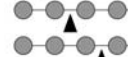
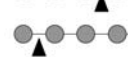




**Figure 2.** Effect of pH and temperature on activity and stability of ManA (●), ManC (■), ManAS289W (○) and ManCW283W (□) using 0.5% locust bean gum galactomannan as substrate (broken lines are used for mutants). A) pH-activity dependence for 213 nM ManA, 104 nM ManC, 276 nM ManAS289W and 249 nM ManCW283S in 40 mM Britton-Robinson. B) pH-stability dependence of 2.13 μM ManA, 1.04 μM ManC, 2.76 μM ManAS289W and 2.49 μM ManCW283S in 40 mM Britton-Robinson buffer after 3 h incubation at 37°C. C) Temperature-activity dependence for the same enzyme concentrations as in A. D) Thermal stability of the same enzyme concentrations as in B at 20–80°C after 3 h incubation in 50 mM sodium acetate pH 5.5. Each experiment was made in triplicate. Standard deviations are shown as error bars.

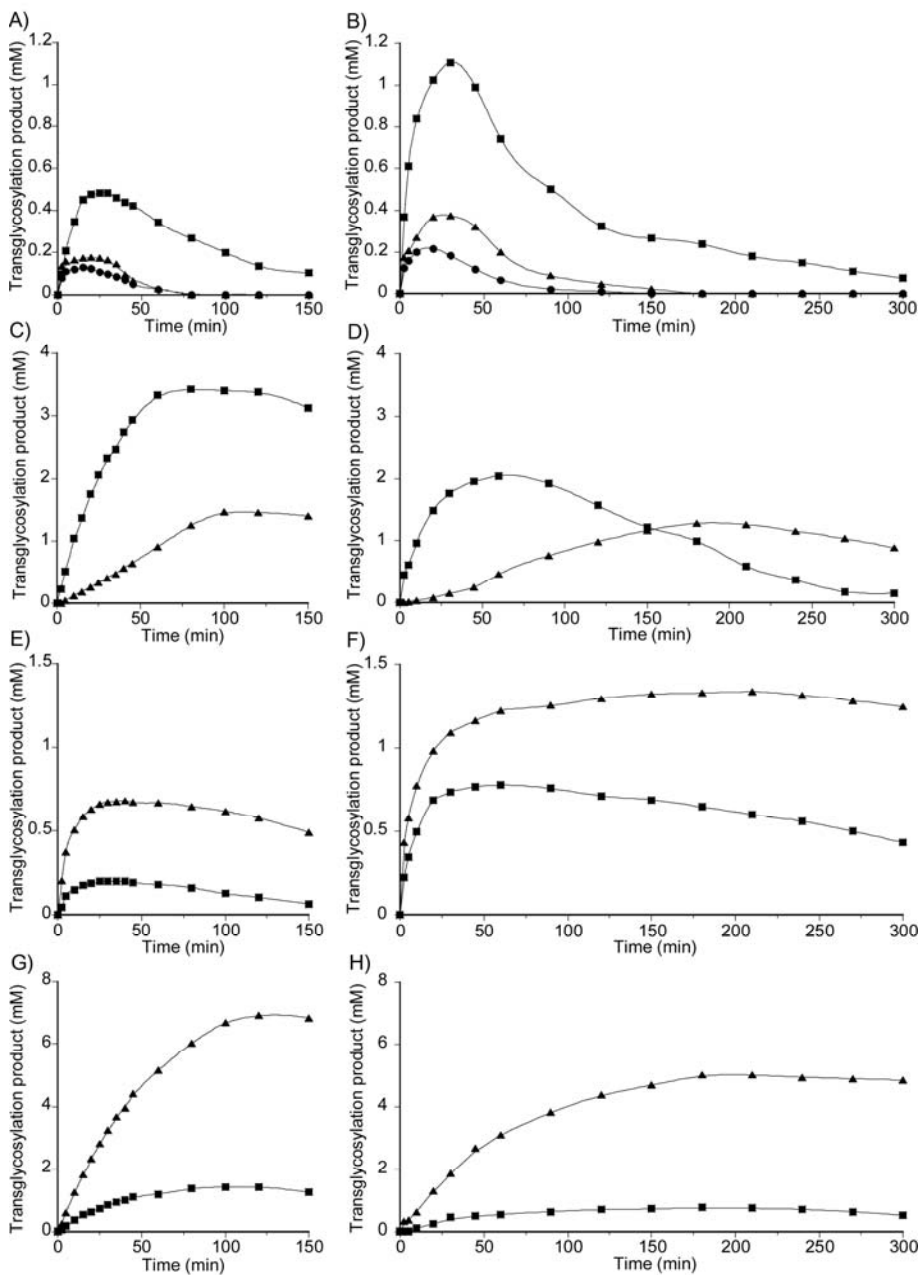




**Figure 3.** Hydrolysis action patterns of ManA (A–C), ManAS289W (D–F), ManC (G–I), and ManCW283S (J–L) towards 0.5 mM M4–M6 in 100 mM sodium acetate pH 5.5 at 37°C. A) 60 nM ManA with M4; B) 30 nM ManA with M5; C) 10 nM ManA with M6; D) 50 nM ManAS289W with M4; E) 28 nM ManAS289W with M5; F) 12 nM ManAS289W with M6; G) 75 nM ManC with M4; H) 15 nM ManC with M5; I) 12 nM ManC with M6; J) 120 nM ManCW283S with M4; K) 32 nM ManCW283S with M5; L) 20 nM ManCW283S with M6. M1 ( $\Delta$ ); M2 ( $\square$ ); M3 ( $\circ$ ); M4 ( $\diamond$ ); M5 ( $\blacktriangle$ ); M6 ( $\blacksquare$ ).

Substrate	ManA	ManA S289W	ManC	ManC W283S
M4 	64%	68%	91%	88%
	36%	32%	9%	12%
				
M5 	100%	100%	96%	100%
				
M6 	88%	88%	92%	94%
	12%	12%	8%	6%

**Figure 4.** Schematics of hydrolysis products from action pattern analysis (Fig. 3) after 20 min reaction by ManA, ManAS289W, ManC or ManCW283S on 0.5 mM manno-oligosaccharides. ●) Mannose residue; ▲) possible cleavage site.



**Figure 5.** Transglycosylation product formation catalysed by ManA (330 nM), ManAS289W (330 nM), ManC (145 nM), and ManCW283S (145 nM) using 30 mM M4 (A–D) or 24 mM M4 as donor with 100 mM M3 as acceptor (E–H) in 100 mM sodium acetate pH 5.5 at 37°C. M5 (▲); M6 (■); M7 (●).

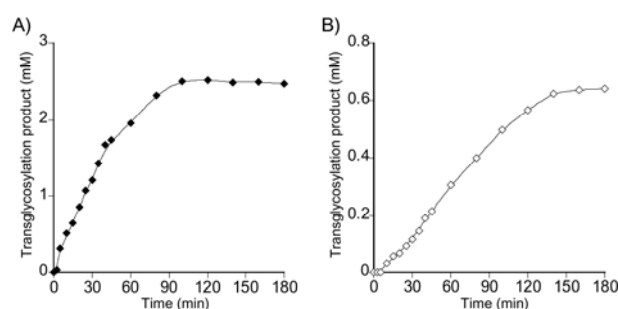
### 3.4 Identification of carbohydrate acceptors for production of novel manno-oligosaccharides

The specificity of ManA and ManC determined by screening with 12 mono-, 15 di-, and 9 trisaccharide acceptor candidates (400 mM; all listed in 2.8) with M4 (14 mM) as donor. ManC transglycosylated M3, isomaltotriose and melezitose, while none of the monosaccharides and disaccharides served as acceptors during 30 min reaction. ManA only used M3 as acceptor. These findings suggest that ManA and ManC require binding at subsite +3 for functional accommodation of an acceptor in transglycosylation. This behaviour is supported by kinetics analysis on manno-oligosaccharides showing poor affinity for M4 while  $K_M$  was 0.6–2.9 mM for M5 and M6 (Table 1) most probably occupying subsite +3 (Fig. 3 and 4). No crystal structure is reported of GH5 endo- $\beta$ -1,4-mannanase with sugar bound at subsite +3, but the models (Fig. 1) suggest ManA Tyr259 and ManC Trp253 are surface exposed and may stack onto a trisaccharide acceptor at subsite +3. An aromatic residue is conserved at this position in fungal GH5 endo- $\beta$ -1,4-mannanases suggesting this site has functional importance in recognition of substrate.

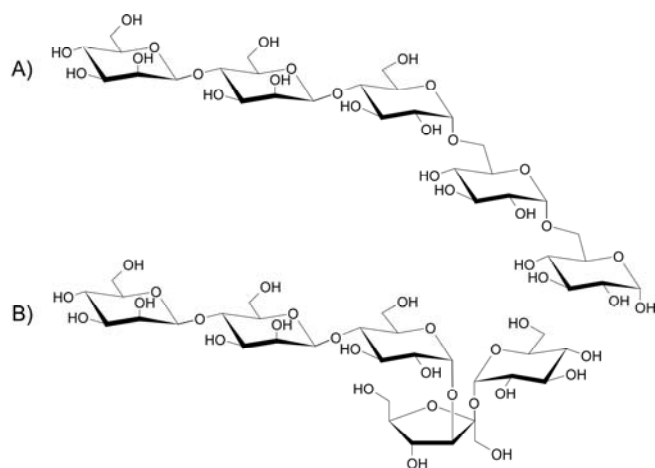
ManC gave highest transglycosylation yields and was used to generate oligosaccharide products from 24 mM M4 with 200 mM isomaltotriose or melezitose as acceptor (Fig. 6) for NMR structure determination. Two products were obtained in a ratio of about 5:1 with each acceptor due to transfer of mannobiose and mannotriose to give highest yield (sum of penta- and hexasaccharide products) of manno-isomaltotriose and manno-melezitose of 2.51 and 0.64 mM after 120 and 180 min reaction (Fig. 6) calculated to 10% and 3% total yields, respectively, based on the donor concentration. MALDI-TOF MS showed molecular mass with  $\text{Na}^+$  adducts of the products with M3 (100 mM), isomaltose and melezitose to be  $m/z$  851 and 1013 (Supplementary Fig. S4) indicating the predominant and minor products to be a pentasaccharide and a hexasaccharide, respectively.

The structures of the major transglycosylation products: mannobiosyl-

isomaltotriose, mannobiosyl-melezitose, and M5 were assigned by 2D NMR (Supplementary Table S2). Similarly to M5, the mannobiosyl-isomaltotriose ( $\beta$ -mannopyranosyl-(1 $\rightarrow$ 4)- $\beta$ -mannopyranosyl-(1 $\rightarrow$ 4)- $\alpha$ -glucopyranosyl-(1 $\rightarrow$ 6)- $\alpha$ -glucopyranosyl-(1 $\rightarrow$ 6)- $\alpha$ -glucopyranoside; Fig. 7A) and mannobiosyl-melezitose ( $\beta$ -mannopyranosyl-(1 $\rightarrow$ 4)- $\beta$ -mannopyranosyl-(1 $\rightarrow$ 4)- $\alpha$ -glucopyranosyl-(1 $\rightarrow$ 3)- $\beta$ -fructofuranosyl-(2 $\rightarrow$ 1)- $\alpha$ -glucopyranoside; Fig. 7B) showed a  $\beta$ -1,4 linkage between the mannobiosyl and trisaccharide acceptor, as identified by the downfield shift of the C4, indicating  $\beta$ -1,4 regioselectivity. Noticeably, mannobiosyl-melezitose also contained minor compounds identified as mannobiosyl 1,6 linked to the fructosyl group, as indicated by the downfield shift of the C6 in fructose residue, and two mannobiosyl groups linked to one melezitose acceptor, which appeared as a small peak at  $m/z$  1175.3 in MALDI-TOF MS (Supplementary Fig. S4E). The minor transglycosylation products: mannotriosyl-isomaltotriose and mannotriosyl-melezitose, could not be purified in sufficient amounts enabling the 2-D NMR analysis. MALDI-MS, however, identified that these products were  $\text{Na}^+$  adducts of hexasaccharides (Supplementary Fig. S4D,F).



**Figure 6.** Progress of total transglycosylation products (sum of penta- and hexasaccharide products) formation catalysed by ManC (145 nM) using 30 mM M4 with 200 mM isomaltotriose (A) or 200 mM melezitose (B) in 100 mM sodium acetate pH 5.5 at 37°C during 180 min.



**Figure 7.** Structure of novel manno-oligosaccharides. A)  $\beta$ -Manp-(1 $\rightarrow$ 4)- $\beta$ -Manp-(1 $\rightarrow$ 4)- $\alpha$ -Glc p-(1 $\rightarrow$ 6)- $\alpha$ -Glc p-(1 $\rightarrow$ 6)- $\alpha$ -Glc p; B)  $\beta$ -Manp-(1 $\rightarrow$ 4)- $\beta$ -Manp-(1 $\rightarrow$ 4)- $\alpha$ -Glc p-(1 $\rightarrow$ 3)- $\beta$ -Furf-(2 $\rightarrow$ 1)- $\alpha$ -Glc p.

#### 4. Conclusion

The *A. nidulans* FGSC A4 endo- $\beta$ -1,4-mannanase ManC showed 30–80% and 2–3 fold higher activity towards mannans and catalytic efficiency towards manno-oligosaccharides, respectively, compared to ManA and moreover had eight fold higher transglycosylation capacity. While ManA seemed to have strict acceptor specificity in transglycosylation reactions and accepted only manno-oligosaccharides, ManC could also use isomaltotriose and melezitose as acceptors resulting in novel  $\beta$ -mannobiosyl- and  $\beta$ -mannotriosyl-oligosaccharides, that have interest as potential prebiotics. In ManC, Trp283 at subsite +1 is involved in both manno-oligosaccharide hydrolysis and transglycosylation. Moreover this Trp residue contributed to the polysaccharide substrate specificity by discriminating the mannans with varying degree of galactose side chain substitution as well as glucose backbone composition.

#### Acknowledgements

Anne Blicher is thanked for amino acid analysis. We are grateful to Atsuo Kimura for providing isomaltotriose and to Louise Enggaard Rasmussen for maintaining the *Pichia pastoris* transformant strains. Jørn Dalgaard Mikkelsen and

Anne Meyer are thanked for discussions on the enzymes. The spectra at 800 MHz were obtained on the Bruker Avance 800 spectrometer of the Danish Instrument Center for NMR Spectroscopy of Biological Macromolecules. Bent O. Petersen and Jens Ø. Duus are thanked for assisting with NMR assignments. This study was supported by the Danish Strategic Research Council's Committee on Food and Health (FøSu, to the project 'Biological Production of Dietary Fibres and Prebiotics' no. 2101-06-0067), the Carlsberg Foundation, the Danish Research Council for Natural Sciences, the Centre for Advanced Food Studies and an H.C. Ørsted postdoctoral fellowship from DTU (M.J.B.).

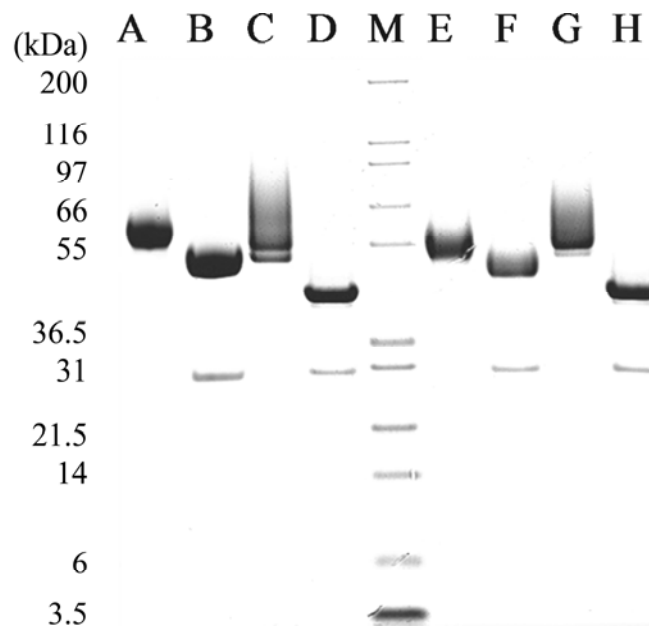
#### References

- [1] L.R.S. Moreira, E.X.F. Filho, An overview of mannan structure and mannan-degrading enzyme systems, *Appl. Microbiol. Biot.* 79 (2008) 165–178.
- [2] S. Dhawan, J. Kaur, Microbial mannanases: An overview of production and applications, *Crit. Rev. Biotechnol.* 27 (2007) 197–216.
- [3] R. Schroder, R.G. Atkinson, R.J. Redgwell, Re-interpreting the role of endo- $\beta$ -mannanases as mannan endotransglycosylase/hydrolases in the plant cell wall, *Ann. Bot.* 104 (2009) 197–204.
- [4] K.W. Waldron, C.B. Faulds, Cell wall polysaccharides: composition and structure, in: J. P. Kamerling, G-J. Boons, Y.C. Lee, A. Suzuki, N. Taniguchi, A.G.J. Voragen (Eds.), *Comprehensive glycoscience/Introduction to Glycoscience Synthesis of Carbohydrates*, vol. 1, Elsevier, Oxford, United Kingdom, 2007, pp 181–201.
- [5] I. Asano, K. Hamaguchi, S. Fujii, H. Iino, *In vitro* digestibility and fermentation of manno-oligosaccharides from coffee mannan, *Food Sci. Technol. Res.* 9 (2003) 62–66.
- [6] U. Hoshino-Takao, S. Fujii, A. Ishii, L.K. Han, H. Okuda, T. Kumao, Effects of manno-oligosaccharides from coffee mannan on blood pressure in Dahl salt-sensitive rats, *J. Nutr. Sci. Vitaminol.* 54 (2008) 181–184.
- [7] T. Kumao, S. Fujii, A. Asakawa, I. Takehara, I. Fukuhara, Effect of coffee drink containing manno-oligosaccharides on total amount of excreted fat in healthy adults, *J. Health Sci.* 52 (2006) 482–485.
- [8] R.P. de Vries, J. Visser, *Aspergillus* enzymes involved in degradation of plant cell wall polysaccharides, *Microbiol. Mol. Biol. Rev.* 65 (2001) 497–522.

- [9] B.L. Cantarel, P.M. Coutinho, C. Rancurel, T. Bernard, V. Lombard, B. Henrissat, The Carbohydrate-Active EnZymes database (CAZy): an expert resource for glycogenomics, *Nucleic Acids Res.* 37 (2009) D233–D238.
- [10] D. Hogg, G. Pell, P. Dupree, F. Goubet, S.M. Martin-Orue, S. Armand, H.J. Gilbert, The modular architecture of *Cellvibrio japonicus* mannanases in glycoside hydrolase families 5 and 26 points to differences in their role in mannan degradation. *Biochem. J.* 371 (2003) 1027–1043.
- [11] P. Ademark, A. Varga, J. Medve, V. Harjunpää, T. Drakenberg, F. Tjerneld, H. Stålbrand, Softwood hemicellulose-degrading enzymes from *Aspergillus niger*: Purification and properties of a  $\beta$ -mannanase, *J. Biotechnol.* 63 (1998) 199–210.
- [12] M. Evodia Setati, P. Ademark, W.H. van Zyl, B. Hahn-Hagerdal, H. Stålbrand, Expression of the *Aspergillus aculeatus* endo- $\beta$ -1,4-mannanase encoding gene (*man1*) in *Saccharomyces cerevisiae* and characterization of the recombinant enzyme, *Protein Expres. Purif.* 21 (2001) 105–114.
- [13] H. Stålbrand, M. Siika-Aho, M. Tenkanen, L. Viikari, Purification and characterization of two  $\beta$ -mannanases from *Trichoderma reesei*, *J. Biotechnol.* 20 (1993) 229–242.
- [14] B.Z. Xu, P. Hägglund, H. Stålbrand, J.C. Janson, Endo- $\beta$ -1,4-mannanases from blue mussel, *Mytilus edulis*: purification, characterization, and mode of action, *J. Biotechnol.* 92 (2002) 267–277.
- [15] L. Anderson, P. Hägglund, D. Stoll, L. Lo Leggio, T. Drakenberg, H. Stålbrand, Kinetics and stereochemistry of the *Cellulomonas fimi*  $\beta$ -mannanase studied using H-1-NMR, *Biocatal. Biotransfor.* 26 (2008) 86–95.
- [16] A.M. Larsson, L. Anderson, B.Z. Xu, I.G. Munoz, I. Uson, J.C. Janson, H. Stålbrand, J. Stahlberg, Three-dimensional crystal structure and enzymic characterization of  $\beta$ -mannanase Man5A from blue mussel *Mytilus edulis*, *J. Mol. Biol.* 357 (2006) 1500–1510.
- [17] E. Sabini, H. Schubert, G. Murshudov, K.S. Wilson, M. Siika-Aho, M. Penttilä, M. The three-dimensional structure of a *Trichoderma reesei*  $\beta$ -mannanase from glycoside hydrolase family 5, *Acta Crystallogr. D.* 56 (2000) 3–13.
- [18] L.E. Tailford, V.M.A. Ducros, J.E. Flint, S.M. Roberts, C. Morland, D.L. Zechel, N. Smith, M.E. Bjornvad, T.V. Borchert, K.S. Wilson, G.J. Davies, H.J. Gilbert, Understanding how diverse  $\beta$ -mannanases recognize heterogeneous substrates, *Biochemistry* 48 (2009) 7009–7018.
- [19] G.M. Gübitz, M. Hayn, M. Sommerauer, W. Steiner, Mannan-degrading enzymes from *Sclerotium rolfsii*: Characterisation and synergism of two endo  $\beta$ -mannanases and a  $\beta$ -mannosidase. *Bioresour. Technol.* 58 (1996) 127–135.
- [20] Y.L. Zhang, J.S. Ju, H. Peng, F. Gao, C. Zhou, Y. Zeng, Y.F. Xue, Y. Li, B. Henrissat, G.F. Gao, Y.H. Ma, Biochemical and structural characterization of the intracellular mannanase *AaManA* of *Alicyclobacillus acidocaldarius* reveals a novel glycoside hydrolase family belonging to clan GH-A, *J. Biol. Chem.* 283 (2008) 31551–31558.
- [21] G. Davies, B. Henrissat, Structures and mechanisms of glycosyl hydrolases, *Structure* 3 (1995) 853–859.
- [22] B. Henrissat, G. Davies, Structural and sequence-based classification of glycoside hydrolases, *Curr. Opin. Struct. Biol.* 7 (1997) 637–644.
- [23] V. Harjunpää, A. Teleman, M. Siikaaho, T. Drakenberg, Kinetic and stereochemical studies of manno-oligosaccharide hydrolysis catalysed by  $\beta$ -mannanases from *Trichoderma reesei*, *Eur. J. Biochem.* 234 (1995) 278–283.
- [24] V. Harjunpää, J. Helin, A. Koivula, M. Siika-aho, T. Drakenberg, A comparative study of two retaining enzymes of *Trichoderma reesei*: transglycosylation of oligosaccharides catalysed by the cellobiohydrolase I, Cel7A, and the  $\beta$ -mannanase, Man5A, *FEBS Lett.* 443 (1999) 149–153.
- [25] M. Hrmova, R.A. Burton, P. Biely, J. Lahnstein, G.B. Fincher, Hydrolysis of (1,4)- $\beta$ -D-mannans in barley (*Hordeum vulgare* L.) is mediated by the concerted action of (1,4)- $\beta$ -D-mannan endohydrolase and  $\beta$ -D-mannosidase, *Biochem. J.* 399 (2006) 77–90.
- [26] H.J. Gilbert, H. Stålbrand, H. Brumer, How the walls come crumbling down: recent structural biochemistry of plant polysaccharide degradation, *Curr. Opin. Plant Biol.* 11 (2008) 338–348.
- [27] J. Le Nours, L. Anderson, D. Stoll, H. Stålbrand, L. Lo Leggio, The structure and characterization of a modular endo- $\beta$ -1,4-mannanase from *Cellulomonas fimi*, *Biochemistry* 44 (2005) 12700–12708.
- [28] J. E. Galagan, S.E. Calvo, C. Cuomo, L.J. Ma, J.R. Wortman, S. Batzoglou, S.I. Lee, M. Bastuerkmen, C.C. Spevak, J. Clutterbuck, V. Kapitonov, J. Jurka, C. Sczzocchio, M.L. Farman, J. Butler, S. Purcell, S. Harris, G.H. Braus, O. Draht, S. Busch, C. D'Enfert, C. Bouchier, G.H. Goldman, D. Bell-Pedersen, S. Griffiths-Jones, J.H. Doonan, J.Yu, K. Vienken, A. Pain, M. Freitag, E.U. Selker, D.B Archer, M.A. Penalva, B.R. Oakley, M. Momany, T. Tanaka, T. Kumagai, K. Asai, M. Machida, W.C. Nierman, D.W. Denning, M.X. Caddick, M. Hynes, M. Paoletti, R. Fischer, B.L. Miller, P.S. Dyer, M.S. Sachs, S.A. Osmani, B.W. Birren, Sequencing of *Aspergillus nidulans* and comparative analysis with *A. fumigatus* and *A. oryzae*, *Nature* 438 (2005) 1105–1115.

- [29] S. Bauer, P. Vasu, S. Persson, A.J. Mort, C.R. Somerville, Development and application of a suite of polysaccharide-degrading enzymes for analyzing plant cell walls, *PNAS* 130 (2006) 11417–11422.
- [30] S.F. Altschul, T.L. Madden, A.A. Schäffer, J. Zhang, Z. Zhang, W. Miller, D.J. Lipman, Gapped BLAST and PSI-BLAST: a new generation of protein database search programs, *Nucleic Acids Res.* 25 (1997) 3389–3402.
- [31] J. Söding, A. Biegert, L.N. Lupas, The HHpred interactive server for protein homology detection and structure prediction, *Nucleic Acids Res.* 33 (2005) W244–W248.
- [32] I.N. Shindyalov, P.E. Bourne, Protein structure alignment by incremental combinatorial extension (CE) of the optimal path, *Protein Eng.* 11 (1998) 739–747.
- [33] B. Wallner, A. Elofsson, Can correct protein models be identified?, *Protein Sci.* 2003. 12: 1073–1086.
- [34] M. Hilge, S.M. Gloor, W. Rypniewski, O. Sauer, T.D. Heightman, W. Zimmermann, K. Winterhalter, K. Piontek, High-resolution native and complex structures of thermostable  $\beta$ -mannanase from *Thermomonospora fusca* - substrate specificity in glycosyl hydrolase family 5, *Struct. Fold Des.* 6 (1998) 1433–1444.
- [35] O. Emanuelsson, S. Brunak, G. von Heijne, H. Nielsen, Locating proteins in the cell using TargetP, SignalP, and related tools, *Nat. Protoc.* 2 (2007) 953–971.
- [36] E. Gasteiger, C. Hoogland, A. Gattiker, S. Duvaud, M.R. Wilkins, R.D. Appel, A. Bairoch, Protein identification and analysis tools on the ExPASy Server, in: J.M. Walker (Ed.), *The Proteomics Protocols Handbook*, Humana Press, New Jersey, 2005, pp. 571–607.
- [37] N. Blom, T. Sicheritz-Ponten, R. Gupta, S. Gammeltoft, S. Brunak, Prediction of post-translational glycosylation and phosphorylation of proteins from the amino acid sequence, *Proteomics* 4 (2004) 1633–1649.
- [38] M. Dubois, K.A. Gilles, J.K. Hamilton, P.A. Rebers, F. Smith, Colorimetric method for determination of sugars and related substances, *Anal. Chem.* 28 (1956) 350–356.
- [39] G.L. Miller, Use of dinitrosalicylic acid reagent for determination of reducing sugar, *Anal. Chem.* 31 (1959) 426–428.
- [40] A.F. Mohun, I.J.Y. Cook, An improved dinitrosalicylic acid method for determining blood and cerebrospinal fluid sugar levels, *J. Clin. Pathol.* 15 (1962) 169–180.
- [41] H.T.K. Britton, R.A. Robinson, Universal buffer solutions and the dissociation constant of veronal, *J. Chem. Soc.* (1931) 1456–1462.
- [42] R.F. McFeeters, A manual method for reducing sugar determinations with 2,2'-bicinchoninate reagent, *Anal. Biochem.* 103 (1980) 302–306.
- [43] H. Mori, K.S. Bak-Jensen, T.E. Gottschalk, M.S. Motawia, I. Damager, B.L. Moller, B. Svensson, Modulation of activity and substrate binding modes by mutation of single and double subsites+1/+2 and -5/-6 of barley  $\alpha$ -amylase 1, *Eur. J. Biochem.* 268 (2001) 6545–6558.
- [44] H. Rantanen, L. Virkki, P. Tuomainen, M. Kabel, H. Schols, M. Tenkanen, Preparation of arabinoxylobiose from rye xylan using family 10 *Aspergillus aculeatus* endo-1,4- $\beta$ -D-xylanase, *Carbohydr. Polym.* 68 (2007) 350–359.
- [45] I. Arisan-Atac, R. Hodits, D. Kristufek, C.P. Kubicek, Purification, and characterization of a  $\beta$ -mannanase of *Trichoderma reesei* C-30, *Appl. Microbiol. Biot.* 39 (1993) 58–62.
- [46] P. Häggglund, T. Eriksson, A. Collen, W. Nerinckx, M. Claeysens, H. Stålbrand, A cellulose-binding module of the *Trichoderma reesei*  $\beta$ -mannanase Man5A increases the mannan-hydrolysis of complex substrates, *J. Biotechnol.* 101 (2003) 37–48.
- [47] V. Puchart, M. Vrsanská, P. Svoboda, J. Pohl, Z.B. Ogel, P. Biely, Purification and characterization of two forms of endo- $\beta$ -1,4-mannanase from a thermotolerant fungus, *Aspergillus fumigatus* IMI 385708 (formerly *Thermomyces lanuginosus* IMI 158749), *Biochim. Biophys. Acta.* 1674 (2004) 239–250.
- [48] C. Notredame, D.G. Higgins, J. Heringa, T-Coffee: A novel method for fast and accurate multiple sequence alignment, *J. Mol. Biol.* 302 (2000) 205–217.
- [49] P. Gouet, E. Courcelle, D.I. Stuart, F. Metoz, ESPript: multiple sequence alignments in PostScript, *Bioinformatics* 15 (1999) 305–308.

Supplementary documents



**Supplementary Figure S1.** SDS-PAGE of purified and deglycosylated ManA, ManC, ManAS289W and ManCW283S; Lane A, 7  $\mu$ g ManCW283S; Lane B, 7  $\mu$ g deglycosylated ManCW283S; Lane C, 5  $\mu$ g ManAS289W; Lane D, 5  $\mu$ g deglycosylated ManAS289W; Lane E, 5  $\mu$ g ManC; Lane F, 5  $\mu$ g deglycosylated ManC; Lane G, 5  $\mu$ g ManA; Lane H, 5  $\mu$ g deglycosylated ManA; M, Marker: Mark12 unstained protein standard marker (Invitrogen); endoglycosidase H migrates as a 29 kDa band seen in lane B, D, F, and H.

**ManC**  $\alpha 0$   $\beta 1$   $\beta 2$   $\beta 3$

1 10 20 30 40

```

ManC M..IFSTLLSLALLA.....TTATARKGFVITKCKDKFLDKGKDFYFAGSNA
ManA M.KFSQALLSLASLA..LAAALPHASTPVYTPSTTPSPPTPSASGSFATTSKIQFVIDGEAGYFPGSNA
HjMan5A_1qnr MMMLSKSLLSAATAASALAAVL.....QPVPRAS.SFVTISGTFNIDGKVGYFAGTNC
SlMan4_1rh9 M..NNSIILIFVAIILIFPNEFSKP.....TRAFSNNNFVYTDGTHFALNGKSLYINGFNA
CmMan5A_1luuq MKNIIAIVIVGFVSILLLAACDKKTPVAESNSAVAPTANVATSPAHEHFVRVNGGHFELQGKPYVITGVNM
MeMan5A_2c0h M.....LLTALAVLFA.....STGCQARLSVSGTNLNLYNGHHIFLSGANQ
TfMan_1bqc .....GLHVKNKRLYEANGOEFIIRGVSH

```

**ManC**  $\alpha 1$

50 60 70 80 90 100

```

ManC ...YYFFP.....NNQTDVELGLSAAKKAGLLVFRWGFNDKNVYIYEDGLPYGEGGAGTTEVV
ManA ...YWIGF.....LKNNSDVLDFDHMASSGLRILRWGFNDVNNTA.....PDG.....SVY
HjMan5A_1qnr ...YWCFS.....LTNHADVSTFHSISSGLKVVRRWGFNDVNTQ.....PSFG.....QIW
SlMan4_1rh9 ...YWLMY.....IAYDPSTRIKVTNTFQQAASKYKMNVARWAFSHGGSRFLQ...SAPG.....
CmMan5A_1luuq ...YWYAA...LGAPNEVGDRDLAKELDNLKAIQVNNLRWLVAVSEKSEINSA...VWPA.....
MeMan5A_2c0h ...AWVNYARDFGHNQYSKGGKSTFESTLSDIQSHGGMNSVRLHLEGEST.....PEFD.....
TfMan_1bqc PHNWYPQH.....TQAFADIKSHGANTVRLVLSNG.....VWWS.....

```

**ManC**  $\alpha 2$   $\beta 4$

110 120 130 140 150

```

ManC FQWWQNGTSTID...LDFDKVNNAAKRTGKILVTLVNWADYGGMDVYTVNLGG.....
ManA FQLHQDGKSTINTGKDLRLDYVHSAEKHGKILINFWNYWDDYGGMAYMAYRG.....
HjMan5A_1qnr FQKLSATGSTINTGADGLGLDYVISEAKKYGHLIMSLVNWDAFGGKKQYVEWAVQRGKL.....
SlMan4_1rh9 .....VYNEQMFGLDFVISEAKKYGHLIMSLVNWDAFGGKKQYVEWAVQRGKL.....
CmMan5A_1luuq .....VINGFGNYDETLGLDYLLVLEAKRDMTVVLYFNFWQWSSGGMQYMAWIEGEPVQDPNVINEW
MeMan5A_2c0h .....NNGYVIGDNTLIDMRAVLAARHN...LILFFLWNGA.....PEFD.....
TfMan_1bqc .....KNGPQVAVVLSLCKQNR...LILCML.....

```

**ManC**  $\alpha 3$   $\beta 5$

160 170 180 190

```

ManC ...QYHDDF...RLPQKKAYKRYVKEMVTR.....YRNSPAIMAWELANEPKRC.....
ManA ...GDKADW...ENEGIQAAVQAYVEAVVVR.....YINSTAVFAWELANEPKRC.....
HjMan5A_1qnr ...GNATTWY...TNTAQTQYRKYVCAVVR.....YANSTAFWELANEPKRC.....
SlMan4_1rh9 ...TSDDDFY...TNPVVRGFYKNNVAVLTVRNVNITKVAYKDDPTILSWELANEPKRC.....
CmMan5A_1luuq EAFMAKSASFY...RSEKARQEYRKTLEKIIITRVNSINGKAYVDDATIMSWQLANEPKRC.....
MeMan5A_2c0h ...VKQSTHRLNGLMVDTRKLSQYIDHAKPMANA.....LNKEKALGGWDTNNEPGEIKPFGES
TfMan_1bqc ...VHDTTGY...GEQSGASTLQAVDYWIE.LKSV...LQGEEDYVLIINNEPVG.....

```

**ManC**  $\alpha 4$

200 210 220 230 240 250

```

ManC .....GADGVRNLPASDECTPELTLTSWIDEMSTYVRRLDPE...HHLVTVWCGEG.GFNYSDD..
ManA .....TGCEPSVLHNWIEKTSAFIKGLDE...KHLVLCIGDEGFGLDTGSD..
HjMan5A_1qnr .....NGCSTDIVQWATSVSQYVKSLS...NHLVTLGDEGLGLSTG.D..
SlMan4_1rh9 .....PSDLGKTFQNWLEMAAGYKLSLDS...NHLLEIGLEGF...YGNDMR
CmMan5A_1luuq .....GNSQT...TAEKQIYIDVHAAAAYIKTLDA...HHLVSSGSEG.EMGSVNDMQ
MeMan5A_2c0h SSEPCPDTRHLSGSGAGWAGHLYSAQEIGRFVNW...QAAAIKEVDPE...GAMVTVGSWNKADTDA..
TfMan_1bqc .....NDSATVAAAGW...DTSAALQRLRAAGFEHTLVVDAPNWGQDWTNTR

```

**ManC**  $\alpha 5$

260 270 280 290 300

```

ManC .DWAYNGSDGGDF.EAELRLKNIDFGVSHSYPDWWS.....KIVIEWTNKW.....IVDHAARAARRVGGK
ManA GSYFPQYTEGSDFAAALIDTIDFGTSHLYPDSWG.....TNDWGLW.....ITSHAACAAAGK
HjMan5A_1qnr GAYPYTYGEGTDF.AKNVTKSLDFGTSHLYPDSWG.....TNYTWGNGW.....IQTHAAACLAAGK
SlMan4_1rh9 QYNPNYSYIFGNTF..ISNNVQGGIDFAITHMYPNQWLPGLTQEAQDKWASQW.....IQVHIDDSKMLK
CmMan5A_1luuq .....VF..DAHAATPDIDYLYTHMWRINWSWFDKTKPAETWPSAWEKAQNYMRAHIDVAKLNLK
MeMan5A_2c0h MGFHNLSYDHCVLKAGGKSGTLSFYQVHTY..DWQ.....NHFGNES.....PFKHFSNFRLLK
TfMan_1bqc NNADQVY.....ASDPTGNTV..FSSHMY.....GVYSQAST.ITSYLHFVNAAGL

```

**ManC**  $\beta 6$   $\alpha 6$

310 320 330 340 350 360

```

ManC PVVHEEYKWLTPQGRLDNLGTVS..NITREAVGGWQISISLREK..MSDMFW...FGYSGYSYG...
ManA PCVLEEXGVTS.....NHCAIEK..QWQNAALNATGIAADLYW...CYGDTLSSGP...
HjMan5A_1qnr PCVFEEXGAQO.....NPNCTNEA..PWQTTSLTTRGMGGDMFW...CWGDTFANGA...
SlMan4_1rh9 PLLIAEFCGSTKTPGY...TVAKRDNYFEKIYGTIFNCAKSGGPGCGGLFW...CVLGGQMS...
CmMan5A_1luuq PLLVLEFCGLDRDMGYSAMDSTTEYRDNYFRGVFELMLASLEQGGESAGYNIW...ANWNGYRTRANY
MeMan5A_2c0h PMVIGENQLDRHAGMSS.....ESMFEWAY.....TKGYSAGWTSRRTDVWNNQLRGIQHL
TfMan_1bqc PLLIIGFCGHDSHDGNPDDETIMA.....EAERLKLGYIGW...WSGNGGGVVEYLD

```

**ManC**  $\alpha 7$

370 380 390

```

ManC ...RNHDD.....GFTIYLDAAEQELVYKHAKEVKNLNR...
ManA ...SPDD.....GNTFYGGSEEFELVNHVETIERSAK...
HjMan5A_1qnr ...QNSD.....PYTVWYNSNNWQCLVKNHVDIAINGGTTTPPPVSSSTTTSSRTSSPPPPGGSC
SlMan4_1rh9 ...SFD...GYQVVLQESPSTRVI...
CmMan5A_1luuq WWQEGDDFMGDDPPPEEQGMYGVFDTDTSTIAIMKEFNARFPK...
MeMan5A_2c0h ...KSRD...HGQVQFGL...
TfMan_1bqc MVYVFDGDNLSPWG...

```

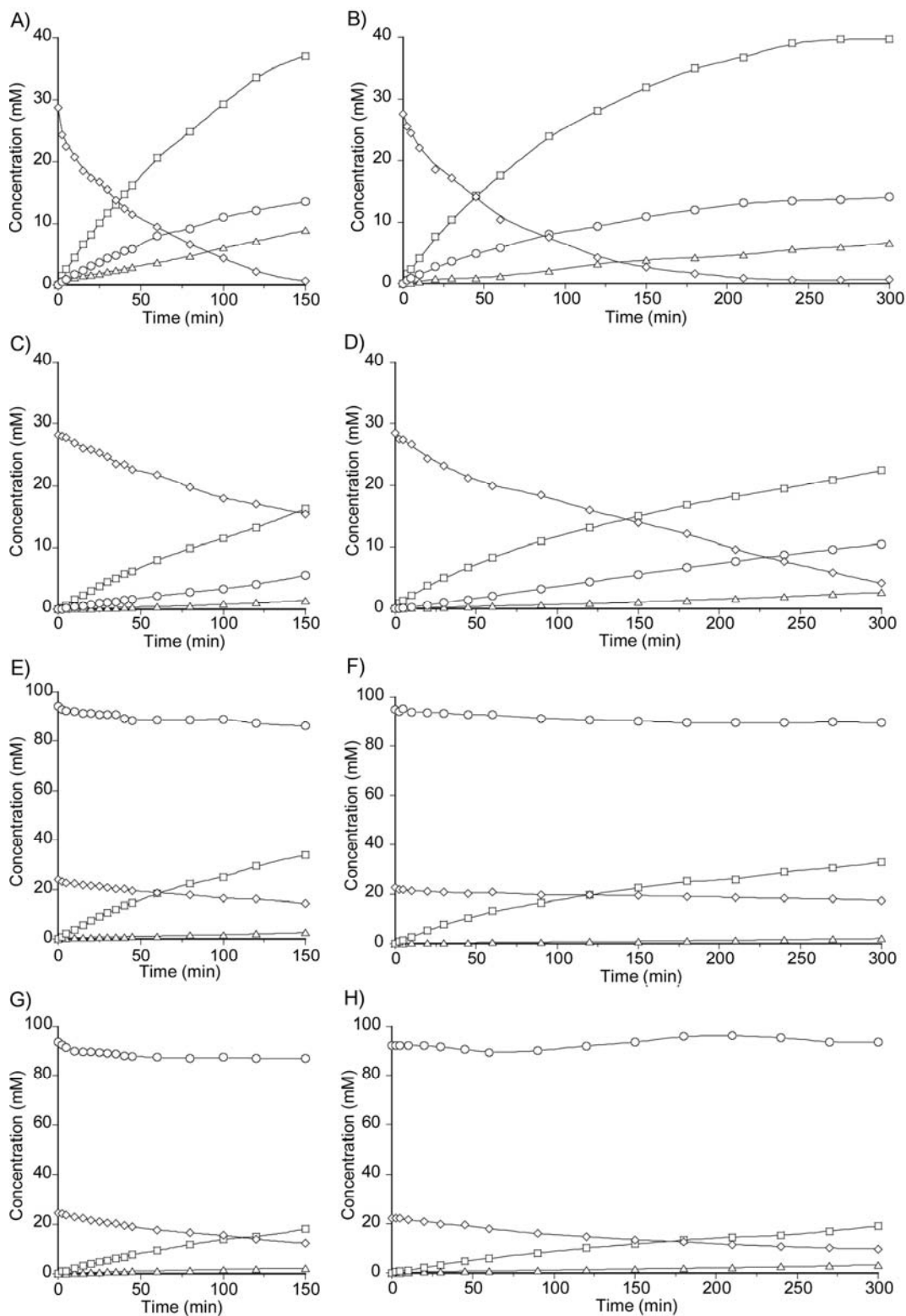


```

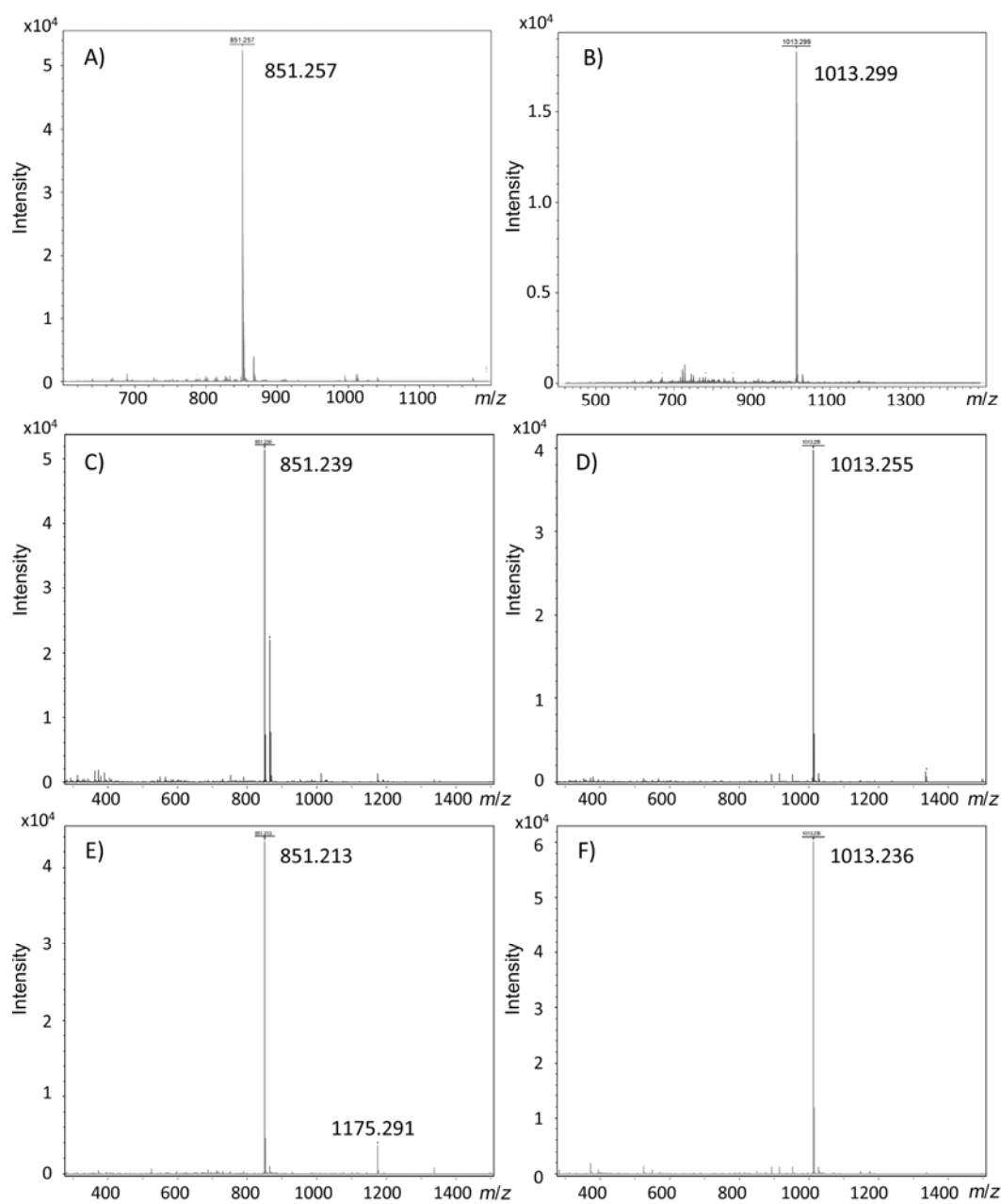
ManC
ManC
ManA
HjMan5A_1qnr  SPLYGQCGGSGYTGPTCCAQGTCTIYSNYWYSQCLNT
SlMan4_1rh9   .....LLQSLAL
CmMan5A_1uuq  .....
MeMan5A_2c0h  .....
TfMan_1bqc    .....

```

**Supplementary Figure S2.** Amino acid sequence alignment of ManA and ManC from *A. nidulans* FGSC A4 and GH5 endo- $\beta$ -1,4-mannanases with reported crystal structures from *Hypocrea jecorina* (HjMan5A\_1qnr; UniProt ID: Q99036), *Solanum lycopersicum* (SlMan4\_1rh9; UniProt ID: Q8L5J1), *Cellvibrio mixtus* (CmMan5A\_1uuq; UniProt ID: Q6QT42), *Mytilus edulis* (MeMan5A\_2c0h; UniProt ID: Q8WPJ2), and *Thermobifida fusca* KW3 (TfMan\_1bqc; UniProt ID: Q9ZF13). The sequence alignment was performed using T-Coffee (<http://tcoffee.vital-it.ch/cgi-bin/Tcoffee/tcoffee.cgi/index.cgi>) [49] and visualised using Easy Sequencing in Postscript (<http://escript.ibcp.fr/ESPrpt/ESPrpt>) [50]; ▼) possible subsite -2 location; ▼) possible subsite +1 and +2 location; ▼) possible subsite +3 location; ▼) mutation position (subsite +1) in present work.



**Supplementary Figure S3.** Progress of transglycosylation reactions (substrates and hydrolysis products) of ManA, ManAS289W, ManC and ManCW283S using 30 mM M4 (A–D) or 24 mM M4 with 100 mM M3 (E–H). A) 330 nM ManA; B) 330 nM ManAS289W; C) 145 nM ManC; D) 145 nM ManCW283S; E) 330 nM ManA; F) 330 nM ManAS289W; G) 145 nM ManC; H) 145 nM ManCW283S; M1, ( $\Delta$ ); M2, ( $\square$ ); M3, ( $\circ$ ); M4, ( $\diamond$ ).



**Supplementary Figure S4.** Molecular masses of transglycosylation products as Na<sup>+</sup> adduct (mass range 300–1500 *m/z*). A), M5: 851.3 *m/z*; B), M6: 1013.3 *m/z*; C), mannbiosyl isomaltotriose: 851.2 *m/z*; D), mannotriosyl isomaltotriose: 1013.3 *m/z*; E), mannbiosyl melezitose: 851.2 *m/z*; F), mannotriosyl melezitose: 1013.2 *m/z*.

**Supplementary Table S1** Primers for construction of the expression plasmids for ManA, ManC, ManAS289W, and ManCW283S

Primer name	Primer sequence	Restriction site
<u>ManA</u>		
Sense	GGGGAATTCCTCCCTCACGCGTCAACACCTGTGTACAC <sup>a</sup>	EcoRI
Antisense	CCC <u>GCGGCCGC</u> CTACTTGGCACTCCTCTCAATCGTCTCG <sup>a</sup>	NotI
<u>ManC</u>		
Sense	GGGGAATTC <u>CGCAAGGG</u> CTTTGTGACCACCAAAGGCG <sup>a</sup>	EcoRI
Antisense	CCC <u>GCGGCCGC</u> CTACCGTCTCCGGTTCAACTTGTTACC <sup>a</sup>	NotI
<u>ManAS289W</u>		
Sense	CTCTACCCGGATT <u>TGGTGGGG</u> CAC <sup>b</sup>	
Antisense	GTGCCCC <u>ACCA</u> ATCCGGGTAGAG <sup>b</sup>	
<u>ManCW283S</u>		
Sense	CTATCCGGA <u>AGTTGG</u> GAGCAAGACC <sup>b</sup>	
Antisense	GGTCTTGCTCCA <u>ACT</u> ATCCGGATAG <sup>b</sup>	

<sup>a</sup> Restriction sites are underlined

<sup>b</sup> Mutation positions are double-underlined

**Supplementary Table S2** <sup>1</sup>H and <sup>13</sup>C NMR data assignment and molecular mass of β-manno-oligosaccharides produced by transglycosylation catalysed ManC using M4 as donor with isomaltotriose or melezitose as acceptor.

Compound (molecular mass) <sup>a</sup>	Chemical shifts (δ, p.p.m.)					
	H-1 C-1	H-2 C-2	H-3 C-3	H-4 C-4	H-5 C-5	H-6a/H-6b C-6
β-Manp-(1,4)-	4.70	4.01	3.60	3.51	3.39	3.89/3.68
	–	–	–	–	–	–
β-Manp-(1,4)-	4.70	4.08	3.77	3.77	3.51	3.87/3.71
	–	–	–	–	–	–
β-Manp-(1,4)-	4.70	4.08	3.77	3.77	3.51	3.87/3.71
	–	–	–	–	–	–
β-Manp-(1,4)-	4.70	4.08	3.77	3.77	3.51	3.87/3.71
	–	–	–	–	–	–
β-Manp	5.13	3.94	3.85	n.d.	n.d.	n.d.
	–	–	–	–	–	–
α-Manp ( <i>m/z</i> 851)	4.86	n.d.	n.d.	n.d.	n.d.	n.d.
	–	–	–	–	–	–
β-Manp-(1,4)-	4.79	4.14	3.82	n.d.	n.d.	n.d.
	101.2	71.0	72.4	n.d.	n.d.	n.d.
β-Manp-(1,4)-	4.75	4.08	3.68	3.58	n.d.	n.d.
	101.3	71.5	n.d.	76.1	n.d.	n.d.
α-Glcp-(1,6)-	4.98	3.62	3.91	3.71	3.85	3.78/3.86
	98.8	72.1	72.7	79.7	n.d.	61.2
α-Glcp-(1,6)-	4.98	3.60	3.75	3.52	3.93	3.79/3.98
	98.8	72.3	n.d.	n.d.	71.2	66.7
α-Glcp	5.26	3.56	n.d.	n.d.	n.d.	n.d.
	93.2	n.d.	n.d.	n.d.	n.d.	n.d.
β-Glcp	4.69	3.28	3.49	n.d.	n.d.	n.d.
( <i>m/z</i> 851)	97.2	75.0	77.1	n.d.	n.d.	n.d.
β-Manp-(1,4)-	4.75	4.12	3.81	3.55	3.55	3.97/n.d.
	100.1	69.7	71.4	66.7	n.d.	n.d.
β-Manp-(1,4)-	4.72	4.05	3.65	3.56	3.81	n.d.
	100.1	n.d.	n.d.	74.9	n.d.	n.d.
α-Glcp-(1,3)-	5.18	3.57	3.72	3.43	3.89	3.75/3.89
	100.3	71.3	72.7	76.3	72.4	60.3
β-Fruf-(2,1)-	?	–	4.31	4.32	4.06	3.99/4.12
	n.d.	103.3	82.9	73.5	79.7	70.3
α-Glcp	5.42	3.53	3.64	3.41	3.92	3.75/3.91
( <i>m/z</i> 851)	91.7	74.8	72.7	69.4	72.0	60.3

<sup>a</sup> molecular mass as Na<sup>+</sup> adduct (estimated mass + 23 *m/z*) determined by MALDI-TOF MS  
n.d., not detected.

Enzyme and Protein Chemistry (EPC) works within protein biochemistry, carbohydrate biochemistry, molecular biology, microbiology and plant biochemistry. The main activities of EPC are related to food and raw materials for food, but the methods and main strategies are relevant to various biotechnological issues. The aim is to explain the molecular mechanisms and interactions relevant for functionality and quality of foodstuffs and raw materials and to identify the biochemical mechanisms connected to health promoting and nutrition related effects of food.

Enzyme and Protein Chemistry  
Department of Systems Biology  
Technical University of Denmark  
Søltofts Plads, Building 224  
DK-2800 Kgs. Lyngby  
Denmark

Phone: +45 4525 2731  
Fax: +45 4588 6307

[www.epc.bio.dtu.dk](http://www.epc.bio.dtu.dk)

ISBN-nr. 978-879149-488-8

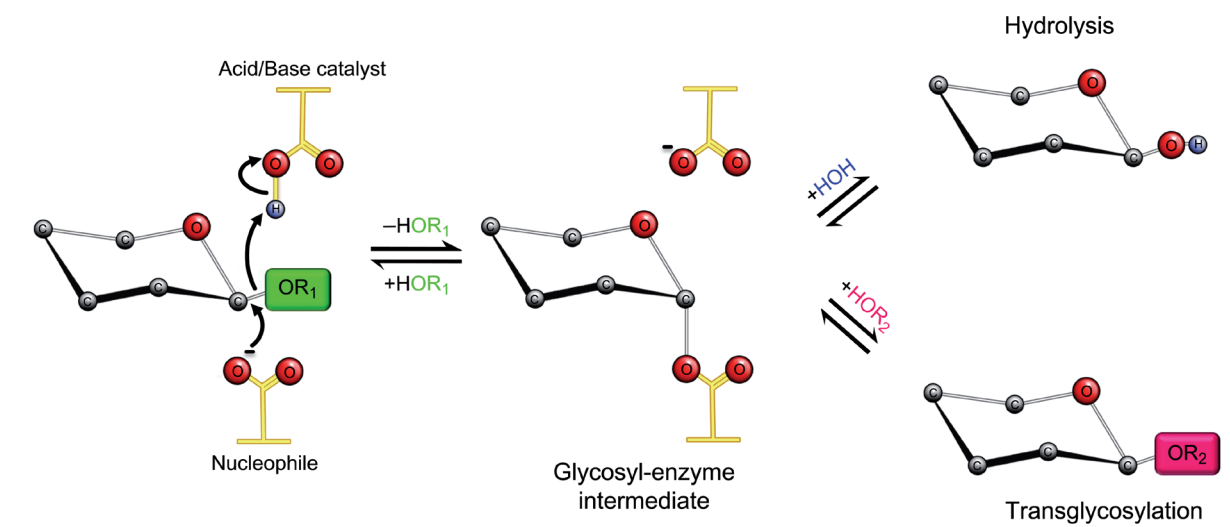


Production and Characterisation of Glycoside Hydrolases from GH3, GH5, GH10, GH11 and GH61 for Chemo-Enzymatic Synthesis of Xylo- and Mannooligosaccharides

Adiphol Dilokpimol



## Production and Characterisation of Glycoside Hydrolases from GH3, GH5, GH10, GH11 and GH61 for Chemo-Enzymatic Synthesis of Xylo- and Mannooligosaccharides



Adiphol Dilokpimol  
Ph.D. Thesis  
June 2010

Enzyme and Protein Chemistry  
Department of Systems Biology